5-2016

Quantum Mechanical Studies of Charge Assisted Hydrogen and Halogen Bonds

Binod Nepal

Utah State University

Recommended Citation

QUANTUM MECHANICAL STUDIES OF CHARGE ASSISTED HYDROGEN

AND HALOGEN BONDS

by

Binod Nepal

A dissertation submitted in partial fulfillment
of the requirements for the degree

of

DOCTOR OF PHILOSOPHY

in

Chemistry

Approved:

_____   _____
Steve Scheiner   Yujie Sun
Major Professor   Committee Member

_____   _____
Alexander I. Boldyrev   T.C. Shen
Committee Member   Committee Member

_____   _____
David Farrelly   Mark R. McLellan
Committee Member   Vice President for Research
                                     and Dean of the School of Graduate Studies

UTAH STATE UNIVERSITY
Logan, Utah

2016

ABSTRACT

Quantum Mechanical Studies of Charge Assisted Hydrogen

and Halogen Bonds

by

Binod Nepal, Doctor of Philosophy

Utah State University, 2016

Major Professor: Dr. Steve Scheiner
Department: Chemistry and Biochemistry

This dissertation is mainly focused on charge assisted noncovalent interactions specially hydrogen and halogen bonds. Generally, noncovalent interactions are only weak forces of interaction but an introduction of suitable charge on binding units increases the strength of the noncovalent bonds by a several orders of magnitude. These charge assisted noncovalent interactions have wide ranges of applications from crystal engineering to drug design. Not only that, nature accomplishes a number of important tasks using these interactions. Although, a good number of theoretical and experimental studies have already been done in this field, some fundamental properties of charge assisted hydrogen and halogen bonds still lack molecular level understanding and their electronic properties are yet to be explored. Better understanding of the electronic properties of these bonds will have applications on the rational design of drugs, noble functional materials, catalysts and so on. In most of this dissertation, comparative studies have been made between charge and neutral noncovalent interactions by quantum mechanical calculations. The

comparisons are primarily focused on energetics and the electronic properties. In most of the cases, comparative studies are also made between hydrogen and halogen bonds which contradict the long time notion that the H-bond is the strongest noncovalent interactions. Besides that, this dissertation also explores the long range behavior and directional properties of various neutral and charge assisted noncovalent bonds.

(396 pages)

PUBLIC ABSTRACT

Quantum Mechanical Studies of Charge Assisted Hydrogen

and Halogen Bonds

by

Binod Nepal, Doctor of Philosophy

Utah State University, 2016

Major Professor: Dr. Steve Scheiner
Department: Chemistry and Biochemistry

Like cement bridges one brick to another, noncovalent forces also bridge two or more molecules together to form a molecular crystal or molecular cluster. Although weaker than the covalent bond, the existence of noncovalent forces can be seen everywhere from liquid water to construction of complex biomolecules like DNA, RNA, proteins etc. An introduction of suitable charge; positive or negative, on the binding units can increase the strength of noncovalent interaction by several orders of magnitude. The primary aim of this dissertation is to explore some fundamental properties of such charge assisted noncovalent interactions which will be helpful for the rational design of molecular crystals, drugs, catalysts and many more. Besides that, this dissertation also makes parallel study between H-bond and halogen bonds and contradicts the long time notion that the H-bond is the strongest noncovalent interaction.

(396 pages)

DEDICATION

I would like to dedicate this work to my son Yubin.

ACKNOWLEDGMENTS

It is giving me a very joyous feeling as well as immense pleasure while writing this important section of my dissertation which I cannot express in words. It is also giving me a very nice flashback of all the time that I spent here in Utah State University. I am remembering all those people whose immense help, support, love and care were vital for the completion of this dissertation.

First of all, I would like to express my deepest gratitude to my advisor Professor Steve Scheiner for his unceasing reinforcement, immense knowledge, expert guidance and motivation throughout my research and study. Had there not been the proper guidance, persistent help and inspiration, I would not be able to present my dissertation in this shape. His knowledge, encouragement and support have been instrumental in becoming a better student, researcher and a good human being.

Next, I am grateful to my supervising committee members Dr. Alexander I. Boldyrev, Dr. David Farrelly, Dr. Yujie Sun and Dr. T. C. Shen for their valuable suggestions, important discussions and precious insights. Dr. Boldyrev also provided me a deep knowledge in spectroscopy and quantum mechanics with his two courses in physical chemistry.

I am equally grateful to Dr. Tapas Kar for his constant help and support during my research work. Dr. Kar always helped me whenever I ended up with some technical difficulties.

CONTENTS

LIST OF TABLES

LIST OF FIGURES

LIST OF SCHEMES

LIST OF ABBREVIATIONS

Abbreviation	Definition
TMA	Trimethyl Amine
TMA+	Tetramethyl Ammonium cation
HBs	Hydrogen Bonds
XBs	Halogen Bonds
AIM	Atoms in Molecules
BSSE	Basis Set Superposition Error
MP2	Second Order Moller-Plesset Perturbation Theory
NBO	Natural Bond Orbital
SAPT	Symmetry Adapted Perturbation Theory
EX	Exchange Repulsion
ES	Electrostatic
IND	Induction
DISP	Dispersion
EXIND	Exchange Repulsion Induction
EXDISP	Exchange Repulsion Dispersion
VSEPR	Valence Shell Electron Repulsion Theory
CPCM	Conductor Polarized Continuum Model
CCSD(T)	Coupled Cluster Single Double (Triple)
DFT	Density Functional Theory
BTP	Bis-Triazole Pyridine

MEP	Molecular Electrostatic Potential
BTB	Bis-Triazole Benzene
DMA	Dimethyl Amine
DMU	Dimethyl Urea
LUMO	Lowest Unoccupied Molecular Orbital

CHAPTER 1

INTRODUCTION

The covalent bond, which is defined as the bond formed by the sharing of electrons between atoms, is largely responsible for the construction of individual molecules. Although, some properties of the substance come from the intrinsic properties of the molecule, some of the properties on the other hand are dependent on how these individual molecules get arranged in a bulk. A very interesting example for this is; properties of 5-Methyl-2-[(2-nitrophenyl) amino]-3-thiophenecarbonitrile molecule, also known as ROY. This molecule in the bulk can have the color red, orange or yellow depending on the arrangement of the molecules in the crystal structure.[1,2] Similarly, a large number of drug molecules exhibit polymorphism which is observed as different solubility, stability and even the different activity inside the body depending on the crystal structure.[3-5] The arrangement of the molecules in a bulk is always dictated by the interaction of one molecule with others which is called intermolecular interaction or noncovalent interaction. The noncovalent interactions not only exist in the condensed phase like solids or liquids but also in the gas phase. The formation of various types of aerosols in the atmosphere are examples of this. The noncovalent interactions are not only intermolecular. If the molecule is big enough, generally in case of organic and biomolecules, noncovalent interactions might be possible within the same molecule and in such a case the noncovalent interaction might affect the conformation of the individual molecules.[6-9]

The collection of noncovalent interactions is very diverse and hence can be classified into various types.[10-12] Among all, the H-bond is undoubtedly the most popular and the most studied one with a history of almost a century.[13-15] Classical definition of the H-bond once proposed by Linus Pauling[16,17] around 1930 is too narrow and is limited to the most electronegative atoms F, O and N as depicted in Fig 1-1 which is still being taught in undergraduate level chemistry.
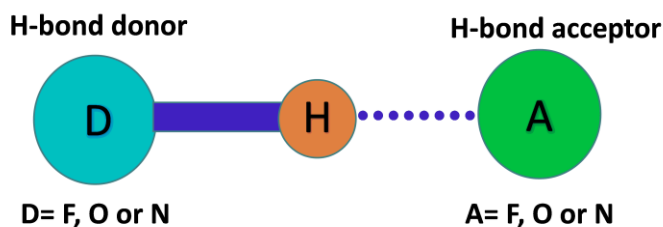
Figure 1-1. Classical depiction of the H-bond.

It was a long time before many experimental as well as quantum mechanical evidences suggested the involvement of less electronegative atoms like P, S, Cl or even the C in a H-bond.[18] For example, the H-bond formed by S-H hydrogen in aryl mercaptans was reported in 1939.[19] The crystallographic evidences of C-H$\cdots$O hydrogen bonds were already published in 1962.[20] The ether hydrochloride complex was already described as H-bonded complex in 1938 where Cl acts as the H-bond donor.[21] Surprisingly, it took so long to formally revise the definition of the H-bond which was done just in 2011 to cover all sorts of observed H-bond interactions.[22]

The newer added member in noncovalent family is the halogen bond in which halogen atom bridges the donor and acceptor atoms as does hydrogen atom in H-bond.[23-25]

It is amazing to see that halogen bond is being developed as the stronger rival of H-bond in terms of energy as well as in applications.[26-30] Although, the experimental evidence of halogen bond was discovered nearly two centuries ago by a chemist Jean-Jacques Colin in a mixture of iodine and ammonia solution, it took almost 150 years for a complete description of the complex.[31] The proper description of the complex was made possible by the separate efforts of Robert Mulliken's and Odd Hassel.[32,33] Unfortunately, the halogen bond was then forgotten for a long time and it has not been more than 15 years or so, the research on halogen bond restarted again. Since then, an overwhelming amount of research both experimentally and theoretically is going on in this field. To date, the halogen bond has been successfully exploited for a number of useful applications like, crystal engineering, anion receptor chemistry, catalysis, drug design, sensing applications and much more.[34-36] The halogen bond was perplexing for a number of chemist as it was not easy to explain why an electronegative halogen atom might be attracted to another electronegative atom.[33] But quantum mechanical calculations provided a very clear picture and molecular level understanding of the halogen bond. The covalently bonded halogen atom when bonded with more electronegative atom forms a positively charged region along the σ bond which is also called σ-hole.[37,38] This positively charge σ-hole can undergo electrostatic interaction with other electronegative atoms or with source of π electrons which is the primary source of attraction for the halogen bond. The type of σ hole interactions is not only limited to the Gr 7A elements of the periodic table. Groups 4A, 5A, 6A or even the 8A elements when covalently bonded with another more electronegative atom can undergo σ hole interactions with another more electronegative atom and such

types of bonding are called tetrel, pnicogen, chalcogen and aerogen bonding respectively.[38-42]

This dissertation is mainly focused on the charge assisted noncovalent interactions mainly hydrogen and halogen bonds. These bonds are often called ionic hydrogen or halogen bonds and they play critical roles in ionic clusters, acid-base equilibria, ion solvation, molecular recognition, ion transports, protein folding and many more.[43] As previously explained, noncovalent interactions are only the weak force of interactions. For example, the H-bond energy of the water dimer is only about 4.9 kcal/mol.[44] Lots of experimental and theoretical research has confirmed that once the charge is introduced into the noncovalently bonded systems, the strength of bonding can be increased by several orders of magnitude.[45-47]

There are mainly three ways of introducing the charge into the noncovalently bonded systems as depicted in the Fig 1-2, which exemplify in the case of H-bond and halogen bond. In the first case, the negative charge is present in the acceptor atom or acceptor group. Such types of bonds are called anionic H-bonds or halogen bonds. In the second case, the positive charge is present in the donor group and such types of bonds are called cationic H-bonds or halogen bonds. The third case is the combination of both where positive charge is developed on the donor group and negative charge on the acceptor group. Similar to the H-bonds or halogen bonds, charge assistance is also possible in case of chalcogen or pnicogen bonds where A and D atoms interact directly with no bridging atoms.
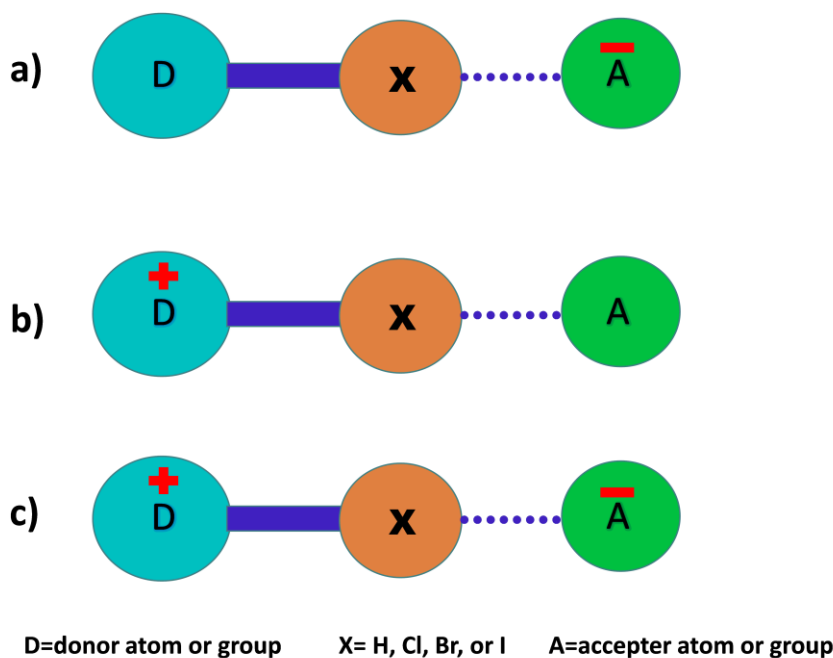
Figure 1-2. Charge assisted H-bond and halogen bond. a) corresponds to anionic H-bond or halogen bond and b) corresponds to cationic H-bond or halogen bond c) corresponds to H-bond or halogen bond assisted by both charges.

Although, ionic H-bonds have been studied for a long time,[48-52] we can find some controversies in the literature in the categorization of some of the charge assisted H-bonds, whether they are truly hydrogen bonds or just some electrostatic interactions. For example, Dougherty's group defined the interaction of benzene and ammonium ion or tetramethyl ammonium ion as purely electrostatic interaction and clearly said that there is no indication of any NH⋯π or CH⋯π interactions.[53] But we can find similar kinds of complexes in the literature being characterized as H-bonded systems.[54,55] These were the cases when the charge is present in only one of the monomer units. But if the charges are present in both of the monomer units, it will even be more difficult to characterize the type of bonding whether it is H-bond (or halogen bond) or the ion pair interactions. For example, in room

temperature ionic liquids (RTILs) which are generally composed of organic cations and inorganic anions, it is not that easy to characterize the types of noncovalent interactions whether it is H-bond or mostly other types of interactions like coulombic interaction.[56]

Although, experimental techniques like microwave spectroscopy, IR or NMR provide a certain degree of understanding for such charge assisted noncovalent interactions, a complete molecular level understanding still might not be possible no matter how advanced instruments that we have access to. Thanks to the development of quantum mechanical methods and powerful supercomputers we have an important tool for molecular level understanding and electronic properties of such noncovalent complexes. Although, a massive number of publications are available in the topic related to charge assisted hydrogen and halogen bonds, many facets of this topic are still devoid of proper understanding. So the primary purpose of this dissertation is to fulfill some of these gaps in the understanding of charge assisted noncovalent interactions mainly hydrogen and halogen bonds. In this dissertation, the electronic properties and the energetics of the charge assisted hydrogen and halogen bonds are compared with their respective neutral analogues. Besides the fundamental properties of the charge assisted hydrogen or halogen bonds, some applications aspects of these bonds especially in anion receptor chemistry, are also discussed. In most of the cases, hydrogen and halogen bonds are studied in parallel. A brief overview of each of the chapters in this dissertation is presented below.

Due to the prevalence CH hydrogens in almost all organic and biomolecules, the carbon donating hydrogen bonds represents one of the most important branches of H-bond in chemistry and biochemistry. But these H-bonds are much weaker than their classical H-

bond analogues.[57,58] It is quite obvious that the presence of positive charge in the proton donor or the negative charge in the proton acceptor can substantially enhance the H-bond energy. Such types of charge assisted CH⋯O and CH⋯N hydrogen bonds are studied quite well.[47] But similar type of studies in case of CH⋯π hydrogen bonds is completely lacking. Chapter 2 of this dissertation is focused on the detailed investigation of the influence of positive charge on these H-bonds in comparison to their neutral analogues in terms of energy as well as other electronic properties. A series of different π electron sources, ethylene, acetylene, butadiene, benzene, phenol, imidazole and indole are taken as proton acceptors which are paired with both positively charged and neutral CH proton donors molecules, trimethyl amine and tetramethyl ammonium respectively.

One of the important applications of C-H H-bond donor molecules is in the field of anion receptor chemistry. Over the past few years, a number of promising experimental results have been published in this field.[59-62] But some of the fundamental questions about these C-H⋯anion H-bonds were still lacking. For example, can these be categorized as truly H-bonds or are they mainly an ionic interaction? How does the strength of these anionic H-bonds vary with amount of charge on the anion? Similarly, is there any substantial effect of the number of acceptors atoms in the anion on the H-bond energy? Chapter 3 is the detailed investigations of such issues on C-H⋯anion H-bonds.

Water is regarded as the universal solvent and is capable of solvating wide ranges of substances. The excellent solvation properties of water are due to its polar nature and its H-bonding capacity. Since C-H⋯anion are quite strong H-bonds,[63-65] it's not surprising to think that such types of H-bonds can be involved in solvation of anions. But such types of

studies at microscopic level are still lacking in the literature. Chapter 3 tries to fulfill this gap and explores several other questions on this topic. For example, how does the magnitude of charge, size, number of the acceptor atoms on the anion affect the energetics solvation? Is this solvation thermodynamically feasible? Can these CH donor molecules form a well-defined solvation shell around the anions?

Normally, particular type of covalent bond has particular bond length and that doesn't vary much from compound to compound. But noncovalent bond lengths vary a good deal from system to system and energetics of the interaction depends on the bond length. The H-bonded or other noncovalently bonded systems are at the equilibrium bond distances when there are no restrictions. Most of the properties of noncovalent interactions are studied at equilibrium bond distances. But the questions always arise, how does the H-bond or other types of noncovalent bond energies vary with distance? Among different types of noncovalent interactions like hydrogen, halogen, pnicogen or chalcogen bonds which one is the most sensitive to bond stretching from their equilibrium geometries? Is it possible to fit this distance dependence to certain equations? How does the charge assisted H-bond differ from its neutral analogue in this respect? The binding energies of noncovalent complexes are normally composed of electrostatic, induction and dispersion components. It will be very interesting to see how do these individual components actually vary with bond distance? Our research group took the first initiative to answer these questions and the results are presented in chapter 5 of this dissertation.

Similar to the covalent bonds, the noncovalent bonds like hydrogen, halogen, chalcogen and pnicogen bonds have certain degree of directional property and they tend to

have linear bond angles as much as possible.[66,67] So most of the properties of the noncovalent bonds are extracted only from the equilibrium bond angle geometries. This type of linearity might not always be possible due to certain restrictions in the molecular systems or due to multiple interactions. Previous study from our group compared the various types of noncovalent interaction in terms of their energy barriers of the bond angle distortion from their equilibrium geometries.[68] But there is still a gap in this issue in case of charge assisted H-bonds. How do the charge assisted H-bonds differ from their neutral analogues for bond angle distortion from their equilibrium geometries? Chapter 6 is a detailed investigation of this question. A number of C-H and N-H hydrogen bond donor systems with both charged and uncharged systems have been studied to address this issue.

Normally, in most of the literature, the H-bond has been reported as the strongest noncovalent interaction. But some of the recent investigations have confirmed that that is not the case. For the analogous systems, halogen bond with iodine is stronger than the H-bond. This discovery leads to replacement of the H-bonds by halogen bonds in a large number of experimental applications like anion receptor chemistry, drug design, catalysis, sensing applications, crystal engineering and many more.[26] Especially, bidentate anion receptors have been very popular at this stage due to their effectiveness in anion binding.[69-71] Despite, an availability of large number of publications, there is still an intriguing question jumbling around the chemist mind, what makes these halogens bond stronger than hydrogen bond and how do they compare with each other in terms of electronic properties? To answer this question, a detailed comparative study of H-bond vs halogen bond is

essential. The effort has been taken to answer this question and the results are presented in chapter 7 of this dissertation.

As already mentioned, halogen bond has been widely utilized to capture selective anions from the aqueous solution. One way of increasing the binding capacity of anion receptor systems is introducing electron withdrawing groups like $-NO_2$, $-COOH$, $-CHO$, $>C=O$ in the system. But electronic effect of such substituent groups on energetics of the binding of the halides is not still not available in the literature and there are also several other fundamental questions regarding this issue. For examples, do the substituents groups have similar effects in H-bonded systems and halogen bonded systems or different? Similarly, the bidentate anion receptor molecules can be cationic or neutral. Which systems will show the higher sensitivity for the substituent? These questions need to be addressed before utilizing the substituent groups in the receptor system for anion binding. All of these fundamental questions have been studied by quantum mechanical methods and results are presented in Chapter 8 of this dissertation.

Quinones are an important class of organic compound which help in electron transfer reaction in many biochemical reactions like photosynthesis and respiration.[72,73] They are also being used as oxidizing reagent in many organic reactions.[74] Many experiments have confirmed that quinones can be activated for reduction by the use of H-bond donor molecules.[75,76] Such activation is described in terms of the stabilization of semiquinone anion radical by charged assisted H-bonds.[77] But one biggest unanswered question in the scientific community is why are electron rich quinones activated more efficiently than electron deficient quinone by H-bond donors. The mystery of this puzzle

has been solved by the quantum mechanical studies on some selected model systems. The results from this study are presented in chapter 9.

The majority of halogen bonds that are studied experimentally or theoretically have carbon as the donor atom. This is not surprising because most of the halogenated organic compounds have halogen atom bonded to the carbon atom. As N is more electronegative than C, it is not difficult to assume that N-X···Y halogen bonds are stronger than C-X···Y halogen bonds where X and Y are the halogen and the acceptor atoms respectively. Few experimental results are available where N-X···Y halogen bonds have been used for crystal engineering.[78-80] One of the very interesting questions on this topic is how do these N-X···Y halogen bonds compare with N-H···Y hydrogen bonds in terms of energetics as well as electronic properties? Similarly, how stronger are the N-X···Y halogen bonds compared with C-X···Y halogen bonds? The detailed comparative investigations on these issues are carried with the model systems saccharin and the N-succinimide as the H-bond donor. The systems are modified to halogen bond donors by replacing H atom by halogen atom. A ranges of molecular systems containing O, N, F lone pairs as well as having π electrons sources are employed as H-bond or halogen bond acceptors. The results are presented in chapter 10 of this dissertation.

References

(1)   Beran, G. J. O. *Chem. Rev.* **2016**, *116*, 5567.

(2)   Yu, L. *Acc. Chem. Res.* **2010**, *43*, 1257.

(3)   Singhal, D.; Curatolo, W. *Advanced Drug Delivery Reviews* **2004**, *56*, 335.

(4)   Rustichelli, C.; Gamberini, G.; Ferioli, V.; Gamberini, M. C.; Ficarra, R.; Tommasini, S. *J. Pharm. Biomed. Anal.* **2000**, *23*, 41.

(5)   O' Nolan, D.; Perry, M. L.; Zaworotko, M. J. *Cryst. Growth Des.* **2016**, *16*, 2211.

(6)   Sharon, A.; Maulik, Prakas R.; Vithana, C.; Ohashi, Y.; Ram, Vishnu J. *Eur. J. Org. Chem.* **2004**, *2004*, 886.

(7)   Matczak-Jon, E.; Videnova-Adrabińska, V.; Burzyńska, A.; Kafarski, P.; Lis, T. *Chem. Eur. J.* **2005**, *11*, 2357.

(8)   Naoda, K.; Mori, H.; Oh, J.; Park, K. H.; Kim, D.; Osuka, A. *J. Org. Chem.* **2015**, *80*, 11726.

(9)   Thomas, S. P.; Veccham, S. P. K. P.; Farrugia, L. J.; Guru Row, T. N. *Cryst. Growth Des.* **2015**, *15*, 2110.

(10)   Scheiner, S. *Acc. Chem. Res.* **2013**, *46*, 280.

(11)   Scheiner, S. *Noncovalent Forces*; Springer International Publishing, 2015.

(12)   Scheiner, S. *Molecular interactions: from van der Waals to strongly bound complexes*; Wiley, 1997.

(13)   Scheiner, S. *Hydrogen Bonding: A Theoretical Perspective*; Oxford University Press, 1997.

(14)   Jeffrey, G. A. *An Introduction to Hydrogen Bonding*; Oxford University Press, 1997.

(15)   Lassettre, E. N. *Chem. Rev.* **1937**, *20*, 259.

(16)   Pauling, L.; Kamb, B. *Linus Pauling: Selected Scientific Papers*; World Scientific Publishing Company, 2001.

(17)   Pauling, L. *The Nature of the Chemical Bond and the Structure of Molecules and Crystals: An Introduction to Modern Structural Chemistry*; Cornell University Press, 1960.

(18)   Gregoret, L. M.; Rader, S. D.; Fletterick, R. J.; Cohen, F. E. *Proteins: Structure, Function, and Bioinformatics* **1991**, *9*, 99.

(19)   Copley, M. J.; Marvel, C. S.; Ginsberg, E. *J. Am. Chem. Soc.* **1939**, *61*, 3161.

(20)   Schwalbe, C. H. *Crystallography Reviews* **2012**, *18*, 191.

(21)   Buswell, A. M.; Rodebush, W. H.; Roy, M. F. *J. Am. Chem. Soc.* **1938**, *60*, 2528.

(22)   Arunan, E.; Desiraju, G. R.; Klein, R. A.; Sadlej, J.; Scheiner, S.; Alkorta, I.; Clary, D. C.; Crabtree, R. H.; Dannenberg, J. J.; Hobza, P.; Kjaergaard, H. G.; Legon, A. C.; Mennucci, B.; Nesbitt, D. J. *Pure Appl. Chem.* **2011**, *83*, 1637.

(23)   Wolters, L. P.; Schyman, P.; Pavan, M. J.; Jorgensen, W. L.; Bickelhaupt, F. M.; Kozuch, S. *WIREs Comput Mol Sci* **2014**, *4*, 523.

(24)   Cavallo, G.; Metrangolo, P.; Milani, R.; Pilati, T.; Priimagi, A.; Resnati, G.; Terraneo, G. *Chem. Rev.* **2016**, *116*, 2478.

(25)   Politzer, P.; Lane, P.; Concha, M. C.; Ma, Y.; Murray, J. S. *J. Mol. Model.* **2007**, *13*, 305.

(26)   Metrangolo, P.; Resnati, G. *Halogen Bonding I: Impact on Materials Chemistry and Life Sciences*; Springer International Publishing, 2015.

(27)   Gilday, L. C.; Robinson, S. W.; Barendt, T. A.; Langton, M. J.; Mullaney, B. R.; Beer, P. D. *Chem. Rev.* **2015**, *115*, 7118.

(28)   Jentzsch, A. V.; Matile, S. In *Halogen Bonding I: Impact on Materials Chemistry and Life Sciences*; Metrangolo, P., Resnati, G., Eds.; Springer International Publishing: Cham, 2015, p 205.

(29)   Lu, Y.; Liu, Y.; Xu, Z.; Li, H.; Liu, H.; Zhu, W. *EXPERT OPIN DRUG DIS* **2012**, *7*, 375.

(30)   Mukherjee, A.; Tothadi, S.; Desiraju, G. R. *Acc. Chem. Res.* **2014**, *47*, 2514.

(31)   Erdelyi, M. *Nat Chem* **2014**, *6*, 762.

(32)   Hassel, O. *Science* **1970**, *170*, 497.

(33)   Mulliken, R. S. *J. Am. Chem. Soc.* **1950**, *72*, 600.

(34)   Kilah, N. L.; Wise, M. D.; Serpell, C. J.; Thompson, A. L.; White, N. G.; Christensen, K. E.; Beer, P. D. *J. Am. Chem. Soc.* **2010**, *132*, 11893.

(35)   Jungbauer, S. H.; Huber, S. M. *J. Am. Chem. Soc.* **2015**, *137*, 12110.

(36)   Wilcken, R.; Zimmermann, M. O.; Lange, A.; Joerger, A. C.; Boeckler, F. M. *J. Med. Chem.* **2013**, *56*, 1363.

(37)   Clark, T.; Hennemann, M.; Murray, J. S.; Politzer, P. *J. Mol. Model.* **2007**, *13*, 291.

(38)   Politzer, P.; Murray, J. S.; Clark, T. *Phys. Chem. Chem. Phys.* **2013**, *15*, 11178.

(39)   Bauza, A.; Quinonero, D.; Deya, P. M.; Frontera, A. *CrystEngComm* **2013**, *15*, 3137.

(40)   Bauzá, A.; Frontera, A. *Angew. Chem. Int. Ed.* **2015**, *54*, 7340.

(41)   Scheiner, S. *J. Chem. Phys.* **2011**, *134*, 094315.

(42)   Wang, W.; Ji, B.; Zhang, Y. *J. Phys. Chem. A* **2009**, *113*, 8132.

(43)   Meot-Ner, M. *Chem. Rev.* **2005**, *105*, 213.

(44)   Feyereisen, M. W.; Feller, D.; Dixon, D. A. *J. Phys. Chem.* **1996**, *100*, 2993.

(45)   Adhikari, U.; Scheiner, S. *J. Phys. Chem. A* **2013**, *117*, 10551.

(46)   Braga, D.; Maini, L.; Grepioni, F.; De Cian, A.; Felix, O.; Fischer, J.; Hosseini, M. W. *New J. Chem.* **2000**, *24*, 547.

(47)   Jesus, A. J. L.; Redinha, J. S. *J. Phys. Chem. A* **2011**, *115*, 14069.

(48)   Davenport, J. N.; Wright, P. V. *Polymer* **1980**, *21*, 287.

(49)   McMichael Rohlfing, C.; Allen, L. C.; Ditchfield, R. *Chem. Phys. Lett.* **1982**, *86*, 380.

(50)   Meot-Ner, M. *J. Am. Chem. Soc.* **1984**, *106*, 278.

(51)   Meot-Ner, M.; Deakyne, C. A. *J. Am. Chem. Soc.* **1985**, *107*, 474.

(52)   Allerhand, A.; von Rague Schleyer, P. *J. Am. Chem. Soc.* **1963**, *85*, 1233.

(53)   Ma, J. C.; Dougherty, D. A. *Chem. Rev.* **1997**, *97*, 1303.

(54)   Koller, J.; Grdadolnik, J.; Hadži, D. *J. Mol. Str.: THEOCHEM* **1992**, *259*, 199.

(55)   Brown, R. J. C. *J. Mol. Struct.* **1995**, *345*, 77.

(56)   Dong, K.; Song, Y.; Liu, X.; Cheng, W.; Yao, X.; Zhang, S. *J. Phys. Chem. B* **2012**, *116*, 1007.

(57)   Gu, Y.; Kar, T.; Scheiner, S. *J. Am. Chem. Soc.* **1999**, *121*, 9411.

(58)   Scheiner, S. *Phys. Chem. Chem. Phys.* **2011**, *13*, 13860.

(59)   Vega, I. E. D.; Gale, P. A.; Light, M. E.; Loeb, S. J. *Chem. Commun.* **2005**, 4913.

(60)   Yoon, D.-W.; Gross, D. E.; Lynch, V. M.; Sessler, J. L.; Hay, B. P.; Lee, C.-H. *Angew. Chem. Int. Ed.* **2008**, *47*, 5038.

(61)   Amouri, H.; Moussa, J.; Malacria, M.; Gandon, V. *Cryst. Growth Des.* **2009**, *9*, 5304.

(62)   Choi, Y.; Kim, T.; Jang, S.; Kang, J. *New J. Chem.* **2016**, *40*, 794.

(63)   Tresca, B. W.; Hansen, R. J.; Chau, C. V.; Hay, B. P.; Zakharov, L. N.; Haley, M. M.; Johnson, D. W. *J. Am. Chem. Soc.* **2015**, *137*, 14959.

(64)   Pedzisa, L.; Hay, B. P. *J. Org. Chem.* **2009**, *74*, 2554.

(65)   Nepal, B.; Scheiner, S. *Chem. Eur. J.* **2015**, *21*, 1474.

(66)   Cybulski, S.; Scheiner, S. *J. Phys. Chem.* **1990**, *94*, 6106.

(67)   Gu, Y.; Kar, T.; Scheiner, S. *J. Mol. Struct.* **2000**, *552*, 17.

(68)   Adhikari, U.; Scheiner, S. *Chem. Phys. Lett.* **2012**, *532*, 31.

(69)   Robinson, S. W.; Mustoe, C. L.; White, N. G.; Brown, A.; Thompson, A. L.; Kennepohl, P.; Beer, P. D. *J. Am. Chem. Soc.* **2015**, *137*, 499.

(70)   Caballero, A.; White, N. G.; Beer, P. D. *Angew. Chem. Int. Ed.* **2011**, *50*, 1845.

(71)   Tepper, R.; Schulze, B.; Jäger, M.; Friebe, C.; Scharf, D. H.; Görls, H.; Schubert, U. S. *J. Org. Chem.* **2015**, *80*, 3139.

(72)   Newman, D. K.; Kolter, R. *Nature* **2000**, *405*, 94.

(73)   Nohl, H.; Jordan, W.; Youngman, R. J. *Advances in Free Radical Biology & Medicine* **1986**, *2*, 211.

(74)   Colucci, M. A.; Couch, G. D.; Moody, C. J. *Org. Biomol. Chem.* **2008**, *6*, 637.

(75)   Uno, B.; Okumura, N.; Goto, M.; Kano, K. *J. Org. Chem.* **2000**, *65*, 1448.

(76)   Gupta, N.; Linschitz, H. *J. Am. Chem. Soc.* **1997**, *119*, 6384.

(77)   Turek, A. K.; Hardee, D. J.; Ullman, A. M.; Nocera, D. G.; Jacobsen, E. N. *Angew. Chem. Int. Ed.* **2016**, *55*, 539.

(78)   Makhotkina, O.; Lieffrig, J.; Jeannin, O.; Fourmigué, M.; Aubert, E.; Espinosa, E. *Cryst. Growth Des.* **2015**, *15*, 3464.

(79)   Hakkert, S. B.; Erdélyi, M. *J. Phys. Org. Chem.* **2015**, *28*, 226.

(80)   Bedin, M.; Karim, A.; Reitti, M.; Carlsson, A.-C. C.; Topic, F.; Cetina, M.; Pan, F.; Havel, V.; Al-Ameri, F.; Sindelar, V.; Rissanen, K.; Grafenstein, J.; Erdelyi, M. *Chem. Sci.* **2015**, *6*, 3746.

CHAPTER 2

EFFECT OF IONIC CHARGE UPON THE CH··π HYDROGEN BOND[1]

Abstract

The CH··π hydrogen bonds (HBs) between trimethylamine (TMA) and an assortment of π-systems are generally weaker than those in which CF_3H serves as proton donor, despite the larger number of CH groups available to serve as donors in the amine. The added positive charge of tetramethylammonium (TMA+) enhances the binding energy by a factor between 4 and 7. The strongest such interaction for TMA+ occurs with indole, bound by 15.5 kcal/mol. Changing from ionic CH··π to NH··π further strengthens the interaction. Conjugation of the π-system improves its proton-accepting capacity, which is further enhanced by aromaticity. Dispersion plays a major role in CH··π HBs: It is the prime contributor in the neutral HBs of TMA, and comparable to Coulombic forces for CF_3H and even in ionic CH··π HBs of TMA+. Many of the results can be understood on the basis of a combination of electrostatic potentials and charge transfers.

2-1. Introduction

Among an assortment of noncovalent interactions that have been recognized over the years,[1-2] hydrogen bonds (HBs) are generally considered the most widespread and important.[3-4] The original consideration of N, O and F as HB donor and acceptor atoms in

---

a DH··A arrangement has been expanded over the years to include other less electronegative atoms like S, Cl, and C.[5-10] Of these, the ability of CH to serve as proton donor has been perhaps most extensively scrutinized, and this growing recognition of CH··O HBs has spawned a diverse literature database that has informed a wide swath of chemistry and biochemistry.[11-18]

In addition to lone pairs, the source of electrons may reside instead in the π-electron system of the proton-acceptor group. Although generally weak, the CH··π HB makes its presence felt in a large number of instances.[19-23] As one example, Brandl et al[24] studied a set of more than a thousand different protein structures which were found to contain over 30,000 C-H π interactions which contribute significantly to the overall stability of the proteins.

Under most circumstances, CH··π HBs are weaker than their classical analogues. For example, the binding energy of methane with the benzene ring, primarily attributed to dispersion, is only around 1.4 kcal/mol.[25-26] On the other hand, in other types of HBs the introduction of a positive charge into the proton donor, or negative on the acceptor, can very substantially enhance the interaction.[27-31] For example, calculations[32] found a complex between trimethylammonium ion and the O acceptor atom of methylacetate that relied solely on CH+··O HBs was bound by 13 kcal/mol. More recently, this research group showed[33] that the introduction of positive charge on the proton donor substantially enhanced the binding energy of several CH··O HBs, by a factor of 4-9. It is tempting to presume that a similar charge-induced magnification might be operating in CH··π HBs as well. Indeed, Dougherty's group synthesized a large number of host molecules[34] which can

extract cations from aqueous solution employing ionic CH··π and NH··π HBs. But there has been little detailed scrutiny of this issue, so a quantitative assessment of the potential strength of CH··π HBs is lacking and perhaps overdue.

Information about this topic ought to have implications for biological systems, including stability of proteins,[35] biochemical reactions,[36] controlling stereochemistry in organic synthesis,[37] and molecular crystal structure.[38] For example, there is a preference within proteins for cationic amine sidechain groups as in lysine and arginine to be oriented[39] toward a nearby aromatic side chain so as to engage in NH^+··π HBs with them. But the charge exerts its effect further along the chain, as in lysine-tryptophan interaction, where the CH_2 group adjacent to the NH_3^+ participates in a CH··π interaction. In another example, D-dopamine binds to the D-2 receptor site[36] via CH··π HBs involving the methylene protons β to the NH_3^+.

Even though a good deal of experimental data reinforce the important role played by ionic CH··π and NH··π bonds in a variety of natural phenomena and chemical reactions, there remain a number of unanswered questions. What factors influence the strength of these bonds, and what is the limit on such strength? How does a single π-bond as in ethylene compare with a series of conjugated π-bonds, or an aromatic system? Is a single CH··π HB preferable to bifurcated or trifurcated arrangements? From a fundamental perspective, is the CH··π pairing a true HB or is it merely a simple Coulombic interaction? Precisely how does charge affect the nature and strength of each interaction, and what are the effects on the preferred geometry?

Quantum mechanical techniques offer an essential means of addressing these questions. In this work, a variety of both CH and NH proton donors are considered for purposes of comparison. CF_3H is a small and relatively simple molecule whose three F atoms impart a fairly strong polar character to the CH bond, making it a potent proton donor. The CH bonds in $N(CH_3)_3$ are less polar, but their number might make up for the weakness of any one individual CH··π bond. This molecule also facilitates a detailed comparison of single vs bifurcated and even trifurcated HBs. The effects of adding a charge can then be easily isolated and studied by consideration of the very similar $N(CH_3)_4^+$ ion. Comparison with the NH donor groups of NH_4^+ reveals any intrinsic differences between NH and CH HBs.

In terms of proton acceptors, a variety of π systems were considered. Ethylene and acetylene both contain a single C-C connection, whereas 1,3-butadiene presents conjugation between a pair of C=C bonds. This conjugation is more complete in the aromatic benzene molecule. The effects of substitution to the aromatic ring are considered by adding an external -OH group to form phenol, or by way of the N atoms in the heteroaromatic imidazole. Lastly, the fusion of a pair of aromatic rings, one of which is heteroaromatic, leads to the indole species. It should be noted that the benzene molecule serves as a model of the Phe residue in proteins; likewise phenol, imidazole, and indole simulate Tyr, His, and Trp, respectively, so the results ought to have implications for noncovalent bonds within proteins.

2-2. Computational Methods

All calculations were carried out using the Gaussian-09 software package.[40] The MP2 method was applied in conjunction with the aug-cc-pVDZ basis set. This level of theory has been found to provide excellent results for these sorts of interactions.[41-51] The binding energies of the complexes were calculated as the differences in energy between the complex and the sum of the monomers in their optimized geometries, corrected for BSSE using the counterpoise procedure.[52] The potential energy surface of each heterodimer was thoroughly searched in order to find all minima, which had no imaginary frequencies. Dimers were examined via the Natural Bond Order (NBO) procedure[53-54] embedded in the Gaussian program. Symmetry Adapted Perturbation Theory (SAPT)[55-56] was carried out via the Molpro suite of programs.[57]

2-3. Results

2-3.1. CHF$_3$ as proton donor

The binding energy of complexes of CF$_3$H with the various π electron systems is reported in the first column of Table 2-1. In some cases more than one minimum was obtained for a particular pair of monomers. Only the most stable complex of the CH··π variety is displayed in the table and in Fig 2-1. The proton of CF$_3$H approaches the π system of each electron donor, although not directly head-on in all cases. The reasons for these deviations are discussed in some detail below.

The interaction with the simple ethylene and acetylene is the weakest, with binding energy of 1.6 kcal/mol. In the case of butadiene, the CF$_3$H proton is drawn toward the two terminal C-C bonds rather than to the central bond. This proclivity can be understood first

on the basis of the normal Lewis structure of butadiene wherein it is the two terminal C=C bonds that involve a π-bond. This pattern is reinforced by the electrostatic potential which is most negative above these terminal C-C bonds, as illustrated in Fig 2-2c. The binding increases along with the size of the donor, up to 3.7 kcal/mol for benzene and 3.9 kcal/mol for phenol. This quantity rises above 4 kcal/mol when heteroatoms are added to the ring, as in imidazole and indole. The intensity of the negative electrostatic potential, indicated by the extent of the red regions in Fig 2-2, correlates nicely with the binding energy.

Turning next to phenol, the CH··π bond in Fig 2-1e is significantly distorted from linearity. The θ(CH··c) angle, where c refers to the center of the phenyl ring, is 147.8°. This bending presumably takes place in order to accommodate an electrostatic attraction between the negative potential around a F atom of CF_3H and the positive region around the OH group of phenol (see Fig 2-2e). One might have anticipated that a CH··O HB to the oxygen of phenol, or OH··F, ought to be stronger than the CH··π bond in Fig 2-1, but this is not the case. Fig 2-10 illustrates five secondary minima for the CF_3H/phenol complex. Structure a is quite similar to the global minimum, with a nearly equal binding energy, differing only in a slight rotation of the proton donor molecule about its C-H axis. Structure b is higher in energy, stabilized by a CH··O HB coupled with OH··F in a cyclic geometry. The CH··O HB appears again in c, and is replaced entirely by a OH··F HB in d. The highest energy dimer e contains no HB at all, with a binding energy of only 1.1 kcal/mol. In this particular pair of molecules, it would appear then that a CH··π HB is more stabilizing than CH··O or OH··F, either singly or in combination.

In the case of heterocyclic imidazole, the high basicity of N leads to an energetic preference for the CH··N over CH··π, especially as the former HB can be reinforced by a weaker CH··F as in f and g in Fig 2-10. The CH··π structure in Fig 2-1 has a binding energy of 4.1 kcal/mol, about 1 kcal/mol smaller than the two former minima. Note the angular distortion of the CH··π bond, with a θ(CH··c) angle of 134°. This angular distortion is again a result of electrostatic forces since Fig 2-2f shows that the most positive region of the imidazole electrostatic potential surrounds the NH group, attracting the F atoms of the CF_3H. (Indeed there are similar angular distortions present for all of the heterocyclic rings with θ(CH··c) between 134° and 149°.) Somewhat less stable are minima h and i in Fig 2-10, both of which contain NH··F HBs, followed finally by structure j with a binding energy of less than 1 kcal/mol, containing a single weak CH··F HB.

In connection with indole, note that there is a stronger interaction with its larger six-membered ring, although the N atom is located in the smaller ring. The electrostatic potential of Fig 2-2g helps explain this distinction, as there is a more intense and extensive negative potential above the larger ring. Without an unprotonated N atom as occurs in imidazole, indole cannot readily engage in a CH··N HB, leaving the CH··π interaction in Fig 2-1 as the dominating attractive force. A secondary minimum was found which contains a NH··F HB, but this structure lies some 3 kcal/mol higher in energy than the global minimum, and another wherein the CF_3H floats above the indole plane, but with its CH turned away from the π-system.

It is frequently observed that the r(CH) bond undergoes a contraction when forming a CH··O HB, and that its stretching frequency is shifted to the blue, both of these patterns

in contrast to trends in HBs in general. The first column of Table 2-2 shows that the CH bond of CF_3H fulfills this pattern, undergoing a small contraction upon formation of the CH··π complexes, on the order of 1-3 mÅ. Consistent with this contraction, the next column shows the CH stretching frequency is shifted to the blue. The largest of these changes is associated with benzene, with $\Delta r(CH)$= -3.1 mÅ and $\Delta \nu(CH)$= 51 cm^{-1}, even though benzene does not form the strongest CH··π bond. Likewise, imidazole induces the smallest shifts even though it represents one of the strongest CH··π complexes; changes for indole are also generally small. The largest changes for benzene may be associated with its near linear CH··π arrangement (see Table 2-1).

Another means of understanding the above trends emerges from NBO analysis. E(2) represents an estimate of the energy involved in a given charge transfer between two specific orbitals. For the CH··π complexes, there is a sizable transfer from the π orbitals of the unsaturated molecule to the $\sigma^*(CH)$ antibonding orbital of CF_3H. These quantities are listed in Table 2-3, and are generally in the range between 2.3 and 4.1 kcal/mol, with the maximum occurring for benzene. This maximum coincides with the largest $\Delta r(CH)$ and $\Delta \nu(CH)$ in Table 2-2. Given that E(2) is dependent upon the overlap between the donor and acceptor orbitals, one may surmise that the smaller magnitudes of E(2) for the heterocyclic rings are likely due to the aforementioned angular distortions of the CH··π systems.

A partitioning of the total interaction energy into its component parts provides another window into the nature of the interaction. The SAPT components are listed in Table 2-4. In most cases, the electrostatic (ES) and dispersion (DISP) terms are comparable to one another, followed by a smaller but still significant induction (IND) energy. The

exceptions are the simple ethylene and acetylene which have a disproportionately smaller dispersion contribution. Each of these components tends to grow in magnitude from top to bottom of Table 2-4, so follow a trend much like the total interaction energy itself. One can thus characterize this set of CH$\cdot\cdot\pi$ bonds as containing roughly equal stabilization from Coulombic and dispersion attractions for the conjugated systems, but with a smaller dispersion component for the simpler C_2H_n molecules.

Pictorial representations of electron redistributions offer a valuable window into the nature of noncovalent interactions. Such plots are generated as the difference in total electron density between the complex on one hand, and the sum of densities of the individual monomers in the same locations. Fig 2-3a illustrates such a redistribution for the $F_3CH\cdot\cdot C_2H_4$ dimer where green represents a loss of density upon formation of the complex, and gains are indicated by purple. The green loss around the bridging proton is typical of H-bonds, and the H-bonding interaction with the ethylene π-system is verified by the purple density increase in that area. The diagram looks much the same for $F_3CH\cdot\cdot C_2H_2$. Whereas the distances in Fig 2-1 suggest that the proton ought to interact approximately equally with the two C=C bonds of butadiene, the density in Fig 2-3b indicates otherwise, that the interaction with one of these two bonds is much stronger. The equivalence of the six C-C bonds in benzene is manifest in the symmetry of the $F_3CH\cdot\cdot$benzene redistribution diagram in Fig 2-3c, as is the case for phenol. This symmetry is broken in the case of imidazole, where it is the π-region above the unprotonated N atom and its neighboring two C atoms that exhibits the bulk of the purple density increase. The interaction with the 5-membered

ring of indole involves the entire ring with the exception of the NH group, and the 6-membered ring resembles the benzene pattern.

2-3.2. N(CH$_3$)$_3$ donor

Another potential CH donor arises when three methyl groups surround a central N atom. The electronegativity of the N imparts a certain level of acidity to the methyl groups, which are then capable of participating in CH··π HBs with π donors. On the other hand, the single N atom of trimethylamine (TMA) is not expected to match the three highly electronegative F atoms of CF$_3$H in terms of polarizing the CH bonds, so weaker CH··π interactions are anticipated. As an added issue, TMA permits the formation of multiple CH··π bonds simultaneously, involving protons either from a single methyl group, or from several individual methyls. One can thus address the question of the relative strengths of a single CH··π bond as compared to several bent bonds of the same sort.

As may be noted by comparison of the first and third columns of Table 2-1, trimethylamine (TMA) forms somewhat weaker interactions with the various π-donors than does CF$_3$H. Given the presence of multiple CH donors on TMA, many of the minima are stabilized by more than one CH··π HB. In the case of acetylene, for example, Fig 2-4 show that three H atoms, all from the same methyl group, are attracted toward the π system, constituting a distorted trifurcated HB. (In fact, NBO analysis in Table 2-3 suggests this complex is stabilized not by CH··π HBs but rather by a transfer from the π orbitals of acetylene into the σ*(CN) antibonding orbital.) Only slightly less stable is a similar configuration, except that each of the three H atoms is associated with a different methyl group. This structure is in fact stabilized purely by CH··π bonds, with no possibility of a

$\pi \rightarrow \sigma^*(CN)$ transfer. Of course, the N atom of TMA can serve as a strong proton-acceptor, so some of the most stable minima contain CH··N HBs. Acetylene is an example, wherein the global minimum contains such a CH··N HB.

The minimum for ethylene is bifurcated in that the two CH groups of TMA interacting with the π system are spread apart such that one is above, and the other below the ethylene plane. This bifurcated arrangement is only very slightly more stable than the trifurcated structure, whether from a single or three separate methyl groups. It might be noted that there are no local minima for either ethylene or acetylene which contain a single CH··π HB. The NBO values in Table 2-3 suggest that the charge transfer from the π orbitals into the $\sigma^*(CH)$ antibonds are considerably smaller here than for CF_3H, even when all are summed together, suggesting very weak CH··π HBs, not only for ethylene and acetylene, but for most of these complexes as well.

Some of the symmetry is lost in the case of conjugated butadiene. The minimum shown in Fig 2-4c has a single CH··π HB, with H··c distance of some 2.88 Å. This weak HB is supplemented by a small amount of transfer, from the butadiene π system to the $\sigma^*(CN)$ antibond of TMA, a sort of tetrel bond. There are two other minima with similar energy, containing respectively 1 or 3 CH··π HBs. As in most of these cases, the global minimum for this pair is stabilized by a HB wherein the N lone pair acts as electron donor, to a C-H bond in butadiene. There is a single CH··π HB in the global minimum of TMA with benzene, barely favored over the approach of 2 or 3 separate CH groups toward the molecule's center. Another sort of structure, slightly less stable, has the N atom approach

the benzene from above. There is no appreciable charge transfer here, and this geometry is probably stabilized primarily by a dipole-quadrupole interaction.

The OH··N HB is a strong interaction by its very nature, so it is not surprising that the global minimum of TMA with phenol contains such a bond. However, there are also a number of minima characterized by CH··π interactions, all with binding energies of 2.5 - 2.7 kcal/mol, depending upon whether there are one, two, or three such bonds. Just as the OH··N HB of phenol is a dominating interaction, so too is the very strong NH··N HB in which the NH of imidazole serves as proton donor. But again, there are a number of stable minima containing CH··π HBs, the most stable of which is illustrated in Fig 2-4f as held together by a pair of CH··π HBs, as well as a CH··N interaction. This structure represents the most strongly bound such complex with TMA, with a binding energy of 4.5 kcal/mol, even more tightly held than another structure which contains three CH··N HBs. As in the case of imidazole, the NH group of indole is also a potent proton donor, so it is not surprising to see a NH··N HB in the global minimum. With the exception of this structure, the most stable complex between TMA and indole includes 2, or arguably 3, CH··π HBs, spanning both rings.

In a molecule like TMA which has nine tightly coupled CH stretches, it is difficult to distinguish the CH stretching modes that correspond to H-bonded protons from those that do not. On the other hand, it is possible to consider any changes of individual CH bond lengths. The CH bonds participating in HBs are generally contracted relative to the isolated TMA monomer. These reductions vary from about 0.6 mÅ for acetylene and indole, up to 4.0 mÅ for the single CH··π bond with benzene, as reported in Table 2-2. Again, it is

emphasized that benzene has a combination of a strong CH··π bond and a nearly linear CH··c arrangement.

Results of SAPT dissection of the binding energy of the various complexes with TMA are reported in Table 2-5. Taking benzene as an example, the electrostatic component of -5.3 kcal/mol for CF_3H is reduced to -3.1 kcal/mol for TMA; likewise for the induction energy, reduced from -3.0 to -2.6 kcal/mol. On the other hand, the dispersion term becomes more attractive, increasing from -5.2 to -7.2 kcal/mol. This pattern is in fact typical of the transition from CF_3H to TMA: reduced ES and IND, but enhanced DISP. The net result is that the TMA complexes are bound primarily by dispersion, which is generally twice as large as ES, which is in turn larger than IND.

The CH··π HBs for TMA exhibit certain differences in electron density redistributions from those involving CF_3H. Whereas most HBs show roughly equal regions of loss around the proton and gain in the lone pair of the proton acceptor, the former losses outweigh the latter gains for TMA. The dominance of the green vs purple regions is exemplified in the cases of benzene and imidazole in Figs 2-3e and 2-3f, respectively. This pattern is common to all the complexes of TMA.

2-3.3. $N(CH_3)_4^+$ donor

The ability of a molecule to donate a proton is greatly enhanced by the presence of a positive charge. The tetramethylammonium $N(CH_3)_4^+$ species (TMA+) thus offers a means to isolate this enhancement for study by comparison with the very similar neutral $N(CH_3)_3$. The minima formed by this cation with the various π-systems are presented in Fig. 2-5, from which it may first be noted that the CH··c distances are considerably shorter

than those of the neutral analogues in Fig 2-4. For example, these HB distances are 3.1 Å for the complex of ethylene with TMA, but shortened to 2.9 Å for TMA+. The energetic magnification of the binding energies is even more dramatic in Table 2-1 where these quantities are 4-7 fold larger for TMA+. The values of 5-17 kcal/mol rank these CH··π HBs among some of the strongest noncovalent interactions in the literature.

In terms of geometry, both ethylene and acetylene engage in trifurcated CH··π HBs, although one of these three HBs is somewhat longer in the case of acetylene. Trifurcation involving three separate methyl groups is again preferred to participation of a single methyl group. The interaction with benzene is dominated by a single CH··π HB, rather short at 2.275 Å. The binding energy exceeds 10 kcal/mol for the other aromatic systems. The hydroxyl of phenol serves as proton acceptor, rather than its role of donor for neutral TMA, supplementing the CH··π, and leading to a total binding energy of 11.4 kcal/mol. Note that the CH··c distance is shorter than R(CH··O) by 0.12 Å in the global minimum of Fig 2-5e. In the case of imidazole, the CH protons prefer to engage with the N lone pair rather than with imidazole's π system. Also, the electrostatic potential of imidazole is most negative in its molecular plane, serving as a powerful pull on the TMA+ cation. Consequently, the CH··π type structure in Fig 2-5 was optimized by forcing the TMA+ to remain above the Im plane; specifically, the N of TMA+ was held directly above the center of Im. Even so, the CH··π complex in Fig 2-5f is bound by 11.3 kcal/mol, with one CH··π interaction considerably stronger than the other two. There are a pair of CH··π HBs in the complex with indole, a single such bond to each of the two aromatic rings, and both shorter than 2.3 Å.

The stronger interactions involving TMA+ are reflected as well in the NBO charge transfer energies in Table 2-3. The values of E(2) for TMA+ are between 2 and 20 times larger than the same quantities for neutral TMA. A comparison of the effects of complexation on the C-H bond lengths for the neutral and cationic proton donors in Table 2-2 is intriguing and perhaps surprising. Despite the much greater strength of the interactions in the cationic dimers, these bonds undergo a generally smaller perturbation. As in their neutral counterparts, these bonds are usually but not always contracted. However, the degree of reduction is generally smaller for the cations. Taking ethylene as an example, r(CH) contracts by 1.0 mÅ when complexed with neutral TMA, but by less than 0.2 mÅ with TMA+. The 4 mÅ contraction of TMA with benzene is reduced to less than 1 mÅ for TMA+.

The added charge enhances the electrostatic component of the interaction energy by a factor of 3 to 6, as is evident from a comparison of the SAPT data for TMA and TMA+ in Tables 2-5 and 2-6, respectively. There is a similar magnification of the induction energy. Dispersion also undergoes an increase albeit by not quite as dramatic a factor. In general, these ionic CH··π complexes are bound by electrostatics and dispersion in roughly equal measure, with IND only slightly smaller.

The density redistribution patterns for these ionic complexes look very much like those for typical HBs, including density loss around the bridging proton, and gain in the region of the π-orbital donors. The purple gain region extends over the entire π system, whether just one C=C bond as in TMA+··C_2H_4 of Fig 2-3g, or the full ring as in the case of larger π systems such as benzene (Fig 2-3h).

2-3.4. NH_4^+ donor

NH_4^+ switches the proton donor atom from C to N, while retaining the potency of a cationic proton donor. The effect of this switch upon the binding energy is evident in the comparison of the two final columns of Table 2-1, where NH_4^+ indeed forms tighter complexes, by roughly a factor of 2, than does TMA+. Indeed, the strongest complex examined in this entire study combines NH_4^+ with indole, with a binding energy of 25 kcal/mol. A single NH··π bond occurs for ethylene and acetylene, as indicated in Fig 2-6, but the interaction is of the bifurcated sort for the larger acceptor molecules, although one of the two NH··c HBs is typically significantly shorter and presumably stronger than the other.

The complex of NH_4^+ with benzene offers a comparison of the different possible modes of binding. The bifurcated arrangement is the global minimum, bound by 18.7 kcal/mol. A single CH··π geometry is less stable, but by only 0.8 kcal/mol, and a trifurcated structure 0.6 kcal/mol higher still. It would appear then that there is nearly free rotation of the NH_4^+ cation above the benzene ring, a quasi-isotropic interaction potential. This behavior contrasts with that of the simpler ethylene π-system. In this case NH_4^+ prefers a single NH··π bond, with a bifurcated structure less stable by 2.7 kcal/mol, followed closely by the trifurcated geometry; a similar pattern is noted for acetylene. As in the case of TMA+, the lone pair of the N atom of imidazole acts as a very strong draw on the NH_4^+ cation. So much so that the NH··π complex displayed in Fig 2-6 is not a true minimum, as it would decay to a NH··N type complex, where the ammonium lies in the imidazole plane.

The structure in Fig 2-6f was obtained only by insisting that the ammonium N atom lie along the perpendicular of the imidazole plane, as was necessary for TMA+/imidazole.

The NH_4^+ cation behaves more like a classical HB donor than the various CH donors in a number of ways. Unlike the r(CH) contractions of the other systems, the NH bond elongates when participating in a HB. Table 2-2 shows that these stretches are of large magnitude, between 14 and 23 mÅ. The longest stretches are associated with the ethylene and acetylene complexes, likely due to the presence of only a single, but linear NH··π bond. Also increased over the CH analogues are the charge transfer stabilization energies E(2) which climb to as high as 23 kcal/mol. Note that the latter value is associated with the complex of NH_4^+ with ethylene, one of the weakest interactions with this cation, but again one which is characterized by a single, linear NH··π HB. The NBO values of E(2) are also disproportionately raised in the NH··π complexes, as compared to CH··π, as is evident in the last column of Table 2-3.

The SAPT dissection of these ionic NH··π complexes in Table 2-7 points to induction and electrostatics as the prime contributing factors, with dispersion playing a smaller, but certainly not insignificant role. A comparison with the data in Table 2-6 shows that the transition from ionic CH··π to NH··π raises both the ES and IND components, but has the reverse effect of a small diminution in the dispersion contribution.

The electron redistribution patterns in these HBs looks much like those for typical HBs with a green loss region surrounding the bridging proton, and purple gain in the area of π system of the electron donor. It is interesting to note a pattern of patterns, as it were. Specifically, as the HB gains strength, progressing from TMA as the weakest proton donor

to NH_4^+ as the strongest, the loss around the proton diminishes while the gain in the π system expands.

2-3.5. NMR Chemical Shifts

Whether red shifting, as are most conventional HBs, or blue-shifting which is true of many CH··O HBs, the NMR chemical shifts of the bridging protons [58-64] appear to make no distinction of that sort. Formation of a HB robs this proton of some of its surrounding electron cloud, and thus reduces its chemical shielding. The change in this chemical shielding is reported in Table 2-8 for the bridging proton in each complex. Focusing first on the simple systems in the first two rows, the loss of shielding is evident by the negative values of $\Delta\sigma$. The magnitude of this change is roughly proportional to the strength of the HB, smallest for TMA and largest for the NH··π HBs of NH_4^+. The situation is somewhat different for butadiene which exhibits no change for CF_3H and a very small positive change for TMA; the two cationic proton donors show the expected deshielding.

The values in the last four rows of Table 2-8 are all positive. This distinction is easily explained by the ring currents within these four aromatic systems, which produce a magnetic field that effectively shields any atom poised above their center. (Similar trends were observed earlier [64] in the case of OH··π interactions.) The value of $\Delta\sigma$ varies between 3.1 and 4.6 ppm for CF_3H, and is not simply related to the binding energy. The values for TMA are somewhat smaller, in the 2.6 – 3.3 ppm range, but again not directly proportional to ΔE; TMA+ shifts are comparable to those of CF_3H, even though the binding energies of the former are much greater. The shifts for the very strongly bound complexes of NH_4^+ with the aromatic systems are positive, but only barely so.

One interpretation of these trends rests on two opposing effects. On one hand, formation of the HB pulls density away from the bridging proton, tending to make σ smaller. But its presence above an aromatic system and its accompanying ring currents pushes σ in the opposite direction. The latter shielding effect wins out in most cases, so Δσ is positive. But the very strong deshielding of NH··π HBs for NH_4^+ more effectively counter the effects of aromatic ring currents, and a smaller positive value of Δσ ensues. Indeed, examination of density shift maps like those in Fig 2-3 reinforce the idea of greater loss of electron density around the bridging proton of NH_4^+ than of the other donors.

2-4. Summary and Discussion

The interactions with the various π-donors follow a pattern in that TMA is the weakest proton donor, followed in order by CF_3H, and then by the two ions TMA+ and NH_4^+. This pattern may be visualized via Fig 2-7 which displays the binding energies of the various complexes. The much stronger binding of the cations, and of NH_4^+ in particular, is plainly evident. It is also clear that there is a relatively small margin between F_3CH and TMA, less than 2 kcal/mol.

This order may be understood to some degree on the basis of electrostatic potentials, illustrated in Fig 2-8. The potentials range between +0.03 (blue) and -0.03 (red) for the two neutrals in a and b, where it is clearly evident that the potential around the CH in CF_3H is considerably more positive than the same areas in TMA. With respect to the two cations, the potential is positive in all directions, so the contours shown vary between +0.15 and +0.22 au. It is clear that the blue positive region is more intense around the protons of NH_4^+.

Comparison of the various contributors to the total interaction energies in Tables 4-7 also reveals some interesting trends. Consistent with the electrostatic potentials, the ES contribution rises steadily as: TMA < CF$_3$H < TMA+ < NH$_4^+$. Not surprisingly, the IND energy follows a similar trend. The dispersion energy, however, is different. First with respect to the two neutral proton donors, there is more dispersion energy in complexes of TMA than with CF$_3$H. Another reversal occurs in the two cations, where TMA+ DISP is larger than the same quantity for NH$_4^+$. In fact, the dispersion associated with the neutral TMA complexes is comparable to, and even larger than, the NH$_4^+$ dispersion energy. The disproportionately larger DISP in the TMA and TMA+ complexes may be due to the larger size of these two monomers, when compared to CF$_3$H and NH$_4^+$. Consequently, it is imperative that any computational study of complexes such as these include accurate assessment of dispersion energy, since it is comparable in magnitude, and sometimes even larger than ES or IND.

Despite its importance to the bonding, the NBO values of E(2) for π→σ*(CH) transfer are not a quantitative indicator of the total binding energy. For example, E(2) for the TMA+ complexes are only slightly larger than the same quantities for F$_3$CH, even though the binding of the former is considerably stronger (see Fig 2-7). Also, even though TMA binds to the π systems almost as strongly as does F$_3$CH, E(2) of the former is much smaller, almost an order of magnitude smaller in some cases, than for the latter. Neither does E(2) accurately reflect the induction component of the interaction energy. Again in a comparison between F$_3$CH and TMA, IND is only slightly smaller for the latter, but E(2) is much smaller.

One final point about E(2) concerns its evaluation via localized NBO orbitals. As such, the π-system of an aromatic molecule like benzene is represented by three separate C=C bonds, rather than the fully delocalized picture. The NBO charge transfer from benzene thus arises from these three C=C bonds, each of which overlaps with the σ*(CH) antibond. In the canonical delocalized picture, the only occupied π-orbital that is not orthogonal to σ*(CH) is the lowest-energy symmetric one, which could make the equivalent transfer of charge.

Complexation causes changes in the C-H and N-H bond lengths. The latter grows longer as is typical of most HBs. The CH bond, on the other hand, contracts. This shortening is of larger magnitude for the weaker CH··π bonds involving F_3CH and TMA, whereas the bond contraction is smaller for the TMA+ cation, less than 1 mÅ. Given the observation that charge is being transferred into the σ* antibonding CH orbital, the contraction of this bond might seem puzzling at first glance. But it must be remembered that these bond length changes are the product of more than one factor. In addition to this charge transfer/hyperpolarization, rehybridization of the CH bonding orbital must be considered as well. A decrease of the p vs s contribution would tend to shorten the bond in question, according to Bent's rule [65-69].

And indeed, the first column of Table 2-9 illustrates that such a diminution of p-contribution occurs for F_3CH. These changes are large enough to overshadow the modest bond-lengthening values of E(2) in Table 2-3, and the result is a bond contraction. These rehybridizations are displayed as the broken blue line in Fig 2-9. Opposing these contractions are bond-lengthening charge transfers into the σ*(CH) antibonding orbital,

illustrated in Fig 2-9 as the solid red curve. The combination of these two factors is chiefly

responsible for the observed changes in the CH bond length, indicated by the solid black

curve. It may be noted that the blue rehybridization curve more closely mimics the pattern

of Δr. The rehybridization of the NH bonding orbital in the NH_4^+ complexes are even larger

in magnitude, as evident in the last column of Table 2-9. But even these quantities are

overwhelmed by the very substantial values of E(2), between 13 and 22 kcal/mol, leading

to the NH bond lengthening. Between these two extremes lies $N(CH_3)_4^+$ where the two

forces are more nearly balanced and only small changes in bond length are observed.

Earlier work [33] had considered the manner in which adding a positive charge can

affect the magnitude of the binding of a methyl amine to a lone pair. Specifically, taking

TMA as a sample neutral amine, the most stable structure contained a trifurcated CH··O

HB to the carbonyl O atom of N-methylacetamide (NMA). The two molecules were bound

by 2.1 kcal/mol. This quantity exceeds the binding energy of the same TMA to the π-

systems of ethylene, acetylene, and butadiene. However, the CH··π bonds are stronger than

CH··O when they engage the aromatic π-systems benzene, phenol, imidazole and indole.

Adding a positive charge to the amine, i.e. changing TMA to TMA+, had magnified by

ninefold the CH··O HB to NMA, bringing the binding energy up to 18.8 kcal/mol. The

charge-induced magnification of the CH··π bonds is again strong, but not quite as dramatic,

raising the binding energy of the various complexes by a factor of 4-7. Consequently, even

the strongest complexes pictured in Fig 2-5 are not quite as strong as the one between

$N(CH_3)_4^+$ and the O lone pairs of NMA. Comparison of NBO values of E(2) suggest a

greater degree of charge transfer stabilization for O lone pairs as compared to π-systems.

Whether lone pair or π-system electron donor, dispersion plays the largest role in binding of the neutral pairs. The situation is different for the ionic pairs: Whereas electrostatic attraction dominates for lone pair donors, it shares nearly equally with induction and dispersion for π-system donors.

There are some data in the literature with which certain of our results can be compared. First with respect to charged systems, experimental measurements[70] of the binding enthalpy of NH_4^+ with benzene and ethylene are equal to 19.3 and 10.0 kcal/mol, respectively. These values compare very well with our corresponding calculated binding energies of 18.7 and 11.0 kcal/mol. ΔH for the TMA+/benzene interaction[71] is 9.4 kcal/mol, also in good agreement with our calculated ΔE of 9.8 kcal/mol.

There are some earlier calculated data on charged systems as well, primarily computed at the MP2 level with various basis sets. The best of these, 6-311+G** calculations[72-73] yielded binding energies of 8.7 and 16.9 kcal/mol for the complexes of benzene with TMA+ and NH_4^+, a bit weaker binding than our own results with the larger aug-cc-pVDZ, 9.8 and 18.7 kcal/mol, respectively. The TMA+/benzene dimer was bound by only 7.5 kcal/mol with 6-31+G**.[74] A smaller 6-31G** basis[75] found a TMA+/benzene binding energy of 9.1 kcal/mol. These lesser quantities are consistent with the importance of dispersion, which is typically saturated only with large basis sets such as the aug-cc-pVnZ series. This same study[75] computed the binding energy of TMA+ with imidazole to be 16.3 kcal/mol, nearly coincident with a 6-31+G** estimate[76] of 16.4 kcal/mol, both only slightly less than our own value of 16.8 kcal/mol. With respect to the NH+··π bond, a recent CCSD(T) computation[77] arrived at a NH_4^+/benzene binding energy within 2% of our own

MP2 result, and confirms the small energy difference between mono, bi, and tridentate structures.

Turning next to neutral dimers, a high-level calculation has been carried out for the neutral $CF_3H\cdots$benzene pair[78] which shows that going beyond MP2 to CCSD(T), and extending to the basis set limit adds only a small increment (0.5 kcal/mol) to the binding energy obtained here. The chlorosubstituted version of F_3CH binds to benzene by 5.5 kcal/mol in a very high level CCSD(T) calculation at the basis set limit.[79] This 1.4 kcal/mol increment of Cl_3CH over F_3CH is consistent with an earlier work.[78] Further, the calculated geometry matches nicely with a recent microwave structure,[80] which also supports our finding that the aromatic benzene molecule binds more strongly to this proton donor than do simple double or triple CC bonds. In the case of another, but related system, the $CH\cdot\pi$ HB in $NCH\cdot$benzene was computed[81] to have a binding energy of 4.6 kcal/mol with a cc-pVTZ basis, slightly larger than our value of 3.7 kcal/mol for F_3CH, consistent with the greater acidity of the former.

In summary, while normally weak, there are a number of means by which $CH\cdot\pi$ HBs can be strengthened. First with respect to the electron donor, there is a trend of increasing HB strength as the simple $C=C$ bond of ethylene or acetylene is conjugated, as in butadiene. The aromaticity of benzene enhances the binding, which is further enhanced by a –OH substituent as in phenol, with even greater effects arising in the heteroaromatic imidazole or indole. Adding electron-withdrawing agents to the proton donor molecule, as in CF_3H, amplifies its proton-donating power, to the point where $CH\cdot\pi$ HBs are comparable to standard $OH\cdot O$ HBs as in the water dimer for example. Even the weaker

proton donor of trimethylamine can form fairly strong HBs, particularly with the heteroaromatic imidazole and indole. But the most effective means of strengthening a CH··π HB is the addition of positive charge to the donor. The binding energy of tetramethylammonium cation to any π-system is very strong indeed, varying from 4.7 kcal/mol for the simple ethylene or acetylene, up to 9.8 kcal/mol for the prototypical aromatic benzene, and as high as 15.5 kcal/mol for indole. There is no single source of the strength of these HBs, which owe their binding to a combination of electrostatic, induction, and dispersion attraction.

References

(1)   Müller-Dethlefs, K.; Hobza, P. Noncovalent Interactions: A Challenge for Experiment and Theory. *Chem. Rev.* **2000,** *100*, 143-167.

(2)   Johnson, E. R.; Keinan, S.; Mori-Sanchez, P.; Contreras-Garcia, J.; Cohen, A. J.; Yang, W. Revealing Noncovalent Interactions. *J. Am. Chem. Soc.* **2010,** *132*, 6498-6506.

(3)   Scheiner, S. *Hydrogen Bonding. A Theoretical Perspective*. Oxford University Press: New York, 1997; p 375.

(4)   Gilli, G.; Gilli, P. *The Nature of the Hydrogen Bond*. Oxford University Press: Oxford, UK, 2009; p 313.

(5)   Arunan, E.; Desiraju, G. R.; Klein, R. A.; Sadlej, J.; Scheiner, S.; Alkorta, I.; Clary, D. C.; Crabtree, R. H.; Dannenberg, J. J.; Hobza, et al. Definition of the Hydrogen Bond. *Pure Appl. Chem.* **2011,** *83*, 1637-1641.

(6)   Biswal, H. S.; Gloaguen, E.; Loquais, Y.; Tardivel, B.; Mons, M. Strength of NH···S Hydrogen Bonds in Methionine Residues Revealed by Gas-Phase IR/UV Spectroscopy. *J. Phys. Chem. Lett.* **2012,** *3*, 755-759.

(7)   Solimannejad, M.; Scheiner, S. Unconventional H-Bonds: SH···N Interaction. *Int. J. Quantum Chem.* **2011,** *111*, 3196-3200.

(8)   Chalasinski, G.; Cybulski, S. M.; Szczesniak, M. M.; Scheiner, S. Nonadditive Effects in HF and HCl Trimers. *J. Chem. Phys.* **1989,** *91*, 7048-7056.

(9)   Latajka, Z.; Scheiner, S. Structure, Energetics and Vibrational Spectrum of H_2O-HCl. *J. Chem. Phys.* **1987,** *87*, 5928-5936.

(10)   Cybulski, S.; Scheiner, S. Hydrogen Bonding and Proton Transfers Involving Triply Bonded Atoms. Hcᵒn and Hcᵒch. *J. Am. Chem. Soc.* **1987,** *109*, 4199-4206.

(11)   Zierke, M.; Smieško, M.; Rabbani, S.; Aeschbacher, T.; Cutting, B.; Allain, F. H.-T.; Schubert, M.; Ernst, B. Stabilization of Branched Oligosaccharides: Lewis Benefits from a Nonconventional C–H···O Hydrogen Bond. *J. Am. Chem. Soc.* **2013,** *135*, 13464-13472.

(12)   Horowitz, S.; Dirk, L. M. A.; Yesselman, J. D.; Nimtz, J. S.; Adhikari, U.; Mehl, R. A.; Scheiner, S.; Houtz, R. L.; Al-Hashimi, H. M.; Trievel, R. C. Conservation and Functional Importance of Carbon-Oxygen Hydrogen Bonding in Adomet-Dependent Methyltransferases. *J. Am. Chem. Soc.* **2013,** *135*, 15536-15548.

(13)   Yang, H.; Wong, M. W. Oxyanion Hole Stabilization by C-H···O Interaction in a Transition State-a Three-Point Interaction Model for Cinchona Alkaloid-

Catalyzed Asymmetric Methanolysis of Meso-Cyclic Anhydrides. *J. Am. Chem. Soc.* **2013,** *135*, 5808-5818.

(14)   Scheiner, S. Contribution of CH··X Hydrogen Bonds to Biomolecular Structure. In *Hydrogen Bonding - New Insights*, Grabowski, S. J., Ed. Springer: 2006; pp 263-292.

(15)   Jones, C. R.; Baruah, P. K.; Thompson, A. L.; Scheiner, S.; Smith, M. D. Can a C-H···O Interaction Be a Determinant of Conformation. *J. Am. Chem. Soc.* **2012,** *134*, 12064-12071.

(16)   Scheiner, S. Weak H-Bonds. Comparisons of CH···O to NH···O in Proteins and PH···N to Direct P···N Interactions. *Phys. Chem. Chem. Phys.* **2011,** *13*, 13860-13872.

(17)   Scheiner, S. Relative Strengths of NH··O and CH··O Hydrogen Bonds between Polypeptide Chain Segments. *J. Phys. Chem. B* **2005,** *109*, 16132-16141.

(18)   Gu, Y.; Kar, T.; Scheiner, S. Comparison of the CH···N and CH···O Interactions Involving Substituted Alkanes. *J. Mol. Struct.* **2000,** *552*, 17-31.

(19)   Nishio, M.; Umezawa, Y.; Fantini, J.; Weiss, M. S.; Chakrabarti, P. CH–p Hydrogen Bonds in Biological Macromolecules. *Phys. Chem. Chem. Phys.* **2014,** *16*, 12648-12683.

(20)   Takahashi, O.; Kohno, Y.; Saito, K. Molecular Orbital Calculations of the Substituent Effect on Intermolecular CH/p Interaction in C_2H_3X--C_6H_6 Complexes (X=H, F, Cl, Br, and OH). *Chem. Phys. Lett.* **2013,** *378*, 509-515.

(21)   Bloom, J. W. G.; Raju, R. K.; Wheeler, S. E. Physical Nature of Substituent Effects in XH/p Interactions. *J. Chem. Theory Comput.* **2012,** *8*, 3167-3174.

(22) Kumar, S.; Mukherjee, A.; Das, A. Structure of Indole···Imidazole Heterodimer in a Supersonic Jet: A Gas Phase Study on the Interaction between the Aromatic Side Chains of Tryptophan and Histidine Residues in Proteins. *J. Phys. Chem. A* **2012,** *116*, 11573-11580.

(23) Ramirez-Gualito, K.; Alonso-Rios, R.; Quiroz-Garcia, B.; Rojas-Aguilar, A.; Diaz, D.; Jimenez-Barbero, J.; Cuevas, G. Enthalpic Nature of the CH/p Interaction Involved in the Recognition of Carbohydrates by Aromatic Compounds, Confirmed by a Novel Interplay of NMR, Calorimetry, and Theoretical Calculations. *J. Am. Chem. Soc.* **2009,** *131*, 18129–18138.

(24) Brandl, M.; Weiss, M. S.; Jabs, A.; Sühnel, J.; Hilgenfeld, R. C-H··p-Interactions in Proteins. *J. Mol. Biol.* **2001,** *307*, 357-377.

(25) Ringer, A. L.; Figgs, M. S.; Sinnokrot, M. O.; Sherrill, C. D. Aliphatic C-H/p Interactions: Methane-Benzene, Methane-Phenol, and Methane-Indole Complexes. *J. Phys. Chem. A* **2006,** *110*, 10822-10828.

(26) Karthikeyan, S.; Ramanathan, V.; Mishra, B. K. Influence of the Substituents on the CH··p Interaction: Benzene–Methane Complex. *J. Phys. Chem. A* **2013,** *117*, 6687-6694.

(27) Ma, J. C.; Dougherty, D. A. The Cation-p Interaction. *Chem. Rev.* **1997,** *97*, 1303-1324.

(28) Meot-Ner, M. Update 1 of Strong Ionic Hydrogen Bonds. *Chem. Rev.* **2012,** *112*, pr22-pr103.

(29) Scheiner, S.; Wang, L. Hydrogen Bonding and Proton Transfers of the Amide Group. *J. Am. Chem. Soc.* **1993,** *115*, 1958-1963.

(30) Cybulski, S. M.; Scheiner, S. Comparison of Morokuma and Perturbation Theory Approaches to Decomposition of Interaction Energy. $(NH_4)^+...NH_3$. *Chem. Phys. Lett.* **1990,** *166*, 57-64.

(31) Scheiner, S.; Redfern, P.; Szczesniak, M. M. Effects of External Ions on the Energetics of Proton Transfers across Hydrogen Bonds. *J. Phys. Chem.* **1985,** *89*, 262-266.

(32) Cannizzaro, C. E.; Houk, K. N. Magnitude and Chemical Consequences of R_3N^+-C-H··O=C Hydrogen Bonding. *J. Am. Chem. Soc.* **2002,** *124*, 7163-7169.

(33) Adhikari, U.; Scheiner, S. The Magnitude and Mechanism of Charge Enhancement of CH··O H-Bonds. *J. Phys. Chem. A* **2013,** *117*, 10551-10562.

(34) Forman, J. E.; Barrans, R. E.; Dougherty, D. A. Circular Dichroism Studies of Molecular Recognition with Cyclophane Hosts in Aqueous Media. *J. Am. Chem. Soc.* **1995,** *117*, 9213-9228.

(35) Gromiha, M. M. Influence of Cation–p Interactions in Different Folding Types of Membrane Proteins. *Biophys. Chem.* **2003,** *103*, 251-258.

(36) Torrice, M. M.; Bower, K. S.; Lester, H. A.; Dougherty, D. A. Probing the Role of the Cation–p Interaction in the Binding Sites of GPCRs Using Unnatural Amino Acids. *Proc. Nat. Acad. Sci., USA* **2009,** *106*, 11919-11924.

(37) Yamada, S.; Iwaoka, A.; Fujita, Y.; Tsuzuki, S. Tetraalkylammonium-Templated Stereoselective Norrish–Yang Cyclization. *Org. Lett.* **2013,** *15*, 5994-5997.

(38)   Dupont, J.; Suarez, P. A. Z.; Souza, R. F. D.; Burrow, R. A.; Kintzinger, J.-P. C-H-p Interactions in 1-n-Butyl-3-Methylimidazolium Tetraphenylborate Molten Salt: Solid and Solution Structures. *Chem. Eur. J.* **2000,** *6*, 2377-2381.

(39)   Gallivan, J. P.; Dougherty, D. A. Cation-p Interactions in Structural Biology. *Proc. Nat. Acad. Sci., USA* **1999,** *96*, 9459-9464.

(40)   Frisch, M. J.; Trucks, G. W.; Schlegel, H. B.; G. E. Scuseria; Robb, M. A.; Cheeseman, J. R.; Scalmani, G.; Barone, V.; B. Mennucci; Petersson, G. A., et al. J. *Gaussian 09*, Revision B.01; Gaussian, Inc: Wallingford CT, 2009.

(41)   Lu, N.; Ley, R. M.; Cotton, C. E.; Chung, W.-C.; Francisco, J. S.; Negishi, E.-I. Molecular Tuning of the Closed Shell C–H$\cdots$F–C Hydrogen Bond. *J. Phys. Chem. A* **2013,** *117*, 8256-8262.

(42)   Hauchecorne, D.; Herrebout, W. A. Experimental Characterization of C–X$\cdots$Y–C (X = Br, I; Y = F, Cl) Halogen–Halogen Bonds. *J. Phys. Chem. A* **2013,** *117*, 11548-11557.

(43)   Li, H.; Lu, Y.; Liu, Y.; Zhu, X.; Liu, H.; Zhu, W. Interplay between Halogen Bonds and p–p Stacking Interactions: CSD Search and Theoretical Study. *Phys. Chem. Chem. Phys.* **2012,** *14*, 9948-9955.

(44)   Azofra, L. M.; Scheiner, S. Substituent Effects in the Noncovalent Bonding of SO_2 to Molecules Containing a Carbonyl Group. The Dominating Role of the Chalcogen Bond. *J. Phys. Chem. A* **2014,** *118*, 3835-3845.

(45) Esrafili, M. D.; Fatehi, P.; Solimannejad, M. Mutual Interplay between Pnicogen Bond and Dihydrogen Bond in HMH···HCN···PH$_2$X Complexes (M = Be, Mg, Zn; X = H, F, Cl). *Comput. Theor. Chem.* **2014,** *1034*, 1-6.

(46) Adhikari, U.; Scheiner, S. Effects of Charge and Substituent on the S···N Chalcogen Bond. *J. Phys. Chem. A* **2014,** *118*, 3183-3192.

(47) Kerdawy, A. E.; Murray, J. S.; Politzer, P.; Bleiziffer, P.; Heßelmann, A.; Görling, A.; Clark, T. Directional Noncovalent Interactions: Repulsion and Dispersion. *J. Chem. Theory Comput.* **2013,** *9*, 2264-2275.

(48) Wu, W.; Zeng, Y.; Li, X.; Zhang, X.; Zheng, S.; Meng, L. Interplay between Halogen Bonds and Hydrogen Bonds in OH/SH···HOX···HY (X = Cl, Br; Y = F, Cl, Br) Complexes. *J. Mol. Model.* **2013,** *19*, 1069-1077.

(49) Pedzisa, L.; Hay, B. P. Aliphatic C-H···Anion Hydrogen Bonds: Weak Contacts or Strong Interactions? *J. Org. Chem.* **2009,** *74*, 2554-2560.

(50) Azofra, L. M.; Scheiner, S. Complexes Containing CO$_2$ and SO$_2$. Mixed Dimers, Trimers and Tetramers. *Phys. Chem. Chem. Phys.* **2014,** *16*, 5142-5149.

(51) Mohan, N.; Vijayalakshmi, K. P.; Koga, N.; Suresh, C. H. Comparison of Aromatic NH···p, OH···p, and CH···p Interactions of Alanine Using MP2, CCSD, and DFT Methods. *J. Comput. Chem.* **2010,** *31*, 2874–2882.

(52) Boys, S. F.; Bernardi, F. The Calculation of Small Molecular Interactions by the Differences of Separate Total Energies. Some Procedures with Reduced Errors. *Mol. Phys.* **1970,** *19*, 553-566.

(53)   Reed, A. E.; Weinhold, F.; Curtiss, L. A.; Pochatko, D. J. Natural Bond Orbital Analysis of Molecular Interactions: Theoretical Studies of Binary Complexes of HF, H_2O, NH_3, N_2, O_2, F_2, CO and CO_2 with HF, H_2O, and NH_3. *J. Chem. Phys.* **1986,** *84*, 5687-5705.

(54)   Reed, A. E.; Curtiss, L. A.; Weinhold, F. Intermolecular Interactions from a Natural Bond Orbital, Donor-Acceptor Viewpoint. *Chem. Rev.* **1988,** *88*, 899-926.

(55)   Szalewicz, K.; Jeziorski, B. Symmetry-Adapted Perturbation Theory of Intermolecular Interactions. In *Molecular Interactions. From Van der Waals to Strongly Bound Complexes*, Scheiner, S., Ed. Wiley: New York, 1997; pp 3-43.

(56)   Moszynski, R.; Wormer, P. E. S.; Jeziorski, B.; van der Avoird, A. Symmetry-Adapted Perturbation Theory of Nonadditive Three-Body Interactions in van der Waals Molecules. I. General Theory. *J. Chem. Phys.* **1995,** *103*, 8058-8074.

(57)   Werner, H.-J.; Knowles, P. J.; Manby, F. R.; Schütz, M.; P. Celani; Knizia, G.; Korona, T.; Lindh, R.; Mitrushenkov, A.; Rauhut, G.; Adler, T. B., et al. *Molpro*, Version 2006; 2010.

(58)   Hopkins, W. S.; Hasan, M.; Burt, M.; Marta, R. A.; Fillion, E.; McMahon, T. B. Persistent Intramolecular C–H···X (X = O or S) Hydrogen-Bonding in Benzyl Meldrum's Acid Derivatives. *J. Phys. Chem. A* **2014,** *118*, 3795-3803.

(59)   Gao, X.; Liu, Y.; Li, H.; Bian, J.; Zhao, Y.; Cao, Y.; Mao, Y.; Li, X.; Xu, Y.; Ozaki, Y.; Wu, J. A Cooperative Hydrogen Bonding System with a C-H···O Hydrogen Bond in Ofloxacin. *J. Mol. Struct.* **2013,** *1040*, 122-128.

(60)   Scheiner, S.; Gu, Y.; Kar, T. Evaluation of the H-Bonding Properties of CH···O Interactions Based Upon NMR Spectra. *J. Mol. Struct. (Theochem)* **2000,** *500*, 441-452.

(61)   Uldry, A.-C.; Griffin, J. M.; Yates, J. R.; Perez-Torralba, M.; Maria, M. D. S.; Webber, A. L.; Beaumont, M. L. L.; Samoson, A.; Claramunt, R. M.; Pickard, C. J., et al. Quantifying Weak Hydrogen Bonding in Uracil and 4-Cyano-4'-Ethynylbiphenyl: A Combined Computational and Experimental Investigation of NMR Chemical Shifts in the Solid State. *J. Am. Chem. Soc.* **2008,** *130*, 945-954.

(62)   Scheiner, S.; Kar, T.; Gu, Y. Strength of the CᵃH·O Hydrogen Bond of Amino Acid Residues. *J. Biol. Chem.* **2001,** *276*, 9832-9837.

(63)   Yates, J. R.; Pham, T. N.; Pickard, C. J.; Mauri, F.; Amado, A. M.; Gil, A. M.; Brown, S. P. An Investigation of Weak CH···O Hydrogen Bonds in Maltose Anomers by a Combination of Calculation and Experimental Solid-State NMR Spectroscopy. *J. Am. Chem. Soc.* **2005,** *127*, 10216-10220.

(64)   Scheiner, S.; Kar, T.; Pattanayak, J. Comparison of Various Types of Hydrogen Bonds Involving Aromatic Amino Acids. *J. Am. Chem. Soc.* **2002,** *124*, 13257-13264.

(65)   Bent, H. A. Electronegativities from Comparison of Bond Lengths in AH and AH$^+$. *J. Chem. Phys.* **1960,** *33*, 1258-1259.

(66)   Alabugin, I. V.; Manoharan, M.; Peabody, S.; Weinhold, F. Electronic Basis of Improper Hydrogen Bonding: A Subtle Balance of Hyperconjugation and Rehybridization. *J. Am. Chem. Soc.* **2003,** *125*, 5973-5987.

(67) Li, A. Y. Chemical Origin of Blue- and Redshifted Hydrogen Bonds: Intramolecular Hyperconjugation and Its Coupling with Intermolecular Hyperconjugation. *J. Chem. Phys.* **2007,** *126*, 154102.

(68) Pluháková, K.; Hobza, P. On the Nature of the Surprisingly Small (Red) Shift in the Halothane···Acetone Complex. *ChemPhysChem.* **2007,** *8*, 1352-1356.

(69) Grabowski, S. J. Red- and Blue-Shifted Hydrogen Bonds: The Bent Rule from Quantum Theory of Atoms in Molecules Perspective. *J. Phys. Chem. A* **2011,** *115*, 12789-12799.

(70) Deakyne, C. A.; Meot-Ner, M. Unconventional Ionic Hydrogen Bonds. 2. NH^+···p. Complexes of Onium Ions with Olefins and Benzene Derivatives. *J. Am. Chem. Soc.* **1985,** *107*, 474-479.

(71) Meot-Ner, M.; Deakyne, C. A. Unconventional Ionic Hydrogen Bonds. 1. CH^{d+}···X. Complexes of Quaternary Ions with n- and p-Donors. *J. Am. Chem. Soc.* **1985,** *107*, 469-474.

(72) Kim, K. S.; Lee, J. Y.; Lee, S. J.; Ha, T.-K.; Kim, D. H. On Binding Forces between Aromatic Ring and Quaternary Ammonium Compound. *J. Am. Chem. Soc.* **1994,** *116*, 7399-7400.

(73) Lee, J. Y.; Lee, S. J.; Cho, H. S.; Cho, S. J.; Kim, K. S.; Ha, T.-K. Ab Initio Study of the Complexation of Benzene with Ammonium Cations. *Chem. Phys. Lett.* **1995,** *232*, 67-71.

(74) Liu, T.; Gu, J.; Tan, X.-J.; Zhu, W.-L.; Luo, X.-M.; Jiang, H.-L.; Ji, R.-Y.; Chen, K.-X.; Silman, I.; Sussman, J. L. Theoretical Insight into the Interactions of TMA-

Benzene and TMA-Pyrrole with B3LYP Density-Functional Theory (DFT) and Ab Initio Second Order Møller-Plessest Perturbation Theory (MP2) Calculations. *J. Phys. Chem. A* **2001,** *105*, 5431-5437.

(75) Pullman, A.; Berthier, G.; Savinelli, R. Theoretical Study of Binding of Tetramethylammonium Ion with Aromatics. *J. Comput. Chem.* **1997,** *18*, 2012-2022.

(76) Liu, T.; Gu, J.; Tan, X.-J.; Zhu, W.-L.; Luo, X.-M.; Jiang, H.-L.; Ji, R.-Y.; Chen, K.-X.; Silman, I.; Sussman, J. L. The Relationship between Binding Models of TMA with Furan and Imidazole and the Molecular Electrostatic Potentials: DFT and MP2 Computational Studies. *J. Phys. Chem. A* **2002,** *106*, 157-164.

(77) Ansorg, K.; Tafipolsky, M.; Engels, B. Cation-p Interactions: Accurate Intermolecular Potential from Symmetry-Adapted Perturbation Theory. *J. Phys. Chem. B* **2013,** *117*, 10093-10102.

(78) Tsuzuki, S.; Honda, K.; Uchimaru, T.; Mikami, M.; Tanabe, K. The Interaction of Benzene with Chloro- and Fluoromethanes: Effects of Halogenation on CH/p Interaction. *J. Phys. Chem. A* **2002,** *106*, 4423-4428.

(79) Fujii, A.; Shibasaki, K.; Kazama, T.; Itaya, R.; Mikami, N.; Tsuzuki, S. Experimental and Theoretical Determination of the Accurate Interaction Energies in Benzene–Halomethane: The Unique Nature of the Activated CH/p Interaction of Haloalkanes. *Phys. Chem. Chem. Phys.* **2008,** *10*, 2836-2843.

(80) López, J. C.; Caminati, W.; Alonso, J. L. The CH···p Hydrogen Bond in the Benzene-Trifluoromethane Adduct: A Rotational Study. *Angew. Chem., Int. Ed. Engl.* **2006,** *45*, 290-293.

(81) Duarte, D. J. R.; de las Vallejos, M. M.; Peruchena, N. M. Topological Analysis of Aromatic Halogen/Hydrogen Bonds by Electron Charge Density and Electrostatic Potentials. *J. Mol. Model.* **2010,** *16*, 737-748.

Tables and Figures

Table 2-1. Binding energies (kcal/mol) of CH··π and NH··π complexes after counterpoise correction, and angular distortion of CH··π HBs for F_3CH as proton donor

proton acceptor	F_3CH	$\theta(CH··c^a)$, degs	$N(CH_3)_3$	$N(CH_3)_4^+$	NH_4^+
ethylene	1.60	172.7	0.83	4.69	11.05
acetylene	1.57	177.8	0.71	4.64	10.50
butadiene	2.53	-	1.66	7.12	14.58
benzene	3.72	179.0	2.17	9.75	18.68
phenol	3.88	147.8	2.69	11.42	19.15
imidazole	4.08	133.9	4.45	11.33[d]	15.68[d]
indole	4.34[b], 4.87[c]	144.5[b],149.4[c]	3.79	15.51	25.04

[a]c represents center of bond or ring
[b]CH poised above 5-membered ring
[c]CH poised above 6-membered ring
[d]optimized with N of proton donor restricted to the imidazole perpendicular.

Table 2-2. Change of r(XH) (mÅ) and ν(CH) (cm-1) caused by formation of CH/NH··π complexes

proton acceptor	F_3CH Δr	F_3CH Δν	$N(CH_3)_3$ Δr	$N(CH_3)_4^+$ Δr	NH_4^+ Δr
ethylene	-0.8	10.9	-0.98, -0.98	-0.18, 0.06, 0.06	23
acetylene	-1.0	16.0	-0.6, -0.58, 0.52	-0.42, 0.08, 0.08	19
butadiene	-1.8	21.4	-1.8	-0.23, -0.13, 0.37	17,1
benzene	-3.1	50.7	-3.96	-0.79, -0.08	14,0
phenol	-1.9	29.5	-1.8, -0.95	-0.85, -0.49, -0.85	14,0
imidazole	-0.5	9.7	-1.56, -1.3	-1.18, 0.17, 1.18	20, 0
indole	-0.7[a], -1.9[b]	10.8[a], 29.8[b]	-0.60, -0.56, -0.21	-1.15, -0.67	14, 5

[a]CH poised above 5-membered ring
[b]CH poised above 6-membered ring

Table 2-3. NBO values of E(2) (kcal/mol) of CH··π and NH··π complexes

proton acceptor	F_3CH	$N(CH_3)_3$	$N(CH_3)_4^+$	NH_4^+
ethylene	3.95	0.38[1]	3.72[2]	22.50
acetylene	3.45	0.49[3,4]	3.88[2]	20.13[3]
butadiene	2.28[3]	0.27	5.71[2,3]	18.66[1,3]
benzene	4.13[5]	1.29[3]	5.16[1,5]	12.68[1,5]
phenol	3.24[3]	2.16[1,3]	6.77[2,6]	12.37[1,5]
imidazole	3.37[3]	3.31[1,7]	7.50[8]	20.21[1,3]
indole	3.56[3,9], 3.71[5,10]	1.94[5,2]	6.43[1,11]	13.26[2,5]

[1] sum of charge transfer over two X-H σ* orbitals
[2] sum of charge transfer over three X-H σ* orbitals
[3] sum of two π orbitals
[4] charge is transferred from CC π to C-N σ* orbital
[5] sum of three π orbitals
[6] sum of three π orbitals and a lone pair
[7] sum of two π orbitals and a lone pair
[8] 5.32 kcal/mol from C-N bond orbitals, plus 2.32 from N lone pairs
[9] CH poised above 5-membered ring
[10] CH poised above 6-membered ring
[11] sum of four π orbitals

Table 2-4. SAPT components of interaction energy (kcal/mol) of CH··π complexes containing F_3CH

proton acceptor	ES	EX	IND	DISP	EX-IND + EX-DISP
ethylene	-3.21	3.54	-1.60	-1.90	1.41
acetylene	-3.03	3.13	-1.30	-1.70	1.08
butadiene	-4.35	5.74	-2.84	-4.11	2.72
benzene	-5.30	7.09	-3.02	-5.15	2.63
phenol	-5.85	8.25	-3.99	-5.94	3.77
imidazole	-5.87	6.89	-3.09	-5.20	2.79
indole	-6.44	9.07	-4.23	-6.91	3.91

Table 2-5. SAPT components of interaction energy (kcal/mol) of CH··π complexes containing TMA

proton acceptor	ES	EX	IND	DISP	EX-IND + EX-DISP
ethylene	-0.82	2.56	-0.58	-2.95	0.85
acetylene	-0.99	2.40	-0.71	-2.15	0.97
butadiene	-2.03	5.22	-1.29	-5.07	1.84
benzene	-3.07	7.78	-2.57	-7.17	3.48
phenol	-3.24	8.34	-2.31	-7.71	3.11
imidazole	-3.38	7.09	-2.33	-6.14	2.70
indole	-4.46	10.60	-3.45	-9.94	4.64

Table 2-6. SAPT components of interaction energy (kcal/mol) of CH··π complexes containing TMA$^+$

proton acceptor	ES	EX	IND	DISP	EX-IND + EX-DISP
ethylene	-5.09	6.49	-4.13	-4.37	2.80
acetylene	-5.41	6.28	-3.62	-4.03	2.36
butadiene	-7.10	9.89	-5.85	-7.01	3.76
benzene	-9.34	12.58	-7.00	-8.95	4.62
phenol	-11.15	13.64	-7.42	-9.83	4.77
imidazole	-11.55	11.76	-3.09	-8.25	4.12
indole	-14.23	17.84	-9.55	-13.04	6.28

Table 2-7. SAPT components of interaction energy (kcal/mol) of NH··π complexes containing NH$_4^+$

proton acceptor	ES	EX	IND	DISP	EX-IND + EX-DISP
ethylene	-11.89	12.79	-14.10	-3.65	7.56
acetylene	-11.70	11.18	-12.18	-3.33	6.10
butadiene	-14.25	15.02	-16.19	-5.30	7.50
benzene	-15.78	15.61	-16.60	-6.51	6.67
phenol	-16.13	16.27	-17.27	-6.76	7.03
imidazole	-13.60	14.64	-14.98	-5.95	6.04
indole	-20.96	19.23	-20.56	-7.98	8.45

Table 2-8. Change in isotropic NMR shielding, Δσ (ppm), of bridging hydrogens occurring upon formation of complex.

proton acceptor	CHF$_3$	N(CH$_3$)$_3$	N$^+$(CH$_3$)$_4$	NH$_4^+$
ethylene	-0.67	-0.27, -0.27	-0.54, -0.70, -0.55	-4.98
acetylene	-0.85	-0.08, -0.08, 0.05	-1.05, -1.00, -0.40	-4.97
butadiene	0.00	0.18	-0.34, -0.90, -0.66	-4.64, -1.58
benzene	4.44	2.70	-0.23, 3.37	0.62, 0.53
phenol	3.80	2.72, 0.35	3.29, -0.7, -0.39	0.03, 0.34
imidazole	3.07	2.63, -0.4	-0.25, -1.3, 3.22	-0.3, 0.53
indole	3.86[a], 4.64[b]	2.94, 3.29, 0.43	-0.21, 4.01, 3.48	1.18, 1.41

[a] poised over five membered ring
[b] poised over six membered ring

Table 2-9. Change in %p character of C spx hybrid as part of C-H or N-H bond of CH··π and NH··π complexes.

proton acceptor	F$_3$CH	NH$_4^+$
ethylene	-0.78	-4.31
acetylene	-0.75	-4.01
butadiene	-0.89	-3.05
benzene	-1.76	-3.27
phenol	-1.57	-2.99
imidazole	-1.32	-3.80
indole	-1.41[a], -1.74[b]	-2.42

[a]CH poised above 5-membered ring
[b]CH poised above 6-membered ring
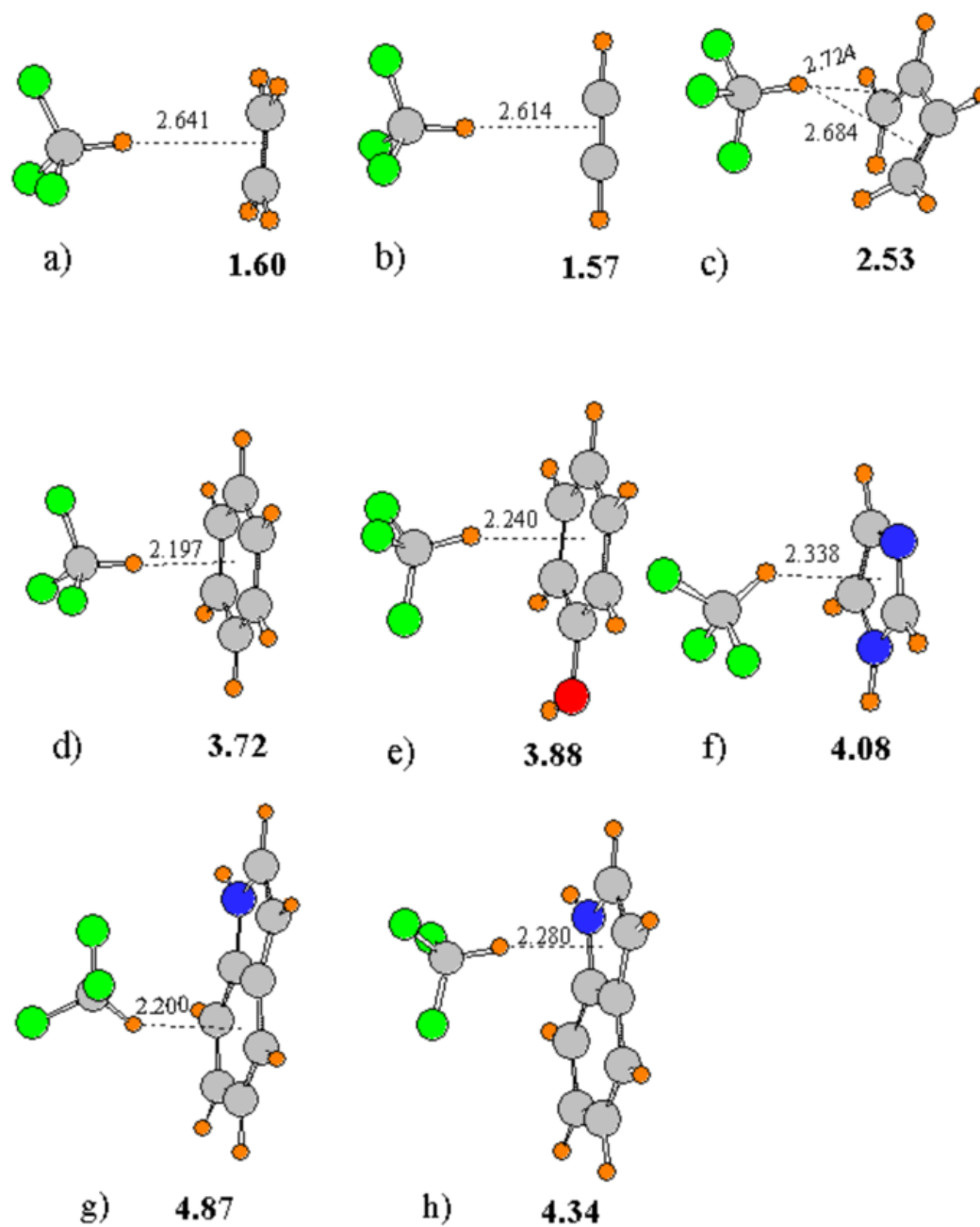
Figure 2-1. CH··π complexes of CHF$_3$ with various π donors. Distances in Å, and counterpoise-corrected binding energies (kcal/mol) displayed in bold.

a) C$_2$H$_4$

b) C$_2$H$_2$

c) C$_4$H$_6$

d) C$_6$H$_6$

e) phenol

f) imidazole

g) indole
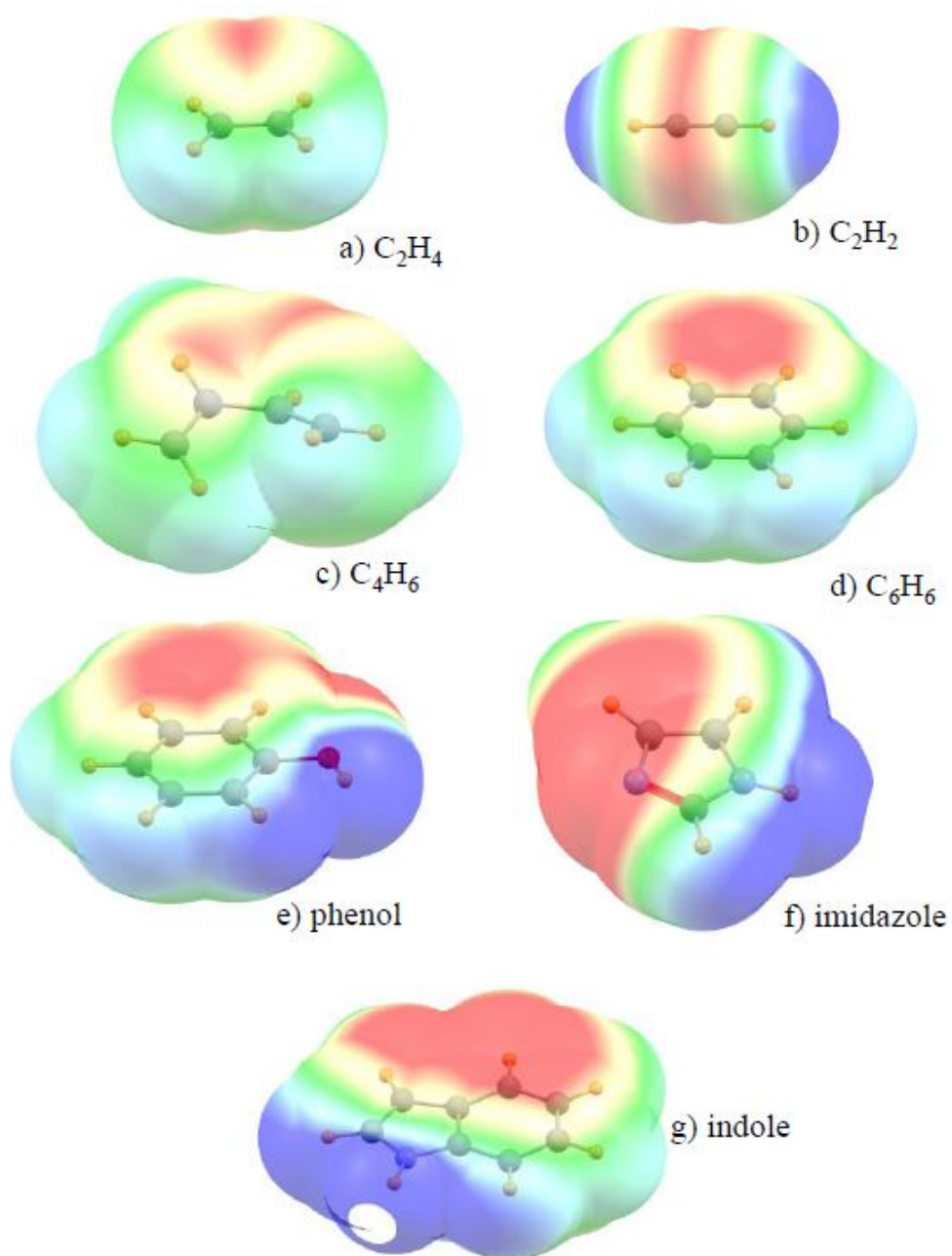
Figure 2-2. Electrostatic potentials on the surface corresponding to 2 x vdW radius. Red and blue colors indicate negative and positive regions, respectively. Maxima and minima correspond to ±0.02 au.
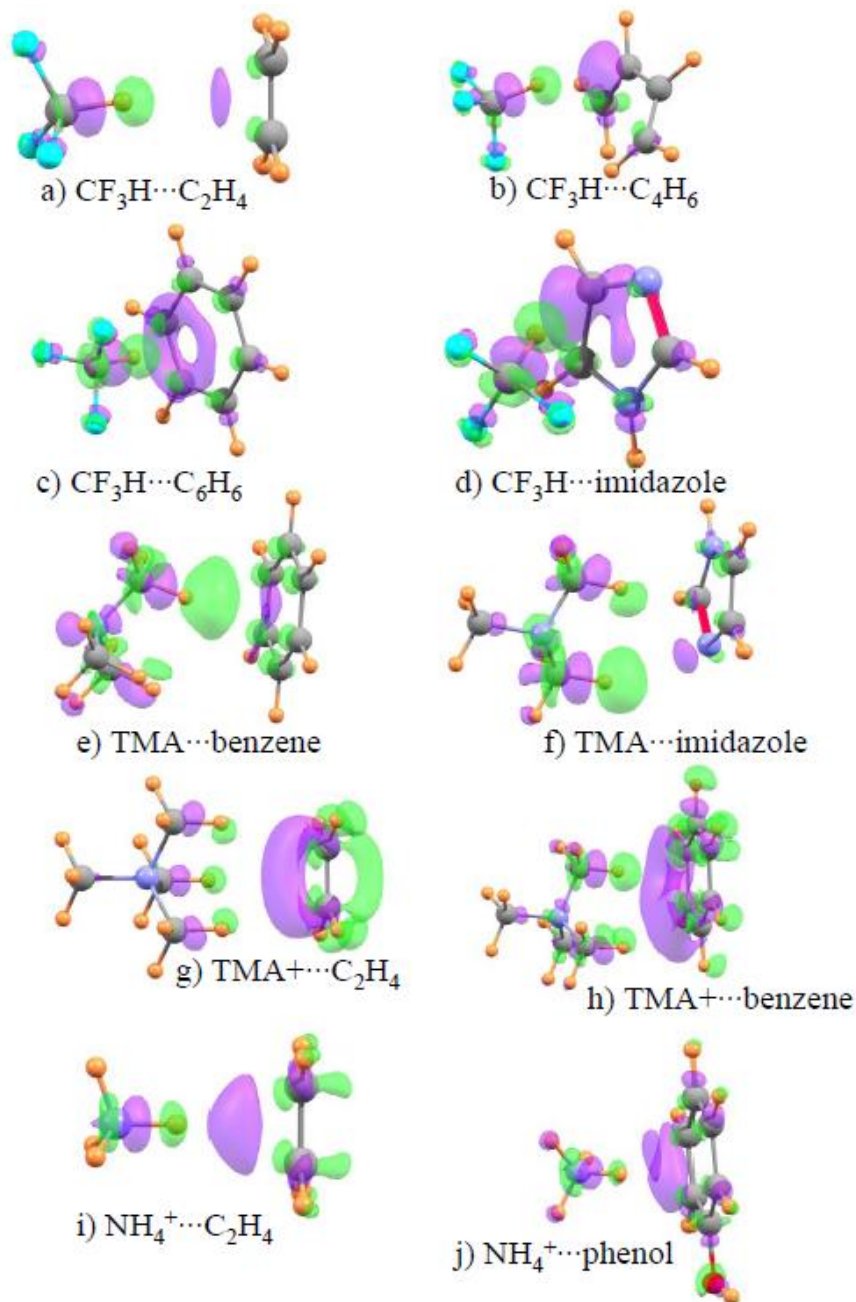
Figure 2-3. Electron density redistributions that accompany formation of the indicated complexes. Purple regions indicate density gain, and losses are green. Isocontours are ±0.0010 au for a-d, ±0.0004 for e, ±0.0006 for f, ±0.0010 for g and h, ±0.0030 for i and j
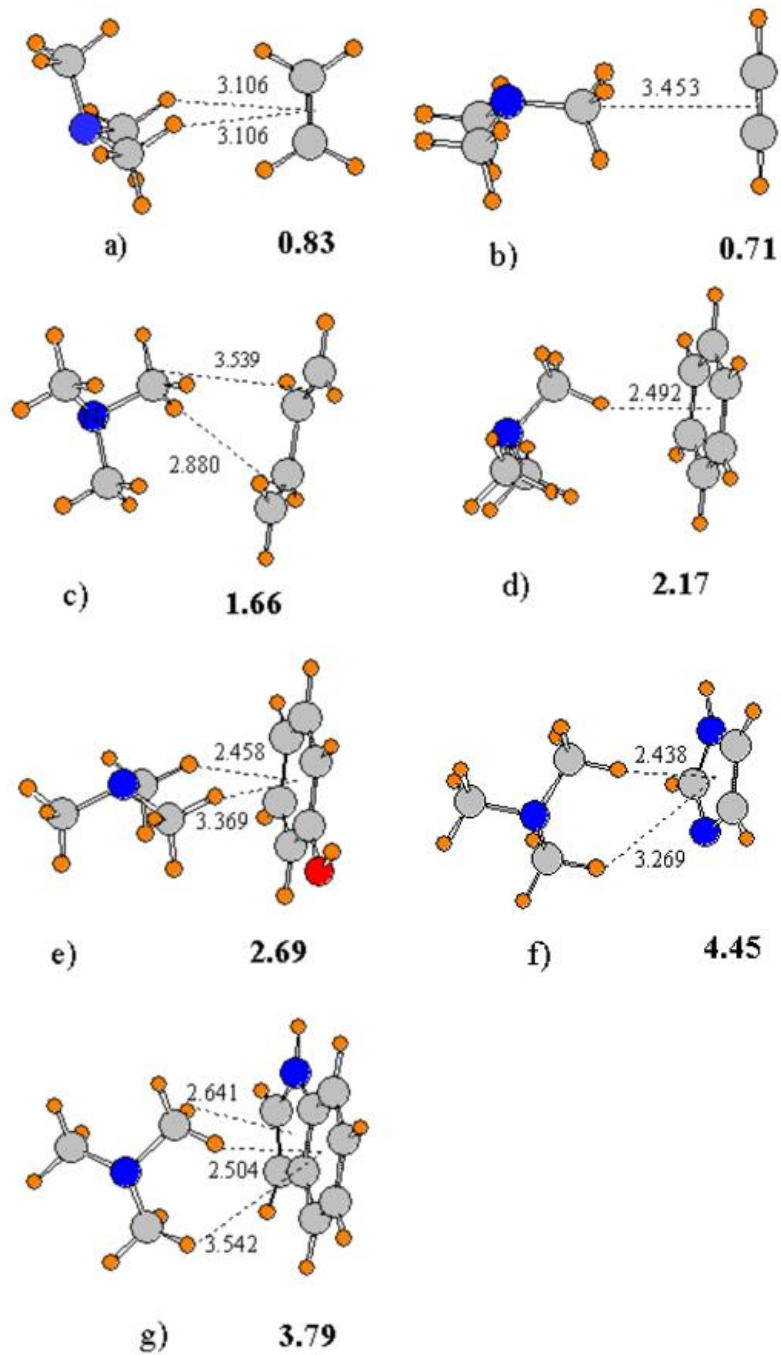
Figure 2-4. CH··π complexes of N(CH₃)₃ with various π donors. Distances in Å, and counterpoise-corrected binding energies (kcal/mol) displayed in bold.
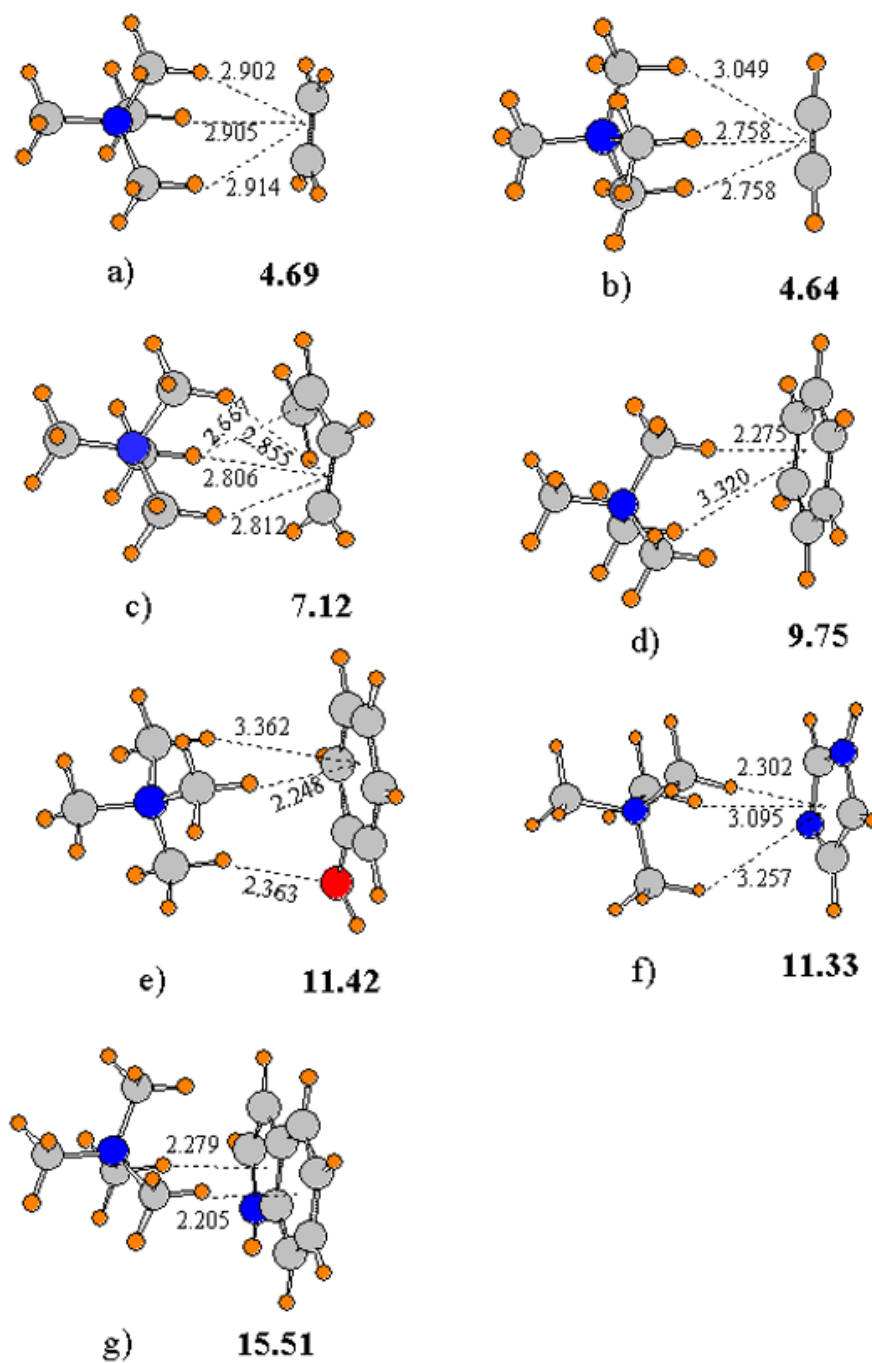
Figure 2-5. Complexes of N(CH$_3$)$_4^+$ with various π donors. Distances in Å, and counterpoise-corrected binding energies (kcal/mol) displayed in bold.
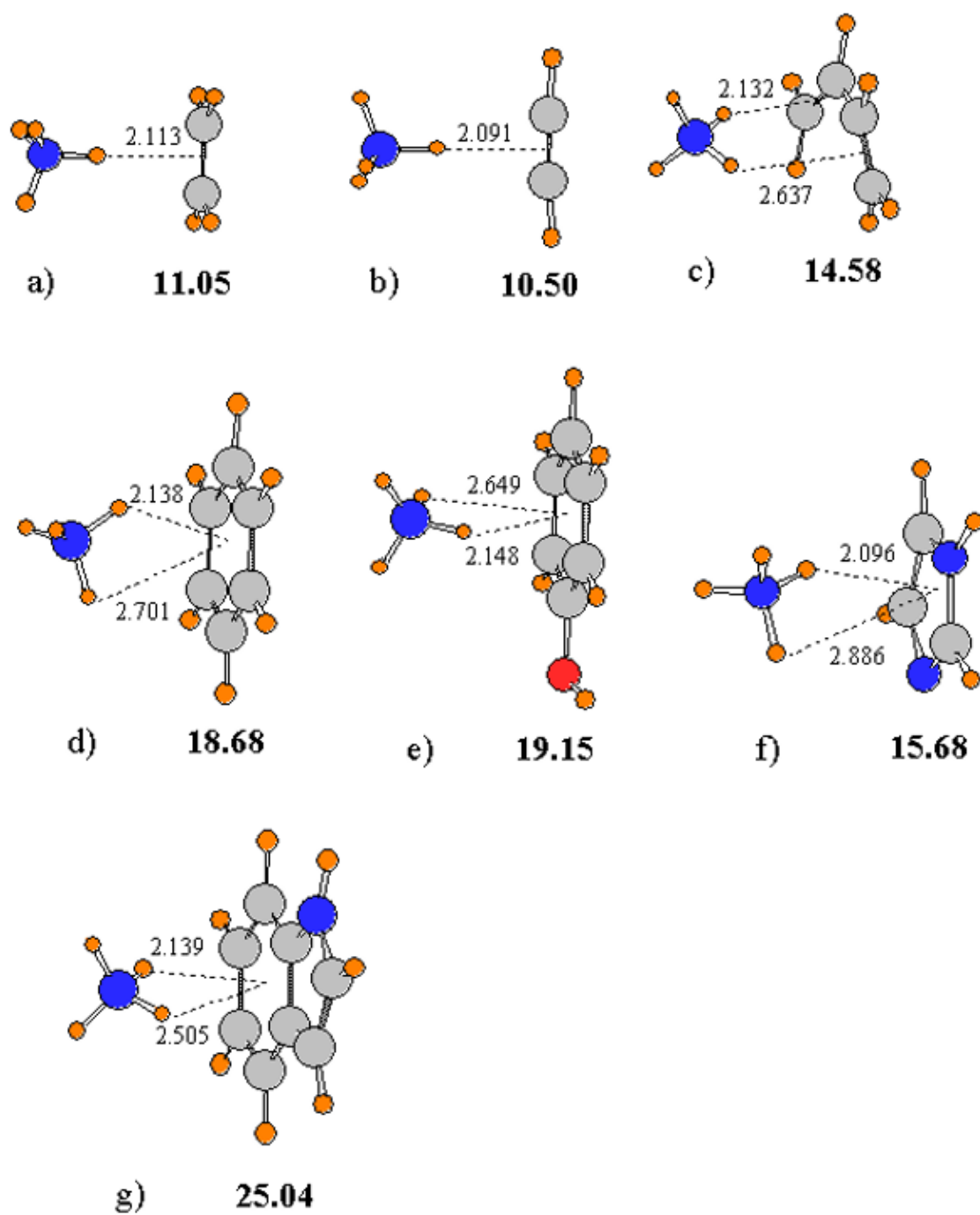
Figure 2-6. CH-π complexes of NH_4^+ with various π donors. Distances in Å, and counterpoise-corrected binding energies (kcal/mol) displayed in bold.
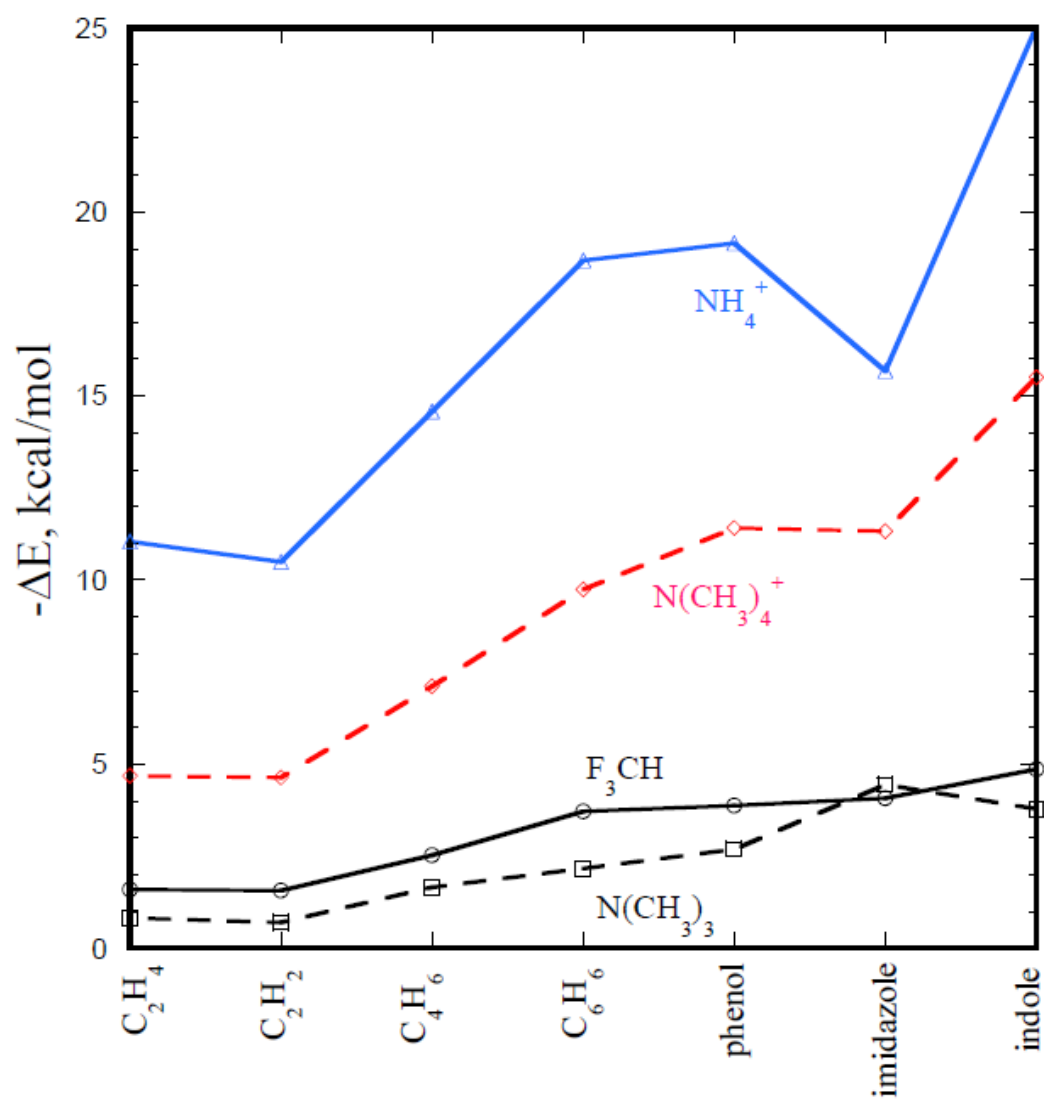
Figure 2-7. Binding energies for the various dimers.

a) CF₃H

b) TMA

c) TMA+

d) NH₄⁺
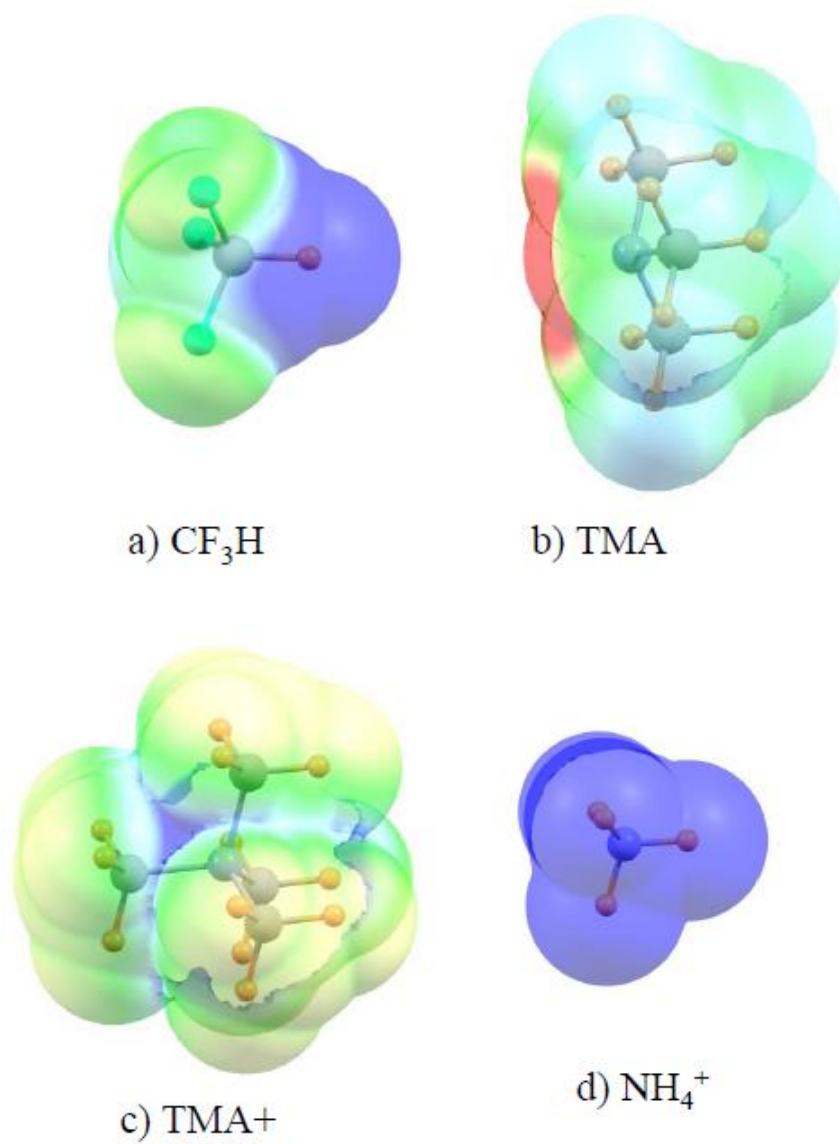
Figure 2-8. Electrostatic potentials lying on the surface corresponding to 1.5 x vdW radius. Colors correspond to +0.03 (blue) and -0.03 au (red) for neutral molecules in a and b, and +0.22 and +0.15 for cations c and d.
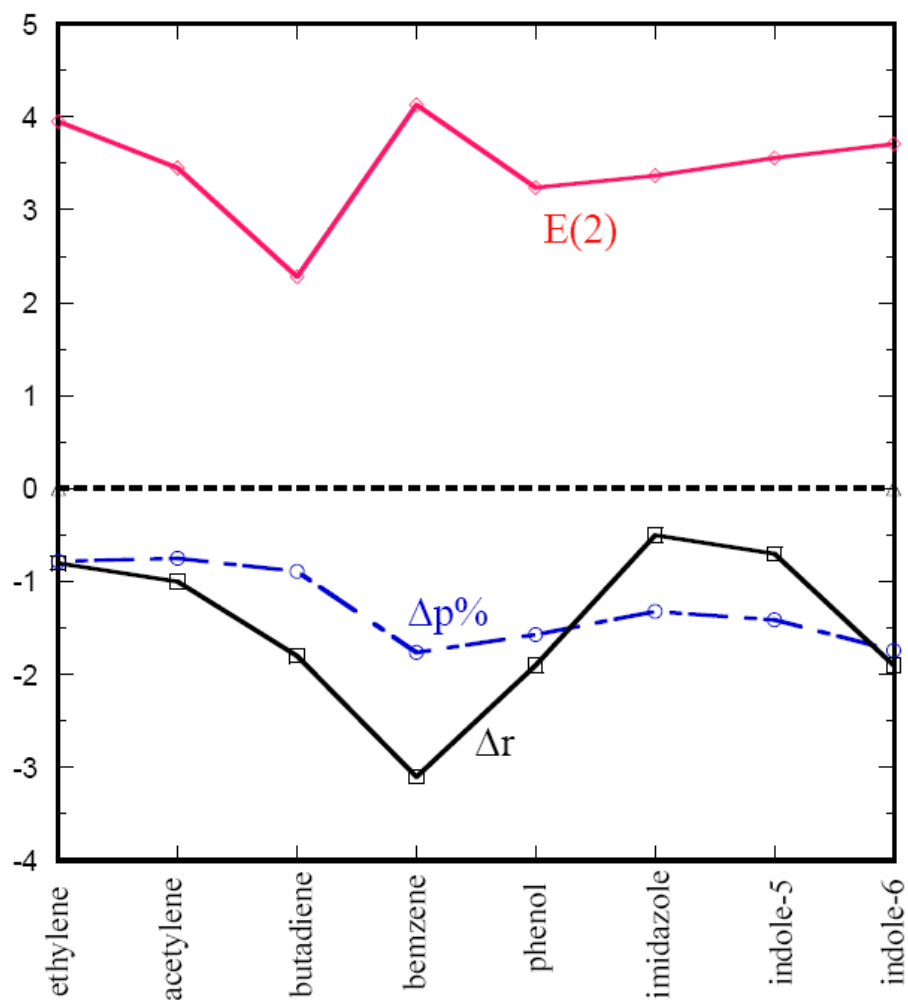
Figure 2-9. Values of properties upon formation of complex of F_3CH with each indicated proton acceptor. Δr represents the change in C-H bond length in mÅ, E(2) refers to charge transfer into σ^*(CH) antibond in kcal/mol, and $\Delta p\%$ represents the change in the p-orbital
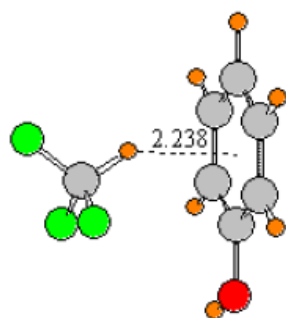
a)   **3.77**

E(2)=3.53

b)   **3.04**

E(2)=1.02 (F$_{LP}$ to OH σ*) and 1.77 (O$_{LP}$ to CH σ*)
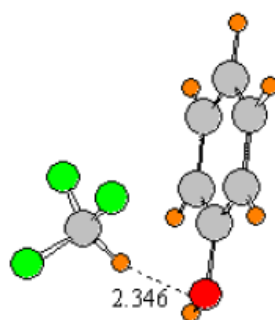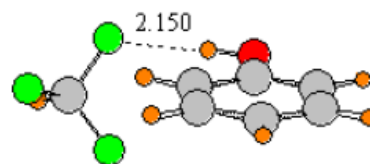
c)   **2.72**

E(2)=3.15

d)   **1.79**

E(2)=3.21
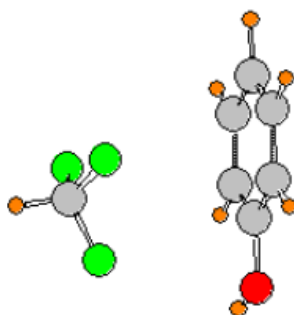
e)   **1.06**
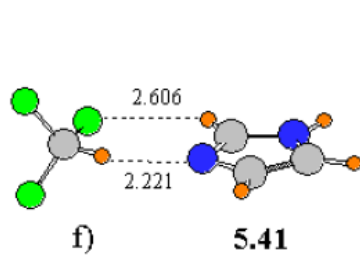
f) **5.41**

E(2)= 7.79 (N_{LP} to CH σ*) and 0.71 (F_{LP} to CH σ*)

g) **5.19**

E(2)= 8.39 (N_{LP} to CH σ*) and 0.39 (F_{LP} to CH σ*)

h) **1.99**

E(2)=3.80

i) **1.98**

E(2)=3.68

j) **0.81**

E(2)=0.68

E(2)=3.73(F$_{LP}$ to NH σ*) and 0.54 (F$_{LP}$ to CH σ*)
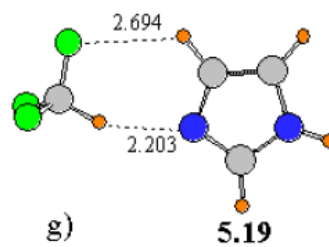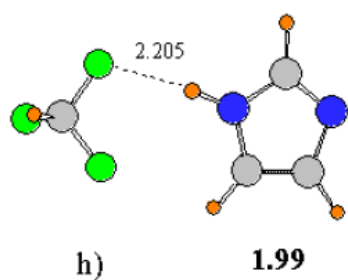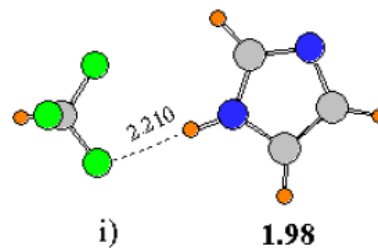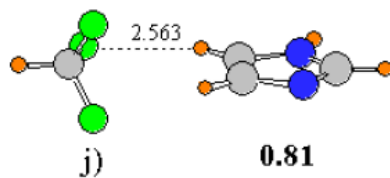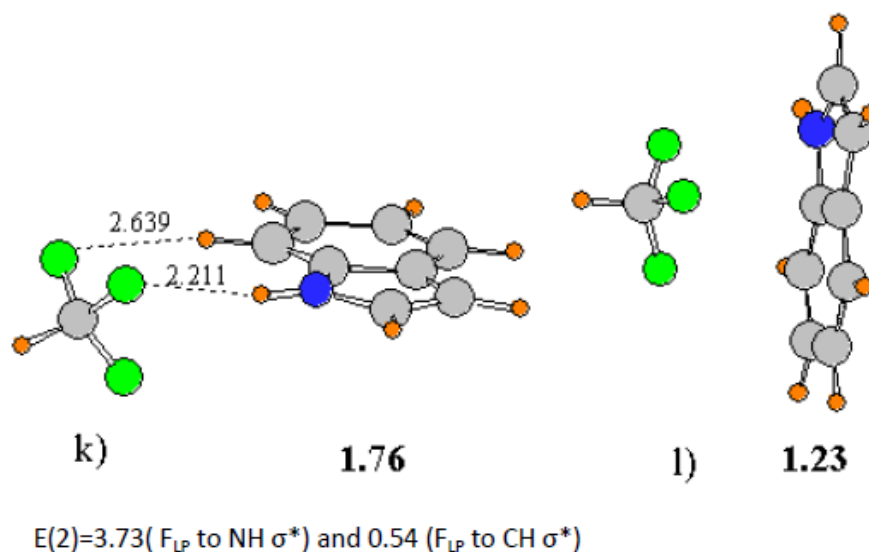
Figure 2-10. Additional minima found for CHF$_3$ complexes. The number in bold represent the BSSE -corrected binding energies and distances in Å. E(2) is the NBO charge transfer stabilization energy (kcal/mol) for the indicated interaction shown by the broken line. In the case of multiple interactions of the same type, E(2) represents the sum.

CHAPTER 3

ANIONIC CH··X⁻ HYDROGEN BONDS. ORIGIN OF THEIR STRENGTH,

GEOMETRY, AND OTHER PROPERTIES[1]

Abstract

CF_3H as proton donor was paired with a variety of anions, and properties assessed via MP2/aug-cc-pVDZ calculations. The binding energy of monoanions halide, NO_3^-, formate, acetate, HSO_4^-, and $H_2PO_4^-$ lie in the 12-17 kcal/mol range, although F^- is more strongly bound by 26 kcal/mol. Dianions SO_4^{2-} and HPO_4^{2-} are bound by 27 kcal/mol, and trianion PO_4^{3-} by 45 kcal/mol. When two O atoms are available on the anion, the CH··O⁻ HB is usually bifurcated, although asymmetrically. The CH bond is elongated and its stretching frequency red-shifted in these ionic HBs, but the shift is reduced in the bifurcated structures. Slightly more than half of the binding energy is attributed to Coulombic attraction, with smaller contributions from induction and dispersion. The amount of charge transfer from the anions to the $\sigma^*(CH)$ orbital correlates with many of the other indicators of bond strength, such as binding energy, CH bond stretch, CH red shift, downfield NMR chemical shift of the bridging proton, and density at bond critical points.

3-1. Introduction

Because of its importance and widespread occurrence, the phenomenon of H-bonding has motivated an enormous amount of investigative effort over the years, culminating in multiple volumes that attempt to summarize a vast amount of data.[1-9] Following its original inception as involving only very electronegative atoms, the concept of H-bonding has continued to broaden and become more general.[10] For example, the proton donor atom can be less electronegative than the usual O, N, or F atoms. In addition to S or Cl,[11] C has also been shown[12-21] to participate in H-bonds (HBs) as the proton donor. In an intriguing and initially surprising contradiction of what had appeared to be an ironclad rule, the C-H stretching frequency of a number of CH··O H-bonds shifts to the blue.[22]

One facet of HBs that is well documented is the strengthening that occurs when one of the two subunits is electrically charged. The neutral water dimer, for example, is bound by some 5 kcal/mol, but if one of the two water molecules is replaced by either OH^- or H_3O^+, the interaction energy climbs[23] by a factor of 5-8. There is growing evidence that such charge amplification applies not only to standard HBs of the OH··O variety, but to their nominally weaker CH··O counterparts. Within the regime of biomolecular structure and function, the CH of a protonated Lys has been observed to attract a Trp sidechain.[24] Upon acquiring some charge from a nearby metal cation, the imidazole sidechain of a His residue forms CH··O HBs with heightened frequency of occurrence, as judged by analysis of the protein data bank.[25] The large number of CH··O H-bonds around the Cu coordination site of amicyanin[26] suggest that charge imparted by metal-coordination

applies more generally to other CH donors as well. Quantum chemical calculations have provided quantitative assessments of the magnification of HB strength associated with $CH^+ \cdot \cdot O$ HBs. Estimates in the 8-15 kcal/mol range derive from a number of such calculations,[27-32] well above the interaction energies of neutral HBs, even conventional ones. More recently, this research group showed[33] that the introduction of positive charge on the proton donor substantially enhanced the binding energy of several $CH \cdot \cdot O$ HBs, by a factor of 4-9.

Just as the introduction of positive charge onto the proton donor magnifies the HB strength, it is logical to suppose the same would be true for a $CH \cdot \cdot X^-$ HB where a neutral donor interacts with an anion. This would appear to be the case in that HBs of this type have been found to be the controlling force in various phenomena in nature including crystal structure,[34-36] binding interactions in anion receptor systems,[37-41] and supramolecular chemistry.[42-45] Over the last few years a number of anion receptors have been synthesized which can capture the anion very efficiently and selectively using CH hydrogen bonds. Lee *et al* synthesized a star shaped macrocycle molecule which can extract certain anions (BF_4^-, ClO_4^- and PF_6^-) in a very efficient manner via CH anion interactions.[42] From a computational perspective, there are calculations in the literature that suggest that CH can indeed serve as a potent donor to an anion. Benzene binds to several anions with a binding energy of 8-9 kcal/mol.[46] Denis and Gancheff applied high-level calculations and observed[47] strong $CH \cdot \cdot$anion HBs between halides, paraffins, olefins, and alkynes.

While clearly suggestive of strong CH··X⁻ interactions, the literature remains rather sketchy in terms of specific questions. In the first place, how sensitive is the interaction to the precise nature of the anion? Are small anions like halide more or less effective in this regard than larger multiatomic species? As the charge on the anion increases it is logical to presume a progressively stronger interaction. But it is not obvious that the interaction would necessarily scale proportionately to the charge, e.g. twice as strong for a dianion as for a monoanion. In the case of an anion such as $HCOO^-$, there are two equivalent proton acceptor atoms. Would a bridging proton prefer to interact primarily with a single O, or would a bifurcated arrangement be superior? As noted above, CH··O HBs are known to shift both to the blue and to the red. Which of these would be characteristic of CH··X⁻ HBs, and what are the underlying reasons behind this particular shift?

The present work represents an attempt to answer these questions in a systematic manner. Quantum calculations are applied to systems that employ CF_3H as proton donor. This molecule was chosen first for being a fairly strong donor, due to the three electron-withdrawing F atoms. Secondly, with only one H atom, it will be straightforward to analyze the single CH··X⁻ HB without the complicating effects of multiple bonds within the same complex. The single CH bond also leads to only one CH stretching mode, uncoupled to others, so as to provide unambiguous data about any change in its frequency. A range of different anions was paired with CF_3H. The halides F^-, Cl^-, and Br^- present a comparison of different size single-atom anions. CN^- is a small diatomic, which can potentially interact through either its N or C atom. The NO_3^- anion contains three equivalent O atoms, so allows a comparison of a single CH··O HB with a bifurcated structure. The same is true for $HCOO^-$

, where comparison with CH_3COO^- speaks to the inductive effect of the methyl group. The effect of greater charge can be examined by a comparison of HSO_4^- with SO_4^{2-}; likewise for the $H_2PO_4^-$, HPO_4^{2-}, PO_4^{3-} triad.

3-2. Computational Details

Most of the calculations were carried out using the Gaussian-09 software package.[48] Dimers were constructed by pairing each anion with CF_3H, and the ensuing potential energy surface was searched for all minima, at the MP2/aug-cc-pVDZ level of theory. This combination has been found to be suitable and accurate for related systems. Normal mode analysis was performed to verify the identification of true minima. The binding energies E_b of the complexes were computed as the difference between the energy of the complex and the sum of the energies of the monomers in their optimized geometries. E_b was corrected for basis set superposition error (BSSE) using the counterpoise procedure.[49] Binding energies were decomposed into various components using Symmetry Adapted Perturbation Theory (SAPT)[50,51] which was implemented in the MOLPRO program suite.[52,53] Hartree-Fock (HF) level of theory was used with the same basis set for SAPT analysis (MP2 is not available). Charge transfer from one monomer to the other was carried out by the Natural Bond Orbital (NBO)[54] method. The bonding structure was also examined via Atoms in Molecules (AIM) theory[55] using the AIMAll program.[56]

3-3. Results

3-3.1. Binding Energies and Geometries

The geometries of the global minima are illustrated in Fig 3-1, along with the counterpoise-corrected binding energies. As may be noted by a quick scan of Table 3-1, among the halides as proton accepter, the binding energy is the highest for F^- at 26.1 kcal/mol, followed in order by Cl^- and Br^-. Only a single minimum was found in the potential energy surface for each halide. The CH··X arrangement in all three of these complexes is linear, which maximizes charge transfer from donor to accepter. The R(H··X) HB length is 1.51 Å for the F^- anion, the shortest of any HB in this study.

Two types of complexes are formed with CN^- anions, with either N or C acting as proton acceptor. These two structures have almost the same energy, with the $CF_3H··NC^-$ geometry the global minimum with binding energy 14.9 kcal/mol (Fig 3-1d), just 0.4 kcal/mol more stable than $CF_3H··CN^-$; the HB length is 0.17 Å shorter for the global minimum. As in the cases of the halides, the CH··X angles are 180° in both. NO_3^- engages in only one minimum, a bifurcated structure in Fig 3-1e, albeit not a symmetrical one with the two R(H··O) HB lengths differing by 0.15 Å. The interaction energies of the CN^- and NO_3^- anions are both between 14 and 15 kcal/mol.

The $HCOO^-$ anion forms a slightly stronger HB with CF_3H, just above 16 kcal/mol. The global minimum in Fig 3-1f is bifurcated, while only one O atom acts as proton acceptor in the second structure, less stable by about 1 kcal/mol. Adding a methyl group raises the binding energy by 0.4 kcal/mol, and the complex of CH_3COO^- with CF_3H in Fig

3-1g is little changed from the formate ion structure. The slightly stronger interaction for acetate is consistent with the idea of the methyl group as electron-donating.

The presence of four O atoms on the HSO_4^- anion reduces the binding energy to 12.3 kcal/mol. The global minimum in Fig 3-1h contains a symmetrical bifurcated HB. There are three other minima with very nearly equal energies. These minima all contain bifurcated HBs, and differ in only minor respects.

One would anticipate that dianions would form stronger interactions than monoanions, and that is indeed found to be the case. The binding energy of SO_4^{-2} with CF_3H is 26.7 kcal/mol, more than double that of HSO_4^-. The minimum in Fig 3-1i contains a nonsymmetric bifurcated arrangement, with one $R(H \cdot \cdot O)$ HB as short as 1.83 Å, and only 19° from full linearity.

The phosphate series comprises charges varying from -1 to -3, and the binding energies are 13.8, 27.6, and 44.6 kcal/mol, respectively. Four different minima were found in the potential energy surface of the complex containing $H_2PO_4^-$ but their energies are very similar, varying within only 1.2 kcal/mol. The global minimum structure (Fig3-1j) is characterized by a bifurcated structure but one $CH \cdot \cdot O$ HB is much shorter and more linear than the second. The second and third minima are stabilized by a single $CH \cdot \cdot O$ HB. The fourth minimum also has a single $CH \cdot \cdot O$ HB which is supplemented by what appears to be a weak $OH \cdot \cdot F$ HB. The global minimum for the dianion HPO_4^{-2} in Fig 3-1k looks very much like that for the monoanion, albeit with shorter HBs. Also like $H_2PO_4^-$, HPO_4^{2-} is also involved in several other minima with similar energies. The very strong proton-attracting power of the PO_4^{-3} trianion is powerful enough to pull the proton entirely off of CF_3H,

forming the HPO_4^{2-} /CF_2H^- pair, which then repel one another. In order to examine the CF_3H/PO_4^{-3} pair, it was therefore necessary to prevent this proton transfer by freezing r(C-H) in CHF_3 to 1.16 Å (the projected C-H bond length in the $H_2PO_4^{-1}$ and HPO_4^{-2} series). This restricted optimization led to a single minimum in Fig 3-1l, with binding energy 44.6 kcal/mol. This structure contains a nearly linear single CH··O HB with R(H··O)=1.46 Å.

3-3.2. Perturbations of Internal Properties

While it is typical of conventional AH··D HBs that the A-H bond elongates upon formation of the bond, and the ν(AH) stretching frequency shifts to the red, it has been observed that many CH··O HBs behave in an opposite fashion. CF_3H, for example, engages in blue-shifting HBs with a number of neutral proton acceptors. There is some question, however, as to the behavior of the CH bond when the very strong HBs are formed with anions.

The second column of Table 3-1 shows that the CH bond stretches in its complexes with the various anions. These stretches can be as large as 64 mÅ. In concert with these stretches is a red shift of the ν(CH) stretching frequency, which can exceed 1000 cm^{-1}. The sole exception to this behavior is the HSO_4^- monoanion, where a very small contraction of less than 2 mÅ is combined with a blue shift of 40 cm^{-1}. These trends are not restricted to the global minima, but are representative of secondary minima as well.

The stretch of the CH bond is commonly attributed to a transfer of charge from the proton acceptor into the σ* antibonding CH orbital. The energetic consequences of these transfers are measured by the NBO second order perturbation energy E(2) that is listed in

the indicated column of Table 3-1. And indeed there is a fairly strong linear correlation between $\Delta r(CH)$ and E(2), with a correlation coefficient R^2 of 0.95. In most cases, the source of the transferred charge is a lone pair of the proton-acceptor atom. However, there are other orbitals that can make minor contributions as well, as for example the $\pi(CH)$ bond orbital of CN^-, or a $\pi(PO)$ orbital of HPO_4^{2-}.

In addition to this charge transfer, or hyperconjugation effect, another issue which has some bearing on the CH bond length is the hybridization of the CH bonding orbital. Pursuant to Bent's rule, an increase in the s contribution to this orbital will cause a contraction of the CH bond. The change in the percentage s contribution to this orbital is listed in the penultimate column of Table 3-1, where it may be seen to vary between 4 and 11%. In most cases, this enhancement of s character is unable to reverse the elongating effects of charge transfer. For example, even though the percentage s contribution rises by 6.8% in the $CF_3H\cdot\cdot F^-$ complex, the 65.8 kcal/mol charge transfer yields a large bond elongation of 55 mÅ and red shift of 760 cm^{-1}. It is only in the $CF_3H\cdot\cdot HSO_4^-$ case where the 3.5% increase in s character is able to overcome the small 10.3 kcal/mol E(2), and produce a slightly shorter CH bond and small blue shift. This small charge transfer is in turn likely due to the two very nonlinear CH$\cdot\cdot$O HBs, both distorted from linearity by 36°.

In overview, the smallest values of E(2), less than 20 kcal/mol, occur for NO_3^-, $HCOO^-$, CH_3COO^-, HSO_4^-, and $H_2PO_4^-$, all of which are anions with a bifurcated structure and thus no single nearly linear HB. And it is these anions which produce the smallest red shift in CF_3H. When the data for the global minima are combined with those related to

secondary minima, the general rule emerges that blue shifts are only observed when there is no HB that is within about 15-20° of linearity.

Another aspect of the footprint of a HB is the downfield NMR chemical shift of the bridging proton. The last column of Table 3-1 reports the change in isotropic shielding of the CF_3H proton upon formation of each complex. These shifts are indeed downfield, and their magnitude is roughly proportional to the strength of the HB. $\Delta\sigma$ is linearly related to E_b, with correlation coefficient $R^2 = 0.92$. There is also a certain degree of correlation between the shift of the CH stretching frequency and $\Delta\sigma$, with a correlation coefficient $R^2 = 0.95$. This correlation is perhaps surprising, since these two quantities reflect very different properties. The change of the IR stretching frequency is the product of a delicate balance between various factors such as exchange repulsion and electrostatic attraction, or hyperconjugation vs rehybridization.[57-69] The proton's NMR shift depends instead on overall electron density or placement of the proton relative to an aromatic ring.[32,58,70-72] It is therefore not entirely surprising to observe a small blue shift of $\nu(CH)$ for $CF_3H\cdot\cdot HSO_4^-$ coupled with a downfield shift of the proton's NMR signal.

3-3.3. AIM Analysis of Bonding

Examination of the electron density and its Laplacian enables the AIM procedure to identify noncovalent bonds, as well as provide an alternate measure of their strength. The values of ρ and $\nabla^2\rho$ for each HB at the bond and ring critical points are displayed in Table 3-4. For most of the complexes, there is only one BCP found between the bridging hydrogen and the anion. AIM supports the idea of a bifurcated HB only for NO_3^- and HSO_4^-. And in these two cases, there is also a ring critical point present, another indicator of a

bifurcated HB. The AIM conclusion of a single HB in the complexes of $HCOO^-$, CH_3COO^- and SO_4^{2-} is at odds with the NBO analysis which indicates a bifurcated HB, even if one is weaker than the other. The electron density at the intermolecular BCPs are in the range of 0.015 to 0.087 au and $\nabla^2\rho > 0$ both of which are consistent with the HB phenomenon.

3-3.4. Energy Decomposition

The total binding energy of each complex was dissected by SAPT and the results are summarized in Table 3-2. The electrostatic attractive term ES is the largest, and varies from a minimum of -16 kcal/mol for HSO_4^-, up to as much as 76 kcal/mol for PO_4^{3-}. The various quantities are displayed as their percent contributions to the total attractive energy in Fig 3-2. It is immediately clear that ES makes the largest contribution, followed by induction IND and then dispersion DISP. The Coulombic attractive term is consistently above 50%, induction between 20 and 40%, and dispersion accounts for 10-15%. It may be noted that the induction is particularly large for the trianion, almost as large as ES. In fact, upon increasing the charge on the anion, for example, going from HSO_4^{-1} to SO_4^{-2} or from $H_2PO_4^{-1}$ to HPO_4^{-2} and PO_4^{-3}, the electrostatic component decreases by 4-5% and induction rises by about the same percentage. Fig 3-3 shows that the total binding energies of the complexes are closely correlated with the electrostatic component with correlation coefficient 0.97. Induction is not quite as closely correlated with R^2 only 0.92.

Another measure of the electrostatic interaction, albeit a more approximate one, is associated with the molecular potential that surrounds each monomer. In particular, the potential on a surface that corresponds to a constant electron density of 0.001 au contains minima, i.e. most negative points. It is these minima which are envisioned to interact with

the positive potential around the proton of CF_3H. The values of these minima are listed in Table 3-3 and bear a strong resemblance to the full binding energy. A plot of E_b vs the min ESP of each anion is nearly linear with correlation coefficient 0.94.

3-3.5. Electron Density Shifts

The shifts in electron density that accompany the formation of a HB are rather characteristic. These shifts are illustrated in Fig 3-4 for the binary complexes of CF_3H with the various anions. Indeed, these maps are fully consistent with what is expected for neutral complexes. There is a (red) charge loss in the region surrounding the bridging proton, matched by a (blue) gain in the area to the immediate left of the proton-accepting atom, whether a single or bifurcated HB. These charge shifts are one visible manifestation of the inductive effect. It is therefore not surprising that the magnitude of IND in Table 3-2 corresponds to the amount of charge shift in Fig 3-4. The latter can be assessed by the size of the region encompassed by a given contour. For example, the red and blue regions in Fig 3-4a for $CF_3H \cdot \cdot F^-$ are larger than the corresponding areas for the other monoanions.

3-4. Summary and Discussion

The binding energies of these $CH \cdot \cdot A^{-n}$ interactions are sensitive to the magnitude of the charge on the anion n, but are less sensitive to the nature of the anion. The various monoanions are bound to CF_3H by some 12-17 kcal/mol, with the exception of the much stronger HB with F- which amounts to 26 kcal/mol. Within this group of monoanions, the binding is inversely related to the number of O atoms on which the charge can be dispersed. That is, formate and acetate with two O atoms, are most strongly bound, and the larger

HSO_4^- and $H_2PO_4^-$ with four O atoms engage in a weaker HB; with three O atoms, NO_3^- forms a HB of intermediate strength. The dianions are bound much more strongly with E_b ~ 27 kcal/mol, and the PO_4^{3-} trianion stronger still, at 45 kcal/mol.

When there are two O anionic atoms available, the CH··O⁻ HB is usually bifurcated, although one CH··O distance is typically shorter, and presumably stronger, than the other. This asymmetry is particularly pronounced in the phosphate series ($H_2PO_4^-$, HPO_4^{-2} and PO_4^{-3}), where the bonding pattern may perhaps better be described as non-bifurcated.

The CH bond is elongated and its stretching frequency red-shifted in these ionic HBs. These quantities are as large as 64 mÅ, and 1000 cm^{-1}, respectively, and are closely related to the binding energy. The degree of this shift is reduced in the bifurcated HBs where neither CH··O configuration is close to linear. This diminution is caused by the reduction in overlap between the electron donor lone pair and the acceptor σ*(CH) antibonding orbital, which in turn decreases the amount of charge transferred into the latter orbital. The formation of the HB also reduces the chemical shielding around the bridging proton, by an amount between 2 and 12 ppm, and this downshift of the NMR signal is also correlated with the strength of the HB.

Decomposition of the interaction energy indicates that these HBs are composed largely of a Coulombic force, with some 52-65% of the binding energy attributed to the electrostatic component. Another 20-38% is due to induction and a smaller residual to dispersion. The increase of charge (mono to di to trianion) enhances all components, especially induction.

NBO analysis quantifies the amount of charge transfer from the anions to the σ*(CH) orbital and E(2) correlates very nicely with many of the other indicators of bond strength. Analysis of the bonding pattern via AIM yields many of the same conclusions, but there are exceptions. AIM indicates a single intermolecular noncovalent bond in the SO_4^{2-}, $HCOO^-$ and CH_3COO^- complexes, whereas there are two HBs within the NBO scheme. The electron density, and its Laplacian at the bond critical point also correlate well with the other properties that measure HB strength.

There are some calculated data in the literature with which comparisons may be drawn. Despite their smaller 6-31+G(d,p) basis set, Kryachko and Zeegers-Huyskens obtained[73] interaction energies of CF_3H with F^- and Cl^- of 27.7 and 16.6 kcal/mol, respectively, close to our own values of 26.2 and 15.2 kcal/mol. Their larger values are likely due to the failure to optimize the geometries of the isolated monomers, which would inflate the binding energy. The red shifts of the CH stretch also dovetailed nicely with our own values in Table 3-1. An earlier work[74] had observed that blue shifts occur in the CH bonds of H_3CX, H_2CO and H_2CF_2 when they are involved in bifurcated arrangements with the Cl^- and Br^- anions. Another work[75] verified the concept observed here that linear CH··X HBs are associated with red shifts, while blue shifts are typical of bifurcated arrangements, using a variety of H_2CZ_n molecules as proton donors. Although the data was more ambiguous due to the complexity of the HB network, this idea finds additional support in complexes of 1,4-pentadiene with superoxide anion radical[76], and for a series of XCH_3 donor groups[77] in which the electron-withdrawing ability of X is varied over a wide range of values. The stretching of the CH bond of CF_3H, along with its red shift, when

involved in a non-bifurcated HB with an oxygen anion has been noted also[78] in a series of substituted phenoxides. With regard to NMR chemical shifts, our values in Table 3-1 for the complexes of CF_3H with F^- and Cl^- anions match nicely with those previously computed,[79] albeit with a smaller basis set.

It might be intriguing to ask which of the two varieties of ion-neutral CH HBs are stronger, cation-neutral $CH^+ \cdots X$ or anion-neutral $CH \cdots X^-$. The present set of calculations has placed the range of binding energies of the latter type, all with CF_3H as neutral donor, in the 12-26 kcal/mol range. An earlier work[33] had employed N-methylacetamide as the common neutral proton acceptor, and observed binding energies to fall within the same range, viz. 19-21 kcal/mol. With regard to NMR chemical shifts, the bridging proton is shifted downfield by 2-9 ppm in the monoanion-neutral pairs, which is larger than the cation-neutral shifts[33] that were 2 ppm or less.

References

 [1]   M. D. Joesten, L. J. Schaad. Hydrogen Bonding; Marcel Dekker: New York, 1974.

[2]   P. Schuster, G. Zundel, C. Sandorfy, Eds. The Hydrogen Bond. Recent Developments in Theory and Experiments; North-Holland Publishing Co.: Amsterdam, 1976.

[3]   P. Schuster. Hydrogen Bonds; Springer-Verlag: Berlin, 1984.

[4]   G. A. Jeffrey, W. Saenger. Hydrogen Bonding in Biological Structures; Springer-Verlag: Berlin, 1991.

[5]   D. Hadzi, Ed. Theoretical Treatments of Hydrogen Bonding; John Wiley & Sons: Chichester, 1997.

[6]   S. Scheiner. Hydrogen Bonding. A Theoretical Perspective; Oxford University Press: New York, 1997.

[7]   G. A. Jeffrey. An Introduction to Hydrogen Bonding; Oxford University Press: New York, 1997.

[8]   S. J. Grabowski, Ed. Hydrogen Bonding - New Insights; Springer: Dordrecht, 2006.

[9]   G. Gilli, P. Gilli. The Nature of the Hydrogen Bond; Oxford University Press: Oxford, UK, 2009.

[10] E. Arunan, G. R. Desiraju, R. A. Klein, J. Sadlej, S. Scheiner, I. Alkorta, D. C. Clary, R. H. Crabtree, J. J. Dannenberg, P. Hobza, H. G. Kjaergaard, A. C. Legon, B. Mennucci, D. J. Nesbitt, *Pure Appl. Chem.* **2011**, *83*, 1637-1641.

[11] H. S. Biswal, S. Wategaonkar, *J. Phys. Chem. A* **2009**, *113*, 12774-12782.

[12] B. K. Mueller, S. Subramanian, A. Senes, *Proc. Nat. Acad. Sci., USA* **2014**, *111*, E888-E895.

[13] M. Zierke, M. Smieško, S. Rabbani, T. Aeschbacher, B. Cutting, F. H.-T. Allain, M. Schubert, B. Ernst, *J. Am. Chem. Soc.* **2013**, *135*, 13464-13472.

[14] S. Horowitz, L. M. A. Dirk, J. D. Yesselman, J. S. Nimtz, U. Adhikari, R. A. Mehl, S. Scheiner, R. L. Houtz, H. M. Al-Hashimi, R. C. Trievel, *J. Am. Chem. Soc.* **2013**, *135*, 15536-15548.

[15] P. Venugopalan, R. Kishore, *Chem. Eur. J.* **2013**, *19*, 9908-9915.

[16] H. Yang, M. W. Wong, *J. Am. Chem. Soc.* **2013**, *135*, 5808-5818.

[17] S. Scheiner. In Hydrogen Bonding - New Insights; Grabowski, S. J., Ed.; Springer, 2006, p 263-292.

[18] P. R. Shirhatti, D. K. Maity, S. Bhattacharyya, S. Wategaonkar, *ChemPhysChem.* **2014**, *15*, 109-117.

[19] C. R. Jones, P. K. Baruah, A. L. Thompson, S. Scheiner, M. D. Smith, *J. Am. Chem. Soc.* **2012**, *134*, 12064-12071.

[20] K. M. Lippert, K. Hof, D. Gerbig, D. Ley, H. Hausmann, S. Guenther, P. R. Schreiner, *Eur. J. Org. Chem.* **2012**, *2012*, 5919-5927.

[21] S. Scheiner, *Phys. Chem. Chem. Phys.* **2011**, *13*, 13860-13872.

[22] B. Michielsen, J. J. J. Dom, B. J. van der Veken, S. Hesse, Z. Xue, M. A. Suhm, W. A. Herrebout, *Phys. Chem. Chem. Phys.* **2010**, *12*, 14034-14044.

[23] S. Gronert, *J. Am. Chem. Soc.* **1993**, *115*, 10258-10266.

[24] C. D. Tatko, M. L. Waters, *J. Am. Chem. Soc.* **2004**, *126*, 2028 - 2034.

[25] A. Schmiedekamp, V. Nanda, *J. Inorg. Biochem.* **2009**, *103*, 1054-1060.

[26] N. Sukumar, F. S. Mathews, P. Langan, V. L. Davidson, *Proc. Nat. Acad. Sci., USA* **2010**, *107*, 6817-6822.

[27] N. Sreerama, S. Vishveshwara, *J. Mol. Struct. (Theochem)* **1985**, *133*, 139-146.

[28] K. S. Kim, J. Y. Lee, S. J. Lee, T.-K. Ha, D. H. Kim, *J. Am. Chem. Soc.* **1994**, *116*, 7399-7400.

[29] C. E. Cannizzaro, K. N. Houk, *J. Am. Chem. Soc.* **2002**, *124*, 7163-7169.

[30] E. S. Kryachko, M. T. Nguyen, *J. Phys. Chem. A* **2001**, *105*, 153-155.

[31] F. M. Raymo, M. D. Bartberger, K. N. Houk, J. F. Stoddart, *J. Am. Chem. Soc.* **2001**, *123*, 9264-9267.

[32] S. Scheiner, T. Kar, J. Pattanayak, *J. Am. Chem. Soc.* **2002**, *124*, 13257-13264.

[33] U. Adhikari, S. Scheiner, *J. Phys. Chem. A* **2013**, *117*, 10551-10562.

[34] I. E. D. Vega, P. A. Gale, M. E. Light, S. J. Loeb, *Chem. Commun.* **2005**, *39*, 4913-4915.

[35] A. Mitra, R. J. Clark, C. T. Hubley, S. Saha, *Supra. Chem.* **2014**, *26*, 296-301.

[36] A. Mitra, C. T. Hubley, D. K. Panda, R. J. Clark, S. Saha, *Chem. Commun.* **2013**, *49*, 6629-6631.

[37] C. A. Ilioudis, D. A. Tocher, J. W. Steed, *J. Am. Chem. Soc.* **2004**, *126*, 12395-12402.

[38] P. A. Gale, *Acc. Chem. Res.* **2006**, *39*, 465-475.

[39] O. B. Berryman, V. S. Bryantsev, D. P. Stay, D. W. Johnson, B. P. Hay, *J. Am. Chem. Soc.* **2006**, *129*, 48-58.

[40] J. Cai, B. P. Hay, N. J. Young, X. Yang, J. L. Sessler, *Chem. Sci.* **2013**, *4*, 1560-1567.

[41] P. A. Gale, N. Busschaert, C. J. E. Haynes, L. E. Karagiannidis, I. L. Kirby, *Chem. Soc. Rev.* **2014**, *43*, 205-241.

[42] S. Lee, C.-H. Chen, A. H. Flood, *Nat Chem* **2013**, *5*, 704-710.

[43] E. A. Katayev, G. V. Kolesnikov, J. L. Sessler, *Chem. Soc. Rev.* **2009**, *38*, 1572-1586.

[44] K. P. McDonald, Y. Hua, S. Lee, A. H. Flood, *Chem. Commun.* **2012**, *48*, 5065-5075.

[45] Y. Hua, A. H. Flood, *Chem. Soc. Rev.* **2010**, *39*, 1262-1271.

[46] V. S. Bryantsev, B. P. Hay, *J. Am. Chem. Soc.* **2005**, *127*, 8282-8283.

[47] P. A. Denis, J. S. Gancheff, *Struct. Chem.* **2014**, *25*, 903-908.

[48] M. J. Frisch, G. W. Trucks, H. B. Schlegel, G. E. Scuseria, M. A. Robb, J. R. Cheeseman, G. Scalmani, V. Barone, B. Mennucci, G. A. Petersson, H. Nakatsuji, M. Caricato, X. Li, H. P. Hratchian, A. F. Izmaylov, J. Bloino, G. Zheng, J. L. Sonnenberg, M. Hada, M. Ehara, K. Toyota, R. Fukuda, J. Hasegawa, M. Ishida, T. Nakajima, Y. Honda, O. Kitao, H. Nakai, T. Vreven, J. A. Montgomery Jr., J. E. Peralta, F. Ogliaro, M. J. Bearpark, J. Heyd, E. N. Brothers, K. N. Kudin, V. N. Staroverov, R. Kobayashi, J. Normand, K. Raghavachari, A. P. Rendell, J. C. Burant,

S. S. Iyengar, J. Tomasi, M. Cossi, N. Rega, N. J. Millam, M. Klene, J. E. Knox, J. B. Cross, V. Bakken, C. Adamo, J. Jaramillo, R. Gomperts, R. E. Stratmann, O. Yazyev, A. J. Austin, R. Cammi, C. Pomelli, J. W. Ochterski, R. L. Martin, K. Morokuma, V. G. Zakrzewski, G. A. Voth, P. Salvador, J. J. Dannenberg, S. Dapprich, A. D. Daniels, Ö. Farkas, J. B. Foresman, J. V. Ortiz, J. Cioslowski, D. J. Fox. Gaussian, Inc.: Wallingford, CT, USA, 2009.

[49] S. F. Boys, F. Bernardi, *Mol. Phys.* **1970**, *19*, 553-566.

[50] R. Moszynski, P. E. S. Wormer, T. G. A. Heijmen, A. van der Avoird, *J. Chem. Phys.* **1998**, *108*, 579-589.

[51] S. Scheiner. Molecular interactions : from van der Waals to strongly bound complexes; Wiley: Chichester [u.a.], 1997.

[52] H.-J. Werner, P. J. Knowles, F. R. Manby, M. Schütz, P. Celani;, G. K. Knizia, T.;, R. Lindh, A. Mitrushenkov, G. Rauhut, T. B. Adler, R. D. Amos, A. Bernhardsson, A. Berning, D. L. Cooper, M. J. O. Deegan, A. J. Dobbyn, F. Eckert, E. Goll, C. Hampel, A. Hesselmann, G. Hetzer;, T. Hrenar, G. Jansen, C. Köppl, Y. Liu, A. W. Lloyd, R. A. Mata, A. J. May, S. J. McNicholas, W. Meyer, M. E. Mura, A. Nicklaß, P. Palmieri, K. Pflüger, R. Pitzer, M. Reiher, T. Shiozaki, H. Stoll, A. J. Stone, R. Tarroni, T. Thorsteinsson, M. Wang, A. Wolf, *Molpro, Version 2006; 2010.*

[53] H.-J. Werner, P. J. Knowles, G. Knizia, F. R. Manby, M. Schütz, *Wiley Interdisciplinary Reviews: Computational Molecular Science* **2012**, *2*, 242-253.

[54] E. D. Glendening, C. R. Landis, F. Weinhold, *J. Comput. Chem.* **2013**, *34*, 1429-1437.

[55] R. F. W. Bader. Atoms in molecules : a quantum theory; Clarendon Press: Oxford; New York, 1990.

[56] T. A. Keith, *TK Gristmill Software, Overland Park KS, USA, 2013.*

[57] Y. Gu, T. Kar, S. Scheiner, *J. Am. Chem. Soc.* **1999**, *121*, 9411-9422.

[58] Y. Gu, T. Kar, S. Scheiner, *J. Mol. Struct. (Theochem)* **2000**, *500*, 441-452.

[59] A. Masunov, J. J. Dannenberg, R. H. Contreras, *J. Phys. Chem. A* **2001**, *105*, 4737-4740.

[60] W. Qian, S. Krimm, *J. Phys. Chem. A* **2002**, *106*, 11663-11671.

[61] K. Hermansson, *J. Phys. Chem. A* **2002**, *106*, 4695-4702.

[62] X. Li, L. Liu, H. B. Schlegel, *J. Am. Chem. Soc.* **2002**, *124*, 9639-9647.

[63] I. V. Alabugin, M. Manoharan, S. Peabody, F. Weinhold, *J. Am. Chem. Soc.* **2003**, *125*, 5973-5987.

[64] J. Joseph, E. D. Jemmis, *J. Am. Chem. Soc.* **2007**, *129*, 4620-4632.

[65] B. Michielsen, W. A. Herrebout, B. J. van der Veken, *ChemPhysChem.* **2008**, *9*, 1693-1701.

[66] S. J. Grabowski, *J. Phys. Chem. A* **2011**, *115*, 12789-12799.

[67] A. Karpfen, *Phys. Chem. Chem. Phys.* **2011**, *13*, 14194-14201.

[68] A. K. Chandra, T. Zeegers-Huyskens, *Chem. Phys.* **2013**, *410*, 66-70.

[69] M. Jabłoński, *J. Comput. Chem.* **2014**, *35*, 1739-1747.

[70] S. Scheiner, T. Kar, Y. Gu, *J. Biol. Chem.* **2001**, *276*, 9832-9837.

[71] S. Scheiner, S. J. Grabowski, T. Kar, *J. Phys. Chem. A* **2001**, *105*, 10607-10612.

[72] B. Nepal, S. Scheiner, *J. Phys. Chem. A* **2014**, *118*, 9575-9587.

[73] E. S. Kryachko, T. Zeegers-Huyskens, *J. Phys. Chem. A* **2002**, *106*, 6832-6838.

[74] A. Y. Li, X. H. Yan, *Phys. Chem. Chem. Phys.* **2007**, *9*, 6263-6271.

[75] A. Y. Li, *J. Mol. Struct. (Theochem)* **2008**, *862*, 21-27.

[76] X. Zarate, M. C. Daza, J. L. Villaveces, *J. Mol. Struct. (Theochem)* **2009**, *893*, 77-83.

[77] L. Pedzisa, B. P. Hay, *J. Org. Chem.* **2009**, *74*, 2554-2560.

[78] J.-M. Fan, L. Liu, Q.-X. Guo, *Chem. Phys. Lett.* **2002**, *365*, 464-472.

[79] S. A. C. McDowell, *Chem. Phys. Lett.* **2007**, *441*, 194-197.

Tables and Figures

Table 3-1. Binding energy Eb, for complexes of indicated anion with CF_3H, along with CH bond length change $\Delta r(CH)$, CH stretching frequency change $\Delta \tilde{v}(CH)$, NBO charge transfer energy E(2) to the CH σ^* of proton donor, %s character change of CH NBO bond orbital, and change in NMR chemical shift of bridging proton.

Anion	E_b kcal/mol	$\Delta r(CH)$ mÅ	$\Delta \tilde{v}(CH)$ cm^{-1}	E(2) kcal/mol	Δs %	$\Delta \sigma$ ppm
F$^-$	26.15	55.0	-760.2	65.84	6.8	-8.64
Cl$^-$	15.16	10.6	-156.5	25.60	4.4	-4.74
Br$^-$	13.19	7.6	-112.6	22.56	4.0	-4.33
CN$^-$	14.89	10.9	-164.9	24.32	4.6	-3.59
NO$_3^-$	14.48	2.4	-22.7	15.92[a]	4.1	-3.72
HCOO$^-$	16.26	6.8	-96.4	15.31[a]	4.5	-4.98
CH$_3$COO$^-$	16.66	7.0	-99.0	15.28[a]	4.6	-4.86
HSO$_4^-$	12.31	-1.8	39.7	10.25[a]	3.5	-2.43
SO$_4^{-2}$	26.70	18.4	-252.9	31.96[a]	6.6	-5.99
H$_2$PO$_4^-$	13.76	5.2	-78.0	18.07[a]	4.1	-3.36
HPO$_4^{2-}$	27.55	37.0	-528.4	49.79[b]	7.2	-7.69
PO$_4^{3-,d}$	44.55	64.1	-1048.6	101.11[Z]	10.8	-12.2

[a]sum of charge transfer from two O atoms

[b]sum of charge transfer from two O atoms and one PO π

[c]sum of charge transfer from one O atom and one PO π

[d] optimized with fixed r(CH)

Table 3-2. SAPT energy components (kcal/mol) for interaction of indicated anion with CF_3H

	complex	ES	EX	IND	DISP	EXDISP+EXIND
1	F^-	-47.25	37.64	-24.53	-7.34	13.60
2	Cl^-	-22.33	14.08	-11.29	-4.17	8.25
3	Br^-	-19.56	12.59	-11.05	-3.98	8.83
4	CN^-	-22.50	13.77	-8.14	-4.04	4.16
5	NO_3^-	-19.37	10.32	-6.24	-4.17	3.45
6	$HCOO^-$	-23.02	12.41	-8.72	-4.50	5.15
7	CH_3COO^-	-23.62	12.88	-9.00	-4.74	5.27
8	HSO_4^-	-16.30	8.413	-5.00	-4.01	2.92
9	SO_4^{-2}	-36.08	20.81	-16.14	-6.79	8.55
10	$H_2PO_4^-$	-20.32	12.04	-7.04	-4.59	3.93
11	HPO_4^{2-}	-42.38	29.31	-21.27	-8.02	11.80
12	PO_4^{3-}	-75.93	62.34	-56.95	-12.9	36.70

Table 3-3. Minimum electrostatic potential of anions on the 0.001 au isodensity contour.

Anion	Min ESP kcal/mol
F^-	-169.04
Cl^-	-139.13
Br-	-131.25
CN^-	-137.70
NO_3^-	-140.68
$HCOO^-$	-152.92
CH_3COO^-	-153.24
HSO_4^-	-128.49
SO_4^{-2}	-235.85
$H_2PO_4^-$	-132.88
HPO_4^{2-}	-239.00
PO_4^{3-}	-334.57

Table 3-4. ρ and $\Delta^2\rho$ (au) at the BCP and RCP for complexes of indicated anion with CF_3H

anion	Critical point	ρ	$\nabla^2\rho$
F^-	BCP	0.0677	0.1980
Cl^-	BCP	0.0245	0.0632
Br-	BCP	0.0208	0.0471
CN^-	BCP	0.0290	0.0854
NO_3	BCP	0.0165	0.0499
	BCP	0.0217	0.0623
	RCP	0.0154	0.0531
$HCOO^-$	BCP	0.0261	0.0728
CH_3COO^-	BCP	0.0267	0.0752
HSO_4	RCP	0.0131	0.051
	BCP	0.0163	0.0481
	BCP	0.0163	0.0481
SO_4^{2-}	BCP	0.0365	0.1118
$H_2PO_4^-$	BCP	0.0276	0.0874
HPO_4^{2-}	BCP	0.0498	0.1489
PO_4^{3-}	BCP	0.0872	0.1418
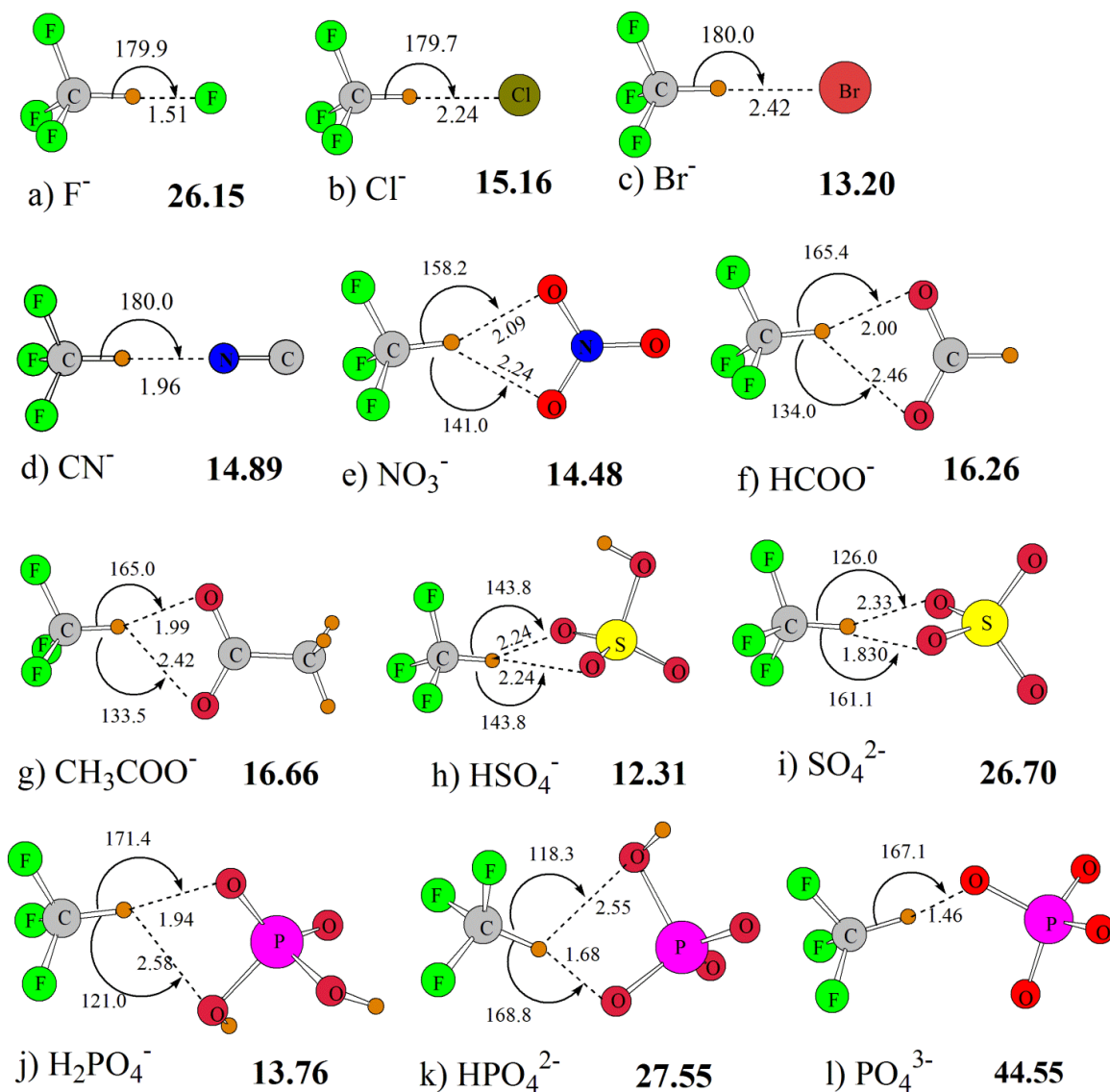
Figure 3-1. Geometries of global minima for complexes of CF3H with indicated anions. Bold number indicates counterpoise-corrected binding energy in kcal/mol. Distances in Å, angles in degs.
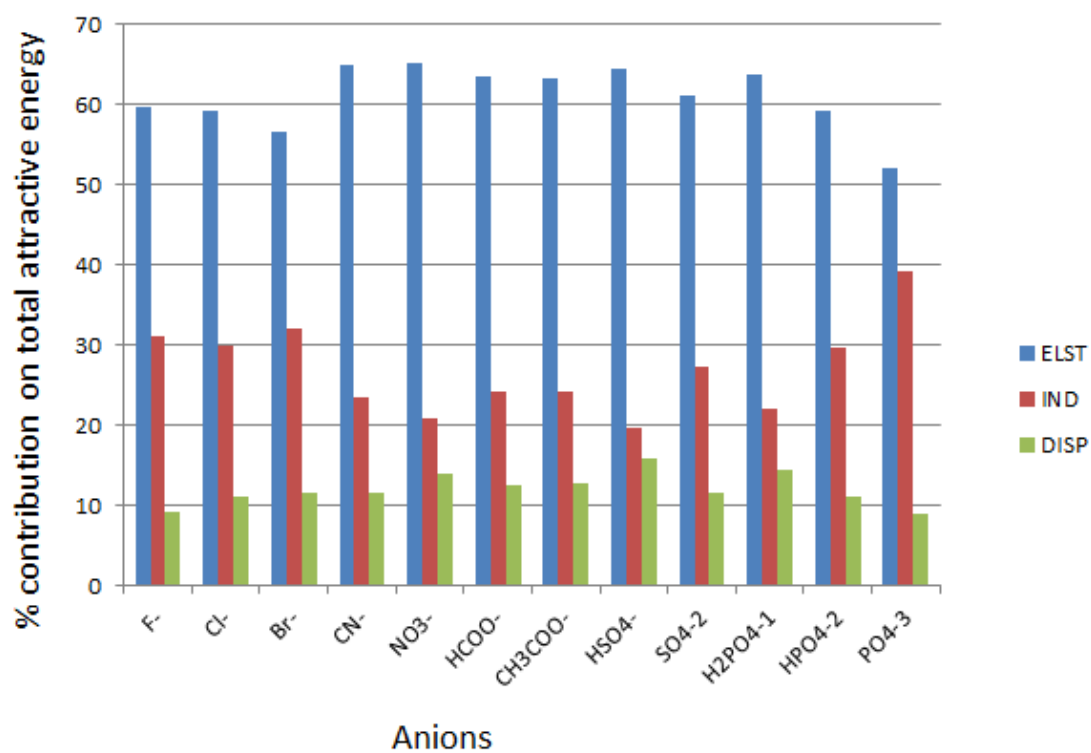
Figure 3-2. Percent contribution of electrostatic, induction and dispersion to total attractive energy based on SAPT analysis.
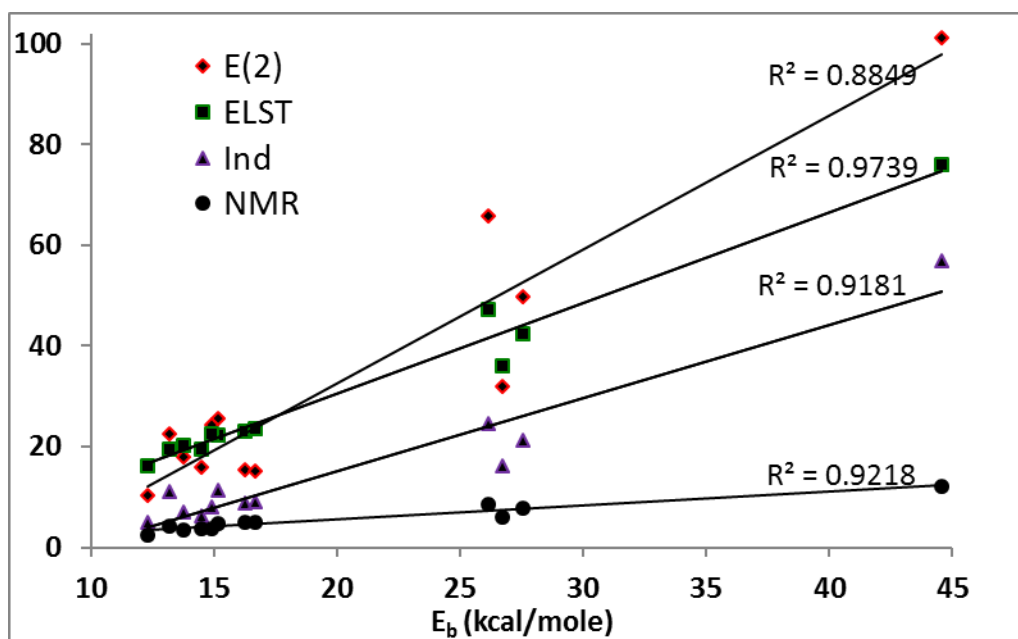
Figure 3-3. Variations of E(2), electrostatic, and induction energies, and $\Delta\sigma$ of bridging proton (ppm), as a function of binding energy (Eb). Vertical axis in units of ppm for NMR data, all others in kcal/mol.

a) CF$_3$H$\cdots$F$^-$

b) CF$_3$H$\cdots$Cl$^-$

c) CF$_3$H$\cdots$Br$^-$

d) CF$_3$H$\cdots$NO$_3^-$

e) CF$_3$H$\cdots$CN$^-$

f) CF$_3$H$\cdots$HCOO$^-$

g) CF$_3$H$\cdots$CH$_3$COO$^-$

h) CF$_3$H$\cdots$HSO$_4^-$

i) CF$_3$H$\cdots$SO$_4^{2-}$

J) CF$_3$H$\cdots$ H$_2$PO$_4^-$

k) CF$_3$H$\cdots$ HPO$_4^{2-}$

l) CF$_3$H$\cdots$ PO$_4^{3-}$
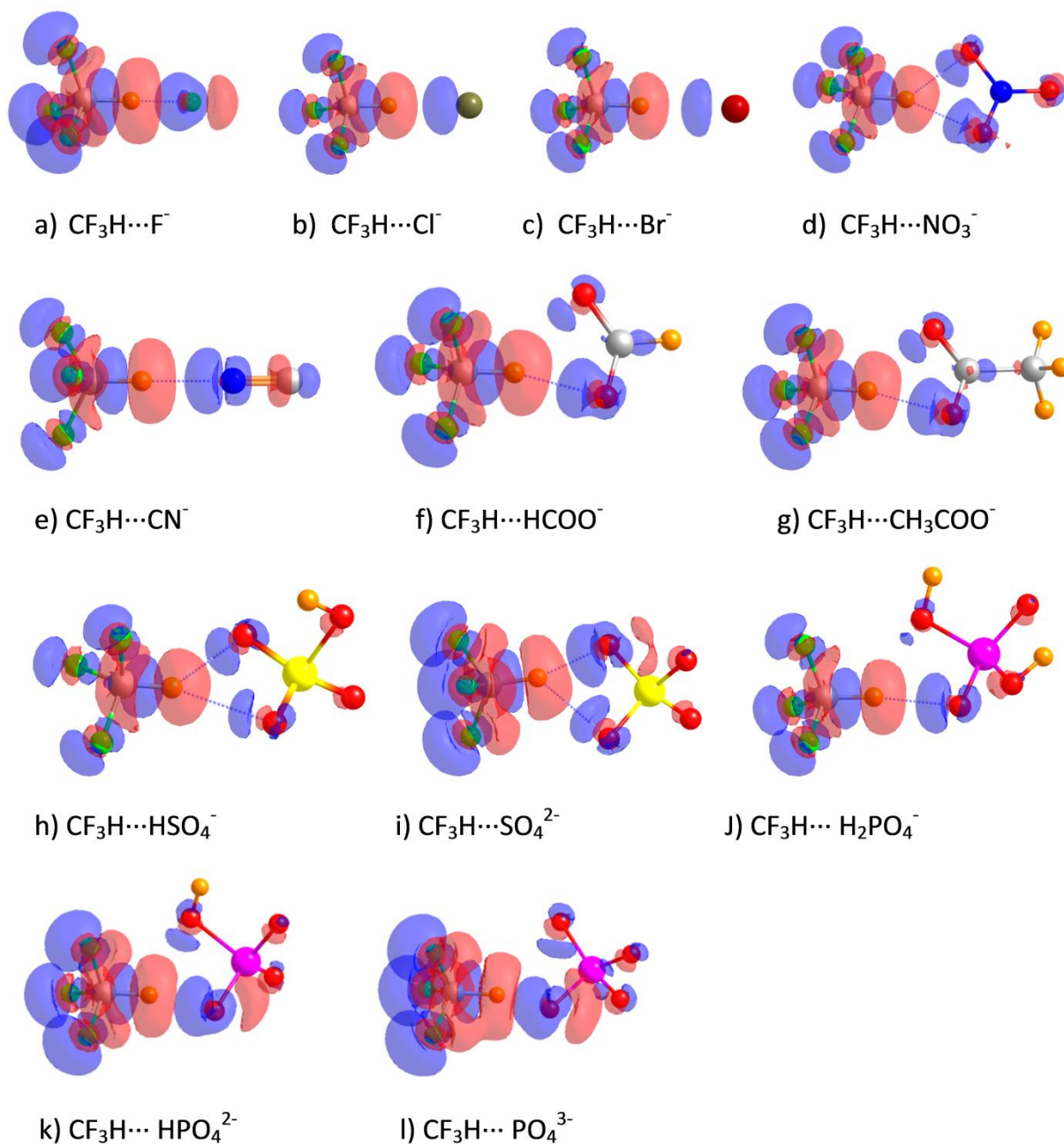
Figure 3-4. Electron density shift map for the global minimum complexes with contour value 0.0015 au. Red/blue color indicates electron density loss/gain.

CHAPTER 4

MICROSOLVATION OF ANIONS BY MOLECULES FORMING CH··X$^-$

HYDROGEN BONDS[1]

Abstract

Various anions were surrounded by n molecules of CF_3H, which was used as a prototype CH donor solvent, and the structures and energies studied by M06-2X calculations with a 6-31+G** basis set. Anions considered included the halides F^-, Cl^-, Br^- and I^-, as well as those with multiple proton acceptor sites: CN^-, NO_3^-, $HCOO^-$, CH_3COO^-, HSO_4^-, $H_2PO_4^-$, and anions with higher charges SO_4^{2-}, HPO_4^{2-} and PO_4^{3-}. Well-structured cages were formed and the average H-bond energy decreases steadily as the number of surrounding solvent molecules rises, even when n exceeds 6 and the CF_3H molecules begin to interact with one another rather than with the central anion. Total binding energies are very nearly proportional to the magnitude of the negative charge on the anion. The free energy of complexation becomes more negative for larger n initially, but then reaches a minimum and begins to rise for larger values of n.

4-1. Introduction

Solvation of ions in various media plays a crucial role in a large number of chemical, biochemical and environmental phenomena. The microsolvation of ionic species occurs not only in the liquid but also in the gas phase in the form of clusters. A number of

_____

[1] Coauthored by Binod Nepal and Steve Scheiner. Reproduced with permission from *Chem. Phys.* ***2015, 463, 137-144***. Copyright 2015, Elsevier.

studies [1-3] show that various types of ionic pollutants, both cationic and anionic, are present in the atmosphere in the form of aerosols causing atmospheric pollution. The study of microsolvation of ions provides an important tool for understanding their structure, energetics, spectroscopic properties, and reaction mechanisms and kinetics in the solution phase as well as in the gas phase. For example, in an ion pair S_N2 reaction between sodium p-nitrophenoxide and halomethanes in acetone [4], the rate of reaction is found to be drastically affected by the microsolvation of anions by acetone molecules. As another example, the α-effect in an S_N2 reaction has been found [5] to be strongly affected by the microsolvation of anions by solvent molecules. Additionally, the properties of isolated ions can be substantially different from their solvated cluster structure. For example, the isolated $(SO_4)^{2-}$ ion is unstable in the gas phase as a dianion due to its very high Coulombic repulsion; the same is true [6] for PO_4^{3-}. However, these same ions become stable when microsolvated by a cluster of solvent molecules, or in the solid state [7,8].

Since water is the most common and the most abundant solvent in nature, most studies of microsolvation of anions have been centered on aqueous systems. Water interacts with the ionic species via its strong H-bonding capacity as well as charge-dipole interactions. On the other hand, a great deal of recent work has shown that the CH group can serve as a potent proton donor in H-bonds (HBs) in parallel fashion to OH and NH donors [9-26]. CH··X HBs are quite prevalent in nature, in biological [27-35] as well as chemical [36-44] contexts. The ability of CH to act in this capacity is related first to the hybridization of the C atom, in the order sp > sp^2 > sp^3. The placement of electron-withdrawing substituents on the C atom, e.g. F or Cl, helps to polarize the CH bond, thereby

strengthening the incipient HB. As with more conventional HBs, a cationic CH donor is particularly powerful [45-49], with related $CH^+··X$ HBs surpassing some of the strongest conventional HBs. Likewise, one would expect that a $CH··X^-$ HB with an anion ought to be quite strong as well, for which there is some evidence [50-55].

Hence, one would anticipate that a CH-donating solvent could serve in a microsolvating role, as do OH and NH donors. However, there has been very limited work to date dealing with clusters in which CH··O HBs play a dominant role. Indeed the first direct evidence of aromatic CH··O HBs in gas phase clusters did not arise until 2005 [56] wherein 1,2,4,5-tetrafluorobenzene served as proton donor to a variety of bases. In terms of calculations, most work has been limited to only small clusters [57-62]. For example, homo-oligomers of CH_3CN up to tetramer were examined [63] so as to measure the degree of cooperativity, as were clusters of H_2CO up to the pentamer level [64]. In a similar vein, aldehyde clusters up to the octamer [65] all contained CH··O HBs. H_2CO was inserted into cyclic clusters of HF and HOH [66] with a particular interest in the frequency shift of the CH bonds. But there is little that deals with larger clusters in which a central species is surrounded by a number of CH proton donors, as a simulation of the first steps of solvation. And data is even more limited when it comes to the microsolvation of anions by such donors.

This work is intended to answer a number of fundamental questions on this topic. As an overarching issue, how effective are CH donors in forming clusters around an anion? Do these molecules form well defined solvation shells around an anion? How does one anion differ from another in terms of the structure and energetics of these clusters? Do

dianions and trianions behave qualitatively differently than do monoanions? For those anions that have more than one proton-accepting atom, do they engage in bifurcated CH··X HBs or is there a preference for single, linear bonds?

Quantum chemical calculations have been recruited in an effort to answer these questions. Such calculations permit the study of a given number of surrounding solvent molecules without complications of smaller and larger clusters complicating the analysis. For any given cluster, all minima on the surface can be identified, and ordered with respect to energy. Analysis of each structure provides unambiguous information about the nature of the forces that hold it together, those between solvent molecules as well as ion-solvent. The comparison of data for different numbers of solvent molecules n reveals whether there is a smooth progression as n increases, or a break in character at some particular cluster size.

F_3CH was chosen as the CH proton donor for a number of reasons. The three strongly electron-withdrawing F atoms make the CH group particularly polar and a correspondingly good donor. Indeed, this molecule has been used in numerous studies [67-74] for just this reason. Secondly, the presence of only a single CH proton on the molecule simplifies the analysis, allowing a focus on a particular CH··O HB, as compared to larger molecules with numerous protons. A number of different anions were taken as proton acceptors, due in part to their ability to form strong HBs. Secondly, as anions, they would be unlikely to act as proton donors to the F atoms of F_3CH which would complicate the analysis. The first group of anions selected for study were the halides: F^-, Cl^-, Br^- and I^-. Their simplicity offers a first step, and their varying size provides a gradation of charge

density. CN^- is an interesting anion as both atoms are potential proton acceptors, as is the π-system that connects them. There are several proton-accepting atoms present in the NO_3^- and $HCOO^-$ anions; extension to CH_3COO^- permits an examination of the effect of an alkyl group. HSO_4^- and $H_2PO_4^-$ each present four possible proton-accepting O atoms. It is then possible to study how increasing the charge on the anion affects the results by including SO_4^{2-}, HPO_4^{2-}, and the triply charged PO_4^{3-}.

4-2. Computational Details

Calculations were carried out with Gaussian-09 [75], applying the M06-2X [76] variant of density functional theory, in conjunction with the 6-31+G** basis set. The LAND2Z pseudopotential [77] from the EMSL basis set library [78] was used for I. Geometries were fully optimized and assured to be minima via vibrational calculations that found all positive frequencies. Binding energies were computed as the difference between the energy of the complex and the sum of the energies of fully optimized monomers. Each binding energy was corrected for basis set superposition error using the counterpoise method [79,80], evaluating the superposition error between each pair of molecules within the cluster, both solute-solvent and solvent-solvent pairs.

4-3. Results and Discussion

4-3.1. Halide Ions

The optimized geometries of the fluoride anion complexes are presented in Fig 4-1. In some cases, notably for n=4, there was a second minimum encountered, some not much higher in energy. The solvating CF_3H molecules generally adopt the classic

arrangements around these halides, viz. those that might be predicted by VSEPR. But this is not always the case, and there are some other geometries that can be quite competitive in energy in some cases. More specifically, a linear arrangement is preferred for n=2, but a bent structure occurs for Br^- and I^-, which is only slightly higher in energy. For n=3, the planar and trigonal pyramids are both minima for these same two anions, with I^- showing a slight preference for the latter. The tetrahedral and square planar geometries are both minima for all four halides, with the former slightly favored. A trigonal bipyramid represents the global minimum for n=5, and octahedral arrangement for n=6.

There are certain perturbations from the standard structures that are noted. Most notably, the n=2 geometries are not necessarily strictly linear, with $H \cdot\cdot X \cdot\cdot H$ angles varying between 163° for F^-, 114° for Cl^-. Two structures with very similar energies are observed for Br^- and I^-, one with a $\theta(H \cdot\cdot I \cdot\cdot H)$ angle of 105-109° and the other with 180°. It may be noted as well that for n<6, the CH groups point directly toward the central anion, with $\theta(CH \cdot\cdot X)$ angles in the neighborhood of 180°. The exception to this rule is the hexacoordinated F^-, where the $\theta(CH \cdot\cdot F)$ angles for $F^-(CF_3H)_6$ are around 130-150°. This disruption of the linear HBs is likely due to the small size of the F^- anion. which would pull the various protons too close to one another without any such distortion.

When *n* grows larger than 6, the structures become less regular, less symmetric. The heptameric arrangement around F^-, for example, shows $R(H \cdot\cdot F^-)$ over a range covering 1.985 to 2.192 Å, and 1.997 - 2.221 Å for n=8. Also, the H-bonds grow less linear. Several of these HBs vary by as much as 70° from linearity for the octamer. In summary, since the central halide cannot fully accommodate more than 6 HBs, these solvating molecules turn

so that they engage in HBs with their neighboring solvent molecules. The level of misalignment with the central halide varies from one molecule to the next: the $\theta(CH\cdot\cdot F^-)$ angle varies from 168° down to 111°. And indeed, this inter-solvent H-bonding is evident in the NBO analysis as well, which reveals charge transfers from the F lone pairs of one molecule to the $\sigma^*(CH)$ antibonding orbitals of another. The same sort of pattern is evident which illustrate the geometries of the various clusters for the other halide anions.

As the number of solvent molecules rises, they become further separated from the halide anion, as may be seen by the average $R(X\cdot\cdot H)$ distances displayed in Table 4-1. This increasing distance, shown pictorially in Fig 4-2, is very nearly linearly related to *n*, and is most sensitive to the growing solvation shell size for the smallest F^- anion, where each additional molecule elongates the HB distance by 0.10 Å. It is interesting to note that the linearity of each curve continues beyond n=6, even after some of the solvent molecules shift their HBs from the central halide to one another.

In concert with the progressively longer HBs, the average HB energy declines regularly with *n*. This quantity was computed as the total complexation energy divided by the number of solvent molecules *n*. As indicated in Table 4-2 and Fig 4-3, this mean HB energy decline is nearly proportional to *n*, with the exception of fluoride where a slight asymptotic behavior is apparent. The absence of any clear break around n=6 is consistent with Fig 4-2, and suggests that the complexation energy does not suffer when the solvent molecules begin to bind to one another.

A more complete treatment of the thermodynamics of binding of F_3CH to the halides is presented in Table 4-3. These quantities were evaluated at 298 K and 1 atm. The

changes in entropy are negative, and progressively so with larger n, which is consistent with the process of binding multiple species into a single entity. The favorable enthalpy of binding is manifested by the progressively larger negative values of ΔH as n increases, consistent with the electronic energies in Table 4-2. Reflecting the smaller average binding energies as n increases (Table 4-2), ΔH behaves in an asymptotic manner. After accounting for the negative entropy change, ΔG is much less negative than ΔH, and even positive for some of the larger clusters. As illustrated in Fig 4-4, ΔG first becomes more negative as n increases, reaches a minimum, and then begins to climb. This shape can be attributed to two factors. First, ΔH does not decrease linearly with n, but rather flattens out, due to the progressively smaller individual HB energy as illustrated in Fig 4-3. ΔS, on the other hand, does not flatten with increasing n; in fact the $\Delta S/n$ ratio becomes larger as n increases. Thus ΔS becomes more prominent for larger n, while ΔH plays a diminishing role, accounting for the curvature of the ΔG curve. ΔG reaches a maximal negative value for small clusters; n=4 for F^- and Cl^-, 3 for Br^-, and 2 for I^-. And consistent with the energetic data, ΔG also obeys the trend that F^- forms the strongest bonds: $F^- < Cl^- < Br^- < I^-$.

4-3.2. CN^-, NO_3^-, $HCOO^-$ and CH_3COO^-

The optimized geometries of the CN^- complexes with increasing number of CF_3H molecules are presented in Fig 4-5. For a single solvent molecule, a proton can be donated to either atom of the CN^- anion, with near equal energy. When n=2, the two CF_3H molecules can either be located at the two ends of CN^-, or both donating a proton to the N atom, again with little energetic difference between the two. All three solvent molecules can donate to N for n=3, or only two of them, with the third interacting with the C; the

latter is favored by 1.5 kcal/mol. The pattern is repeated for larger values of n, wherein most of the CF$_3$H molecules interact with the N, leaving only a single molecule H-bonded to C. As n climbs above 3, the total number of minima increases as well. It is only for n=7 that a second solvent molecule interacts with C. It is for n$\geq$6 that the geometries suggest appreciable intersolvent H-bonding, which is supported by NBO analysis. As in the cases of the halide anions, the average H-bond energy declines smoothly as n increases, with no sharp dropoff at any particular number of solvent molecules.

The same pattern of approximately linear drop of average interaction energy is noted as well for the NO$_3^-$, HCOO$^-$ and CH$_3$COO$^-$ anions as well, as illustrated in Fig 4-6. In fact, the quantitative values indicate that there is little distinction between CN$^-$ and NO$_3^-$ anions with regard to binding energies. The same is true for formate and acetate, which form somewhat stronger bonds, than do CN$^-$ and NO$_3^-$. When the total binding energies are expanded to free energies, one obtains the pattern exhibited in Fig 4-7. Whereas CN$^-$ and NO$_3^-$ have very similar binding energies to F$_3$CH, the former corresponds to a more negative ΔG than does the latter for any value of n; again the HCOO$^-$ and CH$_3$COO$^-$ anions display a stronger interaction than do their smaller counterparts. ΔG is most negative for n=3, as was also the case for Br$^-$.

The presence of 2 or 3 O atoms on each anion creates a tendency for the F$_3$CH proton to engage in bifurcated HBs, although deviation from this pattern is not terribly costly energetically. As n increases it is no longer possible for all solvent molecules to engage in such bifurcated HBs, and single acceptor HBs become more prominent. For

larger values of n, the plane of the anion becomes more crowded, and the solvent molecules consequently deviate further and further from that plane.

4-3.3. HSO_4^-, SO_4^{2-}, $H_2PO_4^-$, HPO_4^{2-} and PO_4^{3-}

The presence of four O atoms on the sulfate and phosphate series presents certain interesting possibilities, as does the differing charge on each of these anions. In the first place, these anions present a larger set of secondary minima. The patterns of average HB energy of the global minima in Fig 4-8 reveal first of all that this quantity is highly dependent upon the total charge. In fact, for any given value of n, the average binding energy is roughly proportional to the charge on the anion. Taking n=3 as an example, the average binding energies for $H_2PO_4^-$, HPO_4^{2-} and PO_4^{3-}, are respectively 13.6, 27.1, and 44.1 kcal/mol. It is also intriguing to note that the nature of the anion is largely irrelevant, in the sense that the SO_4^{2-} and HPO_4^{2-} dianions have nearly identical energies, as do the HSO_4^- and $H_2PO_4^-$, monoanions, true for any given value of n. A third point worthy of note is related to the slopes of the curves. The average binding energies for the anions in Fig 4-8 decline more gradually with n than is the case for the halides in Fig 4-3, or the monoanions in Fig 4-6. For example, this quantity declines from 16.2 kcal/mol for CN^- when n=1 to 10.3 kcal./mol for n=7, a drop of 5.9 kcal/mol or 36%. The same quantities for the HSO_4^- anion drop from 13.9 to 10.0 kcal/mol, declining by only 4.0 kcal/mol which is translates to 28%. While the dianions experience a larger absolute decrease (by 7.8 kcal/mol in the case of SO_4^{2-}) this change is proportionately the same, 27%.

The free energies of binding in Fig 4-9 also present certain comparisons with the smaller anions. Like the binding energies, ΔG is also very sensitive to the total charge. For

the monoanions, ΔG can be as large as -11 kcal/mol, comparable to the smaller monoanions. But for higher charges, this quantity can be quite large, even in excess of -180 kcal/mol for PO_4^{3-}. It is also interesting to note that the value of n for which ΔG exhibits a minimum is closely related to the total charge. This minimum occurs for n=3 for the monoanions, rises to 6-7 for the dianions, and has not yet reached a minimum for the PO_4^{3-} trianion, even for n as large as 10.

The overall pattern for the HSO_4^-, SO_4^{2-} series is consistent with the earlier anions in that the proton of each CF_3H molecule prefers a position roughly midway between two O atoms, in bidentate CH··O HBs. This situation becomes less tenable for larger values of n, at which point non-bifurcated HBs begin to proliferate. In contrast, the $H_2PO_4^-/HPO_4^{2-}/PO_4^{3-}$ series displays a propensity for single, linear CH··O HBs, even when this leaves the proton-accepting ability of O atoms unsatisfied. As a final point, it might be noted that the very high charge of PO_4^{3-} induced a spontaneous proton transfer from one of the CF_3H molecules, for n=1-4. In order to avoid this transfer, geometry optimizations were carried out by fixing all C-H bond lengths to 1.600. (The latter value was chosen based on the optimized CH bond lengths in the $F_3CH\cdots H_2PO_4^-$ and $F_3CH\cdots HPO_4^{2-}$ series of complexes.)

4-3.4. Perturbations in Monomers

The formation of a AH··D HB is well known to induce characteristic changes within the participating monomers. Perhaps most notable of these is the traditional elongation of the A-H covalent bond, accompanied by a red shift of its stretching frequency. However, in a number of cases which have become well known in recent years, these patterns can be reversed in the case of a CH proton donor [81]. The changes undergone in the CH bond

length within CF_3H are reported in Tables 4-4 and 4-5 as the average of all the *n* molecules within a given cluster. In the majority of cases, this bond is stretched, most notably for the fluoride anion. Particularly large stretches are also observed for the multiply charged anions in Table 4-5, again reflecting the strength of the HBs. There is also a clear pattern that the amount of stretching diminishes as the number of solvent molecules enlarges. This pattern mirrors that of the average binding energy, although it is more dramatic. In fact, as n increases further, beyond a first solvation shell, $\Delta r(CH)$ reverses sign in certain cases, reflecting a small contraction. The principal exception to these patterns is associated with the monoanion, where CH bond contractions occur for all size clusters. This reversal may be associated with the predilection for bifurcated HBs for this anion.

It is usually anticipated that the stretch of the CH bond ought to be associated with a red shift of its stretching frequency. This expectation is indeed realized in these clusters, as may be seen by comparison of Tables 4-4 and 4-5 with the frequency shifts. The largest red shift, amounting to 1099 cm^{-1}, occurs for $F_3CH\cdots F^-$, which matches the largest bond elongation of 84 mÅ. Progressive weakening of the average HB via larger numbers of solvent molecules is accompanied by reduced red shift. Those CH bonds which contracted as a result of complexation are also generally characterized by a blue shift of the stretching frequency.

4-4. Conclusions

Very much like the case of H-bonding solvent molecules such as water, CF_3H which engages in non-classical $CH\cdots X$ HBs, forms a well-structured solvation cage around anions of various types. Small numbers *n* of solvent molecules form highly structured

geometries, with the CH··X bonding molecules disposed in well-defined positions. The most stable structures are very much akin to standard ideas of VSEPR theory for the simple halides. For larger anions with multiple H-bond acceptor atoms, the global minima favor simple HBs in many cases, but in others there is a tendency to form bifurcated HBs wherein the bridging proton lies roughly midway between two O atoms. Such bifurcated geometries switch to single proton-acceptor HBs as the number of solvent molecules grows. This pattern is different for the phosphate series however, where linear CH··O HBs are slightly favored, even when such a structure leaves the H-bonding capacity of some O atoms unsatisfied. As n increases beyond 6, steric crowding prevents all of the surrounding CF_3H molecules from forming a CH··X bond with the central anion. As a consequence, some of the solvent molecules reorient so as to engage in CH··F HBs with one another. This process is a gradual one in the sense that these solvent molecules tend to retain at least a marginal engagement with the central anion as well.

The binding energy per solvent molecule undergoes a steady decline as n increases, accompanied by a parallel elongation of the average distance between the central anion and the surrounding solvent molecules. There is no sharp change that occurs for n~6, when solvent molecules disengage from the central anion and form CH··F HBs with one another. In contrast to the asymptotic decline of ΔE, the entropy loss of formation of the complex is nearly a linear function of n, even showing a slight uptick for larger complexes. As a result, the free energy of formation attains its most negative value for a small value of n (2-4) for monoanions, becoming less favorable for larger complexes. The binding energies are roughly proportional to the magnitude of the negative charge on the anion. The value

of *n* for which ΔG is most negative is larger for di and trianions than for monoanions. It should finally be stressed that the results described above relate direct to clusters in the gas phase. Extrapolation to the liquid would involve a much larger number of surrounding solvent molecules, as well as dynamic treatment of molecular motions.

The results presented here were computed with the 6-31+G** basis set. One might wonder if a larger set would significantly alter the trends. In order to examine this possibility, additional calculations were carried out with the much larger and more flexible aug-cc-pVTZ set, within the context of the originally optimized geometries. As may be seen from examination of Table 4-6, such an expansion yielded only very small changes in the binding energies of either a monoanion (F^-) or a dianion (SO_4^{2-}) with any number of F_3CH molecules. Use of the larger set reduced binding energies by only 1-3%. and had no effect on any of the trends. It may thus be concluded that the results presented above are quite insensitive to basis set expansion.

References

[1]   T. Adzuhata, J. Inotsume, T. Okamura, R. Kikuchi, T. Ozeki, M. Kajikawa, N. Ogawa, Anal. Sci. 17 (2001) 71.

[2]   V.L. Bychkov, G.V. Golubkov, A.I. Nikitin, The Atmosphere and Ionosphere: Dynamics, Processes and Monitoring, Springer, 2010.

[3]   A.C. Stern, Air Pollution V1: Air Pollutants, Their Transformation and Transport, Elsevier, 1976.

[4]   Q.-G. Li, K. Xu, Y. Ren, J. Phys. Chem. A 119 (2015) 3878.

[5]   D.L. Thomsen, J.N. Reece, C.M. Nichols, S. Hammerum, V.M. Bierbaum, J. Am. Chem. Soc. 135 (2013) 15508.

[6]   A.I. Boldyrev, J. Simons, J. Phys. Chem. 98 (1994) 2298.

[7]   X.-B. Wang, J.B. Nicholas, L.-S. Wang, J. Chem. Phys. 113 (2000) 10837.

[8]   E. Pluhařová, M. Ončák, R. Seidel, C. Schroeder, W. Schroeder, B. Winter, S.E. Bradforth, P. Jungwirth, P. Slavíček, J. Phys. Chem. B 116 (2012) 13254.

[9]   J.E. Del Bene, I. Alkorta, J. Elguero, Phys. Chem. Chem. Phys. 13 (2011) 13951.

[10]   S. Scheiner, Curr. Org. Chem. 14 (2010) 106.

[11]   S.J. Grabowski, J. Phys. Chem. A 115 (2011) 12789.

[12]   S.A.C. McDowell, A.D. Buckingham, Phys. Chem. Chem. Phys. 13 (2011) 14097.

[13]   M.M. Szczesniak, G. Chalasinski, S.M. Cybulski, S. Scheiner, J. Chem. Phys. 93 (1990) 4243.

[14]   H.S. Biswal, S. Wategaonkar, J. Phys. Chem. A 113 (2009) 12774.

[15]   O. Takahashi, Y. Kohno, S. Iwasaki, K. Saito, M. Iwaoka, S. Tomoda, Y. Umezawa, S. Tsuboyama, M. Nishio, Bull. Chem. Soc. Jpn. 74 (2001) 2421.

[16]   S. Cybulski, S. Scheiner, J. Am. Chem. Soc. 109 (1987) 4199.

[17]   D. Mani, E. Arunan, J. Chem. Phys. 141 (2014) 164311.

[18]   Y. Gu, T. Kar, S. Scheiner, J. Mol. Struct. 552 (2000) 17.

[19]   L. Spada, Q. Gou, S. Tang, W. Caminati, New J. Chem. 39 (2015) 2296.

[20]   N. Lu, R.M. Ley, C.E. Cotton, W.-C. Chung, J.S. Francisco, E.-I. Negishi, J. Phys. Chem. A 117 (2013) 8256.

[21]   B. Michielsen, C. Verlackt, B.J. van der Veken, W.A. Herrebout, J. Mol. Struct. 1023 (2012) 90.

[22]   G. Sánchez-Sanz, C. Trujillo, I. Alkorta, J. Elguero, Phys. Chem. Chem. Phys. 14 (2012) 9880.

[23]   Z. Latajka, S. Scheiner, J. Comput. Chem. 5 (1987) 674.

[24]   W. Zierkiewicz, D. Michalska, T. Zeegers-Huyskens, Phys. Chem. Chem. Phys. 12 (2010) 13681.

[25]   B.G. Oliveira, M.C.A. Lima, I.R. Pitta, S.L. Galdino, M.Z. Hernandes, J. Mol. Model. 16 (2009) 119.

[26]   E. Kryachko, S. Scheiner, J. Phys. Chem. A 108 (2004) 2527.

[27]   S. Horowitz, R.C. Trievel, J. Biol. Chem. 287 (2012) 41576.

[28]   B.K. Mueller, S. Subramanian, A. Senes, Proc. Nat. Acad. Sci., USA 111 (2014) E888.

[29]   M. Zierke, M. Smieško, S. Rabbani, T. Aeschbacher, B. Cutting, F.H.-T. Allain, M. Schubert, B. Ernst, J. Am. Chem. Soc. 135 (2013) 13464.

[30]   S. Scheiner, J. Phys. Chem. B 110 (2006) 18670.

[31]   O. Khakshoor, S.E. Wheeler, K.N. Houk, E.T. Kool, J. Am. Chem. Soc. 134 (2012) 3154.

[32]   D. Sheppard, D.-W. Li, R. Godoy-Ruiz, R. Brschweiler, V. Tugarinov, J. Am. Chem. Soc. 132 (2010) 7709.

[33]   N. Sukumar, F.S. Mathews, P. Langan, V.L. Davidson, Proc. Nat. Acad. Sci., USA 107 (2010) 6817.

[34]   S. Scheiner, J. Phys. Chem. B 109 (2005) 16132.

[35]   Y. Yoneda, K. Mereiter, C. Jaeger, L. Brecker, P. Kosma, T. Rosenau, A. French, J. Am. Chem. Soc. 130 (2008) 16678.

[36]   R. Joseph, A. Nkrumah, R.J. Clark, E. Masson, J. Am. Chem. Soc. 136 (2014) 6602.

[37]   D.A. Leigh, C.C. Robertson, A.M.Z. Slawin, P.I.T. Thomson, J. Am. Chem. Soc. 135 (2013) 9939.

[38]   C.H. Schwalbe, Cryst. Rev. 18 (2012) 191.

[39]   I.D. Madura, J. Zachara, H. Hajmowicz, L. Synoradzki, J. Mol. Struct. 1017 (2012) 98.

[40]   L.-Y. You, S.-G. Chen, X. Zhao, Y. Liu, W.-X. Lan, Y. Zhang, H.-J. Lu, C.-Y. Cao, Z.-T. Li, Angew. Chem. Int. Ed. 51 (2012) 1657.

[41]   K.B. Wiberg, K.M. Lambert, W.F. Bailey, J. Org. Chem. 80 (2015) 7884.

[42]   J. Sandoval-Lira, L. Fuentes, L. Quintero, H. Höpfl, J.M. Hernández-Pérez, J.L. Terán, F. Sartillo-Piscil, J. Org. Chem. 80 (2015) 4481.

[43]   P. Écija, M. Vallejo-López, L. Evangelisti, J.A. Fernández, A. Lesarri, W. Caminati, E.J. Cocinero, ChemPhysChem. 15 (2014) 918.

[44]   P.D. Vaz, M.M. Nolasco, P.J.A. Ribeiro-Claro, Chem. Phys. 427 (2013) 117.

[45]   S. Iwase, B. Xiang, S. Ghosh, T. Ren, P.W. Lewis, J.C. Cochrane, C.D. Allis, D.J. Picketts, D.J. Patel, H. Li, Y. Shi, Nat. Struct. Mol. Biol. 18 (2011) 769.

[46]   A. Schmiedekamp, V. Nanda, J. Inorg. Biochem. 103 (2009) 1054.

[47]   U. Adhikari, S. Scheiner, J. Phys. Chem. A 117 (2013) 10551.

[48]   A. Khrizman, H.Y. Cheng, G. Bottini, G. Moyna, Chem. Commun. 51 (2015) 3193.

[49]   S. Scheiner, J. Phys. Chem. A 119 (2015) 9189.

[50]   M. Lisbjerg, H. Valkenier, B.M. Jessen, H. Al-Kerdi, A.P. Davis, M. Pittelkow, J. Am. Chem. Soc. 137 (2015) 4948.

[51]   H. Yang, M.W. Wong, J. Am. Chem. Soc. 135 (2013) 5808.

[52]   B. Nepal, S. Scheiner, Chem. Phys. Lett. 630 (2015) 6.

[53]   B. Nepal, S. Scheiner, Chem. Eur. J. 21 (2015) 1474.

[54]   L. Pedzisa, B.P. Hay, J. Org. Chem. 74 (2009) 2554.

[55]   B. Nepal, S. Scheiner, Chem. Eur. J. 21 (2015) 13330.

[56]   V. Venkatesan, A. Fujii, N. Mikami, Chem. Phys. Lett. 409 (2005) 57.

[57]   Q. Tang, Q. Li, Comput. Theor. Chem. 1050 (2014) 51.

[58]   D.P. Malenov, G.V. Janjic, D.Ž. Veljkovic, S.D. Zaric, Comput. Theor. Chem. 1018 (2013) 59.

[59]   M. Solimannejad, M. Malekani, I. Alkorta, Mol. Phys. 109 (2011) 1641.

[60]   A.K. Samanta, P. Pandey, B. Bandyopadhyay, T. Chakraborty, J. Phys. Chem. A 114 (2010) 1650.

[61]   S. Scheiner, T. Kar, J. Phys. Chem. B 109 (2005) 3681.

[62]   Q. Li, X. An, B. Gong, J. Cheng, J. Phys. Chem. A 111 (2007) 10166.

[63]   E.M. Cabaleiro-Lago, J.M. Hermida-Ramon, A. Pena-Gallego, E. Martinez-Nunez, A. Fernandez-Ramos, J. Mol. Struct. (Theochem) 498 (2000) 21.

[64]   A. Chaudhari, P.K. Sahu, S.-L. Lee, Int. J. Quantum Chem. 101 (2004) 67.

[65]   T.S. Thakur, M.T. Kirchner, D. Bläser, R. Boese, G.R. Desiraju, Phys. Chem. Chem. Phys. 13 (2011) 14076.

[66]   A. Karpfen, E.S. Kryachko, J. Phys. Chem. A 111 (2007) 8177

[67] P.R. Shirhatti, D.K. Maity, S. Bhattacharyya, S. Wategaonkar, ChemPhysChem. 15 (2014) 109.

[68] P. Ramasami, T.A. Ford, J. Mol. Struct. 1023 (2012) 163.

[69] A. Mukhopadhyay, P. Pandey, T. Chakraborty, J. Phys. Chem. A 114 (2010) 5026.

[70] J.B.L. Martins, J.R.S. Politi, E. Garcia, A.F.A. Vilela, R. Gargano, J. Phys. Chem. A 113 (2009) 14818.

[71] S.A.C. McDowell, Chem. Phys. Lett. 441 (2007) 194.

[72] K. Pluháková, P. Hobza, ChemPhysChem. 8 (2007) 1352.

[73] Y. Gu, T. Kar, S. Scheiner, J. Am. Chem. Soc. 121 (1999) 9411.

[74] P. Hobza, Z. Havlas, Chem. Phys. Lett. 303 (1999) 447.

[75] M.J. Frisch, G.W. Trucks, H.B. Schlegel, G.E. Scuseria, M.A. Robb, J.R. Cheeseman, G. Scalmani, V. Barone, B. Mennucci, G.A. Petersson, H. Nakatsuji, M. Caricato, X. Li, H.P. Hratchian, A.F. Izmaylov, J. Bloino, G. Zheng, J.L. Sonnenberg, M. Hada, M. Ehara, K. Toyota, R. Fukuda, J. Hasegawa, M. Ishida, T. Nakajima, Y. Honda, O. Kitao, H. Nakai, T. Vreven, J. Montgomery, J. A., J.E. Peralta, F. Ogliaro, M. Bearpark, J.J. Heyd, E. Brothers, K.N. Kudin, V.N. Staroverov, R. Kobayashi, J. Normand, K. Raghavachari, A. Rendell, J.C. Burant, S.S. Iyengar, J. Tomasi, M. Cossi, N. Rega, J.M. Millam, M. Klene, J.E. Knox, J.B. Cross, V. Bakken, C. Adamo, J. Jaramillo, R. Gomperts, R.E. Stratmann, O. Yazyev, A.J. Austin, R. Cammi, C. Pomelli, J.W. Ochterski, R.L. Martin, K.

Morokuma, V.G. Zakrzewski, G.A. Voth, P. Salvador, J.J. Dannenberg, S. Dapprich, A.D. Daniels, O. Farkas, J.B. Foresman, J.V. Ortiz, J. Cioslowski, D.J. Fox, Gaussian 09, Wallingford, CT, 2009.

[76]   Y. Zhao, D.G. Truhlar, Theor. Chem. Acc. 120 (2008) 215.

[77]   P.J. Hay, W.R. Wadt, J. Chem. Phys. 82 (1985) 270.

[78]   K.L. Schuchardt, B.T. Didier, T. Elsethagen, L. Sun, V. Gurumoorthi, J. Chase, J. Li, T.L. Windus, J. Chem. Infor. Model. 47 (2007) 1045.

[79]   S.F. Boys, F. Bernardi, Mol. Phys. 19 (1970) 553.

[80]   Z. Latajka, S. Scheiner, J. Chem. Phys. 87 (1987) 1194.

[81]   S. Scheiner, in: C.E. Dykstra, G. Frenking, K.S. Kim, G.E. Scuseria (Eds.), Theory and Applications of Computational Chemistry: The First 40 Years, Elsevier, Amsterdam, 2005, p. 831.

Tables and Figures

Table 4-1. Average H-bond lengths R(H··X) (Å) of the halide complexes with increasing number n of F3CH molecules.

n	F⁻	Cl⁻	Br⁻	I⁻
1	1.420	2.276	2.440	2.712
2	1.614	2.315	2.492	2.743
3	1.720	2.350	2.500	2.794
4	1.800	2.390	2.531	2.830
5	1.867	2.437	2.550	2.873
6	1.984	2.474	2.569	2.890
7	2.063	2.543	2.676	2.966
8	2.146	2.586	2.723	2.988

Table 4-2. Average binding energies (kcal/mol) per F_3CH molecule of halide complexes.

n	F⁻	Cl⁻	Br⁻	I⁻
1	29.31	16.08	14.01	11.69
2	25.05	14.98	13.10	10.33
3	22.08	14.06	12.36	9.31
4	19.66	12.89	11.50	8.47
5	17.50	11.84	10.65	7.76
6	15.93	10.97	9.88	7.15
7	14.60	10.65	9.29	7.12
8	13.57	10.51	9.15	6.80

Table 4-3. Thermodynamic parameters for binding of halide anions by n F$_3$CH molecules at 25 °C and 1 atm. ΔH and ΔG are in units of kcal/mol, and ΔS in cal mol^{-1} K^{-1}.

n	F$^-$			Cl$^-$			Br$^-$			I$^-$		
	ΔS	ΔH	ΔG	ΔS	ΔH	ΔG	ΔS	ΔH	ΔG	ΔS	ΔH	ΔG
1	-24.09	-30.71	-23.53	-20.63	-15.89	-9.74	-20.58	-13.89	-7.75	-20.51	-11.53	-5.41
2	-46.88	-50.26	-36.28	-48.35	-28.51	-14.09	-43.97	-25.01	-11.90	-44.40	-19.57	-6.33
3	-82.33	-64.75	-40.20	-75.54	-39.29	-16.77	-74.18	-34.73	-12.61	-70.11	-25.50	-4.60
4	-107.42	-75.50	-43.47	-98.75	-47.98	-18.54	-101.37	-42.33	-12.11	-97.31	-30.40	-1.39
5	-147.37	-82.78	-38.84	-130.07	-54.38	-15.60	-127.23	-48.71	-10.78	-118.54	-33.98	1.36
6	-172.51	-89.20	-37.77	-156.32	-59.72	-13.11	-159.01	-52.72	-5.31	-138.44	-36.84	4.44
7	-237.31	-94.34	-23.59	-212.16	-66.88	-3.62	-219.20	-57.19	8.16	-207.52	-42.29	19.58
8	-286.66	-99.12	-13.65	-270.93	-75.08	5.70	-279.63	-63.75	19.62	-250.42	-45.29	29.37

Table 4-4. Average CH bond length change (mÅ) within CF$_3$H upon complexation of monoanions with n CF$_3$H molecules (mÅ).

n	F$^-$	Cl$^-$	Br$^-$	I$^-$	CN$^-$	NO$_3^-$	HCOO$^-$	CH$_3$COO$^-$
1	83.94	9.67	7.05	5.16	10.70	1.22	3.56	4.08
2	29.62	6.52	5.03	3.57	8.96	0.04	5.85	6.66
3	15.98	4.41	3.28	2.73	4.88	-0.46	3.17	5.41
4	9.47	3.27	1.94	2.31	2.64	-0.46	3.46	2.88
5	6.07	2.04	1.28	1.42	0.02	-1.17	0.57	0.65
6	-2.83	1.35	0.48	1.46	-0.90	-2.69	-0.71	-0.89
7	0.19	-1.56	-2.71	-0.96	-2.32	-1.40	-0.83	-1.76
8	0.50	-2.58	-2.81	-1.45				

Table 4-5. Average CH bond length change (mÅ) within CF_3H upon complexation of mono-, di- and trianions with n CF_3H molecules (mÅ).

n	HSO_4^-	SO_4^{2-}	$H_2PO_4^-$	HPO_4^{2-}	PO_4^{3-}
1	-3.48	11.84	4.14	41.15	-
2	-2.89	7.60	2.42	22.85	-
3	-2.80	4.36	2.16	10.94	-
4	-2.11	2.51	-0.18	12.16	-
5	-2.84	1.39	-0.67	6.21	62.67
6	-2.69	0.86	-1.82	5.03	31.12
7	-2.68	1.09	-3.11	4.96	24.56
8		0.71		2.82	16.83
9		0.02		3.29	13.79
10		0.44		2.80	9.97

Table 4-6. Binding energies (kcal/mol) of complexes of anions with n CF_3H molecules, calculated by M06-2X method with two different basis sets.

	F^-		SO_4^{2-}	
n	6-31+G**	aug-cc-pVTZ	6-31+G**	aug-cc-pVTZ
1	29.31	28.29	28.79	28.37
2	50.09	48.89	54.86	54.01
3	66.25	64.48	77.72	76.19
4	78.65	76.39	98.47	96.56
5	87.51	85.41	116.96	114.54
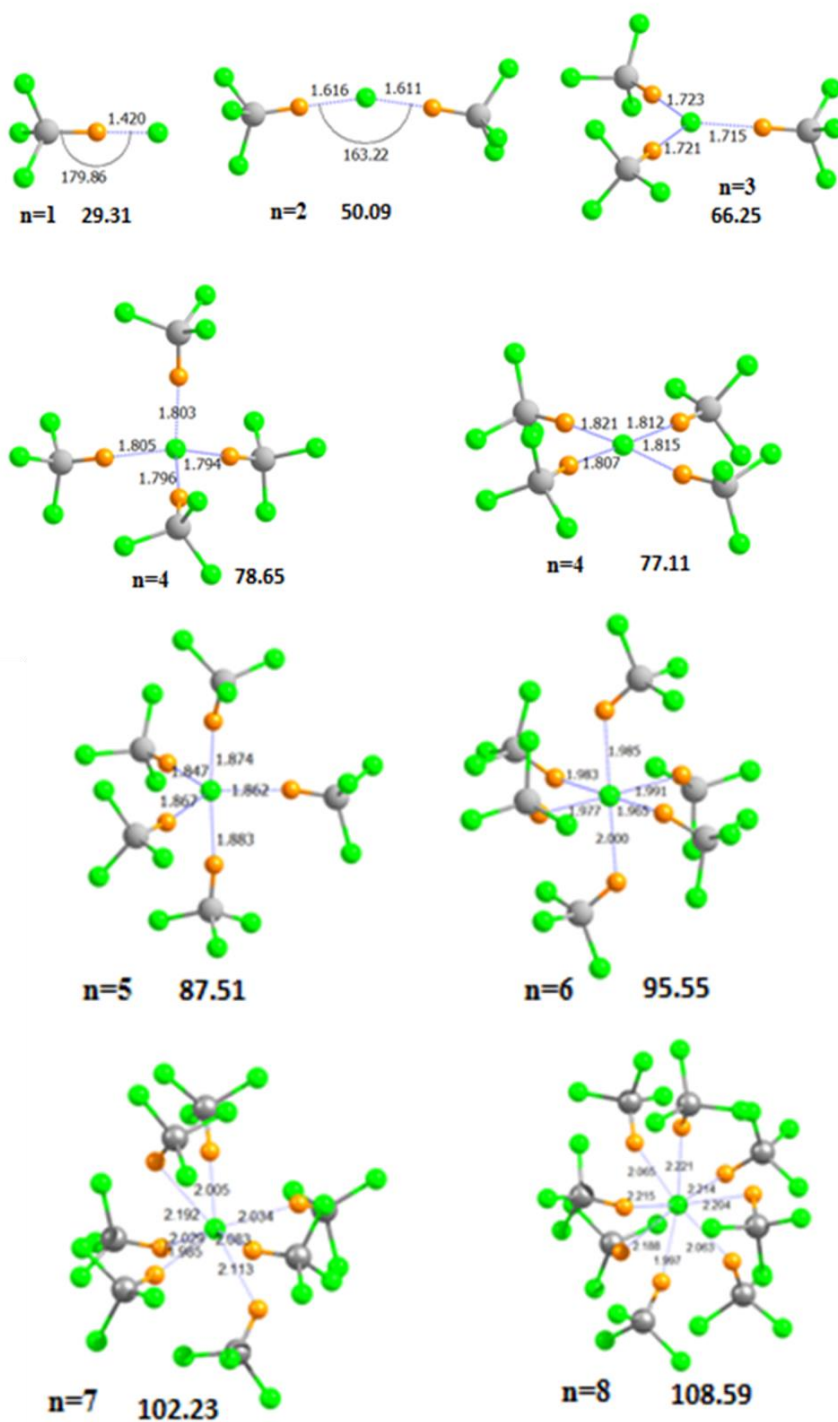
Figure 4-1. Optimized geometries of complexes with n molecules of CF$_3$H surrounding the F- anion. Distance in Å, and binding energies in kcal/mol.
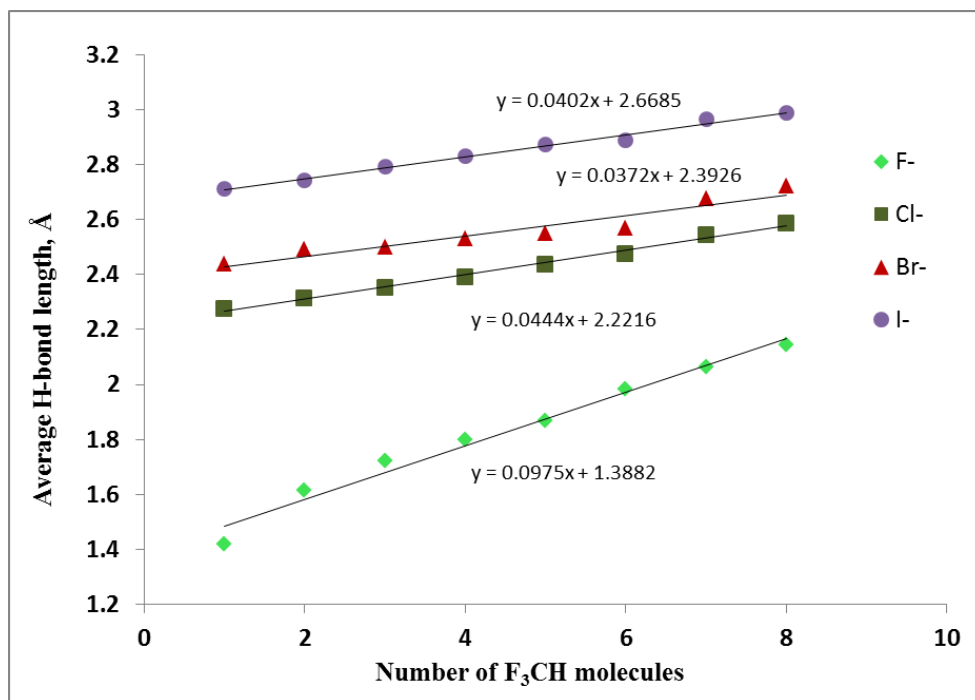
Figure 4-2. Average H-bond length vs number n of surrounding F_3CH molecules for complexes with halide anions.
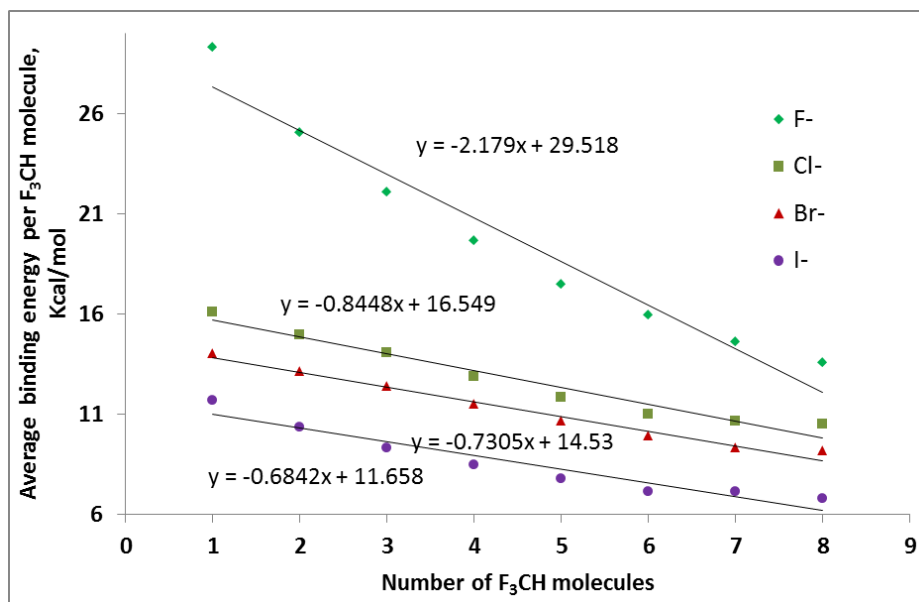
Figure 4-3. Average H-bond energy vs number n of surrounding F_3CH molecules for complexes with halide anions.
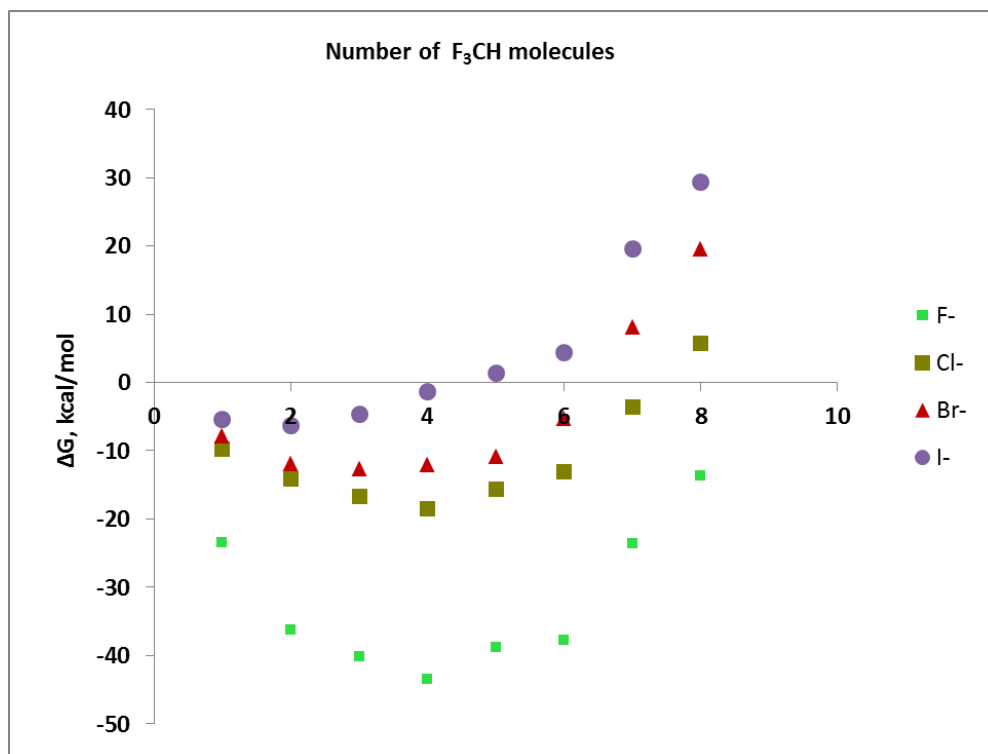
Figure 4-4. Free energy of complexation for binding of halides as function of number of F₃CH molecules.
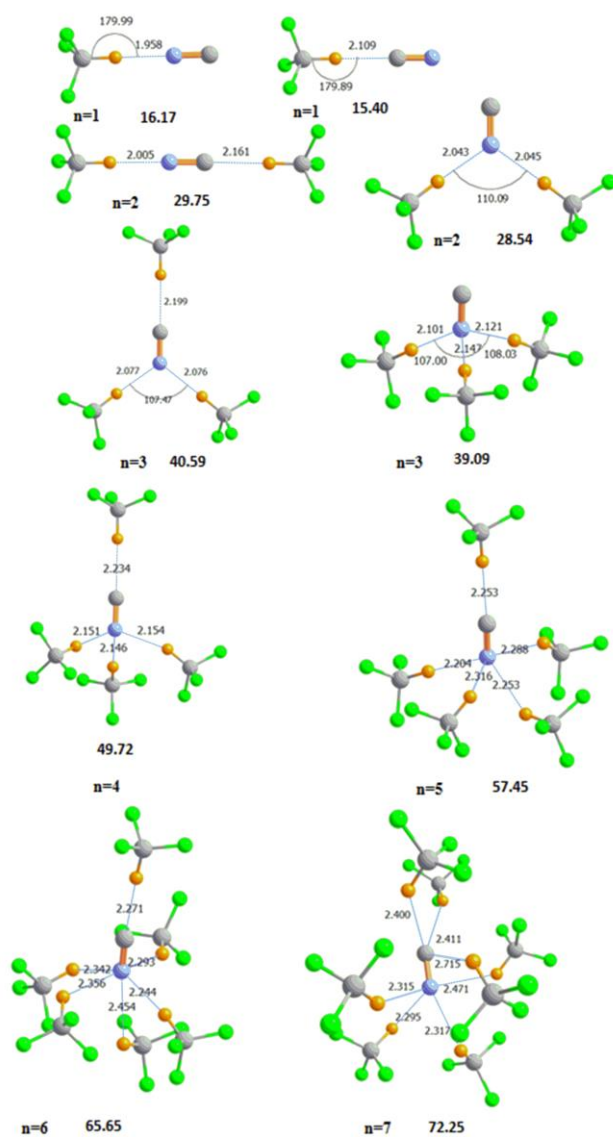
Figure 4-5. Optimized geometries of complexes with n molecules of CF₃H surrounding the CN- anion. Distance in Å, angles in degs, and binding energies in kcal/mol.
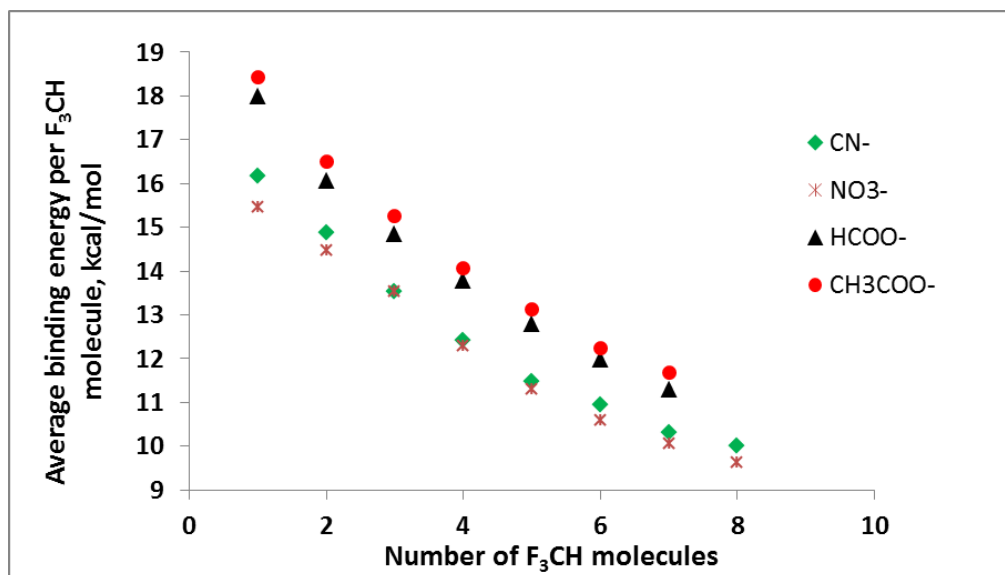
Figure 4-6. Average H-bond energy vs number n of surrounding F_3CH molecules for complexes with CN^-, NO_3^-, $HCOO^-$ and CH_3COO^-.
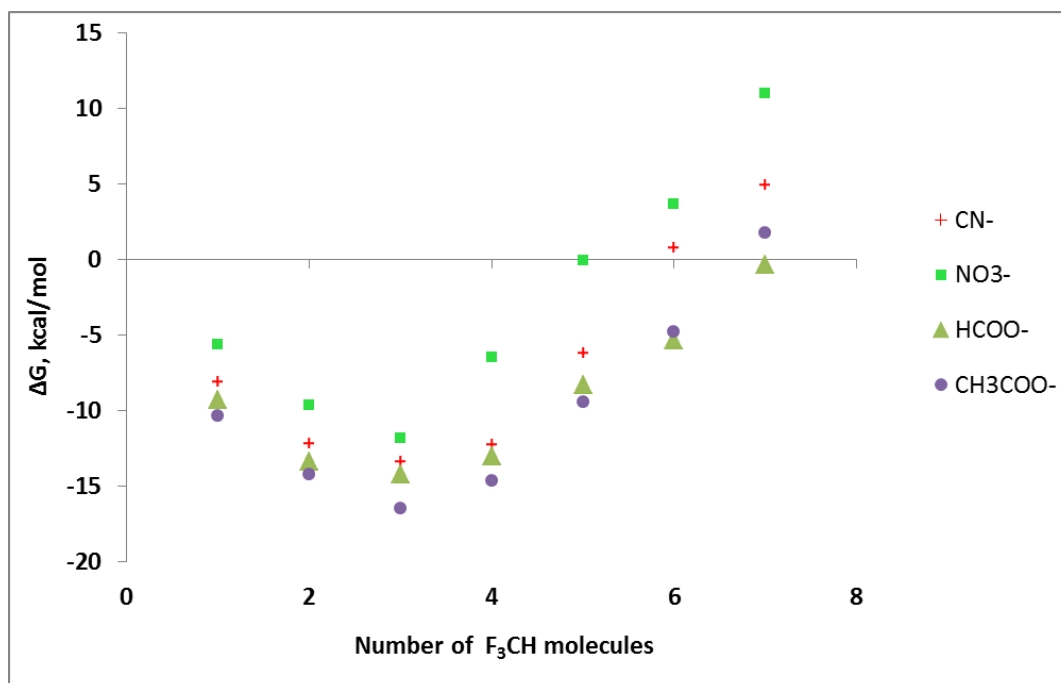
Figure 4-7. Free energy of complexation for binding of CN^-, NO_3^-, $HCOO^-$ and CH_3COO^- with n molecules of F_3CH.
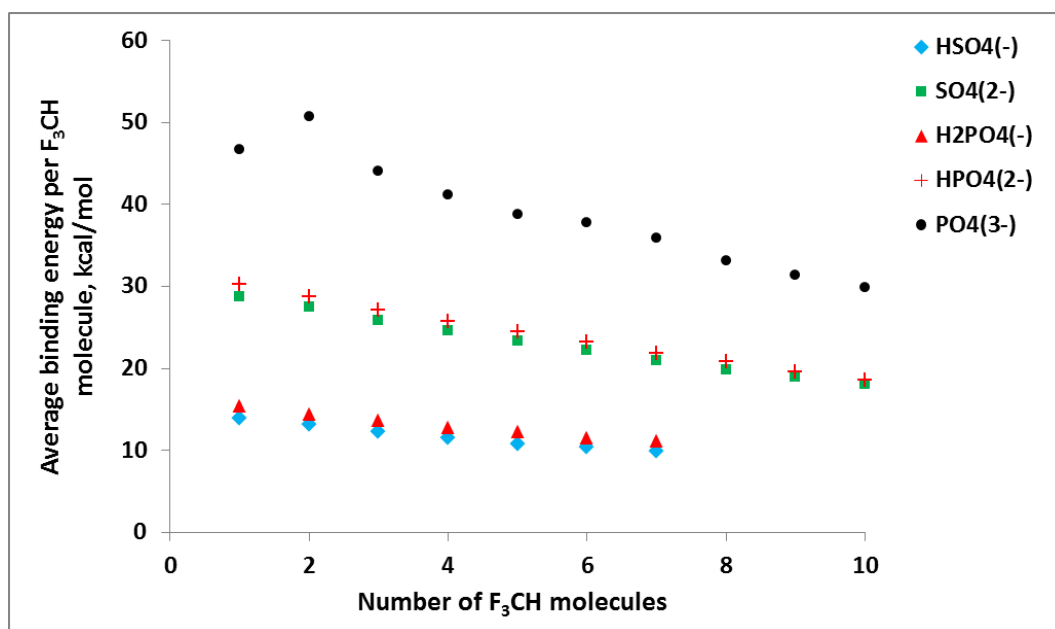
Figure 4-8. Average H-bond energy vs number n of surrounding F_3CH molecules for complexes with HSO_4^-, SO_4^{2-}, $H_2PO_4^-$, HPO_4^{2-} and PO_4^{3-}.
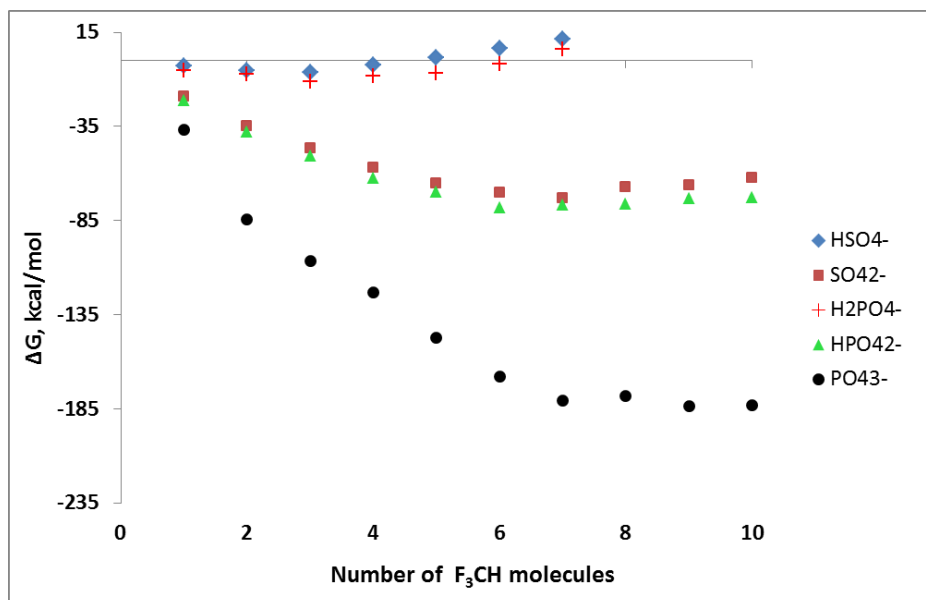
Figure 4-9. Free energy of complexation for binding of HSO_4^-, SO_4^{2-}, $H_2PO_4^-$, HPO_4^{2-} and PO_4^{3-} with n molecules of F_3CH.

CHAPTER 5

ANGULAR DEPENDENCE OF HYDROGEN BOND ENERGY IN NEUTRAL AND

CHARGED SYSTEMS CONTAINING CH AND NH PROTON DONORS1

Abstract

The effects of angular distortions on the H-bond energy are computed in both

neutral and ionic complexes. F_3CH, NCH, and $HNCH^+$ are taken as CH donors and $HCNH$,

$HCNH^+$, and NH_4^+ are NH donors. Ionic complexes are more strongly bound and suffer a

greater loss of H-bond energy upon angular distortion. However, when bending force

constants k are normalized against intrinsic H-bond strength E_b, the k/E_b ratios are similar,

only slightly larger for NH than for CH donors, and with only small perturbations caused

by overall charge. The source of destabilization arising from angular deformation is traced

to exchange repulsion.

5-1. Introduction

After many decades of study, the hydrogen bond (HB) has become arguably the

most thoroughly examined and understood [1-3] of all noncovalent interactions. Because

the HB frequently occurs within the framework of a large system, where it is only one of

many forces that factor into the overall geometry, and is typically not strong enough to

_____

control the structure in and of itself, HBs are usually not free to adopt their optimal internal

geometry. Moreover, the system of interest, whether a large macromolecule or a smaller system immersed in aqueous solvent, is commonly undergoing rapid fluctuations that include the distortions and even breakage of HBs. The sensitivity of HBs to deformation, both stretching and bending, is therefore one of their most important properties.

It is commonly accepted that HBs strive toward linearity, wherein the bridging H atom lies along the axis between the electron donor D and acceptor A atoms, i.e. $\theta(AH\cdot\cdot D)$ tends toward 180°. The energetic cost of distortion from this optimal geometry has been examined in a number of studies, which show [4-9] some dependence upon the specifics of the HB, e.g. the atoms involved, the strength of the bond, and so on. Most of the earlier work has focused on conventional HBs wherein the bridging proton lies between electronegative N, O, or F atoms.

With the growing acceptance of the existence of the CH$\cdot\cdot$D HB, where carbon takes the place of more electronegative atoms as a proton donor [10-12], has come an interest in the elucidation of its properties and how they might differ from conventional HBs. One early study [13] suggested that the angular dependence of CH$\cdot\cdot$O HBs is very much like that of OH$\cdot\cdot$O analogues, at least qualitatively, although certain differences were apparent as well. This study was hardly representative of such bonds in general, though, as only a single proton acceptor molecule (H_2O) was considered. Some of the differences were attributed to the weakness of CH$\cdot\cdot$O HBs in comparison to OH$\cdot\cdot$O. However, this factor can be eliminated if the proton acceptor contains a negative charge, leading to a much stronger CH$\cdot\cdot$D$^-$ HB.

And indeed, the angular dependence of such strong unconventional HBs has scarcely been examined to date. The current work represents an attempt to fill in this gap, considering $CH \cdot \cdot D^-$ HBs for a variety of different anions. By the same token, a strong HB can be generated by placing a positive charge on the proton donor, so the study extends also to $CH^+ \cdot \cdot D$ HBs which can then be compared to their anionic counterparts. Work of this type would not be complete without comparison to more conventional HBs. For this reason, comparisons encompassing a range of different $NH^+ \cdot \cdot D$ HBs can identify fundamental distinctions between HBs involving CH and NH donors, all of which are strengthened by a charge on one of the species. For purposes of expanding the range of system types considered, these ionic systems are compared to their neutral counterparts.

5-2. Methods

Geometries were optimized at the MP2 level using the aug-cc-pVDZ basis set, as implemented in the Gaussian-09 suite of programs [14]. This level of theory is widely used in the literature and provides accurate data for systems of this sort [15-22]. Interaction energies were partitioned into separate contributions by Symmetry Adapted Perturbation Theory (SAPT) [23,24] at the Hartree-Fock level with the same aug-cc-pVDZ basis set as implemented in the MOLPRO software [25]. Charge transfer from electron donor to acceptor was measured via the Natural Bond Orbital (NBO) method [26,27], also with the aug-cc-pVDZ basis set.

5-3. Results

CF$_3$H represents a simple molecule capable of forming CH··D HBs by virtue of its three electron-withdrawing F atoms, and has been commonly used [28-38] as a model CH proton donor in the past. The optimized geometries for complexes combining CF$_3$H with various anions, each involving a different proton-accepting atom, are displayed in Fig 5-1. The equilibrium θ(CH··X) angle lies within 5° of linearity in all four cases. The binding energy E_b was taken as the difference in energy between the optimized complex and the sum of monomer energies, in their optimized geometries; basis set superposition error was corrected by the counterpoise procedure [39,40]. This quantity is displayed by the bold numbers in Fig 5-1.

Another means of examining ionic H-bonds places a positive charge on the proton donor. The HCNH$^+$ cation can act as donor first through its CH end which serves as a good point of comparison with neutral CF$_3$H. These same acceptors can also form a HB with the NH end of HCNH$^+$, offering an interesting and direct comparison between CH and NH donor groups. The corresponding equilibrium structures indicate NH engages in somewhat stronger HBs than CH even if the HB lengths do not always reflect this energetics. The strength of the cationic donor is weakened a bit if the sp-hybridization of HCNH$^+$ is changed to sp^3 in the NH$_4^+$ cation.

In order to unambiguously identify the effect of charge upon the HB energetics, a number of neutral-neutral complexes were considered as well. For example, the F$_3$CH···OH$^-$ anionic complex was transformed to its neutral analogue by adding a proton to the anion: F$_3$CH···OH$_2$. Similarly, the cation-neutral complexes were mutated to the

neutral-neutral by removal of a proton from the donor: e.g. $HNCH^+\cdots OH_2$ changed to $NCH\cdots OH_2$.

So as to examine the sensitivity of each system to bending of the HB, the equilibrium angle was changed in small increments in both directions. With this angle fixed, and the intermolecular HB length also held constant, the remainder of the geometry was fully optimized, including the internal geometries of the individual monomers. In most cases, the energy varies quadratically with angular distortion. That is, the energy can be closely fit to the expression

$$E = -E_b + \tfrac{1}{2} k (\Delta\theta)^2 \tag{1}$$

where k represents a bending force constant, $\Delta\theta$ the distortion of the HB angle from its optimized value, and E_b is the binding energy of the fully optimized complex. θ was varied to encompass distortions of as much as $\pm 65°$ from its equilibrium value in order to fit the data to Eq 1. The fit of the calculated data points in Fig 5-2 by the corresponding parabolas can be seen to be quite good for the neutral-anion systems containing F_3CH as proton donor. Similarly good fits were realized for the other systems considered here.

The first two columns of Table 5-1 report the values obtained for the bending force constant and the optimized binding energy for the ionic complexes, and the corresponding values for their neutral counterparts are displayed in Table 5-2. The binding energies of the $F_3CH\cdots$anion complexes vary from 14.5 kcal/mol for $F_3CH\cdots CN^-$ up to 24.4 kcal/mol for $F_3CH\cdots OH^-$. These values are far higher than the corresponding binding energies of the neutral complexes involving F_3CH again as proton donor, roughly 3 kcal/mol as may be seen in the first rows of Table 5-2. In fact, comparison of these two tables vividly illustrates

the magnifying effect of charge on the HB energies, for any sort of donor or acceptor. Whereas the largest HB energy for the neutral complex is 10.7 kcal/mol, for $CNH\cdots NH_3$, all of the charged HBs are more strongly bound than this quantity, up to a maximum of 33.1 kcal/mol for $HCNH^+\cdots NH_3$.

Of particular importance here are the bending force constants k which embody the sensitivity of the HB energy to angular distortion. These constants are generally larger for the charged systems as well. Using the same pair of systems as an example, k for the neutral $CNH\cdots NH_3$ system is less than half that for the ionic $HCNH^+\cdots NH_3$. The force constants for the systems where F_3CH serves as proton donor are particularly sensitive to the presence of charge. When paired with a neutral acceptor, k remains below 3 kcal mol^{-1} rad^{-2}, but this value rises to between 10 and 18 kcal mol^{-1} rad^{-2} when the acceptor is an anion.

It is generally expected that the more strongly bound complexes will also be more sensitive to angular distortion. For example, Fig 5-3 illustrates a nearly linear relationship between E_b and k. As a means of normalizing this overall tendency, the k/E_b ratio provides a measure of the intrinsic sensitivity of a given system to angular distortion. This ratio is displayed in the third column of Tables 5-1 and 5-2, where it may be seen that the magnifying effects of charge upon both HB energy and force constant are largely neutralized. That is, the k/E_b ratios of the neutral and charged HB systems are much more similar to one another. For example, this ratio is equal to 1.11 and 1.50 rad^{-2} for $HCNH^+\cdots NH_3$ and $CNH\cdots NH_3$, respectively.

The range of these quantities for each of a given set of systems can be used to better understand the principles at work. Table 5-3 characterizes each set by the nature of the

proton donor. Considering F_3CH as donor, its HB energy with various anions varies between 15 and 24 kcal/mol, whereas the same quantity lies in the 3.1-3.3 kcal/mol range when paired with a neutral acceptor. The range of k is likewise considerably higher for the anionic acceptors. On the other hand, the ranges of the k/E_b ratio are more similar. For example, the range for $F_3CH\cdots$anion is only a bit larger than that for $F_3CH\cdots$neutral. The other CH donor displays somewhat different behavior in that the ionic complexes with $HNCH^+$ as donor have a k/E_b ratio a bit smaller than that of its neutral NCH donor analogue. Whether ionic or neutral, changing from CH donor to NH raises this ratio a small amount. Like the CH donors, k/E_b is smaller for the ionic $NH^+\cdot$neutral complexes than for their $NH\cdot$neutral counterparts, up to a maximum of 1.8 rad^{-2} for the latter.

As another point of interest, the penultimate column of Tables 5-1 and 5-2 reports a quantity related to the HB strength. Rather than the total binding energy, E(2) instead represents an energetic measure of the NBO charge transfer that takes place from the lone pairs of the proton acceptor atom to the antibonding σ^* orbital of the CH/NH bond. Although there is a general tendency for some correlation between E(2) and E_b, any such correlation is far from perfect. These deviations suggest that the strengths of these HBs are due only in part to this measure of charge transfer.

The last column of Tables 5-1 and 5-2 reflects the competition between the acid and base for the bridging proton. Specifically, E_a-E_b refers to the difference between the deprotonation energy of the acid on the left, and the protonation energy of the base on the right. Considering the first row of Table 5-1 as an example, it takes 51.03 kcal/mol more energy to remove the proton from F_3CH than is released when Cl^- attracts the proton to

form HCl. $HCNH^+$ and OH_2 are more nearly balanced in that the removal of the proton from $HCNH^+$ requires almost the same amount of energy as is released when water acquires a proton to form OH_3^+.

In summary, ionic HBs are invariably more strongly bound than their neutral counterparts, and they also have correspondingly larger bending force constants k. Whether neutral or charged, the NH group tends to form stronger HBs than does CH, although not necessarily by a wide margin. These patterns are altered, however, when one considers the normalized sensitivity to angular distortion, characterized by k/E_b. This quantity lies in the neighborhood of 1 rad^{-2}, but is somewhat smaller for systems containing CH donors F_3CH and $HNCH^+$, and larger for NCH as donor. In terms of this normalized quantity, there is not a dramatic difference between CH and NH donors.

5-3.1. Energy Components

While it had been an element of conventional wisdom for some time that the weakening of the HB associated with its bending arises from a reduction in electrostatic attraction between the two subunits, recent work [41-45] has laid the blame largely at the feet of exchange repulsion. The bending of the H-bond acts in some cases to destabilize the electrostatic attraction, and in others to have the opposite effect wherein Coulombic forces favor a bent structure. Dispersion and induction generally favor a certain amount of nonlinearity as well. But angular distortions raise the exchange repulsion by a substantial amount, overwhelming any stabilizing influences of the other components. And indeed this same principle is not limited to HBs, but is seen in halogen, chalcogen, and pnicogen bonds as well [41].

However, there has been little inquiry into the factors that contribute to the distortion energy of unconventional CH··X HBs, nor of ionic HBs in general. In order to address this question, the interaction energy of each of the systems was decomposed into its constituent factors via the SAPT procedure. This decomposition provides not only the electrostatic (ES), induction (IND), dispersion (DISP), and exchange (EX) energies, but also the combined exchange-induction (EXIND) and exchange-dispersion (ESDISP) terms.

The changes in each of these terms that arise when the H-bond is distorted by 30° are reported in Tables 5-4 and 5-5 for the charged and neutral systems, respectively. While there is a good deal of variability in the numerical values from one complex to the next, there are certain features that they share. In the first place, the angular distortion results in a more attractive (more negative) electrostatic attraction, in some cases by more than 2 kcal/mol. The same can be said of the IND energy, although the quantitative amount differs from the ES stabilization, sometimes larger and sometimes smaller. The changes in the dispersion energy are smaller in magnitude, but also consistently more stabilizing as the H-bond is distorted. The various exchange terms in the next three columns behave in quite the opposite fashion. All of these quantities become more positive, i.e. more repulsive, when the H-bond is misoriented, and by quite sizable amounts.

Taking the $HNCH^+\cdots OCH_2$ system as an example of the typical system, the ES, IND, and DISP terms combined would stabilize a 30° bend by 3.6 kcal/mol, but the combined exchange terms push the energy up by the larger amount of 5.6 kcal/mol. The

end result of adding together all of these contributions is a 1.95 destabilization, as displayed in the penultimate column of Table 5-4.

It may be noted that there are certain exceptions to the above trends. In particular, some of the systems containing F_3CH as proton donor show little sensitivity of the ES term to distortion. The most notable outlier is the $F_3CH\cdots OH^-$ complex where the bend causes a loss of not only electrostatic attraction, but also induction energy. And indeed, for this same system, the exchange terms behave in an opposite way than in all of the other systems, becoming less positive. This discrepant behavior was traced to a substantial reorientation of the complex: When the F_3CH molecule is rotated 30° away from the O proton acceptor, the OH^- anion undergoes a 27° reorientation such that $\theta(C\cdot\cdot OH)$ changes from 121° in the fully optimized structure to 148°.

These results, qualitatively similar for all of the systems, lead to the conclusion that it is exchange which is responsible for the weakening of these H-bonds upon angular distortion. Moreover, this same principle applies to CH and well as conventional H-bonds, and for cationic and anionic systems as well as neutral complexes. It should be further stressed that this conclusion comports with the same observation for a variety of other neutral H-bonds, as well as halogen, chalcogen, and pnicogen bonds [41].

5-4. Conclusions

In summary, all sorts of HBs, whether CH or NH donor, cationic, anionic, or neutral, suffer a loss of binding energy as angular deformations are introduced into the geometry of the HB. This loss of energy is very roughly proportional to the intrinsic strength of the HB, as measured by binding energy E_b. This quantity is in turn much larger

for charged than for neutral HBs, and NH acts as a stronger donor than does CH. However, these distinctions are nearly washed out when the HB energy sensitivity to distortion is normalized by dividing the bending force constant by the optimal binding strength. In general, the k/E_b ratios are slightly larger for NH donors than for CH, but only slightly so. Regarding the effect of charge, the ionic $F_3CH\cdot\cdot$anion systems are characterized by a slightly larger k/E_b ratio than their neutral counterparts. On the other hand, the removal of the positive charge induces a small increase in this ratio for both CH and NH ends of the $HNCH^+$ donors.

Energy decomposition reveals that the attractive components of HBs, i.e. electrostatic, induction, and dispersion energies, all become more stabilizing upon angular distortion of the HB. Outweighing this effect, though, is the even larger destabilization caused by increasing exchange repulsion, which is thus identified as the major contributor to the loss of HB energy induced by bending. This phenomenon appears to be a general one, common not only to the ionic and neutral $NH\cdot\cdot D$ and $CH\cdot\cdot D$ HBs considered here, but also to the related halogen, chalcogen, and pnicogen bonds examined earlier.

References

[1]   G.A. Jeffrey, W. Saenger, Hydrogen Bonding in Biological Structures, Springer-Verlag, Berlin, 1991.

[2]   S. Scheiner, Hydrogen Bonding. A Theoretical Perspective, Oxford University Press, New York, 1997.

[3]   G. Gilli, P. Gilli, The Nature of the Hydrogen Bond, Oxford University Press, Oxford, UK, 2009.

[4]   S. Scheiner, J. Mol. Struct. 177 (1988) 79.

[5]   S.M. Cybulski, S. Scheiner, J. Phys. Chem. 93 (1989) 6565.

[6]   S.M. Cybulski, S. Scheiner, J. Phys. Chem. 94 (1990) 6106.

[7]   S. Scheiner, X. Duan, Phys. Chem. Chem. Phys. 60 (1991) 874.

[8]   X. Duan, S. Scheiner, J. Am. Chem. Soc. 114 (1992) 5849.

[9]   S. Scheiner, L. Wang, J. Am. Chem. Soc. 115 (1993) 1958.

[10]   S. Cybulski, S. Scheiner, J. Am. Chem. Soc. 109 (1987) 4199.

[11]   Y. Gu, T. Kar, S. Scheiner, J. Mol. Struct. 552 (2000) 17.

[12]   E. Kryachko, S. Scheiner, J. Phys. Chem. A 108 (2004) 2527.

[13]   Y. Gu, T. Kar, S. Scheiner, J. Am. Chem. Soc. 121 (1999) 9411.

[14]   M.J. Frisch, G.W. Trucks, H.B. Schlegel, G.E. Scuseria, M.A. Robb, J.R. Cheeseman, G. Scalmani, V. Barone, B. Mennucci, G.A. Petersson, H. Nakatsuji, M. Caricato, X. Li, H.P. Hratchian, A.F. Izmaylov, J. Bloino, G. Zheng, J.L. Sonnenberg, M. Hada, M. Ehara, K. Toyota, R. Fukuda, J. Hasegawa, M. Ishida, T. Nakajima, Y. Honda, O. Kitao, H. Nakai, T. Vreven, J. Montgomery, J. A., J.E. Peralta, F. Ogliaro, M. Bearpark, J.J. Heyd, E. Brothers, K.N. Kudin, V.N. Staroverov, R. Kobayashi, J. Normand, K. Raghavachari, A. Rendell, J.C. Burant, S.S. Iyengar, J. Tomasi, M. Cossi, N. Rega, J.M. Millam, M. Klene, J.E. Knox, J.B. Cross, V. Bakken, C. Adamo, J. Jaramillo, R. Gomperts, R.E. Stratmann, O. Yazyev, A.J. Austin, R. Cammi, C. Pomelli, J.W. Ochterski, R.L. Martin, K. Morokuma, V.G. Zakrzewski, G.A. Voth, P. Salvador, J.J. Dannenberg, S.

Dapprich, A.D. Daniels, O. Farkas, J.B. Foresman, J.V. Ortiz, J. Cioslowski, D.J. Fox, Gaussian 09, Wallingford, CT, 2009.

[15]   D. Hauchecorne, N. Nagels, B.J. van der Veken, W.A. Herrebout, Phys. Chem. Chem. Phys. 14 (2012) 681.

[16]   S. Scheiner, J. Phys. Chem. A 115 (2011) 11202.

[17]   D. Hauchecorne, W.A. Herrebout, J. Phys. Chem. A 117 (2013) 11548.

[18]   G. Sanchez-Sanz, C. Trujillo, I. Alkorta, J. Elguero, Phys. Chem. Chem. Phys. 16 (2014) 15900.

[19]   Y. Chen, L. Yao, X. Lin, Comput. Theor. Chem. 1036 (2014) 44.

[20]   M.D. Esrafili, P. Fatehi, M. Solimannejad, Comput. Theor. Chem. 1034 (2014) 1.

[21]   N. Nagels, Y. Geboe, B. Pinter, F.D. Proft, W.A. Herrebout, Chem. Eur. J. 20 (2014) 8433.

[22]   T. Lang, X. Li, L. Meng, S. Zheng, Y. Zeng, Struct. Chem. 26 (2015) 213.

[23]   K. Szalewicz, B. Jeziorski, in: S. Scheiner (Ed.), Molecular Interactions. From Van der Waals to Strongly Bound Complexes, Wiley, New York, 1997, p. 3.

[24]   R. Moszynski, P.E.S. Wormer, B. Jeziorski, A. van der Avoird, J. Chem. Phys. 103 (1995) 8058.

[25]   H.-J. Werner, P.J. Knowles, F.R. Manby, M. Schütz, P. Celani, G. Knizia, T. Korona, R. Lindh, A. Mitrushenkov, G. Rauhut, T.B. Adler, R.D. Amos, A. Bernhardsson, A. Berning, D.L. Cooper, M.J.O. Deegan, A.J. Dobbyn, F. Eckert, E. Goll, C. Hampel, A. Hesselmann, G. Hetzer, T. Hrenar, G. Jansen, C. Köppl, Y. Liu, A.W. Lloyd, R.A. Mata, A.J. May, S.J. McNicholas, W. Meyer, M.E. Mura,

A. Nicklaß, P. Palmieri, K. Pflüger, R. Pitzer, M. Reiher, T. Shiozaki, H. Stoll, A.J. Stone, R. Tarroni, T. Thorsteinsson, M. Wang, A. Wolf, MOLPRO, 2010.

[26]   A.E. Reed, L.A. Curtiss, F. Weinhold, Chem. Rev. 88 (1988) 899.

[27]   A.E. Reed, F. Weinhold, L.A. Curtiss, D.J. Pochatko, J. Chem. Phys. 84 (1986) 5687.

[28]   I. Alkorta, S. Maluendes, J. Phys. Chem. 99 (1995) 6457.

[29]   B. Reimann, K. Buchhold, S. Vaupel, B. Brutschy, Z. Havlas, V. Spirko, P. Hobza, J. Phys. Chem. A 105 (2001) 5560.

[30]   E.S. Kryachko, T. Zeegers-Huyskens, J. Mol. Struct. 615 (2002) 251.

[31]   L. Pejov, K. Hermansson, J. Chem. Phys. 119 (2003) 313.

[32]   S.K. Rhee, S.H. Kim, S. Lee, J.Y. Lee, Chem. Phys. 297 (2004) 21.

[33]   J.L. Alonso, S. Antolínez, S. Blanco, A. Lesarri, J.C. López, W. Caminati, J. Am. Chem. Soc. 126 (2004) 3244

[34]   S.A.C. McDowell, Chem. Phys. Lett. 441 (2007) 194.

[35]   K. Pluháková, P. Hobza, ChemPhysChem. 8 (2007) 1352.

[36]   K.S. Rutkowski, S.M. Melikova, P. Rodziewicz, W.A. Herrebout, B.J. van der Veken, A. Koll, J. Mol. Struct. 880 (2008) 64.

[37]   A. Mukhopadhyay, P. Pandey, T. Chakraborty, J. Phys. Chem. A 114 (2010) 5026.

[38]   P.R. Shirhatti, D.K. Maity, S. Bhattacharyya, S. Wategaonkar, ChemPhysChem. 15 (2014) 109.

[39]   S.F. Boys, F. Bernardi, Mol. Phys. 19 (1970) 553.

[40]   Z. Latajka, S. Scheiner, J. Chem. Phys. 87 (1987) 1194.

[41]   U. Adhikari, S. Scheiner, Chem. Phys. Lett. 532 (2012) 31.

[42]   A.J. Stone, J. Am. Chem. Soc. 135 (2013) 7005.

[43]   S.M. Huber, J.D. Scanlon, E. Jimenez-Izal, J.M. Ugalde, I. Infante, Phys. Chem. Chem. Phys. 15 (2013) 10350.

[44]   L. Wang, J. Gao, F. Bi, B. Song, C. Liu, J. Phys. Chem. A 118 (2014) 9140.

[45]   M. Kolár, J. Hostaš, P. Hobza, Phys. Chem. Chem. Phys. 16 (2014) 9987.

Tables and Figures

Table 5-1. Measures of sensitivity of binding energy to angular distortion of H-bond for anion-neutral and cation-neutral H-bonded complexes. k represents the force constant, E_b is counterpoise-corrected binding energy and E(2) is the NBO charge transfer.

complex	k kcal mol^{-1} rad^{-2}	E_b kcal/mol	k/E_b rad^{-2}	E(2) kcal/mol	$(E_a-E_b)^a$ kcal/mol
$F_3CH\cdots Cl^-$	11.23	15.16	0.74	25.60	51.03
$F_3CH\cdots NC^-$	10.45	14.89	0.70	25.61	47.72
$F_3CH\cdots CN^-$	11.00	14.53	0.76	34.67	29.77
$F_3CH\cdots OH^-$	17.88	24.39	0.73	64.92	-8.48
$HNCH^+\cdots FH$	5.90	11.33	0.52	21.80	72.33
$HNCH^+\cdots OH_2$	19.06	19.97	0.95	58.19	21.30
$HNCH^+\cdots OCH_2$	17.14	19.88	0.86	71.42	15.83
$HNCH^+\cdots NH_3$	22.52	24.40	0.92	57.68	-19.95
$HCNH^+\cdots FH$	14.75	14.85	0.99	46.21	54.38
$HCNH^+\cdots OH_2^b$	24.51	24.00	1.02	56.29	3.35
$HCNH^+\cdots OCH_2^b$	21.37	23.88	0.90	61.90	-2.12
$HCNH^+\cdots NH_3^b$	36.60	33.07	1.11	89.96	-37.90
$NH_4^+\cdots FH$	4.93	11.12	0.44	14.71	92.28
$NH_4^+\cdots OH_2$	15.12	19.25	0.79	39.47	41.25
$NH_4^+\cdots OCH_2$	10.87	19.49	0.56	39.79	35.78
$NH_4^+\cdots NH_3$	34.10	25.19	1.35	83.45	0.00

[a]difference between deprotonation energy of acid and protonation energy of base
[b]optimized under restricted condition of fixed r(NH) bond length

Table 5-2. Measures of sensitivity of binding energy to angular distortion of H-bond for neutral-neutral H-bonded complexes. k represents the force constant, E_b is counterpoise-corrected binding energy and E(2) is the NBO charge transfer.

complex	k	E_b	k/E_b	E(2)	$(E_a-E_b)^a$
	kcal mol^{-1} rad^{-2}	kcal/mol	rad^{-2}	kcal/mol	kcal/mol
$F_3CH\cdots NCH$	1.13	3.11	0.36	6.12	210.78
$F_3CH\cdots CNH$	1.41	3.10	0.45	9.62	192.82
$F_3CH\cdots OH_2$	1.74	3.26	0.53	6.90	214.13
$NCH\cdots FH$	2.68	2.61	1.03	5.67	235.39
$NCH\cdots OH_2$	4.13	4.69	0.88	10.16	184.36
$NCH\cdots OCH_2$	6.96	4.27	1.63	9.74	178.89
$NCH\cdots NH_3$	6.94	6.03	1.15	15.50	143.11
$CNH\cdots FH$	5.78	4.08	1.42	11.43	217.44
$CNH\cdots OH_2$	10.18	7.66	1.33	23.21	166.41
$CNH\cdots OCH_2$	13.26	7.30	1.82	23.82	160.94
$CNH\cdots NH_3$	16.13	10.73	1.50	38.19	125.16

^{a}difference between deprotonation energy of acid and protonation energy of base

Table 5-3. Ranges of various quantities for types of H-bonds

complex type	k	E_b	k/E_b
	kcal mol^{-1} rad^{-2}	kcal/mol	rad^{-2}
$F_3CH\cdots$anion	10 - 18	15 - 24	0.7 - 0.8
$HNCH^+\cdots$neutral	6 - 23	11 - 24	0.5 - 0.9
$HCNH^+\cdots$neutral	15 - 37	15 - 33	0.9 - 1.1
$NH_4^+\cdots$neutral	5 - 34	11 - 25	0.4 - 1.4
$F_3CH\cdots$neutral	1.1 - 1.7	3.1 - 3.3	0.4 - 0.5
$NCH\cdots$neutral	3 - 7	3 - 6	0.9 - 1.6
$CNH\cdots$neutral	6 -16	4 - 11	1.4 - 1.8

Table 5-4. Changes incurred in various SAPT components of the interaction energy of ionic systems as a result of 30° angular distortion, as well as change in binding energy E_b. All quantities in kcal/mol.

complex	ES	IND	DISP	EX	EXIND	EXDISP	sum	E_b
$F_3CH\cdots Cl^-$	-0.23	-1.70	-0.40	1.74	1.79	0.14	1.34	1.31
$F_3CH\cdots NC^-$	0.04	-0.85	-0.35	1.44	0.90	0.09	1.27	1.32
$F_3CH\cdots CN^-$	-0.04	-1.28	-0.35	1.51	1.39	0.11	1.34	1.25
$F_3CH\cdots OH^-$	2.32	2.71	-0.11	-	-2.36	-0.12	2.02	2.45
$HNCH^+\cdots FH$	-1.02	-0.52	-0.32	2.07	0.55	0.07	0.83	0.85
$HNCH^+\cdots OH_2$	-1.29	-1.17	-0.46	3.91	1.15	0.13	2.27	2.18
$HNCH^+\cdots OCH_2$	-2.11	-0.97	-0.54	4.56	0.90	0.11	1.95	2.70
$HNCH^+\cdots NH_3$	-0.85	-1.36	-0.44	3.54	1.41	0.12	2.42	2.86
$HCNH^+\cdots FH$	-1.12	-0.66	-0.45	3.16	0.91	0.1	1.94	1.99
$HCNH^+\cdots OH_2$	-1.25	-1.42	-0.54	4.41	1.49	0.16	2.85	2.47
$HCNH^+\cdots OCH_2$	-1.71	-0.96	-0.65	4.89	1.08	0.15	2.80	2.93
$HCNH^+\cdots NH_3$	-0.99	-1.96	-0.65	5.18	2.13	0.20	3.91	4.23
$NH_4^+\cdots FH$	-1.15	-0.50	-0.34	1.84	0.53	0.07	0.45	0.11
$NH_4^+\cdots OH_2$	-1.07	-0.90	-0.38	2.63	0.90	0.11	1.29	1.46
$NH_4^+\cdots OCH_2$	-2.33	-1.23	-0.64	3.97	1.03	0.15	0.95	1.74
$NH_4^+\cdots NH_3$	-0.87	-1.53	-0.53	3.84	1.64	0.18	2.73	3.81

Table 5-5. Changes incurred in various SAPT components of the total binding energy of neutral systems as a result of 30° angular distortion, as well as change in binding energy E_b. All quantities in kcal/mol.

complex	ES	IND	DISP	EX	EXIND	EXDISP	sum	E_b
$F_3CH\cdots NCH$	-0.02	-0.08	-0.12	0.25	0.09	0.02	0.14	0.13
$F_3CH\cdots CNH$	-0.04	-0.12	-0.12	0.27	0.14	0.02	0.15	0.16
$F_3CH\cdots OH_2$	-0.10	-0.13	-0.17	0.43	0.14	0.03	0.20	0.21
$NCH\cdots FH$	-0.32	-0.14	-0.12	0.62	0.14	0.03	0.21	0.25
$NCH\cdots OH_2$	-0.02	-0.12	-0.16	0.60	0.16	0.04	0.50	0.51
$NCH\cdots OCH_2$	-0.35	-0.55	-0.75	1.46	0.45	0.10	0.36	0.22
$NCH\cdots NH_3$	-0.05	-0.23	-0.21	0.94	0.31	0.06	0.82	0.87
$CNH\cdots FH$	-0.75	-0.41	-0.27	1.40	0.42	0.08	0.47	0.57
$CNH\cdots OH_2$	0.01	-0.42	-0.50	2.10	0.68	0.12	1.99	1.15
$CNH\cdots OCH_2$	-2.23	-1.70	-1.40	4.71	1.58	0.32	1.28	1.31
$CNH\cdots NH_3$	-0.23	-0.64	-0.41	2.14	0.83	0.13	1.82	1.87
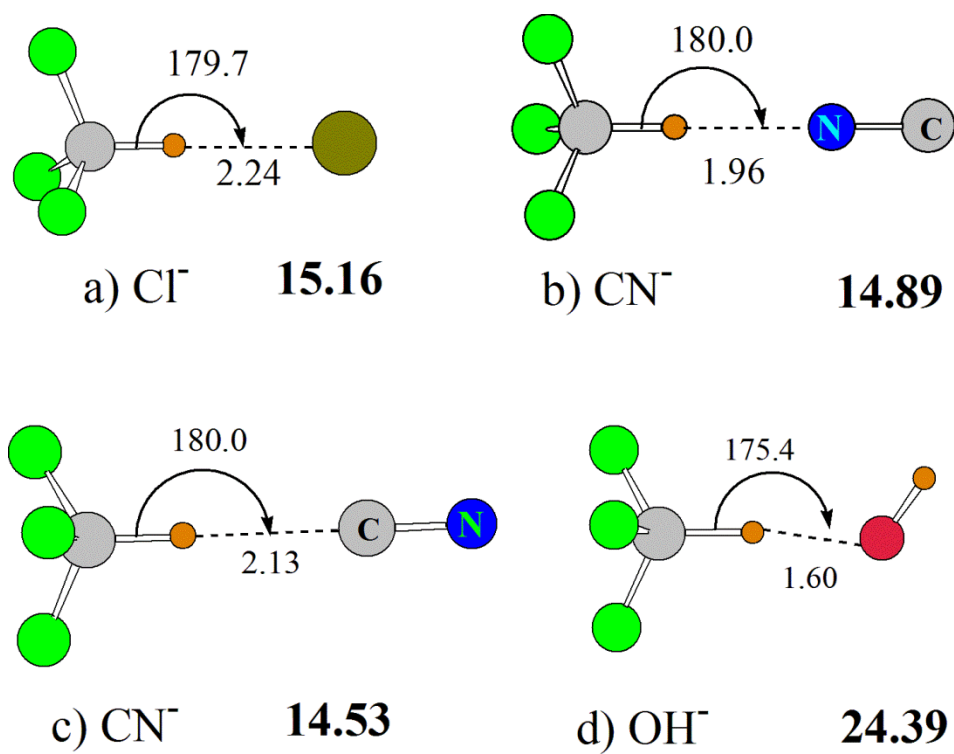
Figure 5-1. Optimized geometries of neutral-anion H-bonded complexes with CF3H as proton-donor. The number in bold indicates counterpoise-corrected binding energy in kcal/mol. Distances are in Å and angles are in degrees.
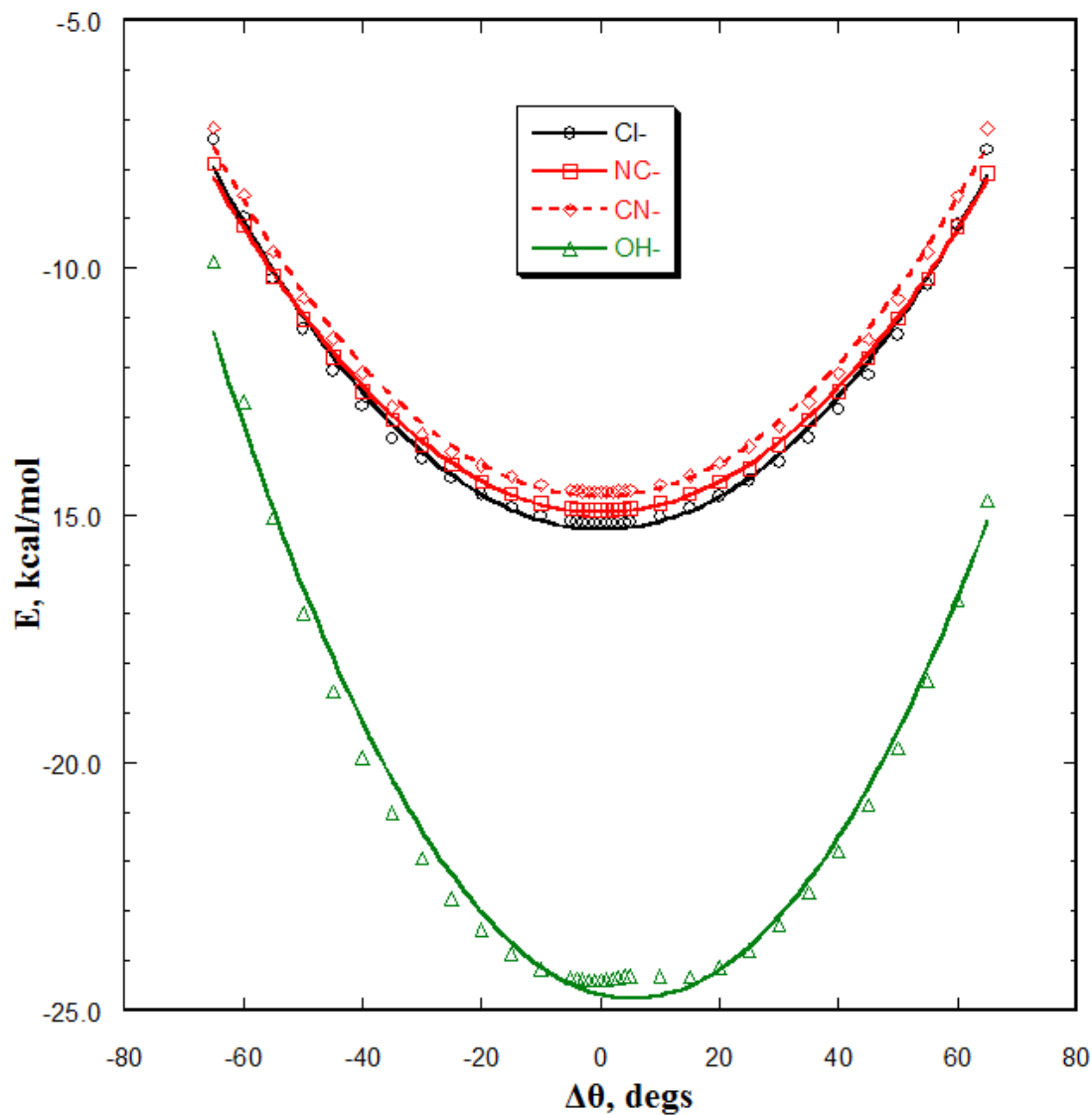
Figure 5-2. Variation of hydrogen bond energy of the neutral-anion complexes in Fig 5-1 with F3CH as proton donor as θ(CH··X) angle deviates from its optimized value. Curves represent the parabolas that are fit to the data points shown.
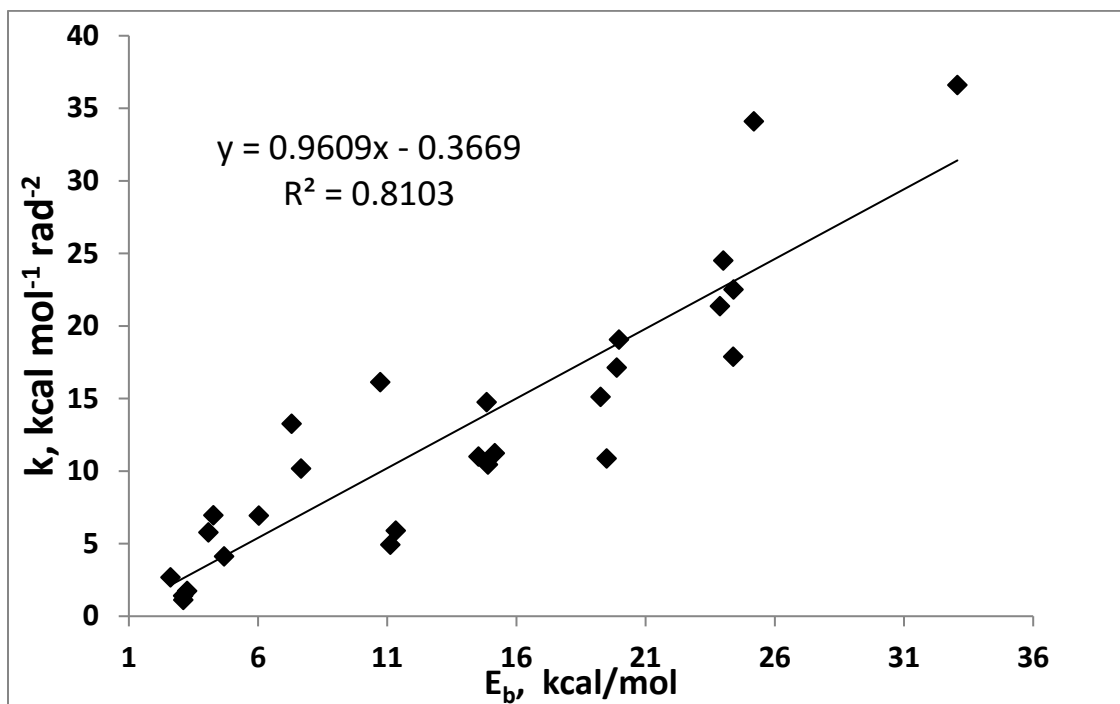
Figure 5-3. Correlation of bending force constant k vs binding energy.

CHAPTER 6

LONG-RANGE BEHAVIOR OF NONCOVALENT BONDS. NEUTRAL AND

CHARGED H-BONDS, PNICOGEN, CHALCOGEN, AND HALOGEN BONDS[1]

Abstract

Ab initio calculations show the drop in interaction energy with bond stretch ΔR can be fit to a common power n, in the functional form ΔR^{-n}. This exponent is smaller for charged H-bonds, as compared to neutral systems, where n varies in the order pnicogen < chalcogen < halogen bond. The decay is slowest for the electrostatic term, followed by induction and then by dispersion. The halogen bond has the greatest sensitivity to bond stretching in terms of all three components. The values of the exponent n are smaller for electrostatic energy than would be expected if it arose purely as a result of classical multipole interactions, such as dipole-dipole for the neutral systems. The exponents are larger when the fitting is done with respect to intermolecular distance R, rather than to its stretch relative to equilibrium length, although still not precisely matching what might be expected on classical grounds.

6-1. Introduction

Over the years, a great deal of information has accumulated regarding molecular interactions. Perhaps the most widely studied of these noncovalent forces is the hydrogen bond (HB), which embodies nearly a century of research [1-15] over the years. The HB was followed in ensuing years by examination of other related noncovalent bonds. The halogen bond, in which the bridging H is replaced by a halogen atom, was the next [16-29] in this chronology. While an attraction between a halogen and another electronegative atom seemed counterintuitive at first, it was realized that the partial negative charge around a halogen atom is quite anisotropic and contains positive as well as negative sub-regions. The electrostatic attraction is supplemented by a transfer of charge from the halogen acceptor atom to the R-X σ^* antibonding orbital, where R represents any atom covalently attached to halogen X. The catalogue of noncovalent bonds was soon enlarged by the finding that the halogen can be replaced by other electronegative atoms, most particularly those of the chalcogen [30-40] and pnicogen [41-51] families.

The vast majority of information that has arisen about these various noncovalent bonds has been concerned with equilibrium geometries, those structures in which the donor and acceptor groups are situated fairly close to one another, where component attractive and repulsive forces balance one another. However, these interactions do not disappear when the two species begin to separate; they are merely weakened. The rate at which this weakening occurs has important implications. For example, if the noncovalent bond strength were to undergo only gradual decline, its effects would be important even if the two relevant groups were removed by fairly long separations. There is presumably a cutoff

distance for each interaction, beyond which any lingering attractive forces are small enough to be comfortably ignored. But what is the cutoff for each sort of noncovalent bond, and how rapidly does the interaction energy approach this threshold? In a related question, what is the functional dependence of interaction energy on the separation distance R? The answers to these questions are especially important to the formulation of empirical functions designed to incorporate the effects of various noncovalent bonds into force fields that are used to simulate the dynamics of various systems.

In terms of explicit consideration of noncovalent bonds that are stretched well beyond their equilibrium separation, the H-bond has motivated a certain amount of limited study. In most cases, the interaction energy has been traced out, point by point, over a range of intermolecular distance. However, few of these studies extended this range of separation beyond 2 or 3 Å. Moreover, there have been scarce attempts to fit these points to a particular function, particularly at long range. There has been even less work in this direction addressing charged HBs, either cation-neutral or anion-neutral. And other noncovalent bonds, most notably the aforementioned halogen, chalcogen, and pnicogen bonds have been largely ignored [52] in terms of their long-range energetics.

The present work represents an attempt to fill in the existing gaps in our knowledge of the long-range behavior of the various sorts of noncovalent bonds. The neutral HB is compared to its ionic analogues, and these systems are then placed in the context of the halogen, chalcogen, and pnicogen bonds. The focus lies on the long range interaction, going out to as far as 11 Å stretched beyond the equilibrium separation. Attempts are made to ascertain which sort of function fits the computed binding energies at these long

separations, and the results compared to what might be expected on simple physical grounds.

6-2. Theoretical Methods

Calculations were carried out at the MP2/aug-cc-pVDZ level of theory, as implemented in the Gaussian-09[53] software package. Each dimer was first fully optimized with no geometrical restraints. In order to examine the sensitivity to intermolecular separation, the optimized distance was stretched in fixed increments: 0.1 Å for the first 6Å, and then 0.2 Å beyond that point. For each intermolecular distance, the remainder of the geometry was fully optimized. The binding energy at each point was computed as the difference between the energy of the heterodimer and the sum of energies of the isolated monomers, again fully optimized. This binding energy was corrected for basis set superposition error via the counterpoise procedure [54]. The interaction energy differs from the binding energy in that it is defined relative to the sum of the energies of the monomers when fixed in the geometry they adopt within the complex. The total interaction energy was dissected into various components by SAPT analysis using the MOLPRO [55] program. Kitaura-Morokuma energy decomposition was carried out using GAMESS [56]. Best fits of the energies to the intermolecular separation were analyzed via KaleidaGraph software.

6-3. Results

The fully optimized geometries of the heterodimers are illustrated in Figs 6-1 to 6-4. Neutral H-bond pairs with OH, FH, and CH proton donors were considered. The bold

numbers in Fig 6-1 indicate the counterpoise-corrected binding energies which span a range from 1.8 kcal/mol for $F_3CH \cdot \cdot NH_3$ to 11.6 kcal/mol for $FH \cdot \cdot NH_3$. The HBs are considerably stronger, with binding energies as large as 41.2 kcal/mol, when an anion is used for proton acceptor, for systems pictured in Fig 6-2. Very strong HBs are also associated with a cationic proton donor, as in the cases depicted in Fig 6-3, considering both NH^+ and CH^+ donor groups. Recent work has focused attention on variants of HBs, where the bridging atom can be pnicogen, chalcogen, or halogen, which are the subject of the systems in Fig 6-4. Such bonds can also be fairly strong, as for example $FBr \cdots NH_3$ which has a binding energy of 14.2 kcal/mol.

Given the wide range of bond strengths in this diverse set of systems, and the interest in the manner, or speed, in which this bond is weakened by stretches, the energetics of stretching were normalized to one another. Specifically, each change in energy arising from a given bond stretch was divided by the full binding energy in the optimized dimer, i.e. the bold numbers in Figs 6-1 to 6-4. The binding energy loss is thus represented as a percent of the full capacity of a given dimer. As an example, the percentage binding energy loss as the HB is stretched is shown for a set of six cationic HBs containing $HCNH^+$ in Fig 6-5. It is immediately clear that the functional dependence of the binding energy percentage losses are quite similar, even though the binding energies themselves cover a wide range of 11-31 kcal/mol. The patterns are also relatively insensitive to whether it is the NH^+ or CH^+ end of the cation that serves as proton donor. This similarity is not limited to only this subset of systems, but is characteristic of all heterodimers.

The percentage bond energy decrease appears to be more or less linear in the first 1 Å of its stretch. A best fit of this quantity to a linear function in this range leads to a slope that characterizes the steepness of this energy loss. These slopes are reported in Table 6-1 where a number of patterns can be discerned. First with regard to neutral HBs, the slope is equal to 60 for conventional HBs HOH··OH$_2$, FH··NH$_3$, and FH··OH$_2$, but 10 units smaller for the CH··N HB in F$_3$CH··NH$_3$, suggesting a slightly more gradual die-off for the latter. The ionic HBs have a smaller slope than their neutral counterparts, in the range between 38 to 49. With the exception of FH··F$^-$, the anionic systems show a more gradual fall-off, but this may be a function of the CH donor. The slopes of the chalcogen-bonded systems are in line with those of the neutral HBs; pnicogen bonds fall more gradually, and halogen bonds more quickly. In fact, the halogen bond of FBr··NH$_3$ shows the largest slope and thus the most rapid loss of binding energy of any of the systems considered here.

As the binding energy loss levels off after the first Å stretch, a linear fit is no longer appropriate for longer intermolecular separations. A fitting was thus adjusted to an inverse ΔR^{-n} decay. That is, the exponent n was fit to the binding energy loss as R increases. No single value of n was appropriate for the entire range of stretching. Instead, this power was fit to individual spans of ΔR, terminating in $\Delta R=11$ Å. In other words, the best value of n was obtained for a range of ΔR from 1 Å to 11 Å. The same process was then undertaken for the 2-11 Å range, followed by 3-11 Å, and so on, terminating in the 10-11 Å range. These best-fit exponents n are listed in Table 6-2 for each set of systems. For example, this exponent is equal to 1.92 for the 1-11 Å range of the neutral HBs, as noted by the first entry in Table 6-2. The exponent rises to 2.10 for the 2-11 Å range, and so on, until reaching a

maximal value of 2.52 for the furthest 10-11 Å range. Note that the values reported in Table 6-2 apply not to a single system, but are instead an average over several. The neutral HB set is thus an average of the four heterodimers in Fig 6-1.

The optimal values of power n are considerably smaller for the charged HBs in the next four columns of Table 6-2. The largest values are associated with the anionic systems, slightly larger than for the cationic HBs. Note that these quantities are consistently larger for the NH end of $HCNH^+$ than for the CH end. Like the short-range behavior described in Table 6-1, the powers of n for the other sorts of bonds vary as pnicogen < chalcogen < halogen bond, again indicating a faster fall-off of binding energy for the latter system, this time for long range.

The quantities in Table 6-2 may perhaps be more readily understood when compared graphically as in Fig 6-6. The larger values of n for the neutral as compared to ionic systems are immediately apparent. Also evident is the order of pnicogen < chalcogen < halogen bond; the neutral HBs are generally similar to the pnicogen bonds. The slightly larger values of n for the anionic, compared to cationic, is also clear in Fig 6-6, as is the smaller values for CH^+ compared to NH^+.

Although appearing to be reaching for an asymptote, the curves in Fig 6-6 have not yet reached a point where they are no longer changing. One might anticipate that at very long range, the only sort of interaction still present is electrostatic. For a pair of neutrals, the largest lingering quantity at this distance would correspond to a dipole-dipole interaction, which classically dies off as R^{-3}. While the curves in the upper part of Fig 6 have not yet attained this value, a power of -3 does appear to be their asymptote. Likewise,

the charged systems in the lower part of Fig 6-6 ought to be striving toward a charge-dipole interaction at very long range, which should have a power dependence of -2. In any case, the exponents for the charged systems are roughly 1 unit smaller than those of the neutral dimers.

6-3.1. Energy Decomposition

The total interaction energy of complexes such as these encompasses a number of different components. The exchange repulsion is expected to be of very short range, dying off very quickly as the electron clouds of the two subunits disengage from one another. Only slightly longer range would be dispersion attraction, typically considered to die off roughly as R^{-6}. Induction energy wherein the charge distributions of each molecule perturb the electron cloud of its partner, should extend a bit further out. The longest range interaction is anticipated to be electrostatic.

Each of these components can be evaluated separately within the framework of SAPT decomposition. The distance dependence of each component is displayed as an example in Fig 6-7 for three of the cationic H-bonded systems. Again, each term is normalized, as a percentage of its value in the equilibrium geometry, so as to maximize the ability for comparison. Fig 6-7c illustrates the very rapid decay of the dispersion attraction, losing nearly all of its value in the first 2 Å of stretch. It may also be noted that the manner of dispersion energy loss is independent of the particular proton donor, as the three curves in Fig 6-7c coincide. Induction energy loss is also rapid, albeit not as abrupt, as is evident in Fig 6-7b. The drop in induction energy is slightly steeper for the $HCNH^+$ donor than for $HNCH^+$ or NH_4^+. The much slower decay of the electrostatic energy is evident in Fig 6-7a.

A stretch of some 6 Å is required before this attractive term is diminished by 90%. As in the case of induction, there is a slightly less gradual drop-off of electrostatic energy for $HCNH^+$ than for $HNCH^+$ or NH_4^+. Exchange repulsion is not explicitly displayed as its very short-range character led to its disappearance for stretches beyond 1 Å.

As was done earlier for the total interaction energy, each individual component can be fit to a function that dies off as ΔR^{-n}, and the value of n extracted for each region of stretch ΔR. These powers can be grouped into regions. In this case, the short range is defined as stretches between 1 and 5 Å, and long range as 5-11 Å. These powers are reported in Tables 6-3 and 6-4 for each of the heterodimers under consideration, with average values displayed in the last row of each section.

For example, the uppermost section of Table 6-3 indicates that the electrostatic component of the neutral HBs, as a group, decays as $\Delta R^{-1.53}$ between 1 and 5 Å, and then as $\Delta R^{-2.41}$ for the 5-11 Å range. The powers are considerably larger for induction and dispersion, indicating their more rapid decline with ΔR. Comparison with the charged HBs in the next two sections indicates the dispersion exponents are little changed by addition of a charge. Induction exponents, however, are considerably smaller, indicating that the charge on one subunit or the other leads to a slower decay of this component. Likewise, the ELST exponents also drop with the introduction of charge, particularly for the 5-11 Å range. The exponents for the other neutral complexes in Table 6-4 are generally similar to the neutral HBs. Overall, these exponents rise slightly in the order pnicogen < chalcogen < halogen-bonded, consistent with the pattern noted earlier for the total interaction energy. Indeed, among all types of noncovalent interactions, the halogen bond has the greatest

sensitivity to bond stretching in terms of all three components. The average exponent for electrostatic, induction, and dispersion energies are 1.78/2.46, 3.86/4.60 and 2.90/4.38, respectively, for the 1-5 Å/5-11 Å regions.

6-4. Discussion

The calculations described here made use of the polarized double-ζ aug-cc-pVDZ basis set. The latter is obviously not the largest basis set one can envision. Larger sets would likely enlarge dispersion energy which tends to correlate with basis set size. Electrostatic and induction components would also change, albeit in a less predictable manner, as the basis set is expanded. However, the emphasis in this work is not on the computation of highly accurate numerical values for each term, but rather the functional dependence of how quickly each diminishes as the participating units are separated from one another. It is not expected that this functional dependence will be very sensitive to basis set size, provided the set is well balanced, and includes polarization and diffuse functions. Moreover, it is reiterated that a large portion of the error arising from deficiencies in the basis set were alleviated by the application of counterpoise correction.

Similar considerations apply to the MP2 treatment of electron correlation. Again, higher orders of perturbation theory would have likely resulted in somewhat different magnitudes of correlation energy, as would other means of computing this quantity, e.g. CCSD(T). But the MP2 treatment ought to provide a relatively accurate portrayal of the way in which correlation affects the rapidity with which each term is diminished with intermolecular separation, which is at the heart of this work. Moreover, this procedure takes

on added importance as it represents the most widely used ab initio procedure to evaluate electron correlation at the present time. (DFT includes correlation as well, but is not an ab initio method.) Accordingly, knowledge of the functional dependence of interaction energy is important as it affects the calculation of a large number of intermolecular contacts.

There might have been an initial expectation that the long-range behavior of these various noncovalent bonds ought to be dominated by electrostatic terms. This does in fact seem to be the case, as the exponents that characterize the die-off of the ELST term are considerably smaller than those for induction and dispersion. Taking the pnicogen-bonded systems as an example, the average exponent in the $\Delta R = 5 - 11$ Å range is 2.24, as compared to values of 4.42 and 4.31 for IND and DISP, respectively. ELST and IND drop less precipitously for the charged systems. In the case of the cation-neutral HBs, their respective exponents in the same range are 1.39 and 2.91. Dispersion energy, on the other hand, is little affected by placing a charge on one of the two subunits.

Further, focusing on the ELST component, it would be logical to presume that the long-range electrostatics of the neutral systems ought to reduce to a dipole-dipole interaction, which classically dies off as R^{-3}. However, a glance at the data in Tables 6-3 and 6-4 indicates the best-fit exponent for the ELST term is smaller than 3 for the neutral pairs, between 2.2 and 2.5. It would appear then that the long-range behavior of the Coulombic attraction cannot be accurately reduced to a simple R^{-3} charge-dipole function. Along similar lines, a R^{-2} dependence might have been anticipated for the charge-dipole interaction of the charged HBs. The long-range ELST exponent for the charged HBs are 1.4 for the cation and 1.6 for the anion, somewhat smaller than the expected value.

Basis set superposition is a recognized source of error in supermolecule calculations of the sort that have been applied to evaluate binding energies in these complexes. Of course, these errors dwindle quickly as the two subunits are distanced from one another, and are not a source of concern for long-range behavior. On the other hand, it is worth considering how this error affects the equilibrium geometries and energetics. Geometries of the various complexes were reoptimized with counterpoise corrections included directly at each step of the optimization. The changes in the H-bond length R and the H-bond angle θ show that inclusion of counterpoise alters equilibrium geometries by only a small amount. The intermolecular distance increases by 0.1 Å or less, and the angle remains within a degree of its uncorrected value, with the exception of a 4° change for $H_3N^+H\cdots FH$. Most importantly, these minor geometrical alterations have virtually no effect upon the binding energies. The reoptimization causes only minute changes in E_b, less than 0.1 kcal/mol. And even these minor effects will be reduced quickly as the two subunits are moved away from one another, especially in the long range which is the focus of this work. The counterpoise correction of the geometry has only very small effects on this quantity as well.

It is well known that any scheme for partitioning the total interaction energy is arbitrary to some degree. It would hence be wise to compare the SAPT values to those computed using a different scheme. The Kitaura-Morokuma (KM) energy partitioning method [57-59] is one of the first devised and has witnessed extensive use over the years, and has demonstrated its usefulness and validity. The KM values of the ES and EX energies are displayed in Table 6-5 alongside the SAPT quantities for the equilibrium geometries of the indicated complexes. In most cases, the values computed by the two methods are very

similar indeed. For example, the two ES values are within 0.1 kcal/mol of one another for the $F_3CH\cdots Cl^-$ complex, and the EX quantities within 0.2 kcal/mol. The SAPT and KM values of ES differ by 0.2 kcal/mol on average, and the EX energies are within 0.5 kcal/mol. While the physical meanings of ES and EX are reasonably similar for KM and SAPT, the second-order quantities are quite different. The SAPT induction energy IND is very roughly analogous to the summation of KM polarization (POL) and charge transfer (CT) energies. The last two columns of Table 6-5 indicate that despite these different definitions, the two partitioning procedures nevertheless yield fairly similar values in most cases. These similarities of the various components lend confidence that the conclusions discussed above for the SAPT analysis would likely be confirmed for other energy decomposition schemes as well.

It might also be stressed that any energy decomposition scheme, and SAPT is no exception, can begin to break down as the two subunits come very close together, and the interaction energy climbs. It is thus reassuring that the KM and SAPT components are as similar as they are even for the most strongly bound complexes, where one subunit carries a charge. For example, the KM and SAPT values of the electrostatic energy for the $FH\cdots F^-$ complex are -74.96 and -75.01 kcal/mol, respectively. Perhaps more importantly, the emphasis here is placed on the long-range behavior, where the SAPT procedure is most trustworthy.

By considering the percent drops in energetic quantities and the stretches of each intermolecular distance from its equilibrium value, the behavior of the various systems have been normalized to one another which allows direct comparisons to be made between

one complex and another, unifying all the different types of H-bonds: strong and weak, and short and long. However, one might also be interested in the raw data itself. That is one might consider correlations between the unnormalized binding energies and the intermolecular distances R, rather than the stretch from equilibrium. In particular, R is defined as the distance between the electron donor and acceptor atoms.

The fitting of E_b to R for the various systems is also made, corresponding to the fits to ΔR in the earlier tables. The patterns are generally similar with two exceptions. First, while the exponents characterizing ΔR^{-n} tend to increase as the range covered expands to longer stretches, the R^{-n} exponents show a tendency to become slightly smaller. Second, the exponents n for the fit to R^{-n} are somewhat larger than those for ΔR^{-n}. Taking the average of the neutral HBs as an example, n reaches 2.52 for the stretching region of $\Delta R=10-11$ Å; the exponent is 3.19 for R. This behavior characterizes all of the neutral systems, whether H-bonding, or halogen, chalcogen, or pnicogen: n is smaller than 3 for ΔR and larger for R. Similarly, for the anionic HBs where n is less than 2 for ΔR, and is slightly larger than 2 for R. In the case of the cationic HBs, the exponents are closer to 2.0 for the fit of E_b to R.

With regard to the individual components, the fits to R also provide larger exponents than do those for ΔR^{-n}. As indicated earlier in Table 6-3, the exponents n for the electrostatic component fit to ΔR^{-n} are 2.4, 1.6, and 1.4 for the neutral, anionic, and cationic HBs, respectively. When fit instead to the actual intermolecular distance R, these exponents rise to the larger values of 3.2, 2.1, and 1.9. Likewise, for the pnicogen, chalcogen, and halogen-bonded systems where these ΔR^{-n} exponents are in the range 2.2-2.5, and those for

R^{-n} are between 3.1 and 3.2. Similar increases are observed also for the induction and dispersion components. The ΔR^{-n} exponents for the neutral systems for the induction energy are 4.4-4.6, compared to 6.0-6.3 for R^{-n}; the corresponding exponents are 2.9-3.0 and 4.0-4.1 for the ionic complexes. The rate of dispersion die-off is relatively insensitive to charge; it diminishes as $\Delta R^{-4.4}$ whereas it is more variable for R, with exponents varying between 5.7 and 6.1. In summary, when fit to R, the electrostatic exponents are closer to the values of 3 and 2 normally expected for neutral and charged dimers, respectively, even if a little larger; likewise for the R^{-6} die-off of the dispersion energy.

References

[1]   R.M. Badger, S.H. Bauer, J. Chem. Phys. 5 (1939) 839.

[2]   G.C. Pimentel, A.L. McClellan, The Hydrogen Bond, Freeman, San Francisco, 1960.

[3]   M.D. Joesten, L.J. Schaad, Hydrogen Bonding, Marcel Dekker, New York, 1974.

[4]   P. Schuster, G. Zundel, C. Sandorfy (Ed.)^(Eds.), The Hydrogen Bond. Recent Developments in Theory and Experiments. North-Holland Publishing Co., Amsterdam, 1976.

[5]   E.N. Baker, R.E. Hubbard, Prog. Biophys. Molec. Biol. 44 (1984) 97.

[6]   Z. Latajka, S. Scheiner, J. Chem. Phys. 87 (1987) 5928.

[7]   G.A. Jeffrey, W. Saenger, Hydrogen Bonding in Biological Structures, Springer-Verlag, Berlin, 1991.

[8]   S. Scheiner, in: Z.B. Maksic (Ed.), Theoretical Models of Chemical Bonding, Springer-Verlag, Berlin, 1991, p. 171.

[9]   S. Scheiner, Hydrogen Bonding. A Theoretical Perspective, Oxford University Press, New York, 1997.

[10]   S. Scheiner, in: Z.B. Maksic, W.J. Orville-Thomas (Eds.), Pauling's Legacy - Modern Modelling of the Chemical Bond, Elsevier, Amsterdam, 1997, p. 571.

[11]   G.R. Desiraju, T. Steiner, The Weak Hydrogen Bond in Structural Chemistry and Biology, Oxford, New York, 1999.

[12]   Y. Gu, T. Kar, S. Scheiner, J. Mol. Struct. 552 (2000) 17.

[13]   S.J. Grabowski (Ed.)^(Eds.), Hydrogen Bonding - New Insights. Springer, Dordrecht, 2006.

[14]   S. Scheiner, L. Wang, J. Am. Chem. Soc. 115 (1993) 1958.

[15]   G. Gilli, P. Gilli, The Nature of the Hydrogen Bond, Oxford University Press, Oxford, UK, 2009.

[16]   O. Hassel, Science 170 (1970) 497.

[17]   S.C. Blackstock, J.P. Lorand, J.K. Kochi, J. Org. Chem. 52 (1987) 1451.

[18]   N. Ramasubbu, R. Parthasarathy, P. Murray-Rust, J. Am. Chem. Soc. 108 (1986) 4308.

[19] J.P.M. Lommerse, A.J. Stone, R. Taylor, F.H. Allen, J. Am. Chem. Soc. 118 (1996) 3108.

[20] P. Auffinger, F.A. Hays, E. Westhof, P.S. Ho, Proc. Nat. Acad. Sci., USA 101 (2004) 16789.

[21] P. Politzer, P. Lane, M.C. Concha, Y. Ma, J.S. Murray, J. Mol. Model. 13 (2007) 305.

[22] A. Karpfen, in: P. Metrangolo, G. Resnati (Eds.), Halogen Bonding. Fundamentals and Applications, Springer, Berlin, 2008, p. 1.

[23] P. Metrangolo, G. Resnati, Halogen Bonding. Fundamentals and Applications, Springer, Berlin, 2008.

[24] K. Eskandari, H. Zariny, Chem. Phys. Lett. 492 (2010) 9.

[25] A.C. Legon, Phys. Chem. Chem. Phys. 12 (2010) 7736.

[26] M. Erdelyi, Chem. Soc. Rev. 41 (2012) 3547.

[27] S.J. Grabowski, Chem. Phys. Lett. 605-606 (2014) 131.

[28] C. Wang, D. Danovich, Y. Mo, S. Shaik, J. Chem. Theory Comput. 10 (2014) 3726.

[29] A. Mukherjee, S. Tothadi, G.R. Desiraju, Acc. Chem. Res. 47 (2014) 2514.

[30] R.E. Rosenfield, R. Parthasarathy, J.D. Dunitz, J. Am. Chem. Soc. 99 (1977) 4860.

[31] T.N.G. Row, R. Parthasarathy, J. Am. Chem. Soc. 103 (1981) 477.

[32]   M. Iwaoka, S. Takemoto, S. Tomoda, J. Am. Chem. Soc. 124 (2002) 10613.

[33]   F.T. Burling, B.M. Goldstein, J. Am. Chem. Soc. 114 (1992) 2313.

[34]   W. Wang, B. Ji, Y. Zhang, J. Phys. Chem. A 113 (2009) 8132.

[35]   U. Adhikari, S. Scheiner, J. Phys. Chem. A 118 (2014) 3183.

[36]   L.M. Azofra, S. Scheiner, J. Phys. Chem. A 118 (2014) 3835.

[37]   V.d.P.N. Nziko, S. Scheiner, J. Phys. Chem. A 118 (2014) 10849.

[38]   X. Guo, Y.-W. Liu, Q.-Z. Li, W.-Z. Li, J.-B. Cheng, Chem. Phys. Lett. 620 (2015) 7.

[39]   L.M. Azofra, I. Alkorta, S. Scheiner, Phys. Chem. Chem. Phys. 16 (2014) 18974.

[40]   L.M. Azofra, S. Scheiner, J. Chem. Phys. 140 (2014) 034302.

[41]   K.W. Klinkhammer, P. Pyykko, Inorg. Chem. 34 (1995) 4134.

[42]   J.S. Murray, P. Lane, P. Politzer, Int. J. Quantum Chem. 107 (2007) 2286.

[43]   J. Moilanen, C. Ganesamoorthy, M.S. Balakrishna, H.M. Tuononen, Inorg. Chem. 48 (2009) 6740.

[44]   S. Scheiner, J. Chem. Phys. 134 (2011) 094315.

[45]   U. Adhikari, S. Scheiner, J. Chem. Phys. 135 (2011) 184306.

[46]   S. Zahn, R. Frank, E. Hey-Hawkins, B. Kirchner, Chem. Eur. J. 17 (2011) 6034.

[47]   S. Scheiner, U. Adhikari, J. Phys. Chem. A 115 (2011) 11101.

[48]   J.E. Del Bene, I. Alkorta, J. Elguero, J. Phys. Chem. A 119 (2014) 224.

[49]   S. Scheiner, Acc. Chem. Res. 46 (2013) 280.

[50]   S. Sarkar, M.S. Pavan, T.N. Guru Row, Phys. Chem. Chem. Phys. 17 (2015) 2330.

[51]   G. Sánchez-Sanz, C. Trujillo, I. Alkorta, J. Elguero, Comput. Theor. Chem. 1053 (2015) 305.

[52]   S. Scheiner, CrystEngComm 15 (2013) 3119.

[53]   M.J. Frisch, G.W. Trucks, H.B. Schlegel, G. E. Scuseria, M.A. Robb, J.R. Cheeseman, G. Scalmani, V. Barone, B. Mennucci, G.A. Petersson, H. Nakatsuji, M. Caricato, X. Li, H.P. Hratchian, A.F. Izmaylov, J. Bloino, G. Zheng, J.L. Sonnenberg, M. Hada, M. Ehara, K. Toyota, R. Fukuda, J. Hasegawa, M. Ishida, T. Nakajima, Y. Honda, O. Kitao, H. Nakai, T. Vreven, J.A. Montgomery, J.E. Peralta, F. Ogliaro, M. Bearpark, J.J. Heyd, E. Brothers, K.N. Kudin, V.N. Staroverov, T. Keith, R. Kobayashi, J. Normand, K. Raghavachari, A. Rendell, J.C. Burant, S.S. Iyengar, J. Tomasi, M. Cossi, N. Rega, J.M. Millam, M. Klene, J.E. Knox, J.B. Cross, V. Bakken, C. Adamo, J. Jaramillo, R. Gomperts, R.E. Stratmann, O. Yazyev, A.J. Austin, R. Cammi, C. Pomelli, J.W. Ochterski, R.L. Martin, K. Morokuma, V.G. Zakrzewski, G.A. Voth, P. Salvador, J.J. Dannenberg, S. Dapprich, A.D. Daniels, O. Farkas, J.B. Foresman, J.V. Ortiz, J. Cioslowski, D.J. Fox, Gaussian 09. Gaussian, Inc, Wallingford CT, 2009.

[54]   S.F. Boys, F. Bernardi, Mol. Phys. 19 (1970) 553.

[55]   H.-J. Werner, P.J. Knowles, F.R. Manby, M. Schütz, P. Celani, G. Knizia, T. Korona, R. Lindh, A. Mitrushenkov, G. Rauhut, T.B. Adler, R.D. Amos, A. Bernhardsson, A. Berning, D.L. Cooper, M.J.O. Deegan, A.J. Dobbyn, F. Eckert, E. Goll, C. Hampel, A. Hesselmann, G. Hetzer, T. Hrenar, G. Jansen, C. Köppl, Y. Liu, A.W. Lloyd, R.A. Mata, A.J. May, S.J. McNicholas, W. Meyer, M.E. Mura, A. Nicklaß, P. Palmieri, K. Pflüger, R. Pitzer, M. Reiher, T. Shiozaki, H. Stoll, A.J. Stone, R. Tarroni, T. Thorsteinsson, M. Wang, A. Wolf, MOLPRO, 2010.

[56]   M.W. Schmidt, K.K. Baldridge, J.A. Boatz, S.T. Elbert, M.S. Gordon, J.H. Jensen, S. Koseki, N. Matsunaga, K.A. Nguyen, S. Su, T.L. Windus, M. Dupuis, J.A. Montgomery, J. Comput. Chem. 14 (1993) 1347.

[57]   K. Kitaura, K. Morokuma, Int. J. Quantum Chem. 10 (1976) 325.

[58]   K. Morokuma, K. Kitaura, in: P. Politzer, D.G. Truhlar (Eds.), Chemical Applications of Atomic and Molecular Electrostatic Potentials, Plenum, New York, 1981, p. 215.

[59]   K. Morokuma, K. Kitaura, in: H. Ratajczak, W.J. Orville-Thomas (Eds.), Molecular Interactions, Wiley, New York, 1980, p. 21.

Tables and Figures

Table 6-1. The coefficients of linear function that fits the plots of % decrease of binding energy from optimal value vs. bond stretching in the region of 0-1 Å.

complex	coefficient	complex	coefficient
neutral H-bonded complexes		pnicogen bonded complexes	
$H_2O{\cdots}HOH$	60.02	$FH_2P{\cdots}NH_3$	54.39
$FH{\cdots}NH_3$	59.64	$ClH_2P{\cdots}NH_3$	51.08
$H_2O{\cdots}HF$	61.37	$BrH_2P{\cdots}NH_3$	50.82
$F_3CH{\cdots}NH_3$	50.17		
anion–neutral H-bonded complexes		chalocogen bonded complexes	
$F_3CH{\cdots}Cl^-$	37.58	$FHS{\cdots}NH_3$	59.16
$F_3CH{\cdots}NC^-$	39.58	$ClHS{\cdots}NH_3$	57.17
$F_3CH{\cdots}OH^-$	40.33	$BrHS{\cdots}NH_3$	56.63
$FH{\cdots}F^-$	48.21		
cation–neutral H-bonded complexes		halogen bonded complexes	
$H_3N^+H{\cdots}OH_2$	46.47	$FCl{\cdots}NH_3$	63.81
$H_3N^+H{\cdots}FH$	40.20	$FBr{\cdots}NH_3$	66.17
$H_3N^+H{\cdots}OCH_2$	44.26	$CF_3Cl{\cdots}NH_3$	58.72
$HF{\cdots}HNCH$	49.40		
$HF{\cdots}HCNH$	43.43		
$H_2O{\cdots}HNCH$	44.14		
$H_2O{\cdots}HCNH$	46.23		
$HCHO{\cdots}HNCH$	42.87		
$HCHO{\cdots}HCNH$	43.99		

Table 6-2. Average exponents n of the power functions ΔR^{-n} that fit the plots of binding energy vs bond stretching at different ranges for non-covalent complexes.

Range Å	H-bond neutral-neutral	H-bond anion-neutral	H-bond cation-neutral (NH_4^+ donor)	H-bond cation-neutral ($HCNH^+$) NH-donor	H-bond cation-neutral ($HCNH^+$) CH-donor	Pnicogen bond	Chalcogen bond	Halogen bond
1-11	1.92	1.31	1.16	1.30	1.18	2.01	2.10	2.23
2-11	2.10	1.43	1.27	1.38	1.28	2.16	2.28	2.39
3-11	2.20	1.49	1.34	1.44	1.35	2.24	2.37	2.48
4-11	2.26	1.52	1.39	1.47	1.39	2.29	2.42	2.53
5-11	2.32	1.56	1.43	1.50	1.43	2.34	2.47	2.56
6-11	2.39	1.62	1.50	1.53	1.47	2.38	2.51	2.60
7-11	2.44	1.65	1.54	1.55	1.49	2.41	2.54	2.62
8-11	2.47	1.66	1.56	1.57	1.51	2.43	2.56	2.63
9-11	2.49	1.68	1.59	1.58	1.52	2.45	2.58	2.65
10-11	2.52	1.69	1.61	1.60	1.54	2.47	2.60	2.66

Table 6-3. The exponent values n of the functions ΔR^{-n} that fit the plots of different components of the binding energy (electrostatic, induction, and dispersion) vs the bond stretching for different H-bonded complexes in different ranges.

complex	ELST			IND			DISP		
	1-5	1-11	5-11	1-5	1-11	5-11	1-5	1-11	5-11
Neutral-neutral H-bonded complexes									
FH···OH$_2$	1.53	1.85	2.33	3.33	3.83	4.63	3.13	3.68	4.53
H$_2$O···HOH	1.40	1.65	2.43	3.30	3.48	4.38	2.98	3.50	4.39
FH···NH$_3$	1.79	2.11	2.58	3.78	4.25	4.97	3.34	3.92	4.75
F$_3$CH···NH$_3$	1.41	1.75	2.28	2.91	3.49	4.41	2.70	3.27	4.15
Average	1.53	1.84	2.41	3.33	3.76	4.60	3.04	3.59	4.46
Anion–neutral H-bonded complexes									
F$_3$CH···Cl$^-$	0.92	1.13	1.49	1.94	2.28	2.89	2.88	3.40	4.31
F$_3$CH···NC$^-$	0.92	1.13	1.44	1.84	2.21	2.79	2.76	3.30	4.14
F$_3$CH···OH$^-$	1.10	1.29	1.60	2.30	2.58	3.07	3.22	3.81	4.60
FH···F$^-$	1.22	1.41	1.67	2.62	2.87	3.26	3.76	4.27	4.90
Average	1.04	1.24	1.55	2.18	2.49	3.00	3.16	3.70	4.49
Cation-neutral H-bonded complexes									
H$_3$NH$^+$···FH	0.81	1.06	1.43	1.87	2.29	2.94	2.88	3.51	4.51
HCNH$^+$···FH	0.88	1.08	1.37	2.10	2.43	2.89	2.92	3.48	4.25
HNCH$^+$···FH	0.84	1.05	1.37	1.95	2.32	2.89	2.85	3.40	4.25
Average	0.84	1.06	1.39	1.97	2.35	2.91	2.88	3.46	4.34

Table 6-4. The exponent values n of the functions ΔR^{-n} that fit the plots of different components of the binding energy (electrostatic, induction, and dispersion) vs the bond stretching for pnicogen, chalcogen and halogen-bonded complexes.

complex	ELST			IND			DISP		
	1-5	1-11	5-11	1-5	1-11	5-11	1-5	1-11	5-11
Pnicogen-bonded complexes									
$FH_2P\cdots NH_3$	1.58	1.85	2.26	3.42	3.80	4.48	2.86	3.47	4.39
$ClH_2P\cdots NH_3$	1.57	1.83	2.24	3.34	3.71	4.40	2.82	3.40	4.29
$BrH_2P\cdots NH_3$	1.55	1.81	2.23	3.29	3.67	4.37	2.79	3.37	4.25
Average	1.57	1.83	2.24	3.35	3.73	4.42	2.82	3.41	4.31
Chalcogen-bonded complexes									
$FHS\cdots NH_3$	1.69	1.95	2.36	3.81	4.00	4.58	2.99	3.57	4.45
$ClHS\cdots NH_3$	1.62	1.91	2.36	3.45	3.80	4.45	2.82	3.39	4.26
$BrHS\cdots NH_3$	1.62	1.92	2.38	3.38	3.74	4.40	2.77	3.34	4.20
Average	1.64	1.93	2.37	3.55	3.85	4.48	2.86	3.43	4.30
Halogen- bonded complexes									
$FCl\cdots NH_3$	1.89	2.15	2.56	4.16	4.34	4.80	3.06	3.66	4.58
$FBr\cdots NH_3$	1.89	2.13	2.50	4.35	4.43	4.72	3.06	3.64	4.50
$CF_3Cl\cdots NH_3$	1.56	1.86	2.32	3.06	3.51	4.29	2.57	3.15	4.06
Average	1.78	2.05	2.46	3.86	4.09	4.60	2.90	3.48	4.38

Table 6-5. Comparison between SAPT and Kitaura-Morokuma components (kcal/mol) for equilibrium geometries.

	ES		EX		IND	
	KM	SAPT	KM	SAPT	KM[a]	SAPT
$H_2O \cdots HOH$	-8.48	-8.40	6.95	6.98	-3.34	-2.98
$FH \cdots NH_3$	-22.81	-22.45	21.47	21.28	-17.86	-13.10
$H_2O \cdots HF$	-14.68	-14.35	12.21	12.24	-8.31	-6.98
$F_3CH \cdots NH_3$	-7.76	-7.66	5.88	5.74	-3.25	-2.41
$F_3CH \cdots Cl^-$	-22.44	-22.33	14.29	14.08	-10.72	-11.29
$F_3CH \cdots NC^-$	-22.76	-22.50	14.01	13.77	-12.36	-8.14
$F_3CH \cdots OH^-$	-47.58	-47.19	40.57	39.26	-40.02	-27.78
$FH \cdots F^-$	-74.96	-75.01	67.05	64.44	-75.91	-52.23
$H_3N^+H \cdots FH$	-13.44	-13.39	6.60	6.74	-6.63	-5.00
$HF \cdots HNCH$	-17.62	-17.26	14.02	14.12	-15.99	-10.82
$HF \cdots HCNH$	-14.12	-13.92	7.86	7.85	-8.44	-5.78
$ClH_2P \cdots NH_3$	-15.90	-15.61	19.71	19.08	-28.81	-16.79
$FHS \cdots NH_3$	-24.55	-24.33	31.71	30.96	-54.95	-34.88
$FCl \cdots NH_3$	-36.69	-35.93	53.01	51.50	102.47	-69.14

HOH---OH$_2$ **5.26**

FH---NH$_3$ **11.63**

FH---OH$_2$ **7.86**

F$_3$CH---NH$_3$ **1.81**
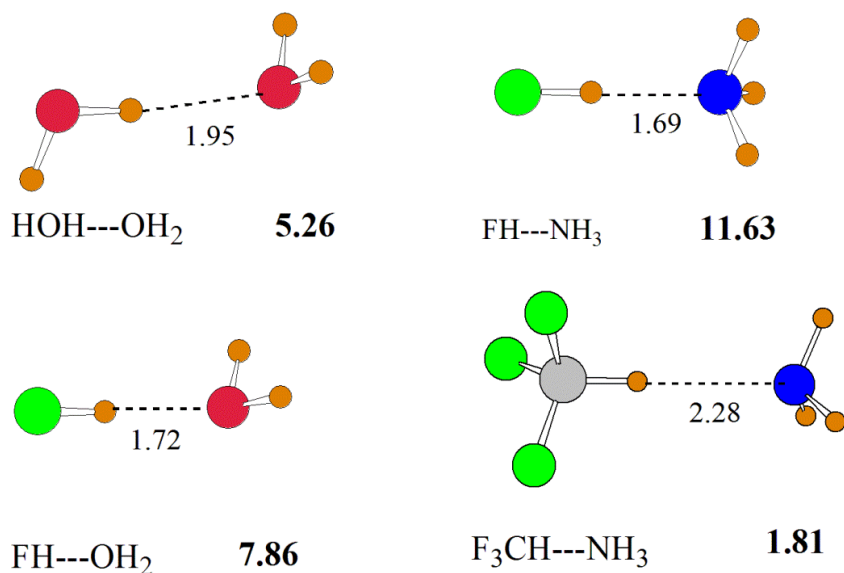
Figure 6-1. Optimized geometries of neutral-neutral H-bonded complexes. The bold number indicates counterpoise-corrected binding energy in kcal/mol, distances in Å.

F$_3$CH---Cl$^-$ **15.16**

F$_3$CH---NC$^-$ **14.89**

F$_3$CH---OH$^-$ **24.39**

FH---F$^-$ **41.16**
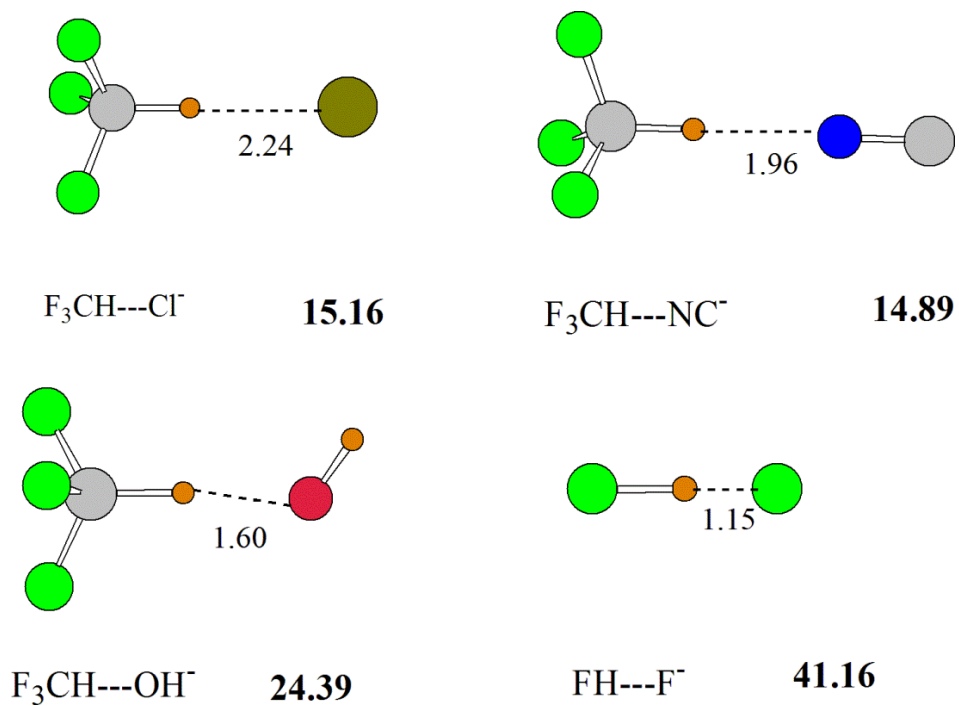
Figure 6-2. Optimized geometries of anion-neutral H-bonded complexes. The bold number indicates counterpoise-corrected binding energy in kcal/mol, distances in Å.
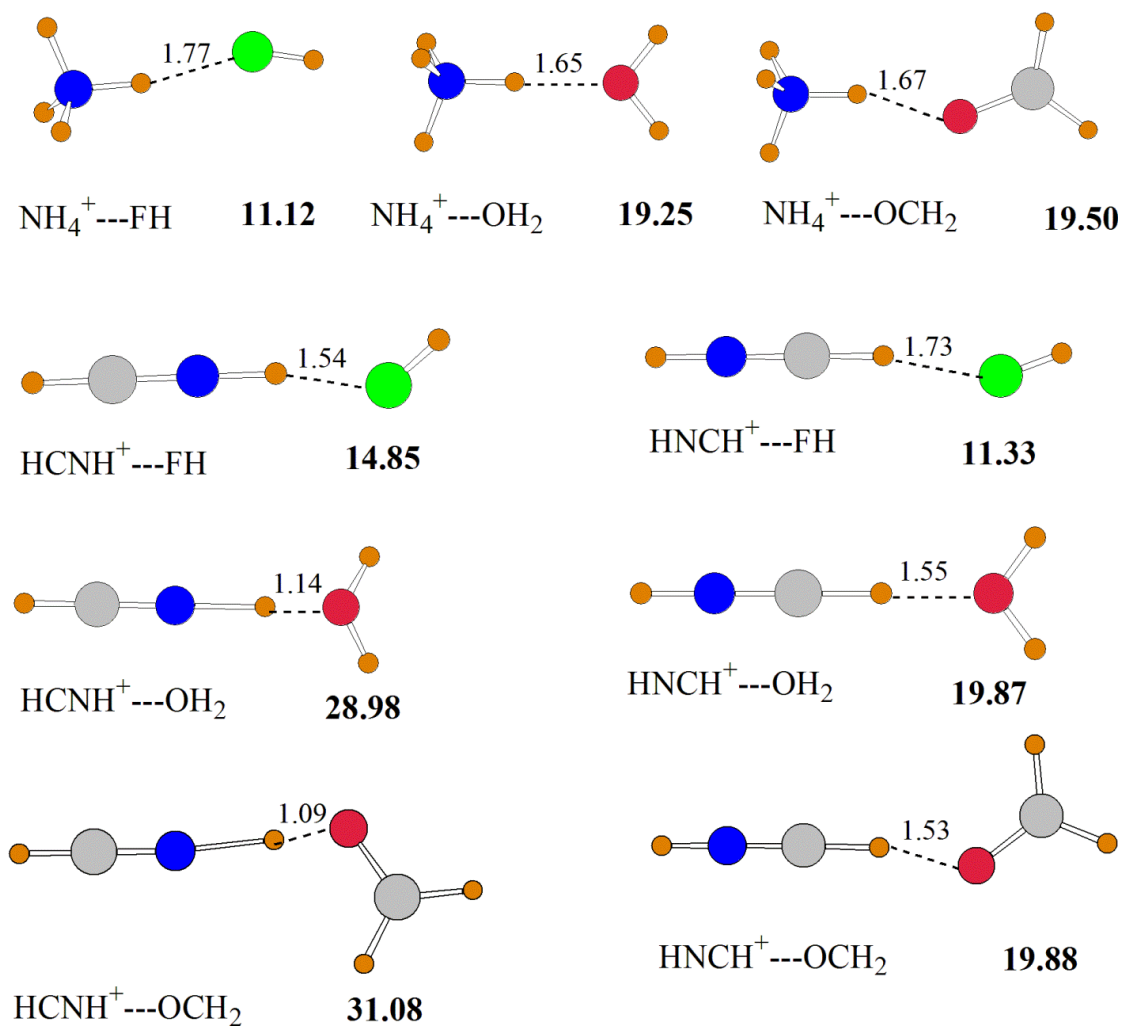
Figure 6-3. Optimized geometries of cation-neutral H-bonded complexes. The bold number indicates counterpoise-corrected binding energy in kcal/mol, distances in Å.
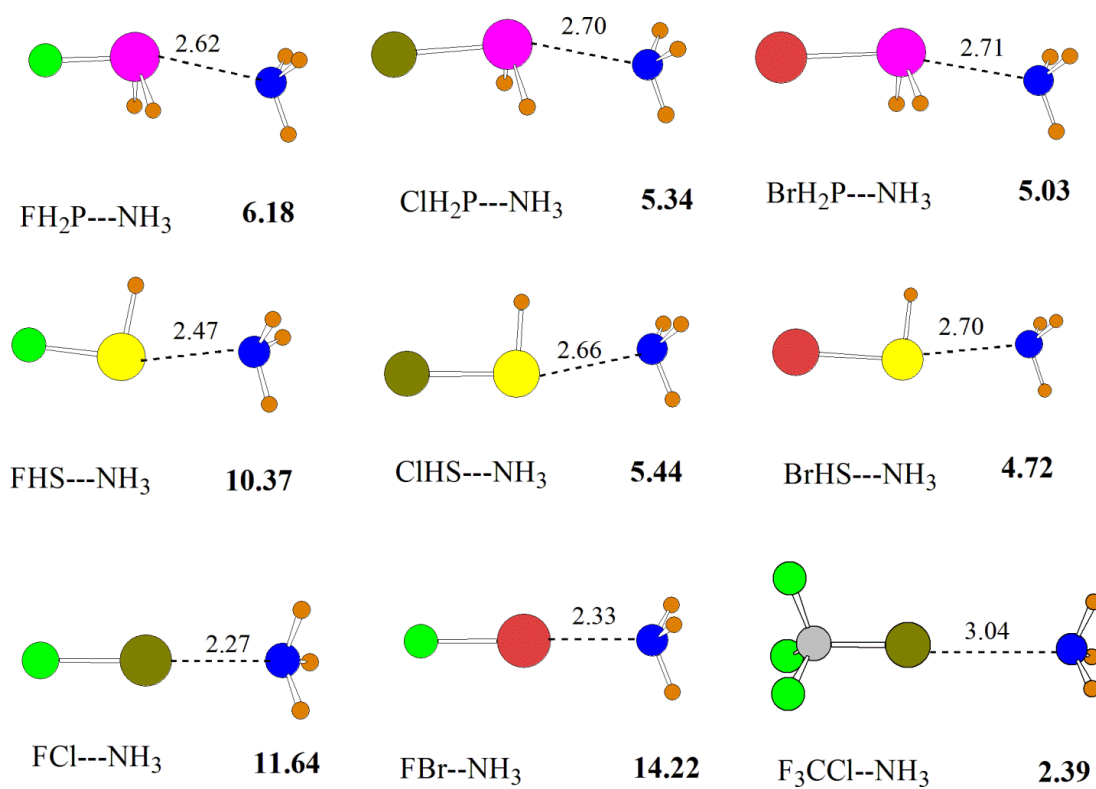
Figure 6-4. Optimized geometries of pnicogen, chlacogen and halogen bonded complexes. The bold number indicates counterpoise-corrected binding energy in kcal/mol, distances in Å.
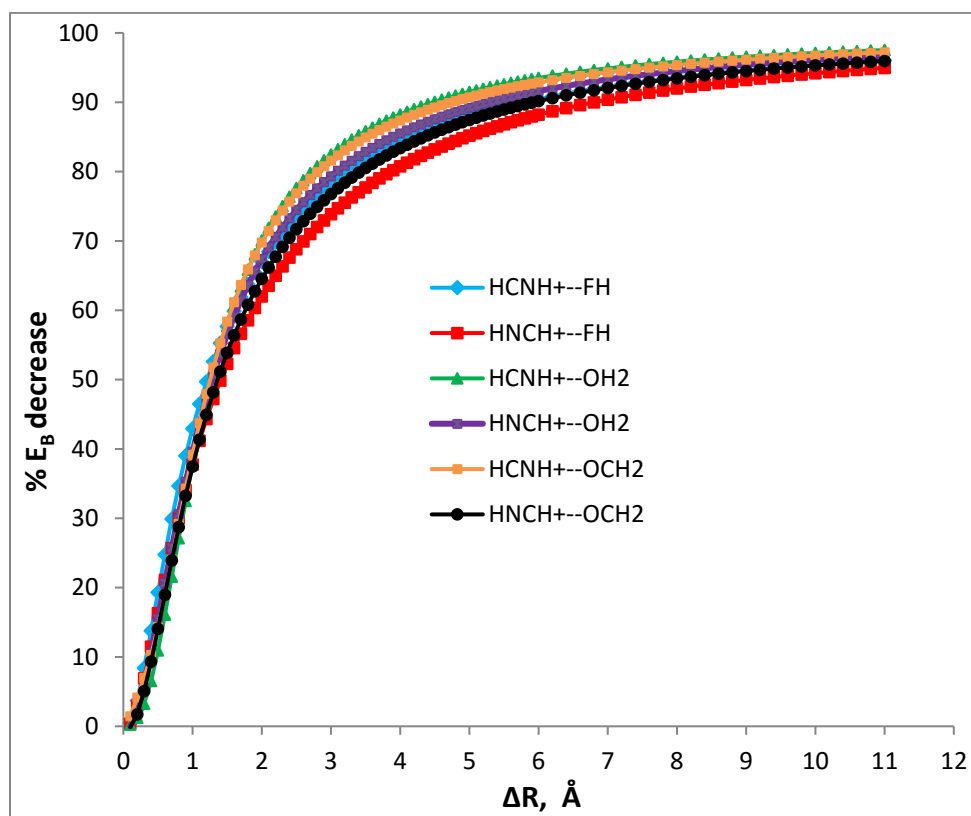
Figure 6-5. Percent decrease of binding energy from the initial value vs bond stretching for cation-neutral H-bonded complexes with $HCNH^+$ as proton donor.
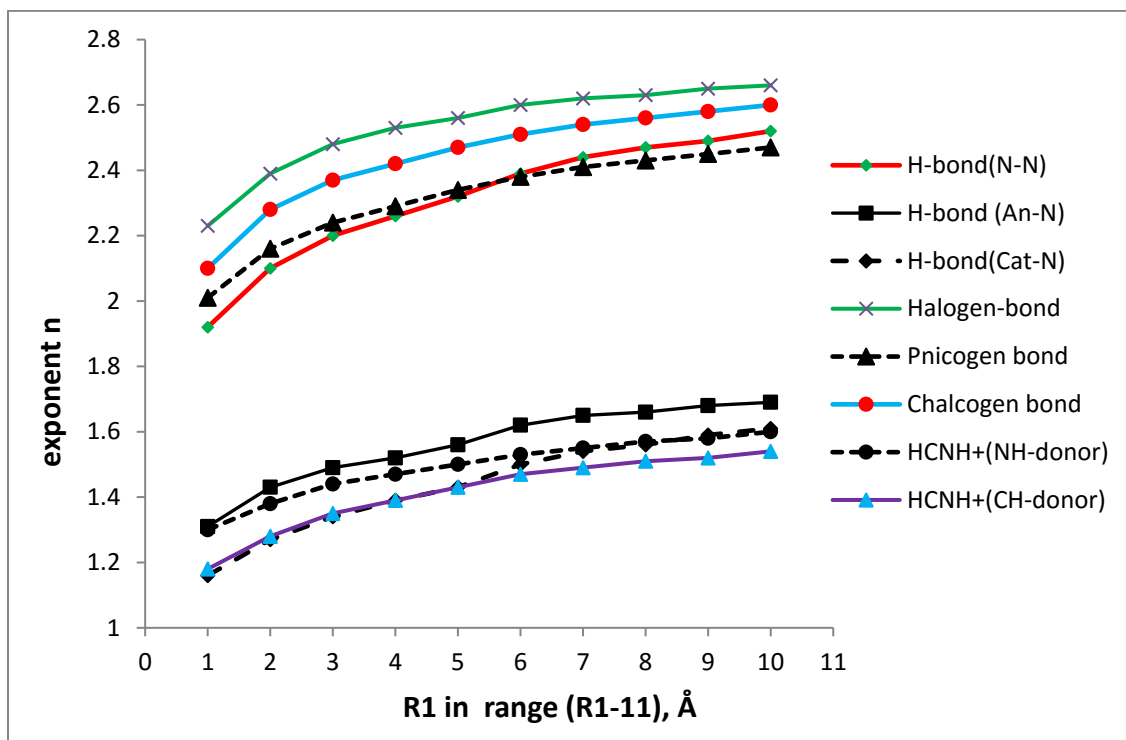
Figure 6-6. Average exponent n of power function $(\Delta R)^{-n}$ vs. range of bond stretching for various complexes. Each value on the x-axis indicates lower value R_1 of the (R_{1-11}) Å range.
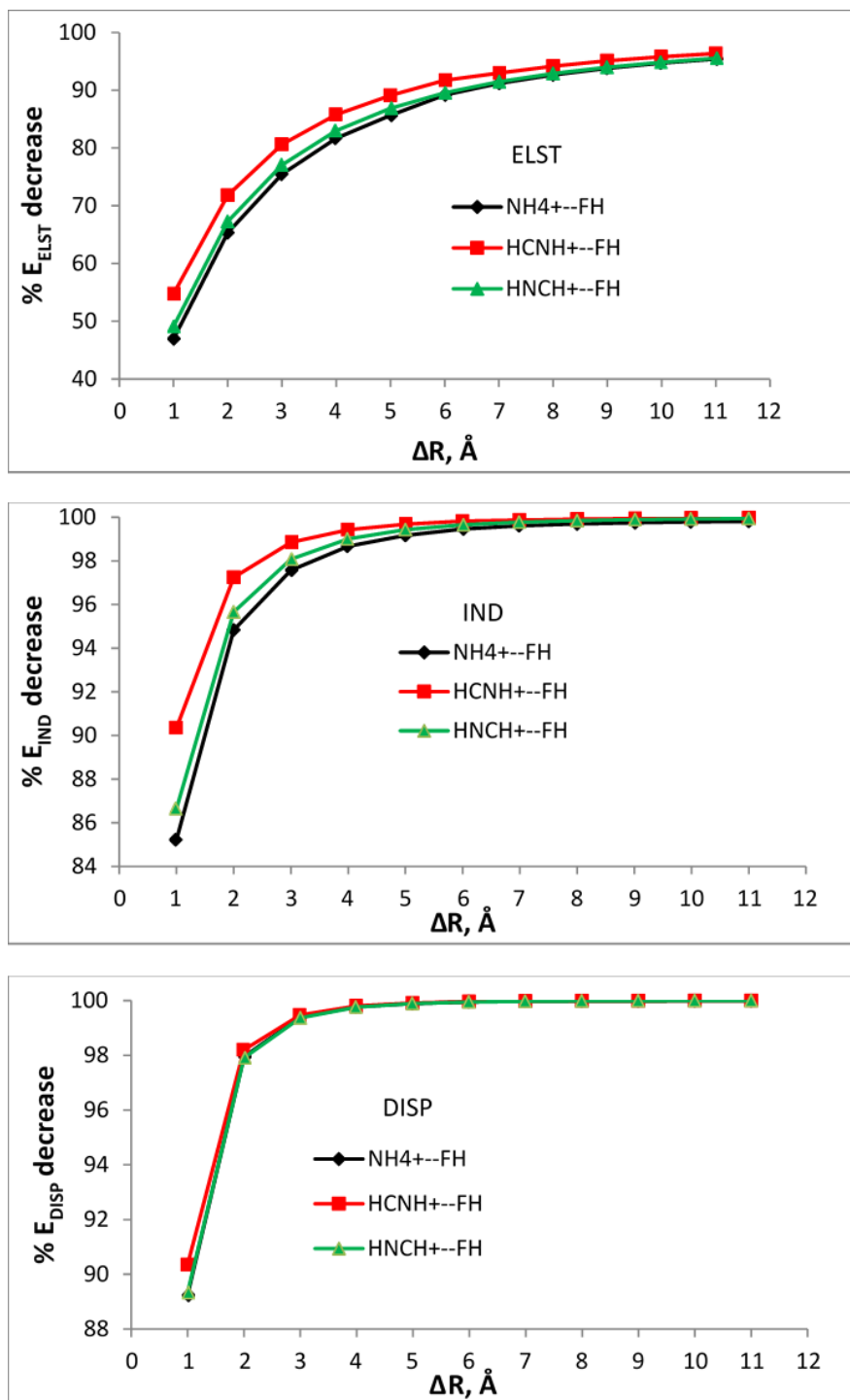
Figure 6-7. Percent decrease of a) electrostatic (ELST), b) induction (IND) and c) dispersion (DISP) components from their equilibrium values due to bond stretching for cation-neutral H-bonded complexes.

CHAPTER 7

COMPETITIVE HALIDE BINDING BY HALOGEN VERSUS HYDROGEN

BONDING. BIS-TRIAZOLE PYRIDINIUM[1]

Abstract

The binding of F^-, Cl^-, Br^-, and I^- anions by bis-triazole-pyridine (BTP) was examined by quantum chemical calculations. There is one H atom on each of the two triazole rings that chelate the halide via H-bonds. These H atoms were replaced by halogens Cl, Br, and I, thus substituting H-bonds by halogen bonds. I-substitution strongly enhances the binding; Br has a smaller effect, and Cl weakens the interaction. The strength of the interaction is sensitive to the overall charge on the BTP, rising as the binding agent becomes singly and then doubly positively charged. The strongest preference of a halide for halogenated as compared to unsubstituted BTP, as much as several orders of magnitude, is observed for I^-. Both unsubstituted and I-substituted BTP could be used to selectively extract F^- from a mixture of halides.

7-1. Introduction

Although the attractive interaction between a halogen and another electronegative atom was first pointed out many years ago,[1-4] our understanding of the halogen bond has recently undergone a rapid acceleration.[5-12] It is now generally understood that when a

---

halogen atom X is covalently bound to another atom, e.g. C, the electrostatic potential around X becomes highly anisotropic. While there exists a belt or equator of negative potential as might be anticipated for an electronegative halogen, a pole of positive potential develops along the extension of the C-X bond. This so-called σ-hole can attract an electronegative atom of a neighboring molecule. This Coulombic attraction is supplemented by the transfer of charge from the neighboring molecule's lone electron pairs into the C-X σ* antibonding orbital under the rubric of polarization or induction energy. Additional attraction arises by way of London dispersion forces. It is worthwhile to note that this bonding mechanism is not limited to halogen atoms, but has been observed for chalcogen,[13-21] pnicogen,[12,22-28] and tetrel[29-36] atoms in the eponymous bonds.

Halogen bonding (XB) has been widely recognized and utilized in crystal engineering over the years.[37-40] But the applications of this phenomenon are diverse, encompassing catalysis,[41-44] biology,[45-48] macromolecular self-assembly,[49,50] and transmembrane transport[51] among numerous others. Due to the fundamental nature of halogen bonding, it may represent an attractive alternative to hydrogen bonding (HB) as a means of selectively coordinating anions in aqueous solution.[52,53]

Particularly intriguing results[54,55] have recently indicated that the binding of halide ions to a bis-triazole-pyridinium (BTP$^+$) species in aqueous solution is greatly enhanced when a H atom is replaced by I on each of the two triazole rings. The authors attributed this selectivity to the superiority of halogen over hydrogen bonds in this environment. These results lead to some very interesting questions which have important implications for the rational design of new halide-binding agents. In the first place, what are the

geometries of the H-bonded and halogen-bonded complexes with the halides? How much more strongly bound are the latter as compared to the former in a quantitative sense? How does the binding depend upon the nature of the halide being captured, and what might be the effect of replacing the I atoms on the triazoles by smaller halogen atoms Br and Cl. How important is the charge on the triazole-containing binding agent: would a neutral or dicationic species function in the same manner? These questions can perhaps best be addressed by quantum chemical calculations, which is the subject of the present work.

7-2. Computational Details

Most of the calculations were carried out with the Gaussian-09 set[56] of codes, using the M06-2X functional[57] within the context of the aug-cc-pVDZ basis set. For the heavy halogen atoms Br and I, the aug-cc-pVDZ-pp pseudo-potential basis set was taken from the EMSL library.[58,59] Binding energies were calculated as the difference between the energy of the complex and the sum of the monomers, in their optimized geometries. Binding energies were corrected for the basis set superposition error via the counterpoise[60] method. Measures of charge transfer were estimated by the natural bond orbital[61] method (NBO), as implemented in the Gaussian-09 software. Aqueous environment was simulated via the Conductor-like Polarizable Continuum Model (CPCM)[62] with water as solvent. The molecular electrostatic potential (MEP) was analyzed via the WFA-SAS program.[63]

The bis-triazole-pyridine (BTP) binding agents tested here are illustrated in Scheme 7-I. X atoms were varied among H, Cl, Br, and I. The neutral molecule was transformed to a monocation by placement of a $-CH_3^+$ on the pyridine N, and to a dication by addition of a methyl to each of the two triazole rings, as indicated.

7-3. Results

In most cases, the optimized geometry of the complex of the anion with the binding agent placed the anion Y^- equidistant between the two binding atoms X. These structures are illustrated for X=H with the monocationic BTP^+ in Fig 7-1. It may be noted that in these cases, the central CH of the pyridine ring also comes close to the anion, in what may be described as a trifurcated CH··Y H-bond. Indeed, for the fluoride and chloride anions, the central HB is shorter than the two peripheral HBs, although the opposite is the case for the larger anions. On the opposite end of the spectrum, the much larger X=I atoms keep the central pyridine H from approaching close enough to the anion to engage in a HB, as is evident in Fig 7-2. In fact, even for the smaller X=Cl complexes, there is no pyridine CH··Y^- HB present. The structures of the complexes for X=Cl and Br are similar.

As illustrated in Scheme 7-I, removal of the -CH_3 group from the pyridine ring leads to an electrically neutral anion binder. The dicationic binder is formed by adding methyls to each of the two triazole rings. The structures of the resulting complexes are similar to those of the monocation, but with respectively longer and shorter intermolecular distances.

The X··Y distances for all the complexes are compiled in Table 7-1 where certain trends are in evidence. For any given binding agent, the intermolecular X··Y distance increases down a column, in the order $Y^- = F^- < Cl^- < Br^- < I^-$, consistent with the growing radius of the anion Y. The increasing size of the halogen atom X attached to the BTP does not have the same effect. In most cases, X=Cl results in a slightly longer X··Y distance than do X=Br or I, although the latter two are quite similar to one another. Not surprisingly,

R(X··Y) is considerably shorter when X=H, due to the much smaller radius of the H atom. With regard to the overall charge on the BTP, the increase from 0 to +1 and then to +2 yields a small but progressive shortening of R(X··Y), indicative of a growing binding strength.

Indeed, the binding energies in Table 7-2 reflect the stronger complexes formed by the ionic BTPs. F$^-$ is clearly the most strongly bound, with a large gap after which the other halides obey the order by Cl$^-$ > Br$^-$ > I$^-$. Unlike the X··Y distances which are relatively insensitive to the identity of the X atom, the binding energies show that X=I is the most strongly bound, followed by Br and then by Cl; the X=H systems tend to fall between X=Cl and X=Br. Overall, the weakest complex is that between the neutral X=Cl BTP and I$^-$, which is bound by 3.2 kcal/mol. The strongest, bound by 24.1 kcal/mol, connects the X=I dicationic BTP^{+2} with F$^-$.

A more complete thermodynamic treatment of the binding yields the quantities displayed in Table 7-3. In all cases ΔS is negative which reflects the process which takes two separate entities into a single complex. The values reported for ΔH are similar to the energies in Table 7-2, differing primarily by the incorporation of vibrational energies into ΔH. The combination of ΔH and ΔS yields the free energies. ΔG is positive for some of the more weakly bound complexes, for example +5.29 kcal/mol for 2H··I$^-$. It turns negative for the more strongly bound dimers, peaking at -16.3 kcal/mol when the dicationic BTP^{+2} with X=I is paired with F$^-$.

As has been observed in the literature, the replacement of H by I strongly enhances the attraction of the BTP for halide anions. The enhancement of the binding of each halide

that results from halogenation of the BTP is reported in Table 7-4. More specifically, the quantities were calculated as the equilibrium ratio of $(2X\cdot\cdot Y^-)/ (2H\cdot\cdot Y^-)$ assuming a Boltzmann distribution, $K=\exp(-\Delta G/RT)$. It is immediately clear that the replacement of H in the BTP by Cl has little if any enhancement effect. Indeed, many of the quantities in the first column of Table 7-4 are less than unity which corresponds to a preference for X=H over X=Cl. An enhancement is apparent for X=Br, particularly for the iodide anion in the last rows. But the largest preference of halide for halogenated BTP over H-bonding BTP is observed for X=I. The enhancement ranges from a factor of 400 up to 1.9×10^7.

It was noted above that F^- forms much stronger complexes with any of the BTPs than do the other halides. These systems could thus be used to selectively bind fluoride in a competition with the other halides. The level of selectivity, again expressed as a ratio of equilibrium populations is exhibited in Table 7-5. The X=Cl BTPs show very little selectivity, with values hovering around unity. X=Br represents an improvement, with ratios between 40 and 2,000. H-bonding BTPs are superior to Br, but the largest selectivity is exhibited by X=I. Even the uncharged BTPs are characterized by a F^- selectivity of roughly 5,000. And this quantity grows larger as charge is placed on the BTP. Consequently, the equilibrium F^-/Y^- population ratio of the dicationic BTP^{+2} with X=I is on the order of 10^6.

There is a crystal structure with which some of our calculated data may be compared. When complexed with Cl^-, a molecule very similar to our monocation with 2 I atoms contained a $R(I\cdot\cdot Cl^-)$ distance [55] in the 3.121 - 3.195 Å range, which compares well with our optimized value of 3.185 Å in Table 7-1. When its 2 H atoms were replaced by I,

other measurements showed that the cationic system displayed an enhancement in its binding of the I$^-$ anion in water [54], consistent with our calculated stronger binding.

As mentioned earlier, the replacement of H by Cl weakens the interaction of the BTP with any anion, while I-substitution leads to a stronger binding energy; the effect of Br is intermediate between Cl and I. This pattern is not consistent with a purely electrostatic effect. The molecular electrostatic potential surrounding each of the monocations is reproduced in Fig 7-3. These maps indicate that the potential is most positive in the unsubstituted BTP$^+$ monocation; halogen-substitution lessens the positive potential. Moreover, the potential in the binding region is not obviously affected by the nature of the halogen, whether Cl, Br, or I. This insensitivity runs counter to the observation of a clear strengthening pattern as the halogen becomes heavier. The electrostatic potential does, though, offer an explanation of the preference of the halide anion Y$^-$ for a position midway between the two halogen X atoms of the BTP$^+$; the potential is most positive (blue) in this region.

These trends can be quantitatively assessed via the evaluation of the maximum of the electrostatic potential on a fixed isodensity contour of 0.001 au, roughly equivalent to the surface envisioned in Fig 7-3. Consistent with this figure, Table 7-6 indicates that the unsubstituted 2H BTP$^+$ has a more positive potential than do the halogenated species. There is a trend for higher potential in the order 2Cl < 2Br < 2I, although this trend is weaker than that exhibited by the total binding energies in Table 7-2. Table 7-6 also obeys the expected pattern that increasing positive charge on the binding agent raises the potential at the maximum, quite dramatically so. Indeed the placing of a single or double positive charge

on BTP roughly doubles or triples the potential maximum, respectively. This strong dependence is not mirrored by the binding energies which rise with increasing charge, but much less dramatically.

Induction appears to offer a better explanation of the observed behavior of the binding energy. In particular, the strongest element of the induction in a halogen bond is associated with charge transfer from the halide lone pairs to the C-X σ* antibonding orbitals. The energetic manifestation of this transfer can be evaluated by the NBO method, and is presented as E(2) in Table 7-7. These values properly reflect the progressively stronger binding from Cl to Br to I. The data also correctly indicate the much stronger binding of F$^-$ than of the other anions, which are not very different from one another. On the other hand, the charge transfer in the H-bonding systems is disproportionately higher than that of the halogen-bonded complexes, so one cannot draw the conclusion that the binding energy is strictly correlated with E(2) for both sorts of bonds. The failure of electrostatic effects to fully account for the differential binding presents a plausible argument that these interactions are better represented as H-bonds or halogen bonds, albeit ionic ones, rather than as simple Coulombic charge-pair interactions.

The results presented here were obtained using a DFT formalism. It would be worthwhile to insure that the values are consistent with a higher level of theory. For this reason, the energetics were recomputed at the ab initio MP2 level, with the same aug-cc-pVDZ basis set, and also in water as solvent. Geometries were taken from the prior M06-2X optimizations, and binding energies were again corrected by the counterpoise procedure. These MP2 calculations were performed for both neutral and monocationic

chelating agents, for 2H and 2I, with all four halide ligands MP2 binding energies for the H-bonded complexes were quite similar to M06-2X quantities, in most cases within 5%. Larger deviations were observed when the H-bonding chelating agents were bound to F^-, where there was a 20% drop. There was also a smaller binding energy of the iodosubstituted chelating agents at the MP2 level, but this change was a fairly uniform decrease of 18-28% for all four halides. Most importantly, none of the trends observed with the M06-2X calculations were altered. The cationic chelator binds the halides more strongly than does its neutral analogue. The energetic order of binding, whether H-bonding or I-bonding, remains $F^- \gg Cl^- > Br^- > I^-$. Also, the 2I chelator binds each halide much more strongly than does 2H.

The symmetrical, largely planar, geometries are not the only ones on the potential energy surface of each complex, although they do generally represent the global minimum. One sort of structure that appears with the neutral BTP places the anion well out of the binder's plane, engaged primarily in a $CH \cdot \cdot Y^-$ H-bond with the pyridine CH. This HB is a distorted one, with $\theta(CH \cdot \cdot Y)$ angles usually less than 150°. (Geometries such as these do not occur for X=H, however.) Like the neutral BTPs, the monocations also display H-bonded minima. In a few cases, their energies are competitive, or even slightly more stable than the symmetric structures. Slightly greater stability is restricted to X=Cl, with $Y=Cl^-$, Br^-, and I^-, where the energies are within 1 kcal/mol of the symmetrical structures. There are no secondary minima in the case of any of the dicationic binders.

7-4. Conclusions

Halide anions generally prefer a location midway between the two H or halogen atoms of the binding agent, whether the latter is neutral or positively charged. The binding energy is largest for the dicationic BTP^{+2}, followed by the monocation and the neutral BTP. The halide binding strength decreases with the size of the anion: F^- >> Cl^- > Br^- > I^-. Replacement of the pair of H atoms of BTP by halogens has a strong effect: the binding is weakened for Cl replacement and strengthened by I substitution; effects with Br are mixed. As a result, the binding of BTP, or any of its charged counterparts, to a halide is strongly enhanced by replacement of H atoms by I. In terms of equilibrium populations, this enhancement can be as large as 10^7. These binding agents, whether cationic or neutral, exhibit a strong preference for F^-. The selectivity for F^- over other halides can be as large as 10^6, for the dicationic BTP^{+2} substituted by I.

References

[1]   F. Guthrie, *J. Chem. Soc.* **1863**, *16*, 239-244.

[2]   O. Hassel, *Science* **1970**, *170*, 497-502.

[3]   J. P. M. Lommerse, A. J. Stone, R. Taylor, F. H. Allen, *J. Am. Chem. Soc.* **1996**, *118*, 3108-3116.

[4]   F. H. Allen, J. P. M. Lommerse, V. J. Hoy, J. A. K. Howard, G. R. Desiraju, *Acta Cryst.* **1997**, *B53*, 1006-1016.

[5]   W. Zierkiewicz, D. C. Bieńko, D. Michalska, T. Zeegers-Huyskens, *J. Comput. Chem.* **2015**, *36*, 821-832.

[6]   P. Deepa, B. V. Pandiyan, P. Kolandaivel, P. Hobza, *Phys. Chem. Chem. Phys.* **2014**, *16*, 2038-2047.

[7]   U. Adhikari, S. Scheiner, *J. Phys. Chem. A* **2012**, *116*, 3487-3497.

[8]   J. P. Anable, D. E. Hird, S. L. Stephens, D. P. Zaleski, N. R. Walker, A. C. Legon, *Chem. Phys. Lett.* **2015**, *625*, 179-185.

[9]   P. Politzer, J. S. Murray. In Noncovalent Forces; Scheiner, S., Ed.; Springer: Dordrecht, 2015, p 357-389.

[10]   S. Scheiner, *CrystEngComm* **2013**, *15*, 3119-3124.

[11]   A. Bauzá, D. Quiñonero, P. M. Deyà, A. Frontera, *CrystEngComm* **2013**, *15*, 3137-3144.

[12]   U. Adhikari, S. Scheiner, *Chem. Phys. Lett.* **2012**, *532*, 31-35.

[13]   R. E. Rosenfield, R. Parthasarathy, J. D. Dunitz, *J. Am. Chem. Soc.* **1977**, *99*, 4860-4862.

[14]   G. R. Desiraju, V. Nalini, *J. Mater. Chem.* **1991**, *1*, 201-203.

[15]   F. T. Burling, B. M. Goldstein, *J. Am. Chem. Soc.* **1992**, *114*, 2313-2320.

[16]   Y. Nagao, T. Hirata, S. Goto, S. Sano, A. Kakehi, K. Iizuka, M. Shiro, *J. Am. Chem. Soc.* **1998**, *120*, 3104-3110.

[17]   S. Scheiner, *J. Chem. Phys.* **2011**, *134*, 164313.

[18]   M. Iwaoka, S. Takemoto, S. Tomoda, *J. Am. Chem. Soc.* **2002**, *124*, 10613-10620.

[19]   V. d. P. N. Nziko, S. Scheiner, *J. Org. Chem.* **2015**, *80*, 2356-2363.

[20]   V. d. P. N. Nziko, S. Scheiner, *J. Phys. Chem. A* **2014**, *118*, 10849-10856.

[21]   L. M. Azofra, S. Scheiner, *J. Phys. Chem. A* **2014**, *118*, 3835-3845.

[22]   K. W. Klinkhammer, P. Pyykko, *Inorg. Chem.* **1995**, *34*, 4134-4138.

[23]   S. Scheiner, *J. Chem. Phys.* **2011**, *134*, 094315.

[24]   S. Scheiner, *Int. J. Quantum Chem.* **2013**, *113*, 1609-1620.

[25]   A. Bauzá, D. Quiñonero, P. M. Deyà, A. Frontera, *Phys. Chem. Chem. Phys.* **2012**, *14*, 14061-14066.

[26]   S. Sarkar, M. S. Pavan, T. N. Guru Row, *Phys. Chem. Chem. Phys.* **2015**, *17*, 2330-2334.

[27]   J. E. Del Bene, I. Alkorta, J. Elguero. In Noncovalent Forces; Scheiner, S., Ed.; Springer: Dordrecht, 2015, p 191-263.

[28]   S. Scheiner, *Acc. Chem. Res.* **2013**, *46*, 280-288.

[29]   I. Alkorta, I. Rozas, J. Elguero, *J. Phys. Chem. A* **2001**, *105*, 743-749.

[30]   Q.-Z. Li, H.-Y. Zhuo, H.-B. Li, Z.-B. Liu, W.-Z. Li, J.-B. Cheng, *J. Phys. Chem. A* **2015**, *119*, 2217-2224.

[31]   Q. Tang, Q. Li, *Comput. Theor. Chem.* **2014**, *1050*, 51-57.

[32]   D. Mani, E. Arunan, *J. Phys. Chem. A* **2014**, *118*, 10081-10089.

[33]   B. Vijaya Pandiyan, P. Deepa, P. Kolandaivel, *Phys. Chem. Chem. Phys.* **2014**, *16*, 19928-19940.

[34]   S. J. Grabowski, *Phys. Chem. Chem. Phys.* **2014**, *16*, 1824-1834.

[35]   K. J. Donald, M. Tawfik, *J. Phys. Chem. A* **2013**, *117*, 14176-14183.

[36]   L. M. Azofra, S. Scheiner, *J. Chem. Phys.* **2015**, *142*, 034307.

[37]   A. Farina, S. V. Meille, M. T. Messina, P. Metrangolo, G. Resnati, G. Vecchio, *Angew. Chem., Int. Ed. Engl.* **1999**, *38*, 2433-2436.

[38]   A. Mukherjee, S. Tothadi, G. R. Desiraju, *Acc. Chem. Res.* **2014**, *47*, 2514-2524.

[39]   D. Cinčić, T. Friščić, W. Jones, *Chem. Eur. J.* **2008**, *14*, 747-753.

[40]   P. Metrangolo, F. Meyer, T. Pilati, G. Resnati, G. Terraneo, *Angew. Chem. Int. Ed.* **2008**, *47*, 6114–6127.

[41]   Y. Takeda, D. Hisakuni, C.-H. Lin, S. Minakata, *Org. Lett.* **2015**, *17*, 318-321.

[42]   F. Sladojevich, E. McNeill, J. Börgel, S.-L. Zheng, T. Ritter, *Angew. Chem. Int. Ed.* **2015**, *54*, 3712-3716.

[43]   F. Kniep, S. H. Jungbauer, Q. Zhang, S. M. Walter, S. Schindler, I. Schnapperelle, E. Herdtweck, S. M. Huber, *Angew. Chem. Int. Ed.* **2013**, *52*, 7028-7032.

[44]   S. M. Walter, F. Kniep, E. Herdtweck, S. M. Huber, *Angew. Chem. Int. Ed.* **2011**, *50*, 7187-7191.

[45]   A. R. Voth, F. A. Hays, P. S. Ho, *Proc. Nat. Acad. Sci., USA* **2007**, *104*, 6188-6183.

[46]   R. Wilcken, M. O. Zimmermann, A. Lange, A. C. Joerger, F. M. Boeckler, *J. Med. Chem.* **2013**, *56*, 1363-1388.

[47]   P. Auffinger, F. A. Hays, E. Westhof, P. S. Ho, *Proc. Nat. Acad. Sci., USA* **2004**, *101*, 16789-16794.

[48]   L. A. Hardegger, B. Kuhn, B. Spinnler, L. Anselm, R. Ecabert, M. Stihle, B. Gsell, R. Thoma, J. Diez, J. Benz, J.-M. Plancher, G. Hartmann, D. W. Banner, W. Haap, F. Diederich, *Angew. Chem. Int. Ed.* **2010**, *50*, 314-318.

[49]   A. Vanderkooy, M. S. Taylor, *J. Am. Chem. Soc.* **2015**, *137*, 5080-5086.

[50]   L. C. Gilday, T. Lang, A. Caballero, P. J. Costa, V. Félix, P. D. Beer, *Angew. Chem. Int. Ed.* **2013**, *52*, 4356-4360.

[51] M. Lisbjerg, H. Valkenier, B. M. Jessen, H. Al-Kerdi, A. P. Davis, M. Pittelkow, *J. Am. Chem. Soc.* **2015**, *137*, 4948-4951.

[52] B. R. Mullaney, B. E. Partridge, P. D. Beer, *Chem. Eur. J.* **2015**, *21*, 1660-1665.

[53] B. R. Mullaney, A. L. Thompson, P. D. Beer, *Angew. Chem. Int. Ed.* **2014**, *53*, 11458-11462.

[54] M. J. Langton, S. W. Robinson, I. Marques, V. Félix, P. D. Beer, *Nat Chem* **2014**, *6*, 1039-1043.

[55] S. W. Robinson, C. L. Mustoe, N. G. White, A. Brown, A. L. Thompson, P. Kennepohl, P. D. Beer, *J. Am. Chem. Soc.* **2015**, *137*, 499-507.

[56] M. J. Frisch, G. W. Trucks, H. B. Schlegel, G. E. Scuseria, M. A. Robb, J. R. Cheeseman, G. Scalmani, V. Barone, B. Mennucci, G. A. Petersson, H. Nakatsuji, M. Caricato, X. Li, H. P. Hratchian, A. F. Izmaylov, J. Bloino, G. Zheng, J. L. Sonnenberg, M. Hada, M. Ehara, K. Toyota, R. Fukuda, J. Hasegawa, M. Ishida, T. Nakajima, Y. Honda, O. Kitao, H. Nakai, T. Vreven, J. Montgomery, J. A., J. E. Peralta, F. Ogliaro, M. Bearpark, J. J. Heyd, E. Brothers, K. N. Kudin, V. N. Staroverov, R. Kobayashi, J. Normand, K. Raghavachari, A. Rendell, J. C. Burant, S. S. Iyengar, J. Tomasi, M. Cossi, N. Rega, J. M. Millam, M. Klene, J. E. Knox, J. B. Cross, V. Bakken, C. Adamo, J. Jaramillo, R. Gomperts, R. E. Stratmann, O. Yazyev, A. J. Austin, R. Cammi, C. Pomelli, J. W. Ochterski, R. L. Martin, K. Morokuma, V. G. Zakrzewski, G. A. Voth, P. Salvador, J. J. Dannenberg, S. Dapprich, A. D. Daniels, O. Farkas, J. B. Foresman, J. V. Ortiz, J. Cioslowski, D. J. Fox. Wallingford, CT, 2009.

[57]   Y. Zhao, D. G. Truhlar, *Theor. Chem. Acc.* **2008**, *120*, 215-241.

[58]   M. W. Feyereisen, D. Feller, D. A. Dixon, *J. Phys. Chem.* **1996**, *100*, 2993-2997.

[59]   K. L. Schuchardt, B. T. Didier, T. Elsethagen, L. Sun, V. Gurumoorthi, J. Chase, J. Li, T. L. Windus, *J. Chem. Infor. Model.* **2007**, *47*, 1045-1052.

[60]   S. F. Boys, F. Bernardi, *Mol. Phys.* **1970**, *19*, 553-566.

[61]   A. E. Reed, L. A. Curtiss, F. Weinhold, *Chem. Rev.* **1988**, *88*, 899-926.

[62]   V. Barone, M. Cossi, *J. Phys. Chem. A* **1998**, *102*, 1995-2001.

[63]   F. A. Bulat, A. Toro-Labbé, T. Brinck, J. S. Murray, P. Politzer, *J. Mol. Model.* **2010**, *16*, 1679-1691.

Tables and Figures

Table 7-1. Optimized distances (Å) from anion to H or halogen atomsa of neutral, singly and doubly charged BTP with different halide anions. 2H indicates H-bonding anion receptors and 2Cl, 2Br, and 2I refer to corresponding halogen-substituted systems.

anion Y^-	2H	2Cl	2Br	2I
neutral BTP				
F^-	2.030	2.697	2.612	2.614
Cl^-	2.579	3.314	3.199	3.226
Br^-	2.729	3.458	3.355	3.390
I^-	2.955	3.643	3.577	3.610
monocation BTP$^+$				
F^-	2.013	2.652	2.577	2.582
Cl^-	2.538	3.264	3.166	3.185
Br^-	2.695	3.416	3.322	3.352
I^-	2.891/2.942	3.607	3.536	3.568
dication BTP^{+2}				
F^-	1.075/ 2.835	2.577	2.492	2.519
Cl^-	2.442	3.169	3.093	3.109
Br^-	2.657	3.346	3.247	3.262
I^-	2.903	3.551	3.458	3.480

aboth distances shown for appreciably asymmetric structures

Table 7-2. Counterpoise-corrected binding energies (kcal/mol) for complexes of neutral, singly and doubly charged BTP with different halide anions.

anion Y^-	2H	2Cl	2Br	2I
neutral BTP				
F^-	9.70	4.20	10.18	16.02
Cl^-	5.44	3.26	6.77	10.33
Br^-	4.77	3.24	6.55	9.88
I^-	4.10	3.21	6.30	9.37
monocation BTP^+				
F^-	13.18	5.93	12.38	18.83
Cl^-	7.35	4.34	8.22	12.16
Br^-	6.42	4.23	7.88	11.59
I^-	5.47	4.10	7.47	10.94
dication BTP^{+2}				
F^-	11.12	9.11	16.87	24.13
Cl^-	8.57	6.11	10.81	15.49
Br^-	7.77	5.82	10.28	14.61
I^-	6.74	5.50	9.60	13.66

Table 7-3. Thermodynamic parameters for binding of halide anions by neutral and charged receptors at 25 °C and 1 atm. ΔH and ΔG are in units of kcal/mol, and ΔS in cal mol^{-1} K^{-1}.

	2H			2Cl			2Br			2I		
	ΔS	ΔH	ΔG	ΔS	ΔH	ΔG	ΔS	ΔH	ΔG	ΔS	ΔH	ΔG
neutral BTP												
F$^-$	-29.63	-9.76	-0.93	-29.07	-4.00	4.67	-28.74	-10.09	-1.52	-34.34	-16.29	-6.05
Cl-	-27.10	-5.27	2.81	-25.03	-3.31	4.15	-24.88	-6.78	0.64	-31.16	-10.33	-1.04
Br-	-30.07	-5.31	3.65	-23.49	-3.32	3.68	-23.92	-6.52	0.61	-30.45	-9.86	-0.78
I$^-$	-33.48	-4.70	5.29	-23.92	-3.11	4.02	-23.65	-6.23	0.82	-28.39	-9.34	-0.88
monocation BTP$^+$												
F$^-$	-28.13	-13.32	-4.94	-30.04	-5.57	3.38	-27.86	-12.42	-4.11	-30.23	-19.01	-10.00
Cl-	-23.74	-7.35	-0.27	-26.11	-4.22	3.56	-25.32	-8.07	-0.52	-28.08	-12.18	-3.81
Br-	-30.74	-7.05	2.11	-26.25	-4.07	3.76	-22.31	-7.84	-1.19	-27.53	-11.65	-3.45
I$^-$	-33.82	-6.14	3.94	-31.89	-4.57	4.94	-22.02	-7.48	-0.92	-26.97	-10.97	-2.92
dication BTP^{+2}												
F$^-$	-24.10	-13.56	-6.38	-33.84	-9.86	0.23	-31.09	-16.83	-7.56	-24.68	-23.66	-16.31
Cl-	-25.85	-8.58	-0.87	-27.16	-5.88	2.22	-26.35	-10.89	-3.04	-22.74	-15.00	-8.22
Br-	-25.49	-7.92	-0.32	-25.39	-5.76	1.81	-25.04	-10.52	-3.05	-20.62	-14.22	-8.08
I$^-$	-18.14	-6.86	-1.45	-24.75	-5.54	1.84	-22.70	-9.92	-3.15	-18.50	-13.20	-7.69

Table 7-4. Preference of halide anion for halogenated vs H-bonding agent expressed as equilibrium ratio.

	2Cl	2Br	2I
	neutral BTP		
F$^-$	7.92E-05	2.70E+00	5.62E+03
Cl$^-$	1.04E-01	3.88E+01	6.60E+02
Br$^-$	9.51E-01	1.68E+02	1.76E+03
I$^-$	8.51E+00	1.88E+03	3.30E+04
	monocation BTP$^+$		
F$^-$	8.07E-07	2.47E-01	5.08E+03
Cl$^-$	1.57E-03	1.52E+00	3.91E+02
Br$^-$	6.19E-02	2.61E+02	1.18E+04
I$^-$	1.85E-01	3.62E+03	1.06E+05
	dication BTP^{+2}		
F$^-$	1.44E-05	7.31E+00	1.87E+07
Cl$^-$	5.46E-03	3.88E+01	2.41E+05
Br$^-$	2.75E-02	9.98E+01	4.82E+05
I$^-$	3.90E-03	1.76E+01	3.71E+04

Table 7-5. Selectivity of binding agent for F- over other halogen anions, expressed as equilibrium ratio.

	2H	2Cl	2Br	2I
	neutral BTP			
Cl$^-$	5.48E+02	4.16E-01	3.82E+01	4.67E+03
Br$^-$	2.26E+03	1.88E-01	3.63E+01	7.24E+03
I$^-$	3.59E+04	3.34E-01	5.17E+01	6.11E+03
	monocation BTP$^+$			
Cl$^-$	2.63E+03	1.35E+00	4.26E+02	3.41E+04
Br$^-$	1.46E+05	1.90E+00	1.38E+02	6.26E+04
I$^-$	3.19E+06	1.39E+01	2.17E+02	1.53E+05
	dication BTP^{+2}			
Cl$^-$	1.08E+04	2.87E+01	2.04E+03	8.41E+05
Br$^-$	2.74E+04	1.44E+01	2.01E+03	1.06E+06
I$^-$	4.08E+03	1.51E+01	1.70E+03	2.05E+06

Table 7-6. Maximum of molecular electrostatic potential, evaluated on the 0.001 au isodensity contour, at the M06-2X/6-311G* level.

	2H	2Cl	2Br	2I
neutral BTP	60.7	38.2	44.5	51.1
monocation BTP$^+$	129.0	90.2	96.6	101.6
dication BTP^{+2}	189.8	151.9	157.6	160.5

Table 7-7. NBO values of E(2) (kcal/mol) for interaction of halide anion with monocationic receptors. Charge transfers from all halide lone pairs to the C-H/X σ* antibonding orbitals.

anion	2H	2Cl	2Br	2I
F$^-$	43.19	8.64	21.57	36.82
Cl$^-$	25.38	4.42	12.91	22.77
Br$^-$	22.06	4.10	11.88	21.17
I$^-$	18.50	4.10	11.14	19.98
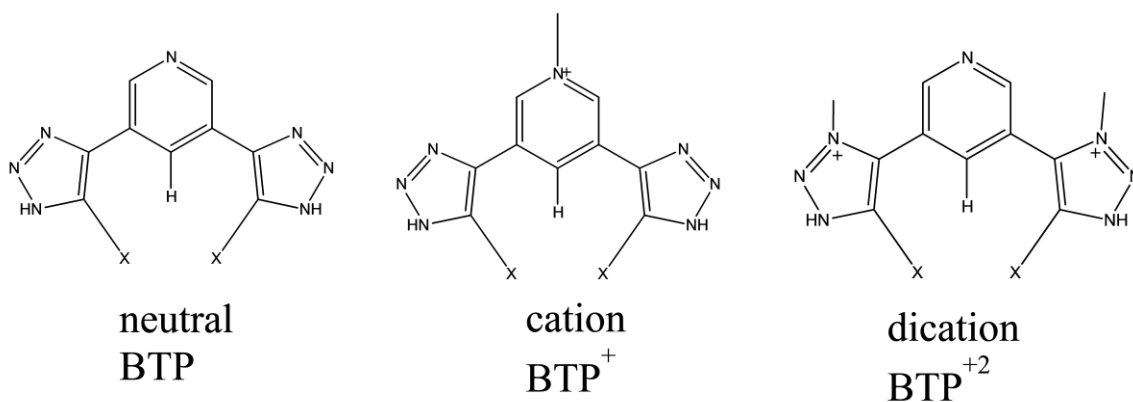
Scheme 7-I. Diagrams of BTP and its charged derivatives.
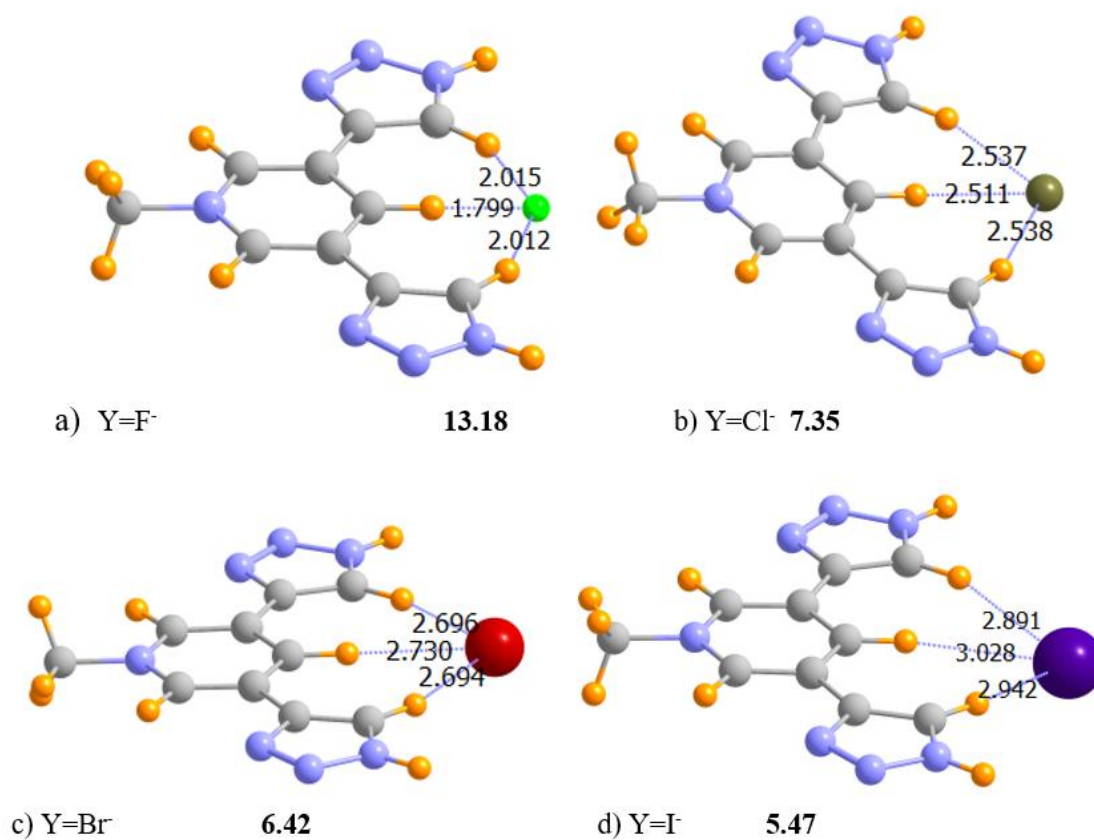
Figure 7-1. Optimized geometries of the complexes of halides with monocationic BTP$^+$ with X=H. The bold number indicates the counterpoise-corrected binding energy (kcal/mol); distances are in Å.
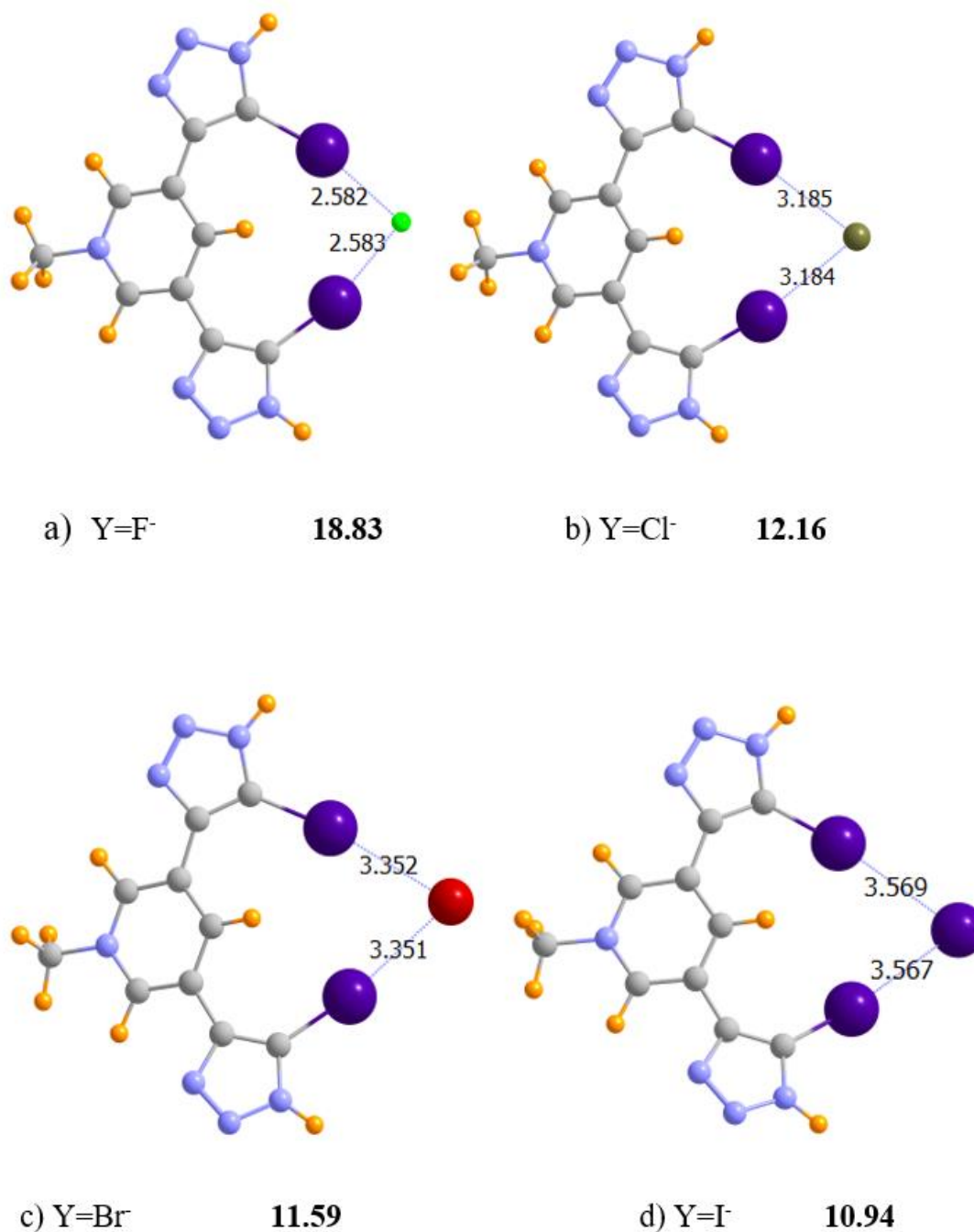
Figure 7-2. Optimized geometries of the complexes of halides with monocationic BTP$^+$ with X=I. The bold number indicates the counterpoise-corrected binding energy (kcal/mol); distances are in Å.

a) X=H

b) X=Cl

c) X=Br

d) X=I
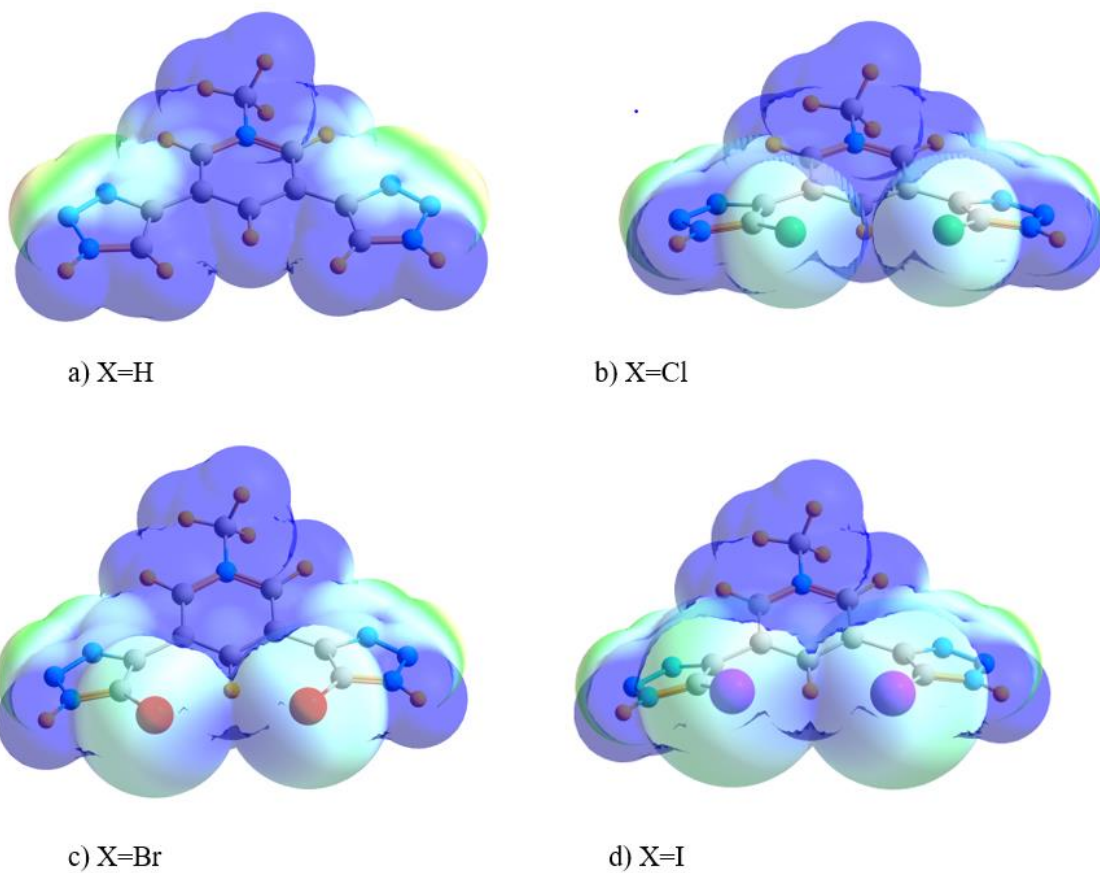
Figure 7-3. Molecular electrostatic potentials of monocationic BTP+.   Potential is illustrated on an isocontour equal to 1.5 times the van der Waals radius of each atom. Most positive potential shown (blue) is 0.15 au, and most negative (red) is 0.0 au.

CHAPTER 8

SUBSTITUENT EFFECTS ON THE BINDING OF HALIDES BY NEUTRAL AND

DICATIONIC BIS-TRIAZOLIUM RECEPTORS[1]

Abstract

The effects of substituent and overall charge upon the binding of a halide anion by a bis-triazolium receptor are studied by M06-2X DFT calculations, with the aug-cc-pVDZ basis set. Comparison is also made between a receptor that engages in H-bonds, with a halogen-bonding species. Fluoride is clearly most strongly bound, followed by Cl^-, Br^-, and I^- in that order. The dicationic receptor engages in stronger complexes, but not by a very wide margin compared to its neutral counterpart. The binding is enhanced as the substituent on the two triazolium rings becomes progressively more electron-withdrawing. Halogen-substituted receptors, whether neutral or cationic, display a greater sensitivity to substituent than do their H-bonding counterparts. Both Coulombic and charge transfer factors obey the latter trends but do not correctly reproduce the stronger halogen vs hydrogen bonding. Both H-bonds and halogen bonds are nearly linear within the complexes, due in part to bond rotations within the receptor that bring the two triazole rings closer to coplanarity with the central benzene ring.

8-1. Introduction

The selective and efficient binding of anions is an important component in a number of chemical, biological, and environmental processes. There has consequently been a progression of works that are aimed at understanding the fundamentals of this process, and thereby improving it, which would have a number of applications in analytical chemistry, catalysis, and so forth. The majority of anion receptor systems make use of noncovalent interactions between the receptor and the anion. Hydrogen bonds (HBs) are the most common[1-4] of these binding forces, which are typically strengthened relative to most other HBs by the presence[5-7] of a full charge on the anion.

However, work in recent years has shown a number of other noncovalent interactions that can be competitive with HBs. For example, highly asymmetric distribution of electron density around electronegative atoms of the chalcogen and pnicogen families allows a means for them to interact attractively with the negatively charged region of a partner.[8-23] The halogen atoms are no exception to this behavior and the rapidly developing exploration[19,24-30] of the eponymous halogen bonds (XBs) has found application in numerous areas of chemistry, such as molecular recognition,[31-33] organocatalysis,[34-37] and crystal engineering.[37-43]

It is no surprise, then, that XBs have found recent application to the field of selective anion binding.[43-49] Many of the binding agents have been bipodal in nature, with two different halogen atoms connecting to the anion via XBs. These interactions have typically been further strengthened by the presence of positive charge on the receptor. The most common groups binding the anions to date have been derivatives of pyridine,[48,50-52]

imidazole,[53-56] and 1,2,3 triazole.[44, 51, 57-61] These binding groups are typically connected to one another with a spacer group, such as a benzene or pyridine ring.

Recent work from this laboratory[62] studied the binding of halides to a receptor composed of a pair of 1,2,3-triazole species placed on either side of a separating pyridine ring. The replacement of the H atoms of the two triazoles by halogen atoms altered the binding, and in particular I-substitution yielded a strong enhancement of the binding of various halides by changing HBs to XBs. Adding positive charge to the receptor furnished another increment to the binding, such that the equilibrium constant could be increased by as much as several orders of magnitude.

However, what this study did not consider at all was how the binding of halides might be affected by the presence of substituents on the receptor. And indeed, this issue of substituent effects represents a gaping hole in our present understanding of differential halide binding, as it has not been examined to date in any systematic manner by either theory or experiment. Based on the major effects that substituents afford to a wide range of chemical properties, e.g. pK_a and reaction rates to name just two, it is easy to imagine a scenario where the judicious choice of a proper substituent could make the difference between an effective and ineffective receptor. In fact, a detailed understanding of substituent effects and their origins might enable the design of a new receptor that has been carefully tuned for optimal desired performance.

The present work addresses this issue in a systematic manner. How strong might these substituent effects be - are they comparable to the rise in binding energy that results from positive charge on the receptor? Do the substituents affect the halogen bonds to the

same degree that they alter the H-bonds? Can this effect be evaluated purely on the basis of the electron-withdrawing or donating capacity of the substituent or are there other phenomena that must be considered? What are the principal contributing factors to the binding, and can they be related simply to Coulombic and/or charge transfer? How might the substituents alter the geometries of both the receptors themselves, and the receptor-halide complex? Does the total charge on the receptor carry the same impact on the binding when there are substituents present? Does the strong preference of the receptor for F^- over other halides that was found earlier carry over when substituents are present?

In order to answer these questions, the bis-triazole receptor (BTB) shown in Scheme 8-I was taken as the starting point. As in many of the systems considered experimentally, I contains a pair of 1,2,3-triazole rings, connected to a central benzene unit. The two H atoms in the Z position of each triazole are replaced by each of 10 different substituents, chosen to span a wide range of electron-withdrawal or release. The dicationic analogues II were constructed by adding a methyl group on each triazole, as illustrated in the bottom of Scheme 8-I. The binding of each of these receptors to F^-, Cl^-, Br^-, and I^- was considered so as to span a wide range of different halides.

8-2. Computational Methods

Computations were carried out with Gaussian 09, Revision D.01 software.[63] Geometry optimizations along with frequency calculations were performed using the DFT M06-2X density functional[64] in conjunction with the aug-cc-pVDZ basis set. With heavier elements Br and I, aug-cc-pVDZ-PP pseudopotentials from the EMSL basis sets library[65-66] were used. Only geometries with all positive vibrational frequencies were taken into

consideration to ensure the obtained structures are in fact true minima. To account for solvent effects, the polarizable conductor calculation model (CPCM) was applied,[67] with water as the solvent. The binding energy of each optimized complex was computed as the difference in energy between the optimized complex and the sum of the energies of separately optimized monomers. The binding energies were corrected for basis sets superposition error (BSSE) using the counterpoise procedure.[68] Charge transfer was assessed using the NBO 6.0 program.[69] Molecular electrostatic potentials were calculated via the WFA- SAS program.[70]

8-3. Results

The geometries of a sample subset of complexes are displayed in Fig 8-1, which illustrate the binding of the F^- anion to both neutral and dicationic receptors, with substituent $Z=NO_2$. The H-bonding species (X=H) are placed on the left and the halogen-bonding receptors (X=I) on the right. These geometries are representative of the trends observed throughout. Comparison of Fig 8-1a with 8-1c illustrates the contraction of the H-bond lengths that occurs when a charge of +2 is placed on the receptor. The distances of F^- to the X=I atoms on the right side of Fig 8-1 are longer, chiefly due to the larger radius of I as compared to H. Again, the dication has shorter halogen bonded distances than does the neutral. Note also that the larger size of I vs H prevents the third H··F^- HB that is present in Figs 1a and 1c from occurring in the halogen-bonded species. In fact, this third HB is only possible for $Y=F^-$, which is at least partly responsible for the much stronger bonding of F^- as compared to the other halides. Fig 8-2 provides a broader picture of how the geometries are affected by the nature of the halide, as well as the charge state of the receptor

and the identity of the binding atom. The substituent chosen for illustration in Fig 8-2 is NH_2, which is on the opposite end of the electron-donation spectrum from NO_2 in Fig 8-1. The fully optimized geometries of all species discussed below are illustrated in the Supplementary Information, and display very similar trends.

The effects of the various substituents on the binding energy are evident in Fig 8-3 which represents the neutral receptors. As one moves from left to right there is a general trend toward larger binding energy. The broken lines refer to the H-bonding molecules, and the halogen bonding species with X=I are indicated by the solid lines. The identity of the halide anion is color coded.

There are several overall trends that are apparent in Fig 8-3. In most cases, the electron-releasing amino group yields the weakest binding and NO_2 the strongest. The solid lines lie above their broken counterparts, which represents the stronger halogen vs H-bonding. This preference for I over H varies from 1.6 to 5.8 kcal/mol, and is generally larger for the more strongly bound species on the right side of Fig 8-3. Another clear trend is the diminishing binding strength of the halides in the order $F^- \gg Cl^- > Br^- > I^-$, whether by a H or halogen-bonding agent.

Within the overall trends are several other interesting patterns. For example, the data for the OCH_3 substituent suggest a real difference between H and X bonding. Methoxy seems to provide anomalously strong binding for the broken curves representing H-bonding, in comparison to their halogen-bonding counterparts, indicated by the solid curves. This distinction is perhaps most readily apparent in the comparison with the similar OH substituent to its immediate right in Fig. 8-3. Examination of the optimized geometries

provides a ready explanation for this apparent paradox. When X=H, the methyl groups are oriented toward that halide, engaging in weak H-bonding with it. These secondary HBs have (H··Y⁻) lengths on the order of 3.5 Å, which are rather long but there are four such bonds in each case, which have a cumulative effect. In addition, there is a Y→σ*(CH) charge transfer observed in the NBO analysis which reinforces this stabilizing effect. However, when X=H is replaced by the much bulkier I, the methyl group is forced into the opposite orientation, where any such interaction is impossible. So one can perhaps attribute the "bumps" in the H-bonding broken curves of Fig 8-2 to this supplementary CH··Y⁻ H-bonding.

Another substituent which behaves in a perhaps surprising pattern is -COOH. When X=H, the COOH group is oriented with its -OH turned toward the halide, and cis to the carbonyl O. However, when the H is replaced by I, -COOH rotates around by 180° such that it is its C=O which is turned toward the binding halide. On the other hand, this reorientation has little effect upon the energetics, since the -COOH does not engage in any bonding with the halide in either of these two conformations, and there is little energetic difference between these two orientations.

The addition of a double positive charge on the receptor leads to stronger binding with the halides, as one would expect. The degree of strengthening is illustrated by comparison of Fig 8-4 with Fig 8-3. Whereas the neutral binding agents with X=H span a range between 3.9 and 16.6 kcal/mol, the minimum and maximum for the dications are 6.9 and 24.0 kcal/mol, respectively. Similarly, for X=I, the range for the neutrals is 8.5-21.1 kcal/mol, and that of the dications is 12.8-29.6 kcal/mol. It is perhaps interesting that the

enlargement of the binding energies induced by a double positive charge is no larger than this.

It is worth noting as well that the patterns for the dications and neutrals are quite similar, with binding energies rising from left to right, as the substituent alters its character from electron-releasing to withdrawing. Also consistent with the neutrals in Fig 8-3, the interactions with X=I are stronger than with X=H for the dications as well. The preference for I over H is larger for the dications, but only slightly so. For example, the largest I/H difference for the neutrals is 8.1 kcal/mol, which occurs for the -COCH$_3$ substituent. The same substituent is responsible for a 9.7 kcal/mol preference of I over H for the dications.

The gap between the solid and broken curves in Fig 8-3 is related to the improved ability of the I-substituted receptor to bind each halide, relative to the unsubstituted species. This gap is largest for F$^-$, roughly 7-8 kcal/mol for the neutral receptors and 8-10 kcal/mol for the dications. In terms of an equilibrium constant, 7 kcal/mol would translate at 25° C to a 10^5 enhancement of the binding of fluoride by I-substitution, and this quantity would be as large as 10^7 for the dicationic receptor. The interactions of the other halides are also strengthened by the I-substitution, but not by quite as much, more in the range of 3-6 kcal/mol.

The magnitude of substituent effect is another important parameter. Turning first to the neutral H-bonding receptors, the broken curves in Fig 8-3, the change of substituent from NH$_2$ to NO$_2$, raises the binding energy by 2-5 kcal/mol, largest for F$^-$ and smallest for I$^-$. This same increment is larger for the halogen-bonding receptors in Fig 8-3, in the range between 3 and 7 kcal/mol. Adding double positive charge to the receptor results in a small

increase of roughly 0.5 kcal/mol in the aforementioned NO_2 - NH_2 difference for the H-bonding receptors, about 0.7 kcal/mol for the halogen bonding agents. In summary, the I-substituted receptors, whether neutral or cationic, display a greater sensitivity to substituent than do their H-bonding counterparts.

Just as in the case of the neutrals in Fig 8-3, the dications also present an anomalously large binding energy for the OMe substituents when X=H, as indicated by the broken curves in Fig 8-4. Again, this effect is the result of secondary H-bonding to the methyl groups. A similar inflation appears in Fig 8-4 for the $COCH_3$ group which has a similar origin: $CH\cdot\cdot Y^-$ H-bonding. This interaction is absent in the neutrals because the $COCH_3$ group adopts the opposite configuration there, with CH_3 trans to the Y^- anion. One may note that the binding energies of the OH substituent in Fig 8-4 are also somewhat higher than in Fig 8-3, relative to the other substituents. Again, secondary H-bonding is the culprit, in this case $OH\cdot\cdot Y^-$.

8-3.1. Electrostatics and Charge Transfer

The interaction of each receptor with a halide will clearly have a strong electrostatic component. The anion will be attracted toward the positive region of the pertinent atom, whether H or I. The molecular electrostatic potential (MEP) surrounding each receptor was evaluated on a surface corresponding to an isodensity contour of 0.001 au. The maximum value of this potential on the binding atom, either H or I, and pointing directly toward the incoming halide, is illustrated in Fig 8-5 for all binding agents. The potential is clearly most positive for the dications, shown in red, compared to the neutrals in green. Secondly, the potentials are uniformly higher for X=H (broken curves) than for X=I (solid). This trend is

opposite to the binding energies in Figs 8-3 and 8-4 where X=I engages in stronger binding with the halides. Another point of difference is related to the magnitudes. As indicated above, the dications bind more strongly to the halides than do the neutrals, but not by a wide margin. The dication/neutral ratio of binding energies is between 1.2 and 2.0. In contrast, however, there is a much larger ratio of electrostatic potentials between the charged and neutral species in Fig 8-5, some three to fourfold. Also, the curves in Fig 8-5 flatten out toward their right extrema, while the binding energies rise up more quickly, suggesting that the MEP does not adequately represent the effects of the strongly electron-withdrawing substituents. Clearly, then, Coulombic forces cannot be considered the only factor, or perhaps even the dominant one, in the binding of halides.

On the positive side, the rise in the potentials from left to right in Fig 8-5 does conform at least in a general sense to the trends in the binding energies in Figs 8-3 and 8-4. It is interesting to note that the broken green curve in Fig 8-5, corresponding to the neutral agents with X=H, shows the same bump at OMe as appears in the four broken curves of Fig 8-3. This similarity, absent in the solid curves of both figures, indicates that the position of the methyl group has an influence on the MEP commensurate with its effect on the binding energy.

The interaction between an anion and receptor can be expected to lead to a substantial polarization component. That is, the presence of the halide ought to induce a shift in electron density within the binding agent, as well as the obvious transfer of density from halide to receptor. The energetic consequence of such charge shifts can be assessed via the NBO procedure. In the case of a $CH \cdot \cdot Y^-$ HB for example, the shift of charge from

the lone pairs of the halide into the σ*(CH) antibonding orbital accounts for a second order perturbation energy E(2); a similar quantity is calculated for a halogen bond where the charge is transferred into the σ*(IC) antibonding orbital. (It should be noted that in a few cases, there is a secondary HB, as for example the -OCH$_3$ substituents mentioned above. In these cases, the E(2) of these secondary interactions with the halide are included in the data below so as to furnish a more complete treatment of charge transfer.)

These values of E(2) are displayed in Figs 8-6 and 8-7 for the neutral and dicationic complexes, respectively, where several familiar trends are again present. These quantities are larger for the dications than for the neutrals, and become larger from left to right in the figures. They are more reflective of the binding energies than are the MEP maxima in Fig 8-5 in that the difference between dication and neutral is not overly dramatic. Also, their shapes are rather similar. They both rise at a good clip, even at the right extrema. Both sorts of curves contain the bump at the OMe substituent for the neutrals, for X=H, but not for X=I. Regarding the dications, both Figs 8-4 and 8-5 contain what appears to be a dip for X=H (which is in reality a supplement to the surrounding substituents from secondary interactions). On the other hand, the NBO values are like MEP quantities in that they are both larger for X=H than for X=I, in contrast to the binding energies. However, the larger values of E(2) for HBs as compared to XBs is not surprising as it is a general feature of NBO E(2), in a wide range of different systems.[71-73]

One may ask whether MEP maxima or NBO quantities represent a better means of predicting or measuring binding strength. Figs 8-8 and 8-9 display the correlation coefficients in a linear fit of E_b to each quantity, respectively. The fits are clearly superior

for E(2) in Fig 8-9. For example, the correlation coefficients are especially good for the halogenated binding agents, whether neutral or dicationic, with $R^2 \geq 0.97$. One might conclude that the energetic representation of interorbital charge transfer, as encapsulated by NBO, provides a more rigorous reproduction of the full binding energy than does the electrostatic approximation, although neither can be said to be perfect.

8-3.2. Geometries

The charge transferred into the $\sigma^*(CH)/(CI)$ antibonding orbitals is well known to lengthen these covalent bonds upon formation of the relevant complexes.[74-78] The elongation that occurs in these bonds obey many of the same patterns as do the binding energies. They are uniformly larger for the halogen than for the H-bonded complexes, and the dicationic systems manifest longer elongations than do the neutrals. Also in parallel with the binding energies, the stretches follow the rule $F^- \gg Cl^- > Br^- > I^-$. In moving from left to right, i.e. from electron-releasing to electron-withdrawing substituents, there is a clear pattern of increase in the elongation. Regarding the range, the smallest stretch amounts to 0.003 Å for the neutral species H-bonded to I^-, and the largest elongation of 0.049 Å occurs for the cationic halogen-bonded receptor interacting with F^-.

Both HBs and XBs have a strong preference for linearity. There is some question as to how the internal restraints within the receptors might accommodate this preference, given their nonplanarity, the difference in length between CH and CI bonds, as well as the variable size of the four halides. All of the complexes are able to maintain near linearity, with the largest deviation being only 14°. There is little distinction between H-bonding vs halogen-bonding receptors, nor does the presence of charge or the degree of electron-

withdrawing character of the substituent have an appreciable effect. In fact, the only substantive trend is that the small size of the fluoride anion leads to about 5° larger deviations from linearity than do the other halides.

The unbound receptors are not planar species. The two triazole rings are rotated around the CN bond connecting them to the central benzene by varying amounts. The φ(CNCC) dihedral angle (where the latter two C atoms lie in the phenyl group) is taken as the measure of this nonplanarity. This nonplanarity lies in the 28-35° range for the neutral H-bonding receptor, and becomes about 8° larger for the analogous dication. The much larger size of the I atom leads to greater nonplanarity in the halogen-bonding receptors, averaging 61° and 69° in the neutral and dications, respectively.

However, the strong HB forces pull the two triazole rings into much closer coplanarity when the anions are bound. The two rings are held within 1° of coplanarity for the F$^-$ anion. Although the larger sizes of the other halides prevent attaining this level of planarity, one can still observe a much diminished φ(CNCC). The measure of nonplanarity decreases on average by 16° upon binding of Cl$^-$, 8° for Br$^-$, and 6° for I$^-$, consonant with the enlarging sizes of these halides. The corresponding reductions for the dicationic H-bonding receptors are 13, 12, and 7°, respectively. The XBs exert a similar pull trying to bring the two triazole rings closer to coplanarity, but the much larger size of the I atoms opposes this trend, keeping φ(CNCC) up around 50-60°. The reduction in this angle arising from binding of the anions is thus only 3-6° for the neutrals and 6-9° for the dications.

8-4. Conclusions and Discussion

The receptors considered here engage in strongly bound complexes with the various halides, in the order $F^- \gg Cl^- > Br^- > I^-$. The binding energies vary from 4 to 21 kcal/mol for the neutral receptors, rising to the 7-30 kcal/mol range for dications. In all cases, the replacement of the H atom of the receptor by I strengthens the interaction. This differential amounts to between 3 and 10 kcal/mol, which equals 20-100% on a percentage basis. The binding grows steadily stronger as the substituent Z becomes more electron-withdrawing. The largest increment, that between the NH_2 and NO_2 substituents, amounts to a 30-50% rise. Sensitivity to substituent is larger for I-substituted receptors than for their H-bonding counterparts, and dicationic receptors of both sorts show a heightened sensitivity. There are minor deviations from the strict ordering of binding energy with electron-withdrawing capacity of the substituent, most of which can be attributed to direct but weak secondary interactions between the halide and the substituent itself.

The total binding energies can be correlated with their chief contributing forces, viz. Coulombic attraction and charge transfer. The former is measured by the magnitude of the MEP on the X=H or I atom to which the halide is attached, and charge transfer is assessed via the NBO second-order perturbation energy. Both of these quantities grow along with the electronegativity of the substituent, but also show certain deviations from the binding energy than do their H-bonding counterparts. Most notably, while the halogen bonding agents (X=I) engage in tighter complexes with the halides, both MEP and E(2) would suggest the opposite pattern. Nonetheless the NBO charge transfer correlates better with the binding energy than does the MEP.

The binding produces certain geometrical changes in the receptors. Chief among these is the elongation of the CH/CI covalent bonds. These stretches are larger for the halogen than for the H-bonded species, and obey trends very much akin to those observed for the energetics. The receptors are able to mold their shape so as to engage in nearly linear HBs/XBs with the bound halide, even accommodating the very large iodide. This linearity is associated with modification of the internal geometry of the receptor, such that the two triazole rings come closer to coplanarity with the central benzene ring than in their unbound state.

Comparison with earlier work[62] enables conclusions to be drawn concerning the effect of the central group to which the two triazole rings are bound. The earlier calculations used a pyridine rather than a benzene ring as a connector, and the two triazole rings were bound to this connector by one of their C atoms, rather than N as here. These changes produced very little effect upon any of the binding energies, with one exception: the H-bonds to fluoride were weakened by some 20-40%.

As one might anticipate in cases involving charged species, there are locations other than the multidentate H-bonding or halogen-bonding sites of interest here that can attract the halide anion. In most cases, the other local minima were of considerably higher energy and thus largely irrelevant to the arguments presented above. The exceptions involved those substituents like -COOH that contain a highly acidic proton that can engage in a $OH \cdot \cdot X^-$ HB with the halide. When F^- interacts with the carboxyl-substituted receptors, the formation of such a $-COOH \cdot \cdot F^-$ HB is energetically preferred over the usual binding site. The same is true for the -OH substituents which can again engage in a $OH \cdot \cdot F^-$ HB. The

ability of such strong proton donors as substituents must therefore be a consideration in the design of halide receptors.

There are other more minor perturbations from the global minimum that occur as secondary minima in a few cases. These other structures involved a rotation of the substituent. Taking OH as an example, the H atom could be oriented toward or away from the incoming halide. In the case of the neutral receptors, the OH favored rotation away from the halide. The other conformation was higher in energy by roughly 1 kcal/mol. The dicationic receptors favored the OH rotated in toward the halide, by something on the order of 5 kcal/mol. Very similar observations apply to several other substituents, specifically OMe, COMe, CHO, and COOH. In any case, it is the global minima that are reported and analyzed here.

Although only recently engendering detailed study, the use of halogen bonding receptors to complex with anions has yielded some related principles. While limited to simpler monodentate receptors and not considering halides directly, Sarwar et al[79] noted a linear free energy relationship between the binding constant and substituent constant or calculated MEP of the substituted iodoperfluoroarene XC_6F_4I receptors. Like our own findings above these authors noted limitations to a purely electrostatic representation of halogen bonding and differences between halogen bonding and hydrogen bonding. The following year saw the examination of a bipodal halogen-bonding receptor[80] in concert with halides, but did not explicitly consider substituent effects, also true of slightly later work.[36] A very recent report confirmed our finding that the binding energy increases with diminished size of the halide,[59] as well as the superiority of halogen bonding through I as

compared to H-bonding, but again little in the way of substituent effects could be gleaned from this work. The amplification of binding energy resulting from replacement of H by I had been noted earlier,[81-83] albeit without direct evaluation of substituent effects, and this same effect can be utilized for catalysis.[51] The same principles appear to apply to tripodal receptors[56] as well.

References

(1)   Hargrove, A. E.; Nieto, S.; Zhang, T.; Sessler, J. L.; Anslyn, E. V. Artificial Receptors for the Recognition of Phosphorylated Molecules. *Chem. Rev.* **2011,** *111*, 6603-6782.

(2)   Malerich, J. P.; Hagihara, K.; Rawal, V. H. Chiral Squaramide Derivatives Are Excellent Hydrogen Bond Donor Catalysts. *J. Am. Chem. Soc.* **2008,** *130*, 14416-14417.

(3)   Doyle, A. G.; Jacobsen, E. N. Small-Molecule H-Bond Donors in Asymmetric Catalysis. *Chem. Rev.* **2007,** *107*, 5713-5743.

(4)   Schreiner, P. R. Metal-Free Organocatalysis through Explicit Hydrogen Bonding Interactions. *Chem. Soc. Rev.* **2003,** *32*, 289-296.

(5)   Nepal, B.; Scheiner, S. Microsolvation of Anions by Molecules Forming CH··X$^-$ Hydrogen Bonds. *Chem. Phys.* **2015,** *463*, 137-144.

(6)   Cybulski, S. M.; Scheiner, S. Hydrogen Bonding and Proton Transfers Involving the Carboxylate Group. *J. Am. Chem. Soc.* **1989,** *111*, 23-31.

(7)   Cybulski, S. M.; Scheiner, S. Comparison of Morokuma and Perturbation Theory Approaches to Decomposition of Interaction Energy. $(NH_4)^+$...NH_3. *Chem. Phys. Lett.* **1990,** *166*, 57-64.

(8)   Desiraju, G. R.; Nalini, V. Database Analysis of Crystal-Structure-Determining Interactions Involving Sulphur: Implications for the Design of Organic Metals. *J. Mater. Chem.* **1991,** *1*, 201-203.

(9)   Burling, F. T.; Goldstein, B. M. Computational Studies of Nonbonded Sulfur-Oxygen and Selenium-Oxygen Interactions in the Thiazole and Selenazole Nucleosides. *J. Am. Chem. Soc.* **1992,** *114*, 2313-2320.

(10)   Scheiner, S. On the Properties of X⋯N Noncovalent Interactions for First-, Second- and Third-Row X Atoms. *J. Chem. Phys.* **2011,** *134*, 164313.

(11)   Nagao, Y.; Hirata, T.; Goto, S.; Sano, S.; Kakehi, A.; Iizuka, K.; Shiro, M. Intramolecular Nonbonded S⋯O Interaction Recognized in (Acylimino)Thiadiazoline Derivatives as Angiotensin II Receptor Antagonists and Related Compounds. *J. Am. Chem. Soc.* **1998,** *120*, 3104-3110.

(12)   Iwaoka, M.; Takemoto, S.; Tomoda, S. Statistical and Theoretical Investigations on the Directionality of Nonbonded S⋯O Interactions. Implications for Molecular Design and Protein Engineering. *J. Am. Chem. Soc.* **2002,** *124*, 10613-10620.

(13)   Nziko, V. d. P. N.; Scheiner, S. Intramolecular S···O Chalcogen Bond as Stabilizing Factor in Geometry of Substituted Phenyl-SF$_3$ Molecules. *J. Org. Chem.* **2015,** *80*, 2356-2363.

(14)   Nziko, V. d. P. N.; Scheiner, S. Chalcogen Bonding between Tetravalent SF$_4$ and Amines. *J. Phys. Chem. A* **2014,** *118*, 10849-10856.

(15)   Azofra, L. M.; Scheiner, S. Substituent Effects in the Noncovalent Bonding of SO$_2$ to Molecules Containing a Carbonyl Group. The Dominating Role of the Chalcogen Bond. *J. Phys. Chem. A* **2014,** *118*, 3835-3845.

(16)   Klinkhammer, K. W.; Pyykko, P. Ab Initio Interpretation of the Closed-Shell Intermolecular E···E Attraction in Dipnicogen (H$_2$E-EH$_2$)$_2$ and (He-EH)$_2$ Hydride Model Dimers. *Inorg. Chem.* **1995,** *34*, 4134-4138.

(17)   Scheiner, S. A New Noncovalent Force: Comparison of P···N Interaction with Hydrogen and Halogen Bonds. *J. Chem. Phys.* **2011,** *134*, 094315.

(18)   Bauzá, A.; Mooibroek, T. J.; Frontera, A. The Bright Future of Unconventional Σ/Π-Hole Interactions. *ChemPhysChem.* **2015,** *16*, 2496-2517.

(19)   Adhikari, U.; Scheiner, S. Sensitivity of Pnicogen, Chalcogen, Halogen and H-Bonds to Angular Distortions. *Chem. Phys. Lett.* **2012,** *532*, 31-35.

(20)   Bauzá, A.; Quiñonero, D.; Deyà, P. M.; Frontera, A. Pnicogen–p Complexes: Theoretical Study and Biological Implications. *Phys. Chem. Chem. Phys.* **2012,** *14*, 14061-14066.

(21)   Sarkar, S.; Pavan, M. S.; Guru Row, T. N. Experimental Validation of 'Pnicogen Bonding' in Nitrogen by Charge Density Analysis. *Phys. Chem. Chem. Phys.* **2015,** *17*, 2330-2334.

(22)   Del Bene, J. E.; Alkorta, I.; Elguero, J. The Pnicogen Bond in Review: Structures, Energies, Bonding Properties, and Spin-Spin Coupling Constants of Complexes Stabilized by Pnicogen Bonds. In *Noncovalent Forces*, Scheiner, S., Ed. Springer: Dordrecht, Netherlands, 2015; Vol. 19, pp 191-263.

(23)   Scheiner, S. The Pnicogen Bond: Its Relation to Hydrogen, Halogen, and Other Noncovalent Bonds. *Acc. Chem. Res.* **2013,** *46*, 280-288.

(24)   Zierkiewicz, W.; Bieńko, D. C.; Michalska, D.; Zeegers-Huyskens, T. Theoretical Investigation of the Halogen Bonded Complexes between Carbonyl Bases and Molecular Chlorine. *J. Comput. Chem.* **2015,** *36*, 821-832.

(25)   Deepa, P.; Pandiyan, B. V.; Kolandaivel, P.; Hobza, P. Halogen Bonds in Crystal Ttf Derivatives: An Ab Initio Quantum Mechanical Study. *Phys. Chem. Chem. Phys.* **2014,** *16*, 2038-2047.

(26)   Adhikari, U.; Scheiner, S. Substituent Effects on $Cl\cdots N$, $S\cdots N$, and $P\cdots N$ Noncovalent Bonds. *J. Phys. Chem. A* **2012,** *116*, 3487-3497.

(27)   Anable, J. P.; Hird, D. E.; Stephens, S. L.; Zaleski, D. P.; Walker, N. R.; Legon, A. C. Characterisation of the Weak Halogen Bond in $N_2\cdots ICF_3$ by Pure Rotational Spectroscopy. *Chem. Phys. Lett.* **2015,** *625*, 179-185.

(28)   Politzer, P.; Murray, J. S. A Unified View of Halogen Bonding, Hydrogen Bonding and Other s-Hole Interactions. In *Noncovalent Forces*, Scheiner, S., Ed. Springer: Dordrecht, Netherlands, 2015; Vol. 19, pp 357-389.

(29)   Scheiner, S. Sensitivity of Noncovalent Bonds to Intermolecular Separation: Hydrogen, Halogen, Chalcogen, and Pnicogen Bonds. *CrystEngComm* **2013,** *15*, 3119-3124.

(30)   Bauzá, A.; Quiñonero, D.; Deyà, P. M.; Frontera, A. Halogen Bonding Versus Chalcogen and Pnicogen Bonding: A Combined Cambridge Structural Database and Theoretical Study. *CrystEngComm* **2013,** *15*, 3137-3144.

(31)   Beyeh, N. K.; Pan, F.; Rissanen, K. A Halogen-Bonded Dimeric Resorcinarene Capsule. *Angew. Chem. Int. Ed.* **2015,** *54*, 7303-7307.

(32)   Jungbauer, S. H.; Bulfield, D.; Kniep, F.; Lehmann, C. W.; Herdtweck, E.; Huber, S. M. Toward Molecular Recognition: Three-Point Halogen Bonding in the Solid State and in Solution. *J. Am. Chem. Soc.* **2014,** *136*, 16740-16743.

(33)   Caronna, T.; Liantonio, R.; Logothetis, T. A.; Metrangolo, P.; Pilati, T.; Resnati, G. Halogen Bonding and p···p Stacking Control Reactivity in the Solid State. *J. Am. Chem. Soc.* **2004,** *126*, 4500-4501.

(34)   Takeda, Y.; Hisakuni, D.; Lin, C.-H.; Minakata, S. 2-Halogenoimidazolium Salt Catalyzed Aza-Diels–Alder Reaction through Halogen-Bond Formation. *Org. Lett.* **2015,** *17*, 318-321.

(35)   Sladojevich, F.; McNeill, E.; Börgel, J.; Zheng, S.-L.; Ritter, T. Condensed-Phase, Halogen-Bonded CF$_3$I and C$_2$f$_5$i Adducts for Perfluoroalkylation Reactions. *Angew. Chem. Int. Ed.* **2015,** *54*, 3712-3716.

(36)   Kniep, F.; Jungbauer, S. H.; Zhang, Q.; Walter, S. M.; Schindler, S.; Schnapperelle, I.; Herdtweck, E.; Huber, S. M. Organocatalysis by Neutral Multidentate Halogen-Bond Donors. *Angew. Chem. Int. Ed.* **2013,** *52*, 7028-7032.

(37)   Walter, S. M.; Kniep, F.; Herdtweck, E.; Huber, S. M. Halogen-Bond-Induced Activation of a Carbon–Heteroatom Bond. *Angew. Chem. Int. Ed.* **2011,** *50*, 7187-7191.

(38)   Mukherjee, A.; Tothadi, S.; Desiraju, G. R. Halogen Bonds in Crystal Engineering: Like Hydrogen Bonds yet Different. *Acc. Chem. Res.* **2014,** *47*, 2514-2524.

(39)   Cinčić, D.; Friščić, T.; Jones, W. Isostructural Materials Achieved by Using Structurally Equivalent Donors and Acceptors in Halogen-Bonded Cocrystals. *Chem. Eur. J.* **2008,** *14*, 747-753.

(40)   Cao, D.; Hong, M.; Blackburn, A. K.; Liu, Z.; Holcroft, J. M.; Stoddart, J. F. Two-Point Halogen Bonding between 3,6-Dihalopyromellitic Diimides. *Chem. Sci.* **2014,** *5*, 4242-4248.

(41)   Bruce, D. W.; Metrangolo, P.; Meyer, F.; Pilati, T.; Präsang, C.; Resnati, G.; Terraneo, G.; Wainwright, S. G.; Whitwood, A. C. Structure–Function Relationships in Liquid-Crystalline Halogen-Bonded Complexes. *Chem. Eur. J.* **2010,** *16*, 9511-9524.

(42)   Turunen, L.; Beyeh, N. K.; Pan, F.; Valkonen, A.; Rissanen, K. Tetraiodoethynyl Resorcinarene Cavitands as Multivalent Halogen Bond Donors. *Chem. Commun.* **2014,** *50*, 15920-15923.

(43)   Troff, R. W.; Mäkelä, T.; Topić, F.; Valkonen, A.; Raatikainen, K.; Rissanen, K. Alternative Motifs for Halogen Bonding. *Eur. J. Org. Chem.* **2013,** *2013*, 1617-1637.

(44)   Schulze, B.; Schubert, U. S. Beyond Click Chemistry - Supramolecular Interactions of 1,2,3-Triazoles. *Chem. Soc. Rev.* **2014,** *43*, 2522-2571.

(45)   Ghosh, S.; Mishra, M. K.; Kadambi, S. B.; Ramamurty, U.; Desiraju, G. R. Designing Elastic Organic Crystals: Highly Flexible Polyhalogenated N-Benzylideneanilines. *Angew. Chem. Int. Ed.* **2015,** *54*, 2674-2678.

(46)   Beale, T. M.; Chudzinski, M. G.; Sarwar, M. G.; Taylor, M. S. Halogen Bonding in Solution: Thermodynamics and Applications. *Chem. Soc. Rev.* **2013,** *42*, 1667-1680.

(47)   Metrangolo, P.; Resnati, G. Halogen Versus Hydrogen. *Science* **2008,** *321*, 918-919.

(48)   Langton, M. J.; Robinson, S. W.; Marques, I.; Félix, V.; Beer, P. D. Halogen Bonding in Water Results in Enhanced Anion Recognition in Acyclic and Rotaxane Hosts. *Nat Chem* **2014,** *6*, 1039-1043.

(49)   Lim, J. Y. C.; Beer, P. D. Superior Perrhenate Anion Recognition in Water by a Halogen Bonding Acyclic Receptor. *Chem. Commun.* **2015,** *51*, 3686-3688.

(50)   Robinson, S. W.; Mustoe, C. L.; White, N. G.; Brown, A.; Thompson, A. L.; Kennepohl, P.; Beer, P. D. Evidence for Halogen Bond Covalency in Acyclic and Interlocked Halogen-Bonding Receptor Anion Recognition. *J. Am. Chem. Soc.* **2015,** *137*, 499-507.

(51)   Jungbauer, S. H.; Huber, S. M. Cationic Multidentate Halogen-Bond Donors in Halide Abstraction Organocatalysis: Catalyst Optimization by Preorganization. *J. Am. Chem. Soc.* **2015,** *137*, 12110-12120.

(52)   Kniep, F.; Walter, S. M.; Herdtweck, E.; Huber, S. M. 4,4′-Azobis(Halopyridinium) Derivatives: Strong Multidentate Halogen-Bond Donors with a Redox-Active Core. *Chem. Eur. J.* **2012,** *18*, 1306-1310.

(53)   Zapata, F.; Caballero, A.; White, N. G.; Claridge, T. D. W.; Costa, P. J.; Félix, V.; Beer, P. D. Fluorescent Charge-Assisted Halogen-Bonding Macrocyclic Halo-Imidazolium Receptors for Anion Recognition and Sensing in Aqueous Media. *J. Am. Chem. Soc.* **2012,** *134*, 11533-11541.

(54)   Walter, S. M.; Kniep, F.; Rout, L.; Schmidtchen, F. P.; Herdtweck, E.; Huber, S. M. Isothermal Calorimetric Titrations on Charge-Assisted Halogen Bonds: Role of Entropy, Counterions, Solvent, and Temperature. *J. Am. Chem. Soc.* **2012,** *134*, 8507-8512.

(55)   Caballero, A.; White, N. G.; Beer, P. D. A Bidentate Halogen-Bonding Bromoimidazoliophane Receptor for Bromide Ion Recognition in Aqueous Media. *Angew. Chem., Int. Ed. Engl.* **2011,** *50*, 1845-1848.

(56)   Chakraborty, S.; Dutta, R.; Ghosh, P. Halogen Bonding Assisted Selective Removal of Bromide. *Chem. Commun.* **2015,** *51*, 14793-14796.

(57)   Zapata, F.; Gonzalez, L.; Caballero, A.; Alkorta, I.; Elguero, J.; Molina, P. Dual Role of the 1,2,3-Triazolium Ring as a Hydrogen-Bond Donor and Anion–Π Receptor in Anion-Recognition Processes. *Chem. Eur. J.* **2015,** *21*, 9797-9808.

(58)   Kilah, N. L.; Wise, M. D.; Serpell, C. J.; Thompson, A. L.; White, N. G.; Christensen, K. E.; Beer, P. D. Enhancement of Anion Recognition Exhibited by a Halogen-Bonding Rotaxane Host System. *J. Am. Chem. Soc.* **2010,** *132*, 11893-11895.

(59)   Tepper, R.; Schulze, B.; Jäger, M.; Friebe, C.; Scharf, D. H.; Görls, H.; Schubert, U. S. Anion Receptors Based on Halogen Bonding with Halo-1,2,3-Triazoliums. *J. Org. Chem.* **2015,** *80*, 3139-3150.

(60)   Kniep, F.; Rout, L.; Walter, S. M.; Bensch, H. K. V.; Jungbauer, S. H.; Herdtweck, E.; Huber, S. M. 5-Iodo-1,2,3-Triazolium-Based Multidentate Halogen-Bond Donors as Activating Reagents. *Chem. Commun.* **2012,** *48*, 9299-9301.

(61)   Lim, J. Y. C.; Cunningham, M. J.; Davis, J. J.; Beer, P. D. Halogen Bonding-Enhanced Electrochemical Halide Anion Sensing by Redox-Active Ferrocene Receptors. *Chem. Commun.* **2015,** *51*, 14640-14643.

(62) Nepal, B.; Scheiner, S. Competitive Halide Binding by Halogen Versus Hydrogen Bonding: Bis-Triazole Pyridinium. *Chem. Eur. J.* **2015,** *21*, 13330-13335.

(63) Frisch, M. J.; Trucks, G. W.; Schlegel, H. B.; Scuseria, G. E.; Robb, M. A.; Cheeseman, J. R.; Scalmani, G.; Barone, V.; Mennucci, B.; Petersson, G. A., et al. *Gaussian 09*, Revision B.01; Wallingford, CT, 2009.

(64) Zhao, Y.; Truhlar, D. G. The M06 Suite of Density Functionals for Main Group Thermochemistry, Thermochemical Kinetics, Noncovalent Interactions, Excited States, and Transition Elements: Two New Functionals and Systematic Testing of Four M06-Class Functionals and 12 Other Functionals. *Theor. Chem. Acc.* **2008,** *120*, 215-241.

(65) Feller, D. The Role of Databases in Support of Computational Chemistry Calculations. *J. Comput. Chem.* **1996,** *17*, 1571-1586.

(66) Schuchardt, K. L.; Didier, B. T.; Elsethagen, T.; Sun, L.; Gurumoorthi, V.; Chase, J.; Li, J.; Windus, T. L. Basis Set Exchange: A Community Database for Computational Sciences. *J. Chem. Infor. Model.* **2007,** *47*, 1045-1052.

(67) Barone, V.; Cossi, M. Quantum Calculation of Molecular Energies and Energy Gradients in Solution by a Conductor Solvent Model. *J. Phys. Chem. A* **1998,** *102*, 1995-2001.

(68) Boys, S. F.; Bernardi, F. The Calculation of Small Molecular Interactions by the Differences of Separate Total Energies. Some Procedures with Reduced Errors. *Mol. Phys.* **1970,** *19*, 553-566.

(69)   Glendening, E. D.; Landis, C. R.; Weinhold, F. NBO 6.0: Natural Bond Orbital Analysis Program. *J. Comput. Chem.* **2013,** *34*, 1429-1437.

(70)   Bulat, F. A.; Toro-Labbé, A.; Brinck, T.; Murray, J. S.; Politzer, P. Quantitative Analysis of Molecular Surfaces: Areas, Volumes, Electrostatic Potentials and Average Local Ionization Energies. *J. Mol. Model.* **2010,** *16*, 1679-1691.

(71)   Scheiner, S. Comparison of CH$\cdots$O, SH$\cdots$O, Chalcogen, and Tetrel Bonds Formed by Neutral and Cationic Sulfur-Containing Compounds. *J. Phys. Chem. A* **2015,** *119*, 9189-9199.

(72)   Azofra, L. M.; Scheiner, S. Complexation of n SO_2 Molecules (n=1,2,3) with Formaldehyde and Thioformaldehyde. *J. Chem. Phys.* **2014,** *140*, 034302.

(73)   Scheiner, S. Detailed Comparison of the Pnicogen Bond with Chalcogen, Halogen and Hydrogen Bonds. *Int. J. Quantum Chem.* **2013,** *113*, 1609-1620.

(74)   Donoso-Tauda, O.; Jaque, P.; Elguero, J.; Alkorta, I. Traditional and Ion-Pair Halogen-Bonded Complexes between Chlorine and Bromine Derivatives and a Nitrogen-Heterocyclic Carbene. *J. Phys. Chem. A* **2014,** *118*, 9552-9560.

(75)   Bauzá, A.; Alkorta, I.; Frontera, A.; Elguero, J. On the Reliability of Pure and Hybrid DFT Methods for the Evaluation of Halogen, Chalcogen, and Pnicogen Bonds Involving Anionic and Neutral Electron Donors. *J. Chem. Theory Comput.* **2013,** *9*, 5201-5210.

(76)   Biswal, H. S. Hydrogen Bonds Involving Sulfur: New Insights from Ab Initio Calculations and Gas Phase Laser Spectroscopy. In *Noncovalent Forces*, Scheiner, S., Ed. Springer: Dordrecht, Netherlands, 2015; Vol. 19, pp 15-45.

(77)   Nziko, V. d. P. N.; Scheiner, S. S···Π Chalcogen Bonds between SF_2 or SF_4 and C–C Multiple Bonds. *J. Phys. Chem. A* **2015,** *119*, 5889-5897.

(78)   Nepal, B.; Scheiner, S. Anionic CH···X⁻ Hydrogen Bonds: Origin of Their Strength, Geometry, and Other Properties. *Chem. Eur. J.* **2015,** *21*, 1474-1481.

(79)   Sarwar, M. G.; Dragisic, B.; Salsberg, L. J.; Gouliaras, C.; Taylor, M. S. Thermodynamics of Halogen Bonding in Solution: Substituent, Structural, and Solvent Effects. *J. Am. Chem. Soc.* **2010,** *132*, 1646-1653.

(80)   Chudzinski, M. G.; McClary, C. A.; Taylor, M. S. Anion Receptors Composed of Hydrogen- and Halogen-Bond Donor Groups: Modulating Selectivity with Combinations of Distinct Noncovalent Interactions. *J. Am. Chem. Soc.* **2011,** *133*, 10559-10567.

(81)   Gilday, L. C.; White, N. G.; Beer, P. D. Halogen- and Hydrogen-Bonding Triazole-Functionalised Porphyrin-Based Receptors for Anion Recognition. *Dalton Trans.* **2013,** *42*, 15766-15773.

(82)   Caballero, A.; Swan, L.; Zapata, F.; Beer, P. D. Iodide-Induced Shuttling of a Halogen- and Hydrogen-Bonding Two-Station Rotaxane. *Angew. Chem. Int. Ed.* **2014,** *53*, 11854-11858.

(83)   Mercurio, J. M.; Knighton, R. C.; Cookson, J.; Beer, P. D. Halotriazolium Axle Functionalised [2]Rotaxanes for Anion Recognition: Investigating the Effects of Halogen-Bond Donor and Preorganisation. *Chem. Eur. J.* **2014,** *20*, 11740-11749.

Schemes and Figures
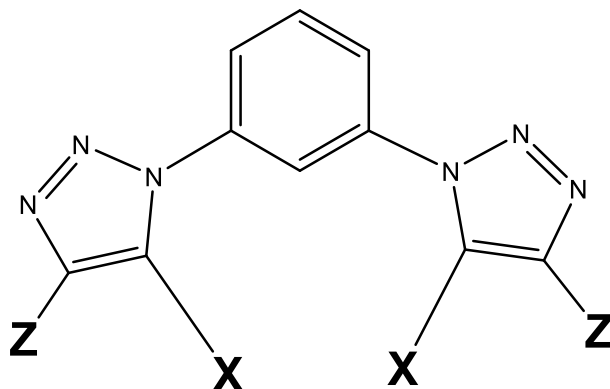
I, neutral
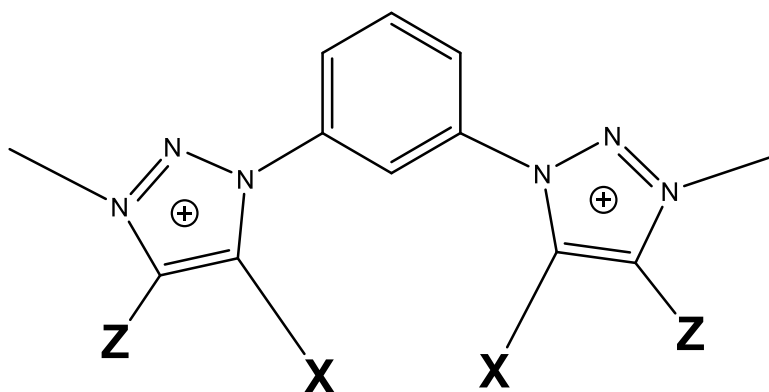
II, dication

X= H, I

Z= H, Me, OH, OMe, NH$_2$, NO$_2$, CHO, COOH, COMe, CN, CF$_3$

Scheme 8-I. Neutral (I) and dicationic (II) bis-triazole benzene (BTB) receptors.
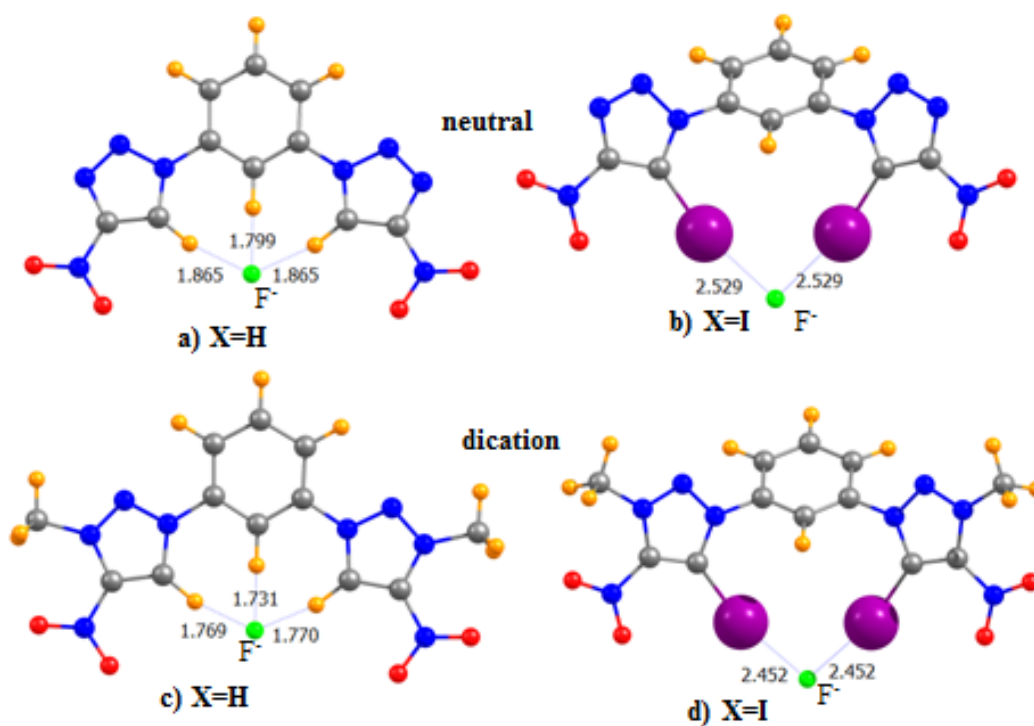
Figure 8-1. Optimized geometries of complexes of F- with neutral and dicationic BTB receptors with X=H (a and c) and X=I (b and d). Distances in Å. C, N, I, O, and H atoms are grey, blue, purple, red, and orange, respectively.
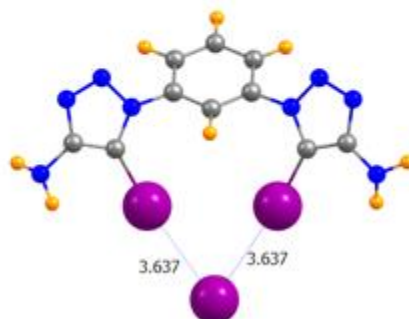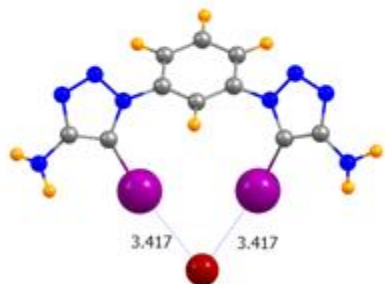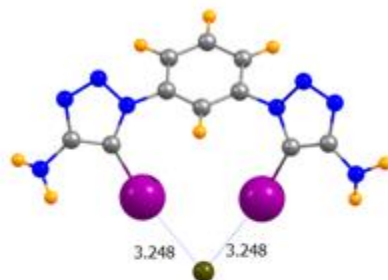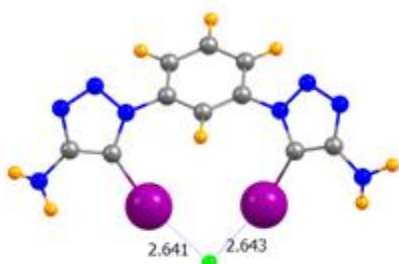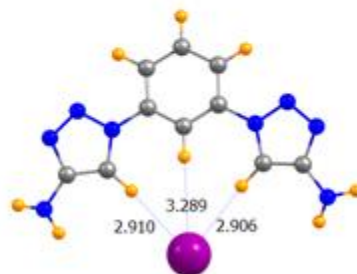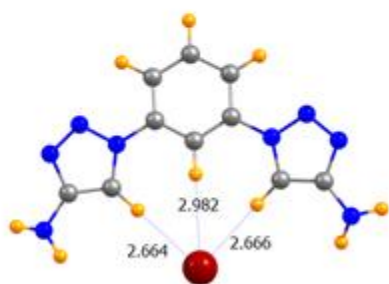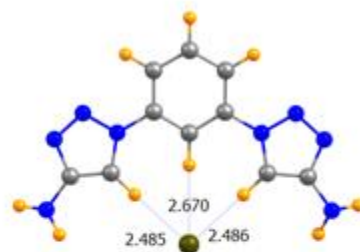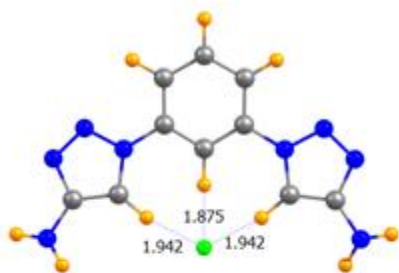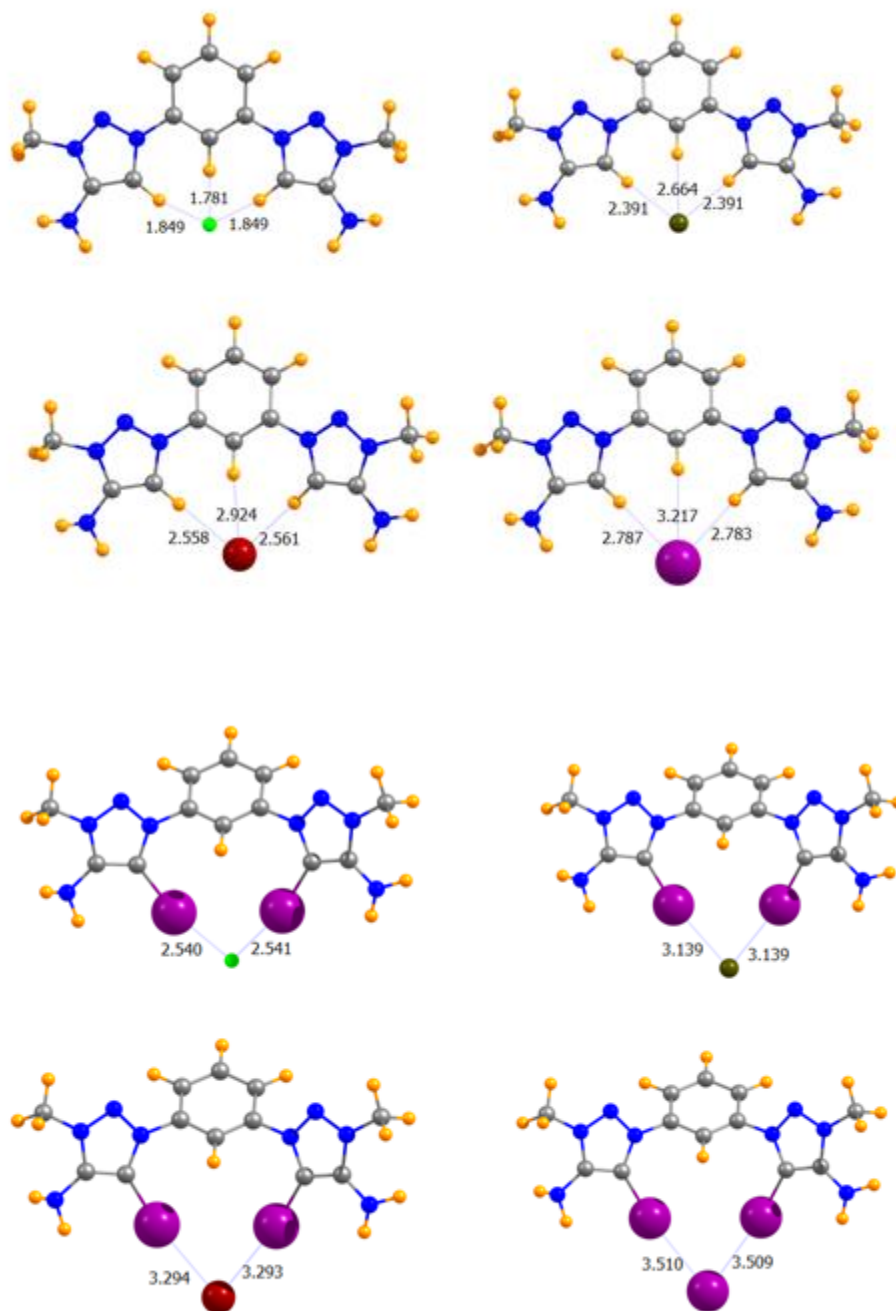
Figure 8-2. Optimized geometries of complexes of halides with neutral and dicationic BTB receptors with X=NH$_2$. Distances in Å. C, N, I, and H atoms are grey, blue, purple, and orange, respectively.
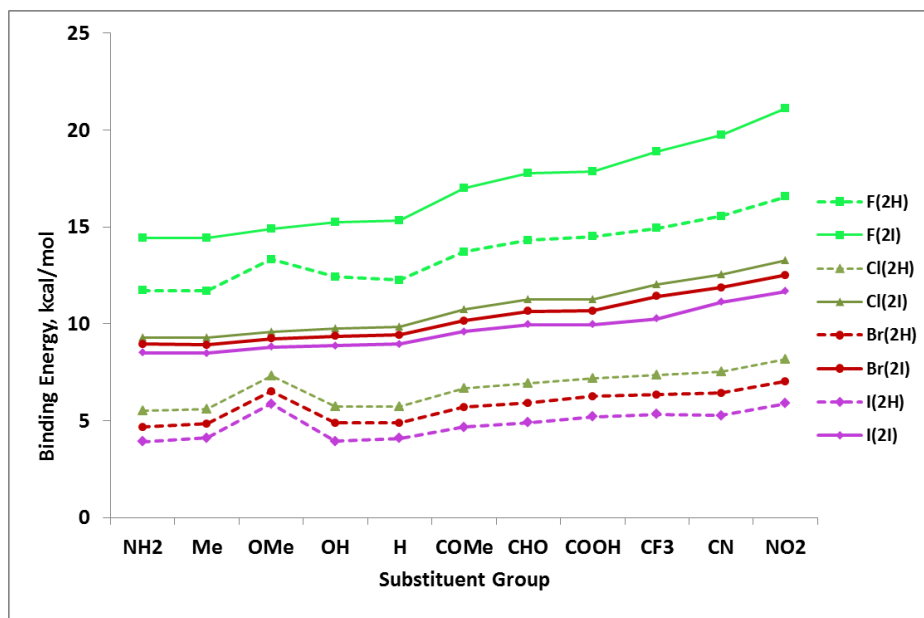
Figure 8-3. Binding energy of halides (Y⁻) to neutral receptors BTB with different substituent groups Z. 2H indicates H-bonding complexes (X=H) and 2I refers to halogen-bonding complexes with X=I.
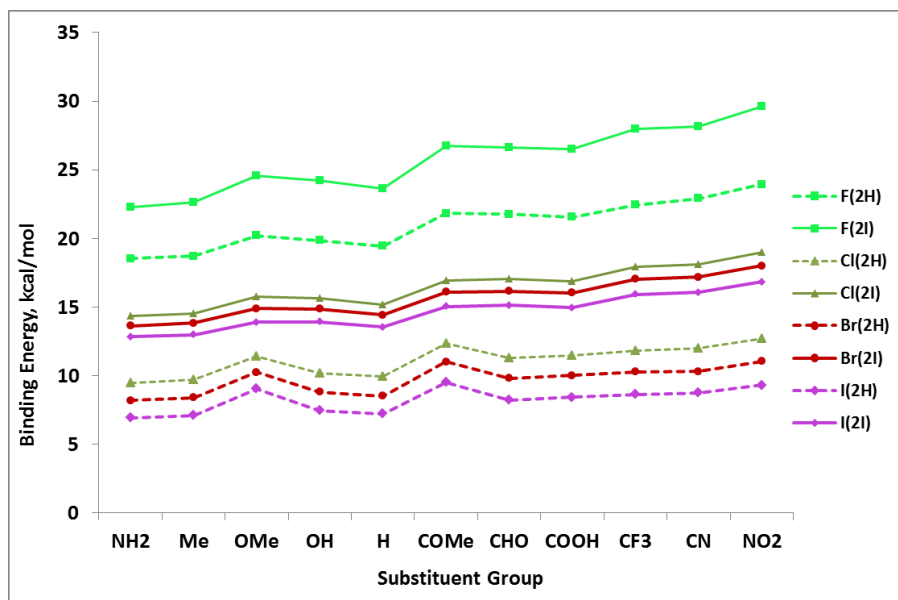
Figure 8-4. Binding energy of halides (Y⁻) to dicationic receptors BTB^{+2} with different substituent groups Z. 2H indicates H-bonding complexes (X=H) and 2I refers to halogen-bonding complexes with X=I.
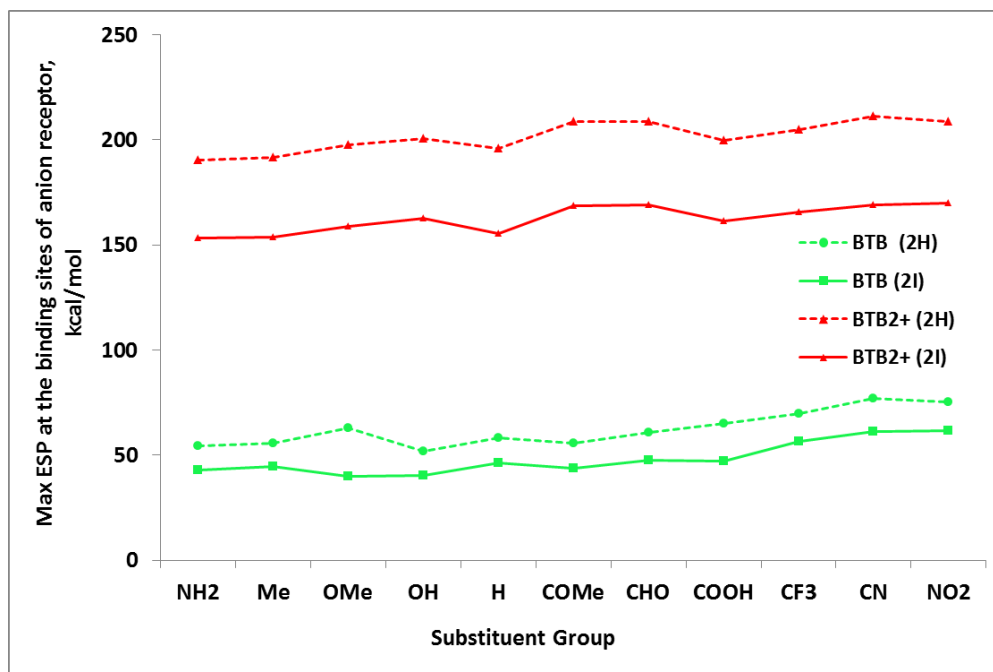
Figure 8-5. Maximum electrostatic potential at the binding sites of BTB receptors with different substituent groups, 2H indicates H-bonding receptors and 2I refers to halogen-bonding receptors.
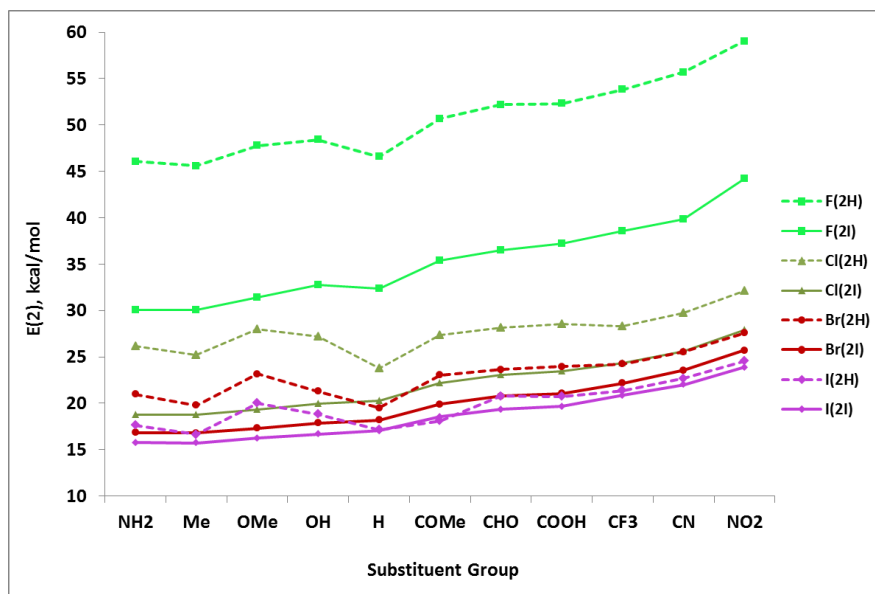
Figure 8-6. NBO charge transfer energy, E(2), from halides to σ*(C-H) or σ*(C-I) antibonding orbitals of neutral receptors BTB with different substituent groups Z. 2H indicates H-bonding complexes (X=H) and 2I refers to halogen-bonding complexes with X=I.
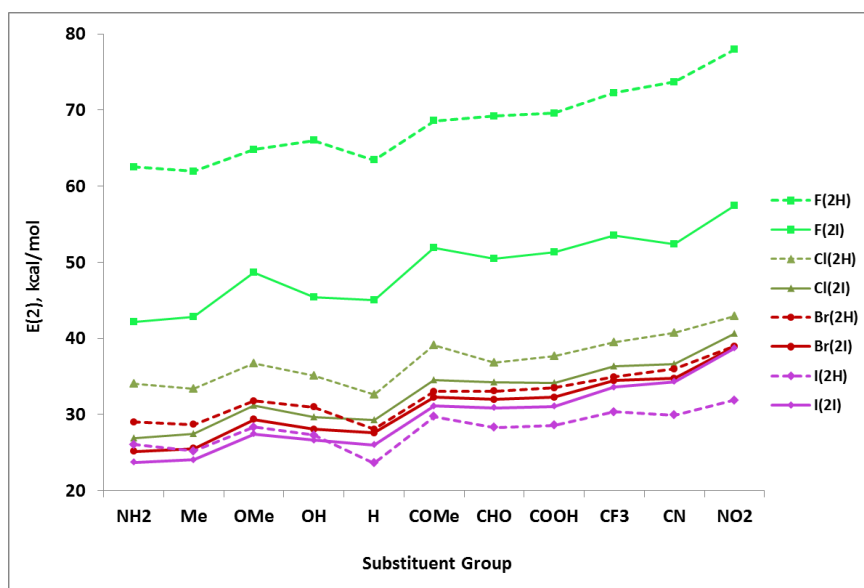
Figure 8-7. NBO charge transfer energy, E(2), from halides to σ*(C-H) or σ*(C-I) antibonding orbitals of dication receptors BTB^{+2} with different substituent groups Z. 2H indicates H-bonding complexes (X=H) and 2I refers to halogen-bonding complexes with X=I.
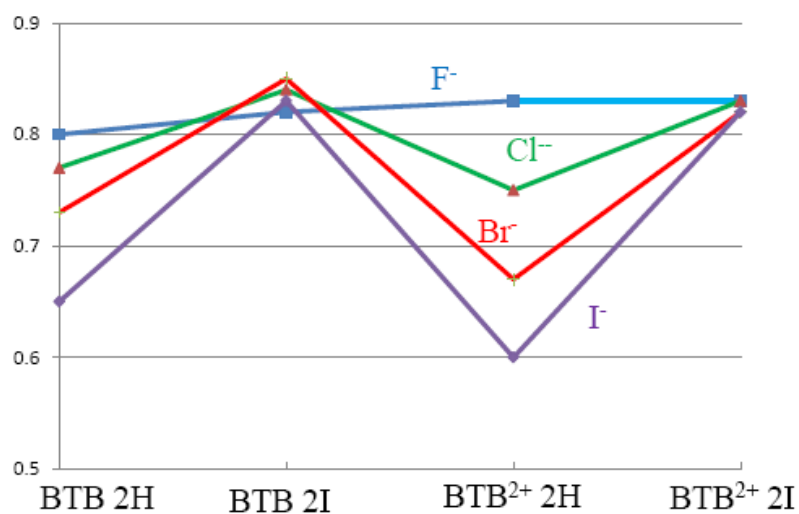
Figure 8-8. Correlation coefficients R2 between the binding energies of the complexes and maximum MEP of the receptors at the binding sites.
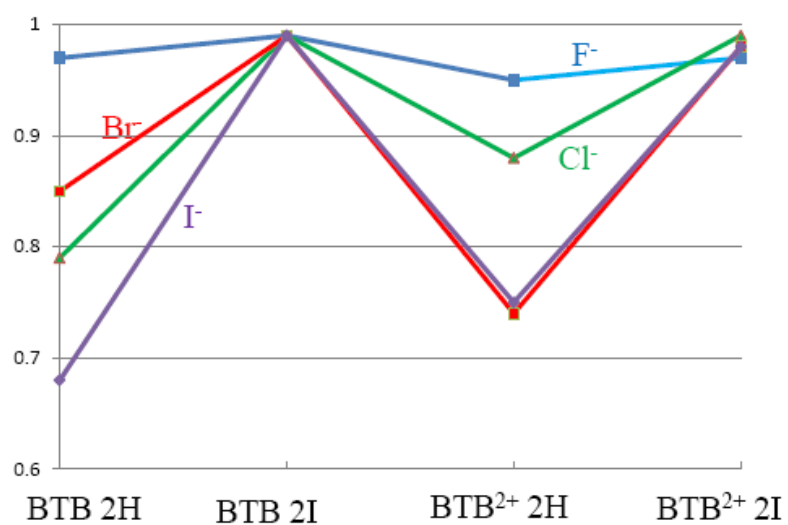
Figure 8-9. Correlation coefficients R_2 between the binding energies of the complexes and NBO charge transfer energies E(2).

CHAPTER 9

ENHANCING THE REDUCTION POTENTIAL OF QUINONES VIA COMPLEX

FORMATION[1]

Abstract

Quantum calculations are used to study the manner in which quinones interact with proton-donating molecules. For neutral donors, a stacked geometry is favored over a H-bond structure. The former is stabilized by charge transfers from the N or O lone pairs to the quinone's π^* orbitals. Following the addition of an electron to the quinone, the radical anion forms strong H-bonded complexes with the various donors. The presence of the donor enhances the electron affinity of the quinone. This enhancement is on the order of 15 kcal/mol for neutral donors, but up to as much as 85 kcal/mol for a cationic donor. The increase in electron affinity is larger for electron-rich quinones, than for their electron-deficient counterparts, containing halogen substituents. Similar trends are in evidence when the systems are immersed in aqueous solvent.

9-1. Introduction

Quinones represent an important class of organic compounds which are present in many biologically active sites. For example, plastoquinone and phylloquinone act as the electron accepters in the electron transport chain in photosynthesis.[1] Ubiquinone is the

---

[1] Coauthored by Binod Nepal and Steve Scheiner. Reproduced with permission from *J. Org. Chem.,***2016**, *81*, 4316-4324. Copyright 2016, American Chemical Society.

electron acceptor in aerobic respiration.[2,3] Several quinone compounds have been found to have anticancer, antibacterial[4-6] and antifungal activity.[7] Similarly, quinone compounds have a wide range of application in synthetic chemistry, catalysis, and electrochemistry.[8-14] Active research continues to assess the usefulness of quinone in lithium-O_2 batteries.[15-17] Quinones are very good oxidizing agents and can undergo one or two electron reduction, forming monoanion and dianion radical, respectively, depending on the conditions. This electron transfer to the quinones can be coupled with proton transfer.[18,19]

A number of studies, both experimental and theoretical, have shown that the redox potential of quinones can be increased by suitable H-bond (HB) donor systems, which assist the electron transfer by stabilizing the resulting radical anion by H-bonding.[20-24] Depending on the solvent media and the pK_a of the HB donor, proton donation may accompany the electron transfer. Various types of HB donors including charged, neutral single-H donor, bidentate etc. have been exploited to activate the oxidizing activity of the quinone compounds.[20,25-27] Interestingly, a number of studies indicate that the HB donors might increase the oxidizing strength of electron-rich quinones but not that much for electron deficient quinones. Very recently, Nocera and Jacobsen's research group published an intriguing article[20] which showed that dicationic HB donors can strongly activate electron-deficient quinones like chloranil, and that the rate of electron transfer can be increased by more than 12 orders of magnitude when coupled with a suitable dicationic H-bond donor. Their study also revealed that an equally acidic HB donor can yield completely different results based on the electrostatic component of H-bond. These cationic donors display greater activation role in electron-deficient quinones.

The kinetics of the electron transfer reaction can be explained in terms of Marcus theory.[28] The rate of electron transfer is dependent on both the free energy change ΔG and the reorganization energy λ. While H-bond donor systems increase the electron transfer rate of quinone systems by making ΔG more negative, they also affect the reorganization energy.[29] A number of articles dealing with this topic suggest that HB donors activate the oxidizing ability of the quinones by stabilizing the radical anion quinone formed subsequent to the electron transfer. One would expect that an anion would participate in a stronger HB than its neutral counterpart. But if that was the only effect, there should not be a large difference between electron-rich and poor quinones, since both of their anion radicals can form this strong H-bond. Another scenario would have HB formation between quinone and HB donor precede the electron transfer. In such case, an electron-rich quinone ought to form a stronger HB. In fact, the electrochemical studies of Nocera and Jacobesen indicated that one HB donor molecule binds to the neutral quinone which is then followed by electron transfer. Finally, the radical anion is additionally stabilized by a second donor molecule.[20]

At this juncture, it remains a bit of a puzzle as to why electron-rich and deficient quinones act differently towards H-bond activation. There is little known about the details or even the fundamental nature of the interaction between a proton donor molecule and quinones, either before or after the electron transfer. There are several important question which await an answer. If the interaction of the proton donor with the quinone precedes electron transfer, what are the geometries, energetics and electronic properties of the complexes? Is a H-bonded geometry indeed the preferred structure, or might another type

of interaction be favored? It is also important to consider how these issues are affected by the proton-donating power of the partner molecule. How does each type of interaction affect the quinone's reduction potential? These same issues must be addressed for the interaction following the addition of an electron. And with respect to trends, why do electron-rich and poor quinones exhibit qualitatively different behavior?

This article reports attempts to answer these questions at the molecular level using quantum mechanical methods. A set of different proton donors is each paired with a range of quinones from very electron-rich to highly deficient. The most stable geometries are ascertained, both before and after an electron is added to the quinone, and the fundamental nature of each interaction is analyzed. The results enable a distinction to be made between electron-rich and poor quinones that is reflective of the experimental results, both *in vacuo* and in solution.

9-2. Computational Details

A series of o-quinones was considered as indicated in the top portion of Scheme 9-I. Either two or four substituents X were added to the quinone in the indicated positions. These substituents included the set NH_2, Me, Cl, and F. The five proton donors considered here are illustrated in the lower half of Scheme 9-I. Dimethylamine (DMA) is the weakest donor examined, and the two alcohols are a bit stronger. Dimethylurea (DMU) is a strong donor, which includes the possibility of engaging in two HBs simultaneously. Strongest of all is the cationic $CNH_2(NHCH_3)_2^+$.

Each of the quinone molecules was paired with a donor system and all the possible minima were identified on the potential energy surface. To ensure each structure represents a true minimum, only geometries with all positive frequencies were taken into account. Density functional theory with M06-2X functional[30] and aug-cc-pVDZ basis set was applied using Gaussian-09 software.[31] A good deal of recent work has supported the ability of this level of theory to treat stacked structures with some accuracy as well as H-bonds.[32-35] Calculations were carried out in the gas phase and in aqueous solvent using the CPCM method.[36] Charge transfers from one monomer to the other, and their energetic effects, were studied by the Natural Bond Orbital (NBO) method.[37] The binding energy of each complexes was calculated as the difference between the energy of the complex and the energy sum of the two monomers in their optimized geometries. Each binding energy was corrected for basis set superposition error using the counterpoise method.[38] The binding energies were further dissected into their constituent components using Symmetry Adapted Perturbation Theory (SAPT)[39] implemented in the MOLPRO software package.[40] Atoms-in-Molecules(AIM)[41] calculations were performed by the AIM ALL program.[42] The electron affinity of each quinone and its various complexes was determined in both vertical and adiabatic schemes. Deprotonation energies were evaluated as the difference in energy between each species, and the entity resulting from removal of the proton of interest.

9-3. Result and Discussion

9-3.1. Monomers

As a first issue, we consider the ease of reduction of the various quinone species. One measure of this property is its electron affinity, eA. The energy released upon acquiring an electron which converts each quinone to its semiquinone radical anion is reported in the first two columns of Table 9-1. The vertical eA was obtained by adding the electron without allowing the geometry to relax, while the adiabatic analogue permitted full geometry optimization of the ensuing anion. The various quinones have been listed in order of greater electron affinity. This order varies from the most electron-donating substituents such as NH$_2$ at the top, down to the electron-withdrawing halogens which have the strongest tendency to attract an excess electron. It is perhaps notable that the F substituent is somewhat less effective than is Cl, as may be seen by comparison of the last two rows. The last column of Table 9-1 displays the energy of the LUMO of the neutral quinone, into which the electron is to be deposited. The electron-withdrawing power of the substituents at the bottom of the table is verified by the stabilization of this molecular orbital. In summary, all three quantities in Table 9-1 agree on the order of reduction potential of the various quinones.

The various proton donor species have varying degrees of ability to engage in a HB with the quinones. The most obvious measure of their acidity in this context is their calculated deprotonation energy, reported in Table 9-2. As expected the amine's NH group requires the most energy to remove its proton, i.e. is the weakest acid, and DMU is the

strongest acid. The two alcohols are intermediate between these extremes, with EtOH slightly stronger. The cationic donor of course requires the least energy to remove a proton.

9-3.2. Geometries and Energetics of Complexes

The quinones form two sorts of complexes with the various neutral proton donors. The first category is characterized by H-bonded structures that take advantage of the two O atoms as proton acceptors. Examples of this sort of structure are provided in Fig 9-1 for the dimethylquinones. A second type of heterodimer displayed in Fig 9-2 is a stacked structure wherein the partner molecule lies above the plane of the quinone ring. As described in greater detail below, these geometries owe their stability in part to charge transfer from the lone pair of an electronegative atom (O or N) to the π^* antibonding orbitals of the quinone C=O bonds. The latter stacked complex is the more stable of the two, with the H-bonded geometries serving as secondary minima.

The BSSE-corrected binding energies of both stacked and H-bonded complexes of each of the quinones with the various H-bond donors are reported in Table 9-3. It is important to note that the cationic donors do not engage in stacked dimers, presumably due to the strength of these charge-amplified H-bonds. The ionic dimers are much more strongly bound, between 18.8 and 34.8 kcal/mol. The binding energies of the neutral HB complexes range between 3.9 and 9.4 kcal/mol, with DMU engaging in the strongest complexes. It might be worthwhile to stress that the greater binding energy of DMU, in comparison to the other neutral donors, is explained in part by its two NH groups, both of which participate in HBs with the quinone O atoms.

In most cases, the strength of the HB follows the anticipated pattern that electron-withdrawing agents such as the halogens weaken the proton-accepting ability of the quinone O atoms. The dimethylamine HB complexes do not obey this trend precisely: for example, the electron-poor QCl_2 and QCl_4 form a stronger HB dimer than does the electron-rich QMe_4, albeit by only a small amount. These deviations are a result of the structures of these particular dimers wherein the amine lies above the quinone plane and the NH··O HBs are supplemented by a certain degree of NH··π H-bonding, as well as some charge transfer from $\sigma(CH)$ the amine to $\pi^*(C=O)$. This auxiliary bonding also accounts for the greater binding energy of the amine than the alcohols which contain a more potent OH proton donor group.

The HB structures contain a strong element of n→σ^* charge transfer, as is typical of H-bonds. These quantities, reported in Table 9-4, reinforce the expected trends. The weakest HBs are formed by the amine NH as compared to the OH of the alcohols. The larger quantities for DMU arise due to the formation of multiple NH··O HBs, and the much higher transfer in the cation donor is typical of ionic HBs. Even more than the total binding energies, the NBO charge transfers obey the trend of diminishing as the quinone electron donor becomes progressively electron poorer, from top to bottom in the table.

As mentioned above the HB minima are secondary to the stacked geometries which form more tightly bound complexes (for the neutral donors). This greater stability margin is as small as 0.4 kcal/mol for the MeOH··QMe_4 dimer but can be as large as 7.8 kcal/mol for the dimer pairing $(Me)_2NH$ with QCl_4. The stacked geometries also contain a heavy element of charge transfer. In the case of dimethylamine and DMU, transfer from the N

lone pair to the $\pi^*(CO)$ antibonding orbitals of the quinone make up the bulk of this quantity, leading to their characterization as lone pair/π complexes. A parallel transfer replaces the N lone pair by the O lone pairs for the two alcohols. The energetic magnitude of these charge transfers is displayed in Table 9-5 for the stacked heterodimers. Just as was noted for the binding energies in Table 9-3, (Me)$_2$NH and DMU whose N atoms donate charge to the quinone present larger values of E(2) than do the O donor alcohols. On the other hand, E(2) is consistently larger for (Me)$_2$NH than for DMU, even though their binding energies tend to have the reverse order. The same may be said for MeOH and EtOH where the latter is more strongly bound even though its E(2) is smaller.

Whereas NBO would characterize the bonding in the stacked structures as primarily of lone pair/π type based upon the orbitals involved in the primary charge transfer, Atoms-in-Molecules (AIM) analysis of the electron density places a bond path between specific atoms of the two molecules, as is typical of AIM. In the case of the stacked geometry of MeOH with Q, for example, the bond path leads from the MeOH O atom to one of the two C atoms bound to O.

It is worth stressing an important set of trends in the energetic data in Table 9-3. As the quinone transitions from electron-rich to poor, i.e. from top to bottom in the table, the HB binding energy tends to diminish. The stacked structures, however, obey an opposite pattern, strengthening as the quinone becomes more electron-deprived. One can understand this behavior on the basis of the charge transfers detailed above. Formation of a HB is weakened as the quinone, and thus its O atoms, become less negative as a result of electron-withdrawing substituents. The stacked dimers are dependent on transfer in the other

direction, to the quinone from the O or N lone pairs of the partner molecule. The presence of electron-withdrawing groups such as halogens can thus be expected to boost this transfer and thus raise the binding energy.

Another view of these trends is purely electrostatic in origin. The molecular electrostatic potentials (MEPs) of three of the quinones are displayed in Fig 9-3 where blue and red colors respectively indicate positive and negative regions. As one transitions from the most electron-releasing NH_2 substituents on the left to the most electron-withdrawing Cl on the right, the red negative regions around the O atoms diminish in magnitude, which would lead to a reduced H-bonding ability, consistent with the pattern in Table 9-3. One may note also a small blue positive region above the midpoint of the two C atoms that are bound to O, an area that might be termed a π-hole. The intensity of this π-hole increases as the substituents become more electron-withdrawing. The magnitude of this hole can be measured by the maximum of the MEP, which is displayed by the numerical values in Fig 9-3, which shows the expected rise as the substituents vary from electron-releasing NH_2 to electron-withdrawing Cl. It follows then that the electrostatic attraction of the quinone to a O or N atom that lies above this π-hole will likewise be enhanced, accounting for the larger binding energies of the stacked geometries from top to bottom in Table 9-3.

Further insight into the stronger binding of the stacked vs the H-bonded structures can be gleaned from a decomposition of the total binding energies. An SAPT analysis reveals that all aspects of the interaction are enhanced in the stacked geometries. The electrostatic component is magnified by a factor of 1.3-2.6. The enlargements of the dispersion is larger, in the 2.1-3.6 range while induction larger still: 2.4-6.0. The increases

in the latter two quantities are consistent with the large induction and dispersion expected for a stacked geometry.

This idea is reinforced by examination of the electronic redistributions caused by formation of the various complexes. Fig 9-4 was computed by subtracting the electron densities of the two individual monomers from that of the full complex. The purple areas represent regions where density is increased as a result of formation of the dimer, and losses are indicated by green. The system chosen for illustration is the DMU/quinone pair. The H-bonded structure on the left shows the classic HB fingerprint of loss surrounding the bridging H atoms, and increases in the regions of the proton-accepting O lone pairs of quinone. The pattern of the stacked structure on the right shows larger contours and thus greater charge shifts. These shifts are also more delocalized involving larger portions of each molecule, consistent with the larger induction energy revealed by SAPT. In more detail, there is substantial charge gain occurring both above and below the quinone O atoms, and losses on the attached C atoms. In the context of DMU, The H atoms suffer some loss, while there appears to be a certain degree of shift from the σ to the π-system in the vicinity of the two N atoms.

NMR chemical shifts of protons are a common indicator of the presence and strength of a HB. But they can also provide information about some of the fundamental characteristics of other types of interactions. The shifts of the H-bonding protons are reported in Table 9-7 relative to the uncomplexed monomer. As expected these protons suffer a loss of shielding, i.e. downfield shift, for each of the H-bonding conformations. Secondly, the shifts are larger for the more strongly H-bonding quinones at the top of Table

9-7 in the and largest for the cationic proton donor that engages in the strongest HBs. For the stacked structures, on the other hand, the same protons are more strongly shielded in the complex than in the monomer, albeit by less than 1 ppm. The density difference map, with its yellow density loss contours around these protons, might have argued for a lower shielding. However, the observed increased shielding may be due to the ring currents within the conjugated quinone system, much as phenyl rings are known to increase the shielding of atoms placed above them.

It might be added finally, that the lone pair→π* transfers that characterize the stacked structures is not particular to 1,2 benzoquinone. Parallel calculations with the 1,4 benzoquinones led to similar results, with stacked dimers preferred over HB structures.

9-3.3. Radical Semiquinone Anion Complexes

After accepting an electron, the quinone transitions to a radical anion semiquinone state. The global minimum for the complexes involving the radicals are of H-bonding type, with binding energies displayed in Table 9-6. The stacked structures common to the neutral quinones do not represent minima on the surface of the semiquinone radicals. Representative structures of the dimethyl semiquinone are illustrated in Fig 9-5. Comparison with the HB geometries in Fig 9-1 indicates little fundamental differences, other than a contraction of the intermolecular distances.

The presence of a full charge on one of the subunits is expected to amplify various facets of the intermolecular interaction. And indeed the binding energies in Table 9-6 are considerably larger than for the neutral HB structures in Table 9-3. The charge

magnification effect is smallest for the amine (3.5 - 6.3 kcal/mol) and largest for DMU with increases between 15.4 and 18.8 kcal/mol. Even more impressive is the increment of 76 - 83 kcal/mol for the cationic proton donor, with binding energies in excess of 100 kcal/mol. In terms of relative growth, the placement of a negative charge on the semiquinone roughly doubles the HB interaction energy of the amine, and magnifies this quantity for the alcohols, DMU, and the cation by respective factors of 2-3, 3-4; and 3-5. Like the neutral systems, the anionic semiquinone HB energies obey the trend amine < alcohol < DMU < cation, although the two alcohols reverse with one another. The expected trend of a weakening HB as one moves down a column of Table 9-6, from electron-rich to electron-deficient semiquinone proton acceptor is not strictly adhered to.

As would be anticipated for the stronger HBs involving the anion, the NBO charge transfers are similarly enlarged when compared to their neutral analogues in Table 9-4. One again sees the similar trend of a general weakening as the semiquinone substituent becomes more electron-withdrawing. Also commensurate with the neutral systems, DMU shows the largest charge transfer and $(Me)_2NH$ the least.

9-3.4. Effect of Complexation upon Reduction

A central issue motivating this work is an elucidation of how the formation of a complex affects the reduction process of each quinone. In other words, does the complexation raise or lower the electron affinity of the quinone. The change in the electron affinity can be equated by simple Hess's Law considerations with the difference between the binding energy of the quinone as compared to the corresponding anionic radical semiquinone. That is, the increase in the electron affinity caused by the formation of the

complex is equal to the increase in the binding energy caused by adding an electron to the quinone:

$$eA(PD\text{-}Q) - eA(Q) \ = \ E_b(Q^-) - E_b(Q) \tag{1}$$

where PD-Q refers to the complex and E_b corresponds to the binding energy of the indicated species with PD.

The quantities in Eq (1) were computed by comparing the binding energies of the anionic radical semiquinones in Table 9-6 with the comparable quantities in Table 9-3 for the neutral quinones. (It should be noted that the more stable of the latter dimers were the stacked structures, not the H-bonded geometries.) The increment of the electron affinity of each quinone associated with its association with the various proton donor molecules is depicted graphically in Fig 9-6.

Focusing first on the neutral proton donors in the lower part of Fig 9-6, these increments are all below 16 kcal/mol. There is a clear trend in that the strongest proton donor, DMU, causes the largest enhancement, and the weakest amine the smallest; the two alcohols are intermediate between these two extremes. There is another pattern present, regardless of the identity of the proton donor. The electron affinity enhancement is largest for the four quinone species on the left, and smallest for those on the right. That is, the electron-rich quinones undergo a larger increase in their electron affinity upon association with a proton-donor molecule than do the electron-deficient species with halogen substituents. In a quantitative sense, this difference between electron-rich and poor quinones is roughly 5 kcal/mol.

It is interesting that there is little difference between the four electron-rich, nor amongst the three electron-poor quinones. It is also intriguing to observe negative quantities when the Me_2NH associates with the three most electron-poor quinones. This result is due to the poor proton-donating ability of this amine. Its H-bonding energy with even the anionic semiquinone (9-10 kcal/mol) is smaller than the strong association energy of the amine in its stacked arrangement with the corresponding neutral quinones (13-14 kcal/mol).

The patterns for the cationic donor in the upper part of Fig 9-6 are a bit different. First of all, the cationic species induces a much larger increment in the quinone's electron affinity, between 75 and 85 kcal/mol. Secondly, the principle observed for the neutrals, that the electron-poor quinones undergo a smaller increment than do their electron-rich counterparts, is largely absent. In fact, it is the unsubstituted quinone that shows the largest increment, and the nominally electron-rich tetraamino-substituted analogue the smallest.

The reader should recall that the most stable complex of each of the neutral proton donors with any of the quinones is a stacked geometry. It might be of interest to wonder how the trends in Fig 9-6 might be affected if the H-bonded geometry were used, not only for the reduced semiquinone, but also for the neutral species. The results in this case are illustrated in Fig 9-8 where it may be seen first that the electron affinity enhancements are quantitatively a bit larger here than in Fig 9-6. But perhaps more importantly, there is much less alteration of the data from left to right. That is, if the H-bonded geometry is used for both the neutral quinone and its anionic correlate, there is a much lesser distinction between electron-rich and poor species. (The results for the cationic donor are identical in Figs 9-6

and 9-8 because it is the H-bonded species which is the global minimum for the neutral as well as anionic quinone.)

One might think there ought to be a connection between the electron affinity of a given species such as a quinone, and the energy of the LUMO into which an added electron would find itself. For example, a lowering of the LUMO energy ε should make the species more attractive to an incoming electron, raising its electron affinity. However, the opposite was noted in the stacked, most stable, geometries of the various quinone/proton donor complexes. The stacking caused the energy of the quinone's LUMO to rise, i.e. become less negative. This rise was on the order of 3-16 kcal/mol. This trend can be understood on the basis of the observation that the formation of the stacked dimer is associated with a certain amount of charge transfer from the proton donor molecule into the quinone. This added electron density would make the quinone less attractive to an incoming electron. And in fact, the degree of increase of ε is roughly proportional to the charge transfers documented in Table 9-5. In any case, this trend is opposite to the aforementioned energetic pattern of enhanced electron affinity of the complex in comparison to the quinone monomer. One can thus conclude that monitoring of the LUMO energy would lead to an incorrect conclusion. It is of interest to note finally that because the formation of a HB results in electron donation from the quinone, the LUMO energy of the quinone drops when this HB is formed.

9-3.5. Solvation Effects

The methods to this point were designed to get to the most fundamental properties of the molecules involved, free of complicating effects. On the other hand, as the practical

applications of these results will generally involve placing the systems within a solvent, it is worthwhile to examine how the principles might be affected by solvation effects. The calculations were repeated by reoptimizing the geometries within the context of aqueous solvation, modeling the effects of hydration by the CPCM approach. The binding energies of the quinones with the various proton donor molecules are reported in Table 9-8. As expected the aqueous environment reduces the various interactions by variable amounts. The binding energies of the amine suffer only a small reduction, on the order of 1 or 2 kcal/mol, with larger decrements for the systems that engage in tighter binding. These reductions tend to be larger for the stacked structures than for the H-bonded geometries. On a percentage basis, the decreases are typically on the order of roughly 15-30%, but larger for the cationic donor, on the order of 70%. The effects of solvation upon the binding energies of the semiquinones are apparent in a comparison of the data in Tables 9-6 and 9-9. One again sees reductions, and of a larger magnitude, roughly 50% for the neutral proton donors, and as much as 85% for the cation.

When all of these solvent effects are considered in terms of the increase of quinone electron affinity caused by complexation, the graphical form of the data is seen in Fig 9-7. Comparison with the unsolvated data in Fig 9-6 reveals a reduction in magnitude of the effects. For example, the gas-phase affinity enhancements were as large as 16 kcal/mol for neutral donors, and up to 85 kcal/mol for the cation. The respective solvated maxima are 4 and 9 kcal/mol. But perhaps most importantly, the patterns are changed only very little. Whether gas-phase or solvated, the electron-rich quinones on the left show the largest change, and the electron-poor quinones the smallest, at least for the neutral donors.

9-4. Conclusions

In summary, the neutral proton donors prefer a stacked geometry over a HB structure with the various quinones. N-containing amine and urea derivative form stronger stacked n→π* complexes with the quinones than do alcohols. Electron-poor quinones, e.g. with halogen substituents, are more strongly bound than are electron-rich quinones, consistent with the idea that electron density is being transferred to the quinone. A cationic proton donor, on the other hand, forms only a H-bonded complex. Following the reduction of the quinone to a radical anion semiquinone, complexation with each proton donor leads to a HB structure, much more strongly bound than the pre-reduced complex. For example, the binding energy with the cationic donor exceeds 100 kcal/mol.

Comparison of the binding energies of the neutral and anionic quinones leads to evaluation of the increase in electron affinity of the quinone associated with its association with each proton donor. This quantity obeys the trend amine < alcohol < urea < cation. The electron affinity increase is as much as 15 kcal/mol for the neutral proton donors, and as high as 85 kcal/mol for the cation. Most importantly, the increased tendency toward reduction caused by the addition of the proton donor molecule is largest for the electron-rich quinones and smallest for the electron-poor species. These same patterns are in evidence when the systems are immersed in aqueous solvent, although the numerical values are smaller. Unlike the other species, the association of the amine induces a reduction in the quinone's electron affinity, albeit only in water. It is reasonable to suppose that the effects of a less polar solvent than water would lead to results intermediate between these two extremes, but still obeying the same patterns.

Turek et al[20] had recently observed that the electron deficient chloranil, corresponding to our QCl$_4$, could be activated as an oxidizing agent via addition of a H-bonding agent. This result is consistent with our own finding that the electron affinity of QCl$_4$ is raised when proton donors such as alcohols or DMU are added, and by much more so when the donor carries a positive charge. It is anticipated that the incorporation of a dicationic species, as examined by Turek et al, into the calculations would cause an even larger enhancement, consistent with their observations.

References

(1)   Biggins, J. *Progress in Photosynthesis Research: Volume 4 Proceedings of the VIIth International Congress on Photosynthesis Providence, Rhode Island, USA, August 10–15, 1986*; Springer Netherlands, 2012.

(2)   Ernster, L.; Dallner, G. *Biochimica et Biophysica Acta (BBA) - Molecular Basis of Disease* **1995**, *1271*, 195.

(3)   Åberg, F.; Appelkvist, E.-L.; Dallner, G.; Ernster, L. *Arch. Biochem. Biophys.* **1992**, *295*, 230.

(4)   Shrestha, J. P.; Chang, C.-W. T. *Bioorg. Med. Chem. Lett.* **2013**, *23*, 5909.

(5)   Shrestha, J. P.; Fosso, M. Y.; Bearss, J.; Chang, C.-W. T. *Eur. J. Med. Chem.* **2014**, *77*, 96.

(6)   Bachur, N. R.; Gordon, S. L.; Gee, M. V. *Cancer Research* **1978**, *38*, 1745.

(7)   Meazza, G.; Dayan, F. E.; Wedge, D. E. *J. Agric. Food. Chem.* **2003**, *51*, 3824.

(8)   DuVall, S. H.; McCreery, R. L. *J. Am. Chem. Soc.* **2000**, *122*, 6759.

(9)   Neumann, R.; Khenkin, A. M.; Vigdergauz, I. *Chem. Eur. J.* **2000**, *6*, 875.

(10)   Wendlandt, A. E.; Stahl, S. S. *J. Am. Chem. Soc.* **2014**, *136*, 11910.

(11)   Tse, D. C.-S.; Kuwana, T. *Anal. Chem.* **1978**, *50*, 1315.

(12)   Caruana, L.; Fochi, M.; Bernardi, L. *Molecules* **2015**, *20*, 11733.

(13)   Zhang, X.-Z.; Du, J.-Y.; Deng, Y.-H.; Chu, W.-D.; Yan, X.; Yu, K.-Y.; Fan, C.-A. *J. Org. Chem.* **2016**, *81*, 2598.

(14)   Grennberg, H.; Gogoll, A.; Baeckvall, J. E. *J. Org. Chem.* **1991**, *56*, 5808.

(15)   Zhu, Z.; Hong, M.; Guo, D.; Shi, J.; Tao, Z.; Chen, J. *J. Am. Chem. Soc.* **2014**, *136*, 16461.

(16)   Pirnat, K.; Dominko, R.; Cerc-Korosec, R.; Mali, G.; Genorio, B.; Gaberscek, M. *J. Power Sources* **2012**, *199*, 308.

(17)   Lee, J.; Kim, H.; Park, M. J. *Chem. Mater.* **2016**.

(18)   Graige, M. S.; Paddock, M. L.; Bruce, J. M.; Feher, G.; Okamura, M. Y. *J. Am. Chem. Soc.* **1996**, *118*, 9005.

(19)   Song, N.; Gagliardi, C. J.; Binstead, R. A.; Zhang, M.-T.; Thorp, H.; Meyer, T. J. *J. Am. Chem. Soc.* **2012**, *134*, 18538.

(20)   Turek, A. K.; Hardee, D. J.; Ullman, A. M.; Nocera, D. G.; Jacobsen, E. N. *Angew. Chem. Int. Ed.* **2016**, *55*, 539.

(21)   Okamoto, K.; Ohkubo, K.; Kadish, K. M.; Fukuzumi, S. *J. Phys. Chem. A* **2004**, *108*, 10405.

(22)   Yuasa, J.; Yamada, S.; Fukuzumi, S. *Angew. Chem. Int. Ed.* **2007**, *46*, 3553.

(23)   Fukuzumi, S.; Kitaguchi, H.; Suenobu, T.; Ogo, S. *Chem. Commun.* **2002**, 1984.

(24)   Uno, B.; Okumura, N.; Goto, M.; Kano, K. *J. Org. Chem.* **2000**, *65*, 1448.

(25)   Staley, P. A.; Lopez, E. M.; Clare, L. A.; Smith, D. K. *J. Phys. Chem. C* **2015**, *119*, 20319.

(26)   Ge, Y.; Miller, L.; Ouimet, T.; Smith, D. K. *J. Org. Chem.* **2000**, *65*, 8831.

(27)   Gupta, N.; Linschitz, H. *J. Am. Chem. Soc.* **1997**, *119*, 6384.

(28)   Marcus, R. A. *Angew. Chem. Int. Ed.* **1993**, *32*, 1111.

(29)   Yago, T.; Gohdo, M.; Wakasa, M. *J. Phys. Chem. B* **2010**, *114*, 2476.

(30)   Zhao, Y.; Truhlar, D. G. *Theor. Chem. Acc.* **2007**, *120*, 215.

(31)   Frisch, M. J.; Trucks, G. W.; Schlegel, H. B.; Scuseria, G. E.; Robb, M. A.; Cheeseman, J. R.; Scalmani, G.; Barone, V.; Mennucci, B.; Petersson, G. A.; Nakatsuji, H.; Caricato, M.; Li, X.; Hratchian, H. P.; Izmaylov, A. F.; Bloino, J.; Zheng, G.; Sonnenberg, J. L.; Hada, M.; Ehara, M.; Toyota, K.; Fukuda, R.; Hasegawa, J.; Ishida, M.;

Nakajima, T.; Honda, Y.; Kitao, O.; Nakai, H.; Vreven, T.; Montgomery Jr., J. A.; Peralta, J. E.; Ogliaro, F.; Bearpark, M. J.; Heyd, J.; Brothers, E. N.; Kudin, K. N.; Staroverov, V. N.; Kobayashi, R.; Normand, J.; Raghavachari, K.; Rendell, A. P.; Burant, J. C.; Iyengar, S. S.; Tomasi, J.; Cossi, M.; Rega, N.; Millam, N. J.; Klene, M.; Knox, J. E.; Cross, J. B.; Bakken, V.; Adamo, C.; Jaramillo, J.; Gomperts, R.; Stratmann, R. E.; Yazyev, O.; Austin, A. J.; Cammi, R.; Pomelli, C.; Ochterski, J. W.; Martin, R. L.; Morokuma, K.; Zakrzewski, V. G.; Voth, G. A.; Salvador, P.; Dannenberg, J. J.; Dapprich, S.; Daniels, A. D.; Farkas, Ö.; Foresman, J. B.; Ortiz, J. V.; Cioslowski, J.; Fox, D. J.; Gaussian, Inc.: Wallingford, CT, USA, 2009.

(32)   Zhao, Y.; Truhlar, D. G. *Acc. Chem. Res.* **2008**, *41*, 157.

(33)   Guin, M.; Patwari, G. N.; Karthikeyan, S.; Kim, K. S. *PCCP* **2011**, *13*, 5514.

(34)   Guin, M.; Patwari, G. N.; Karthikeyan, S.; Kim, K. S. *PCCP* **2009**, *11*, 11207.

(35)   Momeni, Z.; Ebrahimi, A. *Struct. Chem.* **2015**, *27*, 731.

(36)   Cossi, M.; Rega, N.; Scalmani, G.; Barone, V. *J. Comput. Chem.* **2003**, *24*, 669.

(37)   Foster, J. P.; Weinhold, F. *J. Am. Chem. Soc.* **1980**, *102*, 7211.

(38)   Boys, S. F.; Bernardi, F. *Mol. Phys.* **1970**, *19*, 553.

(39)   Szalewicz, K. *WIREs Comput Mol Sci* **2012**, *2*, 254.

(40)   Werner, H.-J.; Knowles, P. J.; Knizia, G.; Manby, F. R.; Schütz, M. *WIREs Comput Mol Sci* **2012**, *2*, 242.

(41)   Bader, R. F. W. *Atoms in Molecules: A Quantum Theory*; Clarendon Press, 1994.

(42)   Keith, T. A. *AIMAll (Version 13.11.04). TK Gristmill Software, Overland Park, KS, USA, 2013.*

Schemes, Figures and Tables
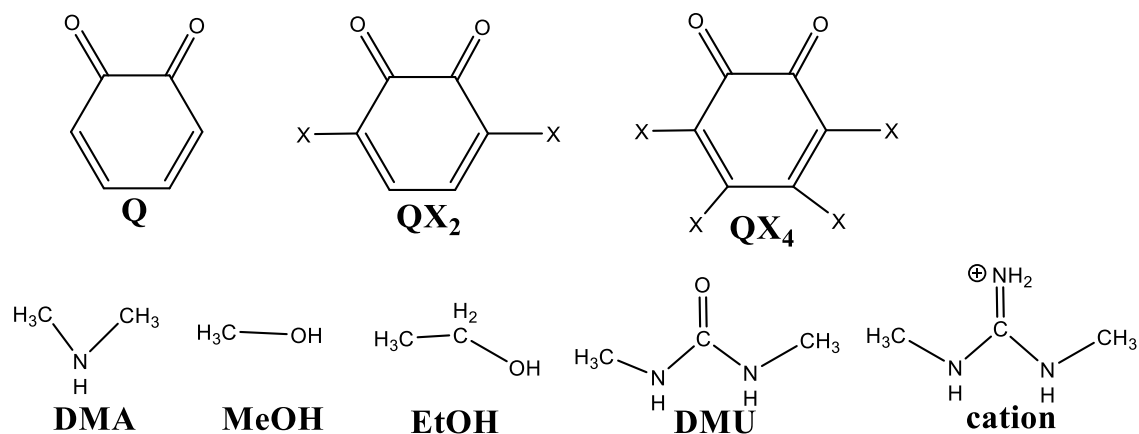
Scheme 9-I. Quinone and proton donor systems studied

Table 9-1. Vertical and adiabatic electron affinity of the various quinone monomers, and the energy of its LUMO (kcal/mol).

quinone	Vertical	Adiabatic	ε(LUMO)
$Q(NH_2)_4$	-27.60	-37.00	-46.43
QMe_4	-34.82	-41.07	-53.21
QMe_2	-39.09	-45.48	-59.49
Q	-42.77	-48.81	-65.66
QCl_2	-56.83	-63.25	-76.96
QF_4	-57.32	-65.61	-80.85
QCl_4	-63.94	-70.10	-81.85

Table 9-2. Deprotonation energies (kcal/mol) of proton donor species

Me$_2$NH	402.95
MeOH	389.77
EtOH	386.97
DMU	369.15
cation	253.16

Table 9-3. Binding energies (kcal/mol) of quinones with various H-bond donors

Quinone	(Me)$_2$NH		MeOH		EtOH		DMU		CNH$_2$(NHCH$_3$)$_2$$^+$
	stacked	HB[a]	stacked	HB	stacked	HB	stacked	HB	HB
Q(NH$_2$)$_4$	8.87	6.01	8.02	6.68	6.58	6.49	11.19	9.37	34.84
QMe$_4$	9.18	6.34	6.85	6.43	7.74	6.28	12.82	8.84	30.46
QMe$_2$	9.92	6.15	6.86	5.94	7.58	5.79	10.79	8.13	27.30
Q	10.21	5.72	6.87	5.58	7.03	5.44	10.73	7.69	26.27
QCl$_2$	12.96	5.98	8.25	4.62	8.54	4.50	13.00	6.43	22.55
QF$_4$	12.96	5.40	8.66	4.05	8.93	3.92	12.63	5.48	18.81
QCl$_4$	13.72	5.90	8.51	4.46	9.00	4.33	13.35	6.01	21.55

Table 9-4. NBO Olp→σ(XH) (X=O,N) charge transfer E(2) (kcal/mol) for HB configurations

	(Me)$_2$NH[a]	MeOH	EtOH	DMU	CNH$_2$(NHCH$_3$)$_2$$^+$
Q(NH$_2$)$_4$	3.19	6.09	6.36	12.67	36.92
QMe$_4$	3.84	6.22	6.09	11.96	28.79
QMe$_2$	4.22	5.68	5.67	10.90	26.42
Q	4.15	5.29	5.21	10.38	24.25
QCl$_2$	4.16	4.62	4.57	8.98	22.28
QF$_4$	3.91	4.24	4.09	8.52	19.69
QCl$_4$	4.11	4.55	3.35	9.02	21.94

Table 9-5. NBO charge transfer E(2) (kcal/mol) for stacked configurations

	(Me)$_2$NH	MeOH	EtOH	DMU
Q(NH$_2$)$_4$	12.80	5.69	6.18	9.35
QMe$_4$	11.93	7.75	6.16	6.21
QMe$_2$	16.00	7.95	6.73	8.65
Q	13.94	8.65	7.05	11.10
QCl$_2$	16.80	9.61	8.62	9.28
QF$_4$	16.64	9.82	8.43	10.88
QCl$_4$	17.10	8.16	6.89	10.42

Table 9-6. Binding energies (kcal/mol) of radical semiquinone anions with various H-bond donors

	(Me)$_2$NH	MeOH	EtOH	DMU	CNH$_2$(NHCH$_3$)$_2$$^+$
Q(NH$_2$)$_4$$^{-\cdot}$	10.37	13.99	14.12	24.75	110.22
QMe$_4$$^{-\cdot}$	12.32	15.95	16.96	26.83	111.83
QMe$_2$$^{-\cdot}$	12.32	15.62	16.68	26.52	110.51
Q-$\cdot$	11.68	15.56	16.61	26.48	111.87
QCl$_2$$^{-\cdot}$	10.51	13.44	14.19	23.10	102.99
QF$_4$$^{-\cdot}$	10.06	13.36	14.16	22.84	101.33
QCl$_4$$^{-\cdot}$	9.81	12.53	13.20	21.43	97.98

Table 9-7. Change in NMR isotropic shielding (ppm) of H-bonding protons due to complexation.

	(Me)$_2$N<u>H</u>		MeO<u>H</u>		EtO<u>H</u>		(CH$_3$N<u>H</u>)$_2$CO^b		CNH$_2$(N<u>H</u>CH$_3$)$_2$$^{+,b}$
	stacked	HB	stacked	HB	stacked	HB	stacked	HB	HB
Q(NH$_2$)$_4$	0.47	-0.69	0.49	-3.47	0.06	-3.49	0.08	-2.38	-4.58
QMe$_4$	0.60	-0.90	0.77	-3.57	0.82	-3.51	0.37	-2.48	-4.15
QMe$_2$	0.66	-0.92	0.85	-3.31	0.87	-3.23	0.52	-2.19	-3.78
Q	0.06	-1.02	0.52	-2.98	0.86	-2.94	0.37	-2.08	-3.52
QCl$_2$	-0.09	-0.98	0.26	-2.75	0.85	-2.65	0.40	-1.61	-3.07
QF$_4$	-0.25	-0.85	0.11	-2.28	0.21	-2.33	0.28	-1.58	-2.79
QCl$_4$	0.21	-0.99	-0.07	-2.70	0.32	-2.64	0.35	-1.62	-3.08

Table 9-8. BSSE-corrected binding energies (kcal/mol) of quinones with various H-bond donors in aqueous solvent

| Quinone	(Me)$_2$NH		MeOH		EtOH		DMU		CNH$_2$(NHCH$_3$)$_2$$^+$
	stacked	HB	stacked	HB	stacked	HB	stacked	HB	HB
Q(NH$_2$)$_4$	5.36	4.65	3.12	5.73	3.98	4.80	5.08	7.19	10.51
QMe$_4$	8.12	4.76	4.39	5.39	5.19	5.26	8.07	6.36	9.49
QMe$_2$	8.96	4.62	4.65	4.99	5.07	4.03	7.55	5.85	8.62
Q	8.61	4.11	4.72	4.82	4.55	4.70	6.64	5.61	8.32
QCl$_2$	11.64	4.17	5.98	4.09	6.02	3.98	8.93	4.63	6.67
QF$_4$	11.58	3.49	6.39	3.74	6.23	3.65	8.94	4.23	6.09
QCl$_4$	12.71	4.04	7.03	4.01	6.73	3.90	10.09	4.46	6.49

Table 9-9. BSSE-corrected binding energies (kcal/mol) of radical semiquinone anions with various H-bond donors in aqueous solvent

	(Me)$_2$NH	MeOH	EtOH	DMU	CNH$_2$(NHCH$_3$)$_2$$^+$
Q(NH$_2$)$_4$$^-\cdot$	4.60	6.86	6.59	9.86	16.72
QMe$_4$$^-\cdot$	5.87	8.35	8.68	11.33	17.88
QMe$_2$$^-\cdot$	5.92	7.96	8.34	10.83	17.04
Q$^-\cdot$	5.18	7.70	8.07	10.40	16.47
QCl$_2$$^-\cdot$	5.58	7.01	7.28	9.27	14.62
QF$_4$$^-\cdot$	5.04	6.74	7.10	6.74	13.87
QCl$_4$$^-\cdot$	5.48	6.83	6.99	6.83	13.91
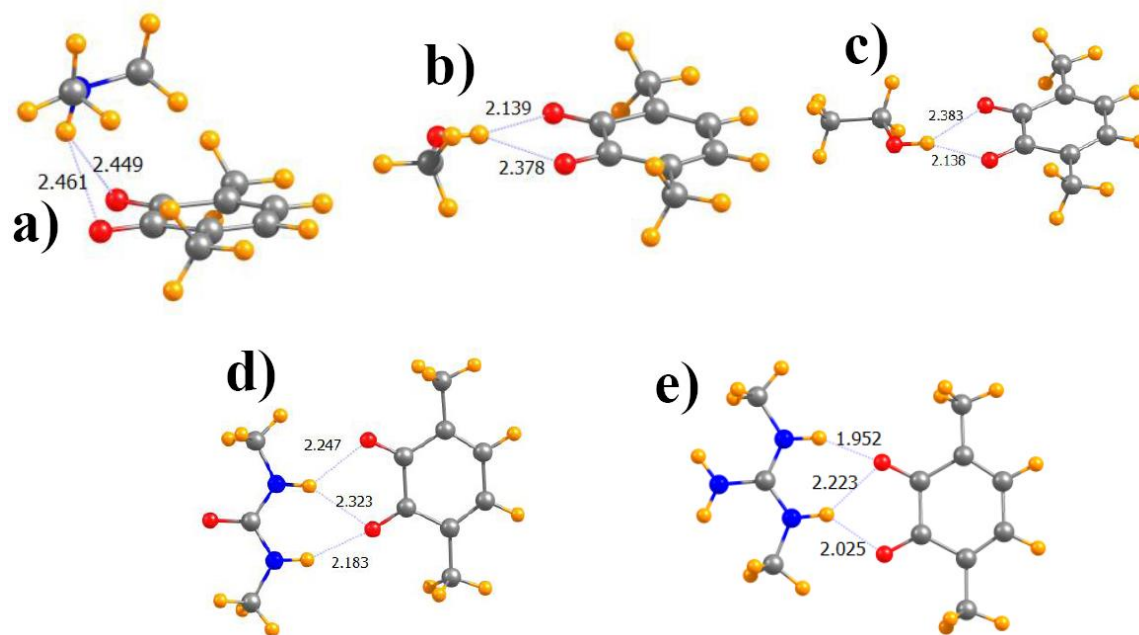
Figure 9-1. H-bonded geometries of complexes formed by dimethylquinone with proton donors a) $(CH_3)_2N$, b) MeOH, c) EtOH, d) dimethylurea, e) $CNH_2(NHCH_3)^{2+}$ cation. Distances in Å.
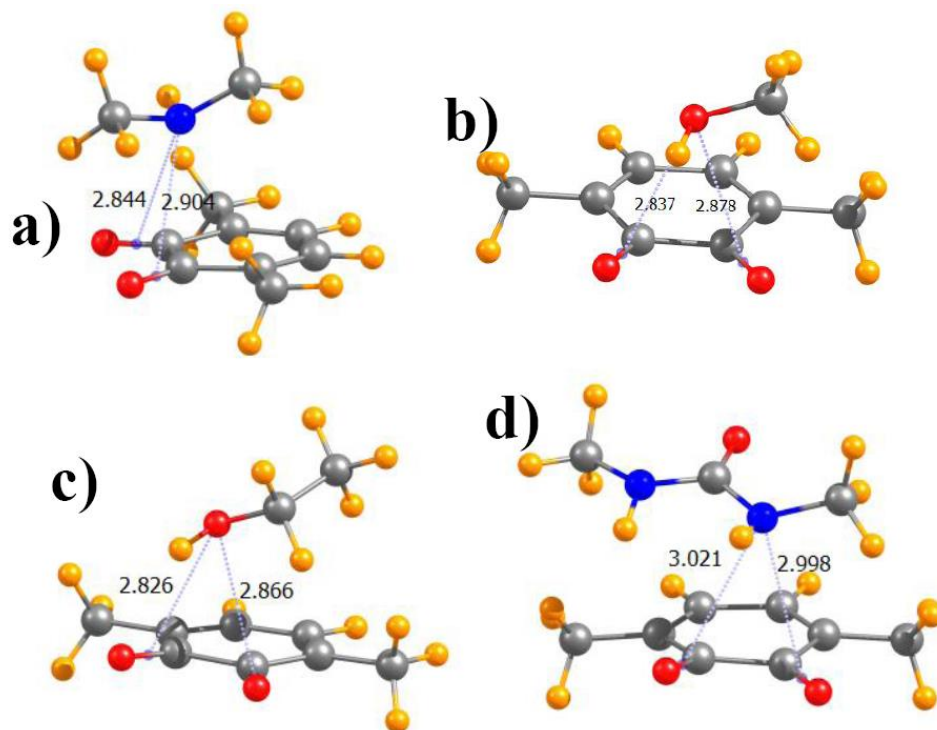
Figure 9-2. Stacked geometries of complexes formed by dimethylquinone with proton donors a) $(CH_3)_2N$, b) MeOH, c) EtOH, d) dimethylurea. Distances in Å.

9.6   20.4   34.0

$Q(NH_2)_4$ Q QCl_4
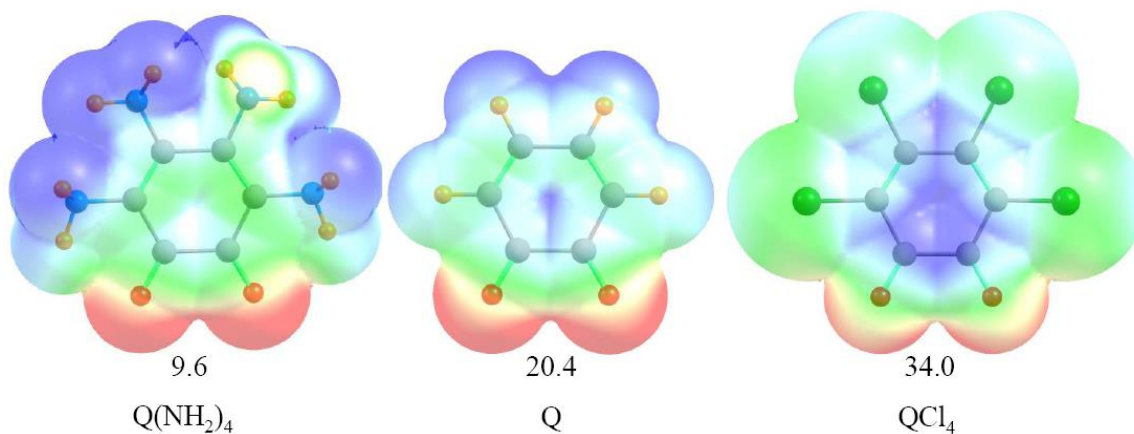
**Figure 9-3.** Molecular electrostatic potential (MEP) surrounding each of the indicated quinones on a surface corresponding to 1.5 x van der Waals radius. Blue and red colors indicate maxima and minima, respectively, ±0.005 au. Numerical values refer to $V_{s,max}$ (kcal/mol) at the π-hole above the C-C bond connecting the two CO groups, on the ρ=0.001 au isodensity surface.
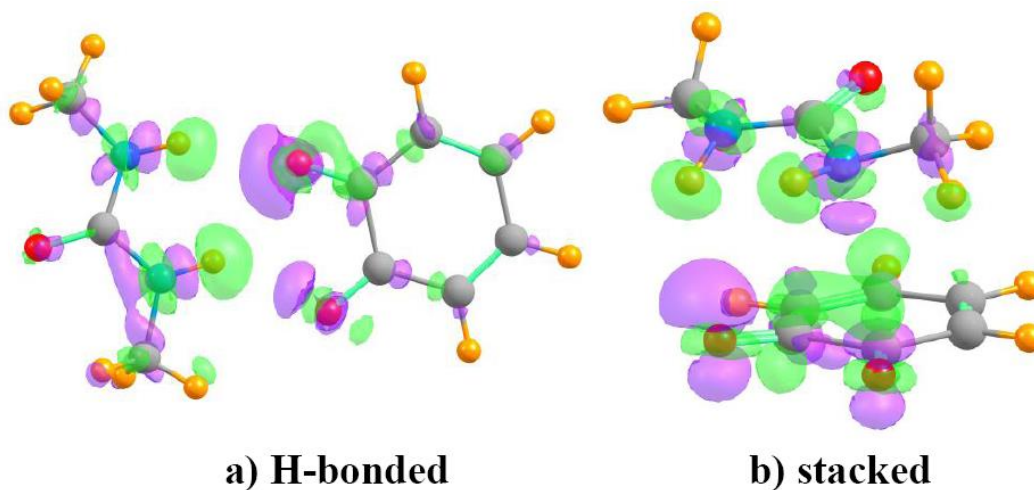
a) H-bonded   b) stacked

Figure 9-4. Electron density difference map of a) H-bonded and b) stacked structures of quinone with dimethylurea. Purple regions indicate increased density resulting from formation of complex; losses are shown in green. Contours represent ±0.001 au.
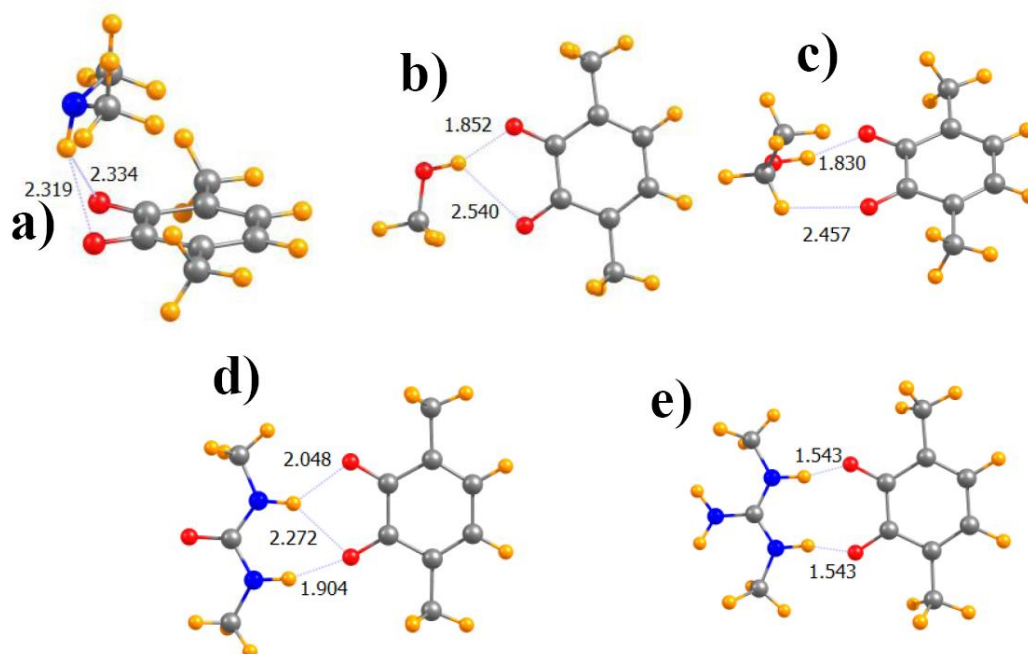
Figure 9-5. Geometries of complexes formed by dimethylquinone anion radical with proton donors a) $(CH_3)_2N$, b) MeOH, c) EtOH, d) dimethylurea, e) $CNH_2(NHCH_3)_{2+}$ cation. Distances in Å.
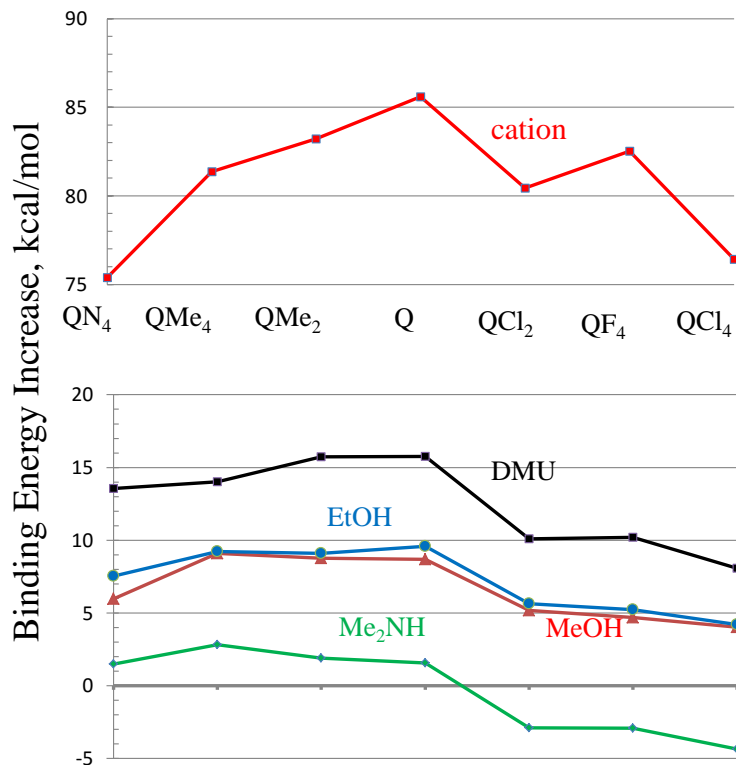
Figure 9-6. Change in binding energy to proton donor molecule caused by reduction of the quinone to radical anion semiquinone.
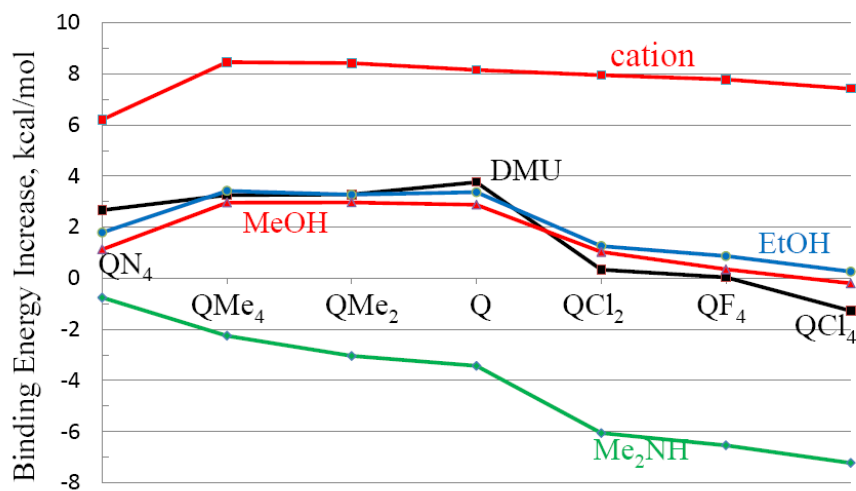
Figure 9-7. Change in binding energy to proton donor molecule caused by reduction of the quinone to radical anion semiquinone in aqueous solvent.
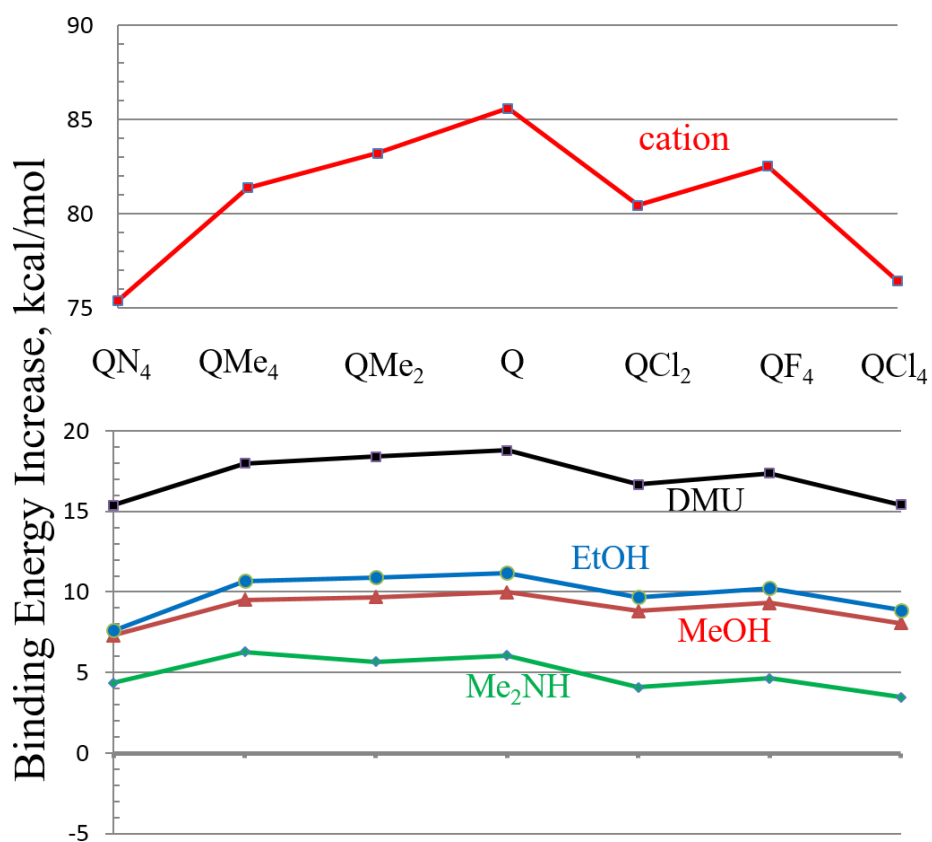
Figure 9-8. Change in binding energy to proton donor molecule caused by reduction of the quinone to radical anion semiquinone, with both complexes in their HB geometries.

CHAPTER 10

NX··Y HALOGEN BONDS. COMPARISON WITH NH··Y H-BONDS AND CX··Y

HALOGEN BONDS[1]

Abstract

Quantum calculations examine how the NH··Y H-bond compares to the equivalent NX··Y halogen bond, as well as to comparable CH/CX donors. Succinimide and saccharin, and their corresponding halogen-substituted derivatives, are chosen as the prototype NH/NX donors, paired with a wide range of electron donor molecules. The NH··Y H-bond is weakened if the bridging H is replaced by Cl, and strengthened by I; a Br halogen bond is roughly comparable to a H-bond. The lone pairs of the partner molecule are stronger electron donors than are π-systems. Whereas Coulombic forces represent the largest fraction of the attractive force in the H-bonds, induction energy is magnified in the halogen bonds, surpassing electrostatics in several cases. Mutation of NH/NX to CH/CX weakens the binding energy to roughly half its original value, while also lengthening the intermolecular distances by 0.3 - 0.8 Å.

10-1. Introduction

The realm of noncovalent interactions is large and diverse and continues to grow. The H-bond (HB) has perhaps attracted the most attention over the past decades,[1, 2] due to its widespread occurrence in important chemical and biological processes. The definition of a HB has greatly expanded from its original inception involving F, O, and N atoms to a growing list[3, 4] of less electronegative atoms as well as π-systems that can serve as electron donors. Many of the intrinsic concepts of the HB have been found to occur as well in related noncovalent bonds[5] where the bridging H is replaced by tetrel, pnicogen, chalcogen, halogen, and even the nominally unreactive aerogen atoms, in the eponymously named bonds.[6-16]

Of the latter sorts of interactions, the halogen bond (XB) has the longest history of inquiry and has been successfully exploited in a number of fields such as crystal engineering, drug development and delivery, catalysis, anion binding and sensing, among many others. Like the HB, the XB owes some of its attractive force to an electrostatic attraction between the bridging atom with a certain amount of positive charge and a negative region of the acceptor molecule. A second contribution arises from charge transfer into the AH/AX σ* antibonding orbital, which typically weakens and lengthens this covalent bond. Due in large measure to its very high electronegativity and low polarizability, the F atom is a reluctant participant in halogen bonding, but the Cl, Br, and I atoms engage in XBs which typically grow stronger as the halogen atom becomes larger. While a great deal has been learned over the years about XBs, most of the systems examined are limited to situations where the bridging halogen is bound to a carbon[17-31] or

other atom.[16,32-37] There is a surprising paucity of information available for systems containing a N-X bond. Taking the parallel world of HBs as an example, there are certainly commonalities between CH and NH HBs, but there are also some significant differences as well. For example, the CH bond often shortens when it engages in a HB and its stretching frequency shifts to the blue, both opposite to what is observed for NH donors. NH HBs are systematically stronger than those with CH donors. It is therefore of some importance to consider the corresponding questions for halogen bonds, viz. how NX halogen bond donors might differ from their CH congeners.

There is a certain amount of information currently available, albeit not as robust as one would like, in the literature about NX halogen bonds.[38-40] Most of this data is structural in nature and derives from crystal studies, as recently summarized by Troff et al.[41] The N-X XB bond in halosuccinimides[42-44] shows up as a short intermolecular contact. Even shorter distances are observed when the XB acceptor is an anion,[41] an amine or triazine[45, 46], or an imine.[47] Halosaccharins have also been observed to engage in XBs[48], including with water and pyridine as halogen acceptor.[49] A very recent study[50] paired halosaccharins with a series of pyridine-N-oxides.

But what remains lacking is a thorough and comprehensive body of information that directly relates and compares NX with CX halogen bonds. Some of the most pressing questions at present begin with a comparison of the energetic and electronic structural features of NX halogen bonds. How does changing the identity of the X atom in the NX bond affect the strength of the interaction, and how do these noncovalent bonds compare with the analogous NH HBs? What is the sensitivity of the NX XB to the nature of the

partner electron donor molecule; how do π-donors compare with lone-pair donors? What are the relative contributions to NX HBs of principal attractive components: electrostatic, induction, and dispersion energy? How does the formation of a NX XB affect the length of the internal covalent N-X bond?

The goal of the present work is to attempt to answer these questions via quantum chemical calculations. We take as a starting point systems where there is available a significant amount of experimental data to serve as a check on the validity of the calculations. The succinimide and saccharin systems fulfill this role, harkening back to their recent study.[41-50] As described below, a wide range of electron donor molecules is considered, including both lone pair and π-donors, and molecules of varying donor ability. Among this list is included both pyridine and pyridine N-oxide, again because of the availability of prior experimental data.

10-2. Computational Methods

Most of the calculations were carried out via the Gaussian-09 package.[51] The geometries were optimized at the MP2 level of theory in conjunction with the aug-cc-pVDZ[52] basis set; the aug-cc-pVDZ-PP[53] pseudopotential was used for the heavier atoms I and Br. The basis sets were taken externally from the EMSL library.[54] Only geometries with non-negative frequencies were taken into consideration to ensure each obtained geometry is in fact a true minimum. The binding energies were calculated as the differences between the energy of the complex and the sum of the monomers, corrected for basis set superposition error using the counterpoise procedure. Charge transfer was examined by Natural Bond Orbital (NBO)[55] calculations using the NBO 6.0 program.[56] The binding

energies were decomposed into various components using Symmetry Adapted Perturbation Theory (SAPT)[57] via the MOLPRO-2010 software package.[58] The HF level of theory and the 6-31+G* basis set for lighter elements, and LANL2DZ basis sets for Br and I, was used for the SAPT analysis.

Extrapolation to complete basis set was performed via a method originally proposed by Truhlar[59] and which has been shown to work well for systems of this type.[60] ChemCraft software[61] was used for visualization of geometries and vibrational frequencies. The molecular electrostatic potentials were analyzed by the Multiwfn software package.[62]

The molecular structures of succinimide and saccharin are displayed in Scheme 10-I. The NH proton of each was replaced in turn by Cl, Br, and I so as to enable the formation of halogen bonds. The nine electron donors considered here are illustrated in Scheme 10-I. They include those that donate electrons via lone pairs, as well as π-donors ethene, acetylene, and benzene.

10-3. Results and Discussion

10-3.1. Optimized Geometries and Binding Energies

The optimized geometries of the H-bonded succinimide complexes with NH_3, H_2O, acetone, pyridine, and pyridine N-oxide are presented on the left side of Fig 10-1. The right side illustrates the structures of the X-bonded complexes, as exemplified by X=Br; the structures for the Cl and I dimers are very similar. The analogous diagrams of the π-complexes with C_2H_4, HCCH, and benzene are displayed in Fig 10-2. There is more

H-bond or halogen bond donors

X=H, Cl, Br, I

N-succinimide

saccharin

H-bond or halogen bond acceptors

NH_3
ammonia

FH
hydrofluoric acid

OH_2
water

acetone

ethene

HC≡CH
ethyne

benzene

pyridine

pyridine-N-oxide
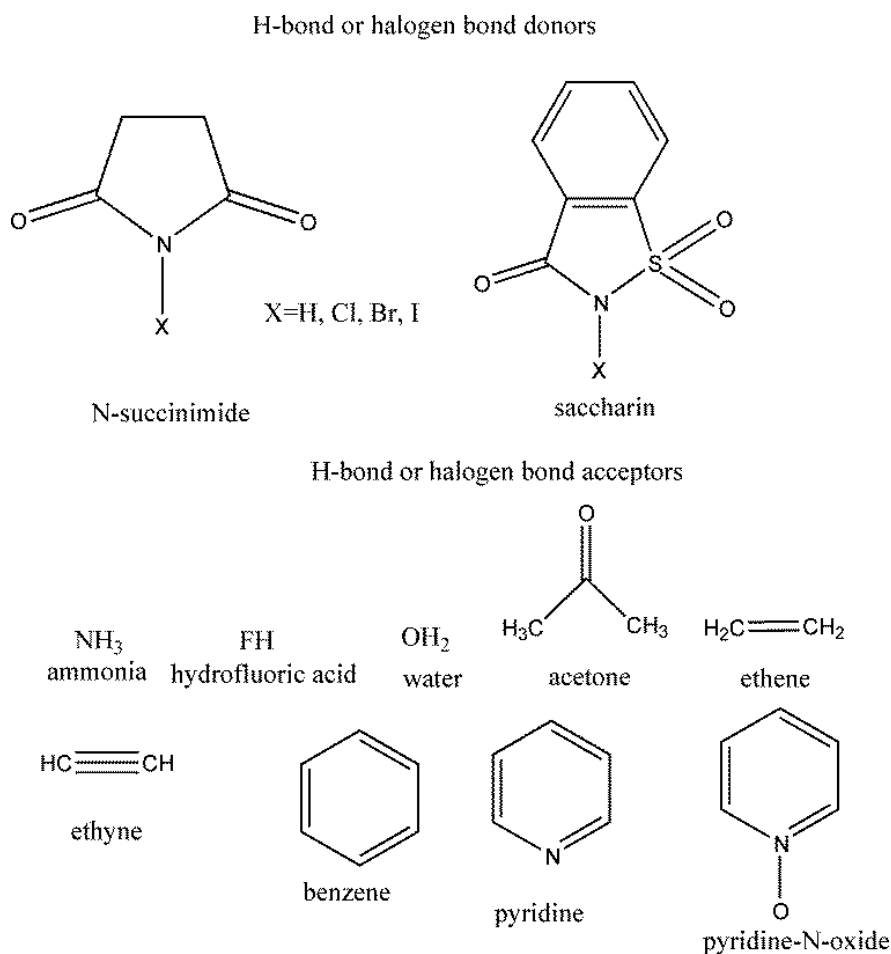
Scheme 10-I. Molecules participating in HB or XB interactions.

diversity in the HF complexes, all of which are illustrated in Fig 10-3. Considering the structures in Fig 10-1, the X-bonded geometries on the right side are all simple and straightforward XBs, with $\theta(NX \cdots Y) \sim 180°$. In contrast, the H-bonded geometries on the left all contain indications of a secondary HB, albeit a weak one in several cases. One of the H atoms of NH_3, for example, is oriented so as to form a secondary $NH \cdots O$ HB. The $OH \cdots O$ HB in the complex with water is as short as the "primary" $NH \cdots O$ HB. There is some

geometrical evidence of subsidiary CH··O HBs in the other HB geometries in Fig 10-1. A secondary HB, also CH··O, appears likely in the HB geometry of acetylene in Fig 10-2. Turning to HF in Fig 10-3, its FH··O HB is shorter and likely stronger than the NH··F HB. When the H atom of succinimide is changed to Cl, this atom is not a strong enough halogen-bonder so one does not see a XB but rather a FH··O HB. Br and I, on the other hand, engage in strong enough XBs that one does see such F··X HBs.

The BSSE-corrected binding energies are reported in Table 10-1. Focusing first on the HB geometries in the first column, succinimide engages in fairly strong complexes when interacting with lone pairs, with binding energies in the 8-10 kcal/mol range. HBs with the π-systems are weaker, between 3.5 and 5.5 kcal/mol, in the order ethene < acetylene < benzene. (The binding energy of acetylene is likely inflated by the presence of the secondary CH··O HB, as is the case also for the OH··O HB for H_2O.) The XB structures in the next three columns obey a consistent pattern: Cl < Br < I. As a general rule of thumb, I XBs are roughly twice as strong as Cl XBs. In most cases, the HB binding energy falls between Br and I. These trends are true whether the bond is formed to lone pairs, or to π-systems. There is one distinction between HB and XB complexes. Ethene forms stronger XBs than does acetylene, in contrast to the HB pattern where it is acetylene that engages in stronger interactions. However, the HB energy of acetylene is likely inflated by the presence of the secondary CH··O HB. Whether HB or XB, pyridine and pyridine-N-oxide form substantially stronger complexes than do the other electron donors studied here.

Table 10-2 lists the intermolecular distances of the various optimized complexes. In most cases, the HBs are shorter than XBs, not surprising in view of the much smaller

atomic radius for H. Within the class of XBs there are two competing trends. The increasing atomic radii would tend toward Cl < Br < I, but the strengthening bond that is associated with larger halogens would push toward an opposite pattern. The final result is a compromise wherein Br generally has the shortest XB and Cl the longest. There is an exception to this trend involving acetone wherein the Cl··O distance is shorter than that for Br, probably due to the presence of a CH··O HB in the former case which draws the two molecules together.

The lower halves of Tables 10-1 and 10-2 allow a comparison of succinimide with saccharin. The latter differs from the former first by the presence of a phenyl group fused to its five-membered ring. Also, one of the two CO groups adjacent to the NX group is replaced by a SO_2 unit. These replacements lead to an overall strengthening of the various bonds, both H and X. The increments are largest for the HBs, ranging up to 2.4 kcal/mol, whereas the increases for the XBs are less than 1 kcal/mol. Importantly, the patterns are largely retained. I-bonds are the strongest of the halogen bonds, and Cl-bonds the weakest. HBs are usually a bit weaker than I-bonds but there are a few exceptions where the reverse if observed, e.g. acetone, pyridine-N-oxide, acetylene, and benzene. The former can be explained by the presence of a pair of CH··O HBs that add to the stability of the HB configuration, while the others would appear to be an intrinsic property of the systems involved.

As a last bit of geometrical information, it is well known that the formation of a HB or XB will typically elongate the pertinent N-H or N-X covalent bond. These bond stretches are contained in Table 10-3 and reproduce some of the energetic trends in Table 10-1 but

not all. Like the binding energies, the stretches increase in the order Cl < Br < I. On the other hand, the NH stretch is less than that for X=Br, although the HB energy is greater than the Br-bond energy. Within the subset of π-donors, the energetic order acetylene < ethene < benzene is altered, with ethene showing the largest bond stretch and acetylene the smallest. The uniformly stronger bonds formed by saccharin vs succinimide are less consistent with respect to bond stretches.

There is always the question as to how well any particular level of theory reproduces data that might be computed at a higher level. In order to address this issue, succinimide, and its three variants of halosubstituted derivatives, was paired with both NH_3 and OH_2, and the binding energies computed at higher levels. The results, displayed in Table 10-4, show that enlargement of basis set from aug-cc-pVDZ to aug-cc-pVTZ, and then extrapolated to complete basis set, each result in a small increase in binding energy, but less than 1 kcal/mol. On the other hand, the improvement of the treatment of electron correlation from MP2 to CCSD(T) leads to only a very small decrease, suggesting MP2 is quite good for treatment of these systems. As a final point of comparison, the M06-2X variant of DFT uniformly overestimates the binding energies, whether compared with MP2 or with CCSD(T).

10-3-2. Electronic Structure Analysis

A myriad of prior studies have pointed to electrostatic attraction as a primary component of both H and X bonds. For that reason, it is instructive to inspect the molecular electrostatic potential (MEP) that surrounds each of the proton or halogen-donor molecules being considered here. These potentials are displayed in Fig 10-4 wherein blue and red

regions correspond respectively to positive and negative regions of the MEP. Each of the molecules contains a blue area at the site of its bonding, i.e. its H or X atom. This blue area is smallest for X=Cl and grows larger for Br and I, and is even broader for H. The numerical values in Fig 10-4 refer to the value of the potential where it reaches its maximal value, $V_{s,max}$, on the contour wherein the electron density is fixed at 0.001 au. These quantities increase in the same Cl < Br < I < H order as the size of the blue region. There are only small differences between the succinimide values in the top of Fig 10-4 and the saccharin quantities in the lower half. It is perhaps important to note that even though X=H is associated with the largest $V_{s,max}$ values, the binding energies of the HB complexes are usually surpassed by those for X=I.

While the MEPs provide useful insights into the electrostatic interactions, they are silent concerning the effects of mutual polarization and charge transfer between the two subunits in each complex. The latter can be understood via NBO analysis which quantifies the energetic consequences of charge transfer between pairs of individual orbitals. It is known that the largest share of charge in H or X-bonded systems is transferred into the $\sigma^*(NX)$ antibonding orbital. These quantities are displayed in Table 10-5 where the donating orbital is either the lone pair(s) or the π-orbitals of the electron donor molecule. It must be recalled that in those cases where a secondary interaction occurs, there are other important charge transfers. For example, the 9.61 kcal/mol E(2) for the HB complex of succinimide with OH_2 is supplemented by an additional 9.08 kcal/mol by the transfer into the $\sigma^*(OH)$ antibonding orbital of the water from the OH··O HB.

With the obvious exception of those cases of a strong secondary interaction, the E(2) quantities mirror the binding energies in Table 10-1 fairly well. Taking the HB systems with succinimide as an example, the acetone < NH_3 < pyridine < pyridine-N-oxide trend in binding energy is the same order as is observed for E(2). The two quantities are even more closely related for the set of six I-bonding systems: FH < OH_2 < acetone < NH_3 < pyridine-N-oxide < pyridine. There are also parallels in that both E(2) and binding energy follow the general pattern of Cl < Br < H < I. The quantities are not as closely related for the various π-complexes in that E(2) is largest for ethene but benzene is more strongly bound. Part of this discrepancy may be related to a secondary charge transfer from the halogen lone pair to the π* orbitals of the alkene.

Given the large values of some of the NBO quantities in Table 10-5, it was considered prudent to examine how sensitive they might be to basis set.[63] Parallel calculations were thus carried out for the aug-cc-pVTZ basis set, and the data compared with aug-cc-pVDZ. Examination focused on those systems with the largest values of E(2) to check for possible basis set inflation. A reduction was observed with the larger basis set, but this decrease was fairly small, only 4-12%, for the I-bonded structures that show the largest values of E(2). For example, E(2) was reduced from 42.2 kcal/mol for the succinimide-I complex with pyridine-N-oxide to 38.7 kcal/mol with the larger basis.

The decomposition of the total binding energy into separate components, each with a physical significance, can add further insights into the nature of the bonding. Fig 10-5 illustrates the fractional contribution of each of the electrostatic (ES, blue), induction (IND, red) and dispersion (DISP, green) components to their total, the entire attractive energy in

the complexes containing succinimide. The distinction between H and X bonds is immediately apparent. The blue electrostatic energy accounts for a large share of the total attraction for the H-bonds in Fig 10-5a, more than 50% in most cases. Induction makes a smaller contribution 20-30%, followed by dispersion at less than 20%. The principal exception is the H-bond to benzene, where the three components are roughly equal. This disproportionately large ES contribution is consistent with the larger values of $V_{s,max}$ for the H-bonding molecules in Fig 10-4.

The pattern is different for the halogen bonds in Fig 10-5. In the first place, induction energy is comparable to and sometimes larger than the electrostatic component. The larger induction is especially noticeable for the three π-systems on the right side, where IND hovers around 50%. But even for the XBs formed to the lone pairs on the left, IND is nearly as large as ES. Where the HBs and XBs are most similar is in the percentage contribution of DISP, which is the smallest of the three components. The three components compose very similar percentages of the total attraction for the corresponding saccharin complexes.

The absolute magnitudes of the various quantities also offer insights into the nature of the interactions. With regard to each attractive term, one sees a clear Cl < Br < I trend. This pattern is especially noticeable with respect to induction energy, where it can increase by a factor of as much as 4 between Cl and I. While obeying the same pattern, dispersion is not quite as sensitive to the nature of the halogen atom. With respect to the nature of the electron donor species, pyridine and pyridine-N-oxide exhibit the largest components in general. Induction and dispersion are disproportionately large for the π-donors ethene,

acetylene, and benzene. The latter is associated with especially high dispersion, while the former shows large induction. The quantities related to H are a bit more variable but generally hover between Cl and I.

10-4. Discussion

The generally lesser ability of π-systems, as compared to lone pairs, to donate protons to XBs matches earlier findings for related pnicogen and chalcogen bonds.[64-67] The Cl < Br < H < I order of binding energy of the N-X donors examined here is consistent with similar patterns observed previously for the many C-X donors that have been studied in the past.[25, 68-75]

It is already well established that NH H-bonds are typically considerably stronger than the related CH HBs. But the comparisons between NX and CX halogen bonds remain relatively unexplored. This issue was examined here in a direct manner by replacing the NH of succinimide by CH_2, so as to retain the basic structure and internal bonding. The resulting 1,3-cyclopentadione was thus taken as the CH donor, and XBs were formed by replacing one of the two H atoms by F, Cl, Br, and I in turn. Each of these molecules was then paired with NH_3 as prototypical electron donor. The counterpoise-corrected binding energies are presented in Table 10-6, along with the optimized intermolecular distances. Also contained in Table 10-6 are the corresponding data for the analogous NH/NX donor succinimide. (Like the complex with succinimide, the H-bonding cyclopentadione complex with NH_3 also contains secondary attractive interactions in addition to the HB.) The first row of Table 10-6 confirms the weaker CH··N HB, as compared to NH··N by a factor of ½. In fact, this weakening CX/NX ratio is fairly typical of the XBs as well.

Consistent with their weaker nature, the various CH/CX complexes are also characterized by longer intermolecular separations, by 0.3 Å for the three XBs, and by 0.8 Å for the HBs.

Another comparison between N and C H/X donors derives from a prior M06-2X/aug-cc-pVDZ study of the CI··N bond between pentafluoroiodobenzene and pyridine[76] which obtained a binding energy of 6.9 kcal/mol. This quantity is considerably smaller than the 12.8 kcal/mol calculated here for the NI··N bond between I-succinimide and pyridine. Pentafluoroiodobenzene was also the I-donor with acetone in another study.[77] At the same level of theory used here, this CI··O XB had a binding energy of 4.9 kcal/mol, less than the 7.6 and 8.5 kcal/mol respectively calculated above for the NI··O bond between acetone and both I-succinimide and I-saccharin. Moreover, this quantity dropped further when some of the electron-withdrawing F atoms were removed from the I donor of the CI··O bond.

A very recent set of calculations[74] dealing with simpler systems affirmed the weaker CX XBs in a set of methyl halide oligomers when compared to the analogous NX XBs in aminohalides, wherein the former amount to roughly 60% of the latter. This weakening is not very different than the 50% reduction noted above for our comparison of succinimide with cyclopentadione in Table 10-5. Calculations on the nitrohalides[78,79] affirmed the I > Br > Cl trend of NX HBs. Recent work by McDowell and Maynard[80] computed the cooperativity experienced by a N-Cl XB when the N atom acts simultaneously as electron donor, but did not draw parallels with the analogous C-Cl XB. With regard to the energy decomposition, earlier calculations[81-83] had also concluded that both dispersion and charge transfer were vital ingredients in XBs, in addition to electrostatics.

There are experimental results available with which we can directly compare some of our data. Puttreddy et al[50] reported the solid state geometrical parameters for complexes of I-succinimide and I-saccharin with pyridine-N-oxide, and Makhotina et al[48] reported analogous quantities for pyridine. In Table 10-7, the numbers outside and inside the parentheses respectively represent our calculated parameters and experimental values from the crystal. The internal N-I bond lengths are reproduced very well by the calculations, while the calculated XB R(I···O/N) distances are a bit longer (by about 0.1 Å). The intermolecular distances in the crystal may be shortened by the strengthening effects of cooperative interactions with neighboring molecules. The XB angles in the final column of Table 10-7 are all close to linearity, both experimental and computed. The association constants measured by Puttreddy et al[50] were also consistent with our finding (Table 10-1) that pyridine-N-oxide is considerably more strongly bound with I-succinimide than are water or acetone. The results of Makhotina et al[48] offer additional support for our calculated finding that I-saccharin forms a stronger I-bond with pyridine than does I-succinimide.

In summary, the calculations presented here indicate that the strength of a XB with Cl as donor is much weaker than the corresponding HB. Replacement of Cl by Br yields a XB that is of comparable strength to the corresponding HB, while I presents the strongest interaction of all. Lone pair electron donors lead to stronger interactions than π-donors, particularly pyridine and pyridine-N-oxide. Mutation of succinimide to the larger NX donor saccharin results in a modest enhancement of the binding. The strengths of the interactions correspond to the NBO charge transfer energies E(2) and to the intensity of the positive MEP in the vicinity of the binding atom, whether H or X, although these

correlations are imperfect. Decomposition of the binding energies suggests that electrostatics account for the lion's share of the HB. The induction energy is substantially larger for the XBs, surpassing electrostatics in a number of cases.

References

1.   G. Gilli and P. Gilli, *The Nature of the Hydrogen Bond*, Oxford University Press, Oxford, UK, 2009.

2.   S. Scheiner, *Hydrogen Bonding. A Theoretical Perspective*, Oxford University Press, New York, 1997.

3.   S. J. Grabowski, ed. *Hydrogen Bonding - New Insights*, Springer, Dordrecht, Netherlands, 2006.

4.   E. Arunan, G. R. Desiraju, R. A. Klein, J. Sadlej, S. Scheiner, I. Alkorta, D. C. Clary, R. H. Crabtree, J. J. Dannenberg, P. Hobza, H. G. Kjaergaard, A. C. Legon, B. Mennucci and D. J. Nesbitt, *Pure Appl. Chem.*, 2011, **83**, 1637-1641.

5.   S. Scheiner, ed. *Noncovalent Forces*, Springer, Heidelberg, 2015.

6.   A. Bauzá and A. Frontera, *Angew. Chem. Int. Ed.*, 2015, **54**, 7340-7343.

7.   M. D. Esrafili and F. Mohammadian-Sabet, *Mol. Phys.*, 2016, **114**, 1528-1538.

8.   S. J. Grabowski, *Phys. Chem. Chem. Phys.*, 2014, **16**, 1824-1834.

9.   S. Scheiner, *J. Phys. Chem. A*, 2015, **119**, 9189-9199.

10. C. Bleiholder, D. B. Werz, H. Koppel and R. Gleiter, *J. Am. Chem. Soc.*, 2006, **128**, 2666-2674.

11. R. Gleiter, D. B. Werz and B. J. Rausch, *Chem. Eur. J.*, 2006, **9**, 2676-2683.

12. P. Sanz, O. Mó and M. Yáñez, *Phys. Chem. Chem. Phys.*, 2003, **5**, 2942-2947.

13. U. Adhikari and S. Scheiner, *Chem. Phys. Lett.*, 2012, **532**, 31-35.

14. P. Metrangolo and G. Resnati, *Science*, 2008, **321**, 918-919.

15. T. Clark, M. Hennemann, J. S. Murray and P. Politzer, *J. Mol. Model.*, 2007, **13**, 291-296.

16. I. Alkorta, F. Blanco, M. Solimannejad and J. Elguero, *J. Phys. Chem. A*, 2008, **112**, 10856-10863.

17. J. P. M. Lommerse, A. J. Stone, R. Taylor and F. H. Allen, *J. Am. Chem. Soc.*, 1996, **118**, 3108-3116.

18. P. L. Wash, S. Ma, U. Obst and J. Rebek, *J. Am. Chem. Soc.*, 1999, **121**, 7973-7974.

19. P. Auffinger, F. A. Hays, E. Westhof and P. S. Ho, *Proc. Nat. Acad. Sci., USA*, 2004, **101**, 16789-16794.

20. P. Metrangolo, H. Neukirch, T. Pilati and G. Resnati, *Acc. Chem. Res.*, 2005, **38**, 386-395.

21.   P. Politzer, P. Lane, M. C. Concha, Y. Ma and J. S. Murray, *J. Mol. Model.*, 2007, **13**, 305-311.

22.   V. d. P. N. Nziko and S. Scheiner, *Phys. Chem. Chem. Phys.*, 2016, **18**, 3581-3590.

23.   K. Raatikainen and K. Rissanen, *Cryst. Growth Des.*, 2010, **10**, 3638-3646.

24.   M. D. Esrafili and N. L. Hadipour, *Mol. Phys.*, 2011, **109**, 2451-2460.

25.   B. Nepal and S. Scheiner, *Chem. Eur. J.*, 2015, **21**, 13330-13335.

26.   S. J. Grabowski, *J. Phys. Chem. A*, 2011, **115**, 12340-12347.

27.   A. Bauzá, D. Quiñonero, A. Frontera and P. M. Deyà, *Phys. Chem. Chem. Phys.*, 2011, **13**, 20371-20379.

28.   I. Alkorta, G. Sanchez-Sanz and J. Elguero, *CrystEngComm*, 2013, **15**, 3178-3186.

29.   D. Hauchecorne and W. A. Herrebout, *J. Phys. Chem. A*, 2013, **117**, 11548-11557.

30.   K. E. Riley, C. L. Ford Jr and K. Demouchet, *Chem. Phys. Lett.*, 2015, **621**, 165-170.

31.   V. d. P. N. Nziko and S. Scheiner, *J. Org. Chem.*, 2016, **81**, 2589-2597.

32.   I. Alkorta, S. Rozas and J. Elguero, *J. Phys. Chem. A*, 1998, **102**, 9278-9285.

33. A. Karpfen, in *Halogen Bonding. Fundamentals and Applications*, eds. P. Metrangolo and G. Resnati, Springer, Berlin2008, vol. 126, pp. 1-15.

34. P. Politzer, J. S. Murray and M. Concha, *J. Mol. Model.*, 2008, **14**, 659-665.

35. S. Scheiner, *Int. J. Quantum Chem*, 2013, **113**, 1609-1620.

36. Q. Li, X. Xu, T. Liu, B. Jing, W. Li, J. Cheng, B. Gong and J. Sun, *Phys. Chem. Chem. Phys.*, 2010, **12**, 6837-6843.

37. A. C. Legon, *Phys. Chem. Chem. Phys.*, 2010, **12**, 7736-7747.

38. M. Bedin, A. Karim, M. Reitti, A.-C. C. Carlsson, F. Topic, M. Cetina, F. Pan, V. Havel, F. Al-Ameri, V. Sindelar, K. Rissanen, J. Grafenstein and M. Erdelyi, *Chem. Sci.*, 2015, **6**, 3746-3756.

39. S. B. Hakkert and M. Erdélyi, *J. Phys. Org. Chem.*, 2015, **28**, 226-233.

40. P. V. Gushchin, M. L. Kuznetsov, M. Haukka and V. Y. Kukushkin, *J. Phys. Chem. A*, 2013, **117**, 2827-2834.

41. R. W. Troff, T. Mäkelä, F. Topić, A. Valkonen, K. Raatikainen and K. Rissanen, *Eur. J. Org. Chem.*, 2013, **2013**, 1617-1637.

42. R. Brown, *Acta Cryst.*, 1961, **14**, 711-715.

43. O. Jaray, H. Pritzow and J. Jander, *Z. Naturforsch B*, 1977, **32**, 1416-1420.

44. K. Padmanabhan, I. C. Paul and D. Y. Curtin, *Acta Crystallographica Section C*, 1990, **46**, 88-92.

45.   K. Raatikainen and K. Rissanen, *CrystEngComm*, 2011, **13**, 6972-6977.

46.   E. H. Crowston, A. M. Lobo, S. Parbhakar, H. S. Rzepa and D. J. Williams, *J. Chem. Soc., Chem. Commun.*, 1984, 276-278.

47.   I. Castellote, M. Moron, C. Burgos, J. Alvarez-Builla, A. Martin, P. Gomez-Sal and J. J. Vaquero, *Chem. Commun.*, 2007, 1281-1283.

48.   O. Makhotkina, J. Lieffrig, O. Jeannin, M. Fourmigué, E. Aubert and E. Espinosa, *Cryst. Growth Des.*, 2015, **15**, 3464-3473.

49.   D. Dolenc and B. Modec, *New J. Chem.*, 2009, **33**, 2344-2349.

50.   R. Puttreddy, O. Jurcek, S. Bhowmik, T. Makela and K. Rissanen, *Chem. Commun.*, 2016, **52**, 2338-2341.

51.   M. J. Frisch, G. W. Trucks, H. B. Schlegel, G. E. Scuseria, M. A. Robb, J. R. Cheeseman, G. Scalmani, V. Barone, B. Mennucci, G. A. Petersson, H. Nakatsuji, M. Caricato, X. Li, H. P. Hratchian, A. F. Izmaylov, J. Bloino, G. Zheng, J. L. Sonnenberg, M. Hada, M. Ehara, K. Toyota, R. Fukuda, J. Hasegawa, M. Ishida, T. Nakajima, Y. Honda, O. Kitao, H. Nakai, T. Vreven, J. A. Montgomery Jr., J. E. Peralta, F. Ogliaro, M. J. Bearpark, J. Heyd, E. N. Brothers, K. N. Kudin, V. N. Staroverov, R. Kobayashi, J. Normand, K. Raghavachari, A. P. Rendell, J. C. Burant, S. S. Iyengar, J. Tomasi, M. Cossi, N. Rega, N. J. Millam, M. Klene, J. E. Knox, J. B. Cross, V. Bakken, C. Adamo, J. Jaramillo, R. Gomperts, R. E. Stratmann, O. Yazyev, A. J. Austin, R. Cammi, C. Pomelli, J. W. Ochterski, R. L. Martin, K. Morokuma, V. G. Zakrzewski, G. A. Voth, P. Salvador, J. J.

Dannenberg, S. Dapprich, A. D. Daniels, Ö. Farkas, J. B. Foresman, J. V. Ortiz, J. Cioslowski and D. J. Fox, Gaussian, Inc., Wallingford, CT, USA2009.

52.   D. E. Woon and T. H. Dunning, *J. Chem. Phys.*, 1993, **98**, 1358-1371.

53.   K. A. Peterson, B. C. Shepler, D. Figgen and H. Stoll, *J. Phys. Chem. A*, 2006, **110**, 13877-13883.

54.   K. L. Schuchardt, B. T. Didier, T. Elsethagen, L. Sun, V. Gurumoorthi, J. Chase, J. Li and T. L. Windus, *J. Chem. Inf. Model.*, 2007, **47**, 1045-1052.

55.   J. P. Foster and F. Weinhold, *J. Am. Chem. Soc.*, 1980, **102**, 7211-7218.

56.   E. D. Glendening, C. R. Landis and F. Weinhold, *J. Comput. Chem.*, 2013, **34**, 1429-1437.

57.   K. Szalewicz, *WIREs Comput Mol Sci*, 2012, **2**, 254-272.

58.   H.-J. Werner, P. J. Knowles, G. Knizia, F. R. Manby and M. Schütz, *WIREs Comput Mol Sci*, 2012, **2**, 242-253.

59.   D. G. Truhlar, *Chem. Phys. Lett.*, 1998, **294**, 45-48.

60.   S. Scheiner, *Comp. Theor. Chem.*, 2012, **998**, 9-13.

61.   G. A. Andrienko, *http://www.chemcraftprog.com*.

62.   T. Lu and F. Chen, *J. Comput. Chem.*, 2012, **33**, 580-592.

63.   K. U. Lao and J. M. Herbert, *J. Chem. Theory Comput.*, 2016.

64.   S. Scheiner and U. Adhikari, *J. Phys. Chem. A*, 2011, **115**, 11101-11110.

65.   M. D. Esrafili and F. Mohammadian-Sabet, *Mol. Phys.*, 2015, **113**, 3559-3566.

66.   A. Bauzá and A. Frontera, *ChemPhysChem*, 2015, **16**, 3108-3113.

67.   F. Zhou, R. Liu, P. Li and H. Zhang, *New J. Chem.*, 2015, **39**, 1611-1618.

68.   S. W. L. Hogan and T. van Mourik, *J. Comput. Chem.*, 2016, **37**, 763-770.

69.   M. D. Esrafili and M. Vakili, *Mol. Phys.*, 2016, **114**, 325-332.

70.   S. A. C. McDowell and Z. L. Holder, *Mol. Phys.*, 2015, **113**, 3757-3766.

71.   Y.-Z. Zheng, G. Deng, Y. Zhou, H.-Y. Sun and Z.-W. Yu, *ChemPhysChem*, 2015, **16**, 2594-2601.

72.   B. Nepal and S. Scheiner, *J. Phys. Chem. A*, 2015, **119**, 13064-13073.

73.   Y. Geboes, N. Nagels, B. Pinter, F. De Proft and W. A. Herrebout, *J. Phys. Chem. A*, 2015, **119**, 2502-2516.

74.   J. Dominikowska, F. M. Bickelhaupt, M. Palusiak and C. Fonseca Guerra, *ChemPhysChem*, 2016, **17**, 474-480.

75.   B. Nepal and S. Scheiner, *ChemPhysChem*, 2016, **17**, 836-844.

76.   Q. Shi, H. Su, Y. Liu, W. Wu and Y. Lu, *Comp. Theor. Chem.*, 2014, **1027**, 79-83.

77.   K. E. Riley, J. S. Murray, J. Fanfrlík, J. Řezáč, R. J. Solá, M. C. Concha, F. M. Ramos and P. Politzer, *J. Mol. Model.*, 2011, **17**, 3309-3318.

78. M. Solimannejad, V. Ramezani, C. Trujillo, I. Alkorta, G. Sánchez-Sanz and J. Elguero, *J. Phys. Chem. A*, 2012, **116**, 5199-5206.

79. M. Solimannejad, N. Nassirinia and S. Amani, *Struct. Chem.*, 2013, **24**, 651-659.

80. S. A. C. McDowell and S. J. Maynard, *Mol. Phys.*, 2016, **114**, 1609-1618.

81. M. Carter, A. K. Rappé and P. S. Ho, *J. Chem. Theory Comput.*, 2012, **8**, 2461-2473.

82. P. Deepa, B. V. Pandiyan, P. Kolandaivel and P. Hobza, *Phys. Chem. Chem. Phys.*, 2014, **16**, 2038-2047.

83. J. Thirman and M. Head-Gordon, *J. Chem. Phys.*, 2015, **143**, 084124.

Tables and Figures

Table 10-1. Counterpoise-corrected binding energies (kcal/mol) of H and X bonded complexes

Succinimide systems				
	H	Cl	Br	I
NH$_3$	8.20	3.83	7.09	9.83
OH$_2$	8.22[d]	2.52	4.11	5.43
FH	10.09[a]	7.22[b]	2.00	2.48
acetone	7.60	3.81	5.83	7.58
pyridine	10.04	5.12	9.21	12.77
Pyridine-N-oxide	10.33	5.63	8.23	10.95
π-complexes				
ethene	3.46	2.37	3.93	5.15
acetylene	4.38	2.16	3.24	4.05
benzene	5.46[c]	3.14	4.46	5.56
Saccharin complexes				
	H	Cl	Br	I
NH$_3$	9.65	4.12	7.91	11.28
OH$_2$	7.92[d]	2.60	4.33	5.92
FH	9.57[a]	5.51[b]	2.07	2.69
acetone	8.77[e]	3.96	6.14	8.48
pyridine	11.53	5.43	10.39	14.66
Pyridine-N-oxide	12.76	6.22	8.79	12.52
π-complexes				
ethene	4.38	2.59	4.36	5.90
acetylene	4.58	2.18	3.37	4.40
benzene	7.29	3.86	4.75	6.15

[a]FH acts as the proton acceptor from NH and as donor to O

[b]no halogen bond; FH acts as the proton donor to O

[c]small negative frequency

[d]NH··O supplemented by OH··O

[e]stabilized by pair of CH··O HBs

Table 10-2. Intermolecular H/X bond distances (Å) of the optimized geometries.

Succinimide systems				
	H	Cl	Br	I
NH$_3$	1.935	2.754	2.608	2.653
OH$_2$	1.996	2.801	2.747	2.810
FH	2.154	-	2.421	3.000
acetone	1.853	2.739	2.907	2.677
pyridine	1.813	2.617	2.421	2.497
Pyridine-N-oxide	1.764	2.720	2.515	2.537
π-complexes				
ethene	2.375	3.046	2.633	2.968
acetylene	2.403	3.101	3.025	3.126
benzene	2.052	3.050	2.965	3.051
Saccharin complexes				
	H	Cl	Br	I
NH3	1.832	2.702	2.536	2.586
OH2	1.931	2.785	2.716	2.762
FH	2.100	-	2.869	2.969
acetone	1.842	2.710	2.588	2.618
pyridine	1.713	2.579	2.332	2.434
Pyridine-N-oxide	1.656	2.723	2.451	2.472
π-complexes				
ethene	2.384	2.997	2.838	2.881
acetylene	2.302	3.070	2.980	3.060
benzene	2.164	3.166	2.968	2.997

Table 10-3. Stretch (mÅ) of the covalent bond, Δr(N-H/X) caused by the formation of the HB/XB.

Succinimide systems			
	H	Cl	Br	I
NH₃	19.2	13.4	32.9	44.7
OH₂	7.9	4.2	8.9	13.6
FH	4.89	-	1.86	3.19
acetone	14.7	5.4	14.9	22.8
pyridine	28.5	19.2	56.1	66.2
Pyridine-N-oxide	23.1	7.8	27.2	41.3
π-complexes			
ethene	4.5	7.3	19.0	26.1
acetylene	4.3	4.2	9.9	12.9
benzene	2.7	3.5	12.0	16.8
Saccharin complexes			
	H	Cl	Br	I
NH3	29.8	13.8	37.5	43.5
OH2	10.8	2.4	6.2	4.4
FH	2.9	-	0.1	-5.7
acetone	14.8	7.4	12.9	17.5
pyridine	43.4	21.4	73.6	71.5
Pyridine-N-oxide	41.0	6.4	30.8	41.2
π-complexes			
ethene	3.7	8.6	22.6	24.2
acetylene	5.7	4.6	9.8	5.7
benzene	4.0	-0.3	12.2	11.3

Table 10-4. NBO charge transfer energies E(2) for transfer into σ*(NH/X) antibonding orbital. All in kcal/mol.

Succinimide systems				
	H	Cl	Br	I
NH$_3$	23.99	8.17	23.05	34.58
OH$_2$	9.61	3.86	8.38	13.13
FH	4.03	-	3.27	4.91
acetone	21.83	4.57	13.21	21.68
pyridine	31.23	10.78	37.36	49.81
Pyridine-N-oxide	34.43	5.68	24.39	42.15
π-complexes				
ethene	7.24	4.34	12.17	19.63
acetylene	5.63	2.91	6.91	9.99
benzene	6.99	2.46	8.44	13.02
Saccharin complexes				
	H	Cl	Br	I
NH$_3$	36.11	9.87	29.82	43.36
OH$_2$	14.40	4.13	9.97	15.43
FH	5.12	-	3.85	5.41
acetone	20.88	5.21	15.76	26.81
pyridine	48.26	11.98	52.86	62.74
Pyridine-N-oxide	54.16	5.32	31.84	53.33
π-complexes				
ethene	7.05	5.19	15.48	26.19
acetylene	7.89	3.28	8.29	12.77
benzene	8.79	1.23	9.32	15.75

Table 10-5. Comparison of counterpoise-corrected binding energies and intermolecular distances for the complexes of substituted 1,3-cyclopentadione and succinimide with NH_3.

|	E_b, kcal/mol		$R(X\cdot\cdot N)$, Å	
	1,3-cyclopentadione	succinimide	1,3-cyclopentadione	succinimide
H	4.31[a]	8.20	2.720	1.935
Cl	1.64	3.83	3.076	2.754
Br	4.91	7.09	2.944	2.608
I	5.42	9.83	2.945	2.653

[a] Not completely H-bonded complex

Table 10-6. Comparison of calculated with experimentally determined geometrical parameters, in parentheses.

complex	$R(N-I)$, Å	$R(I\cdot\cdot\cdot O/N)$, Å	$\theta(N-I\cdot\cdot\cdot O)$, degs
Succinimide-I···Pyridine-N-Oxide	2.090(2.094)	2.537(2.453)	173.(179)
Saccharin-I···Pyridine-N-Oxide	2.107(2.139)	2.472(2.328)	174(177)
Succinimide-I···Pyridine	2.115(2.116)	2.497(2.493)	180(180)
Saccharin-I···Pyridine	2.137(2.254)	2.434(2.254[a])	180(180)

[a] X-ray quality was reported to be poor
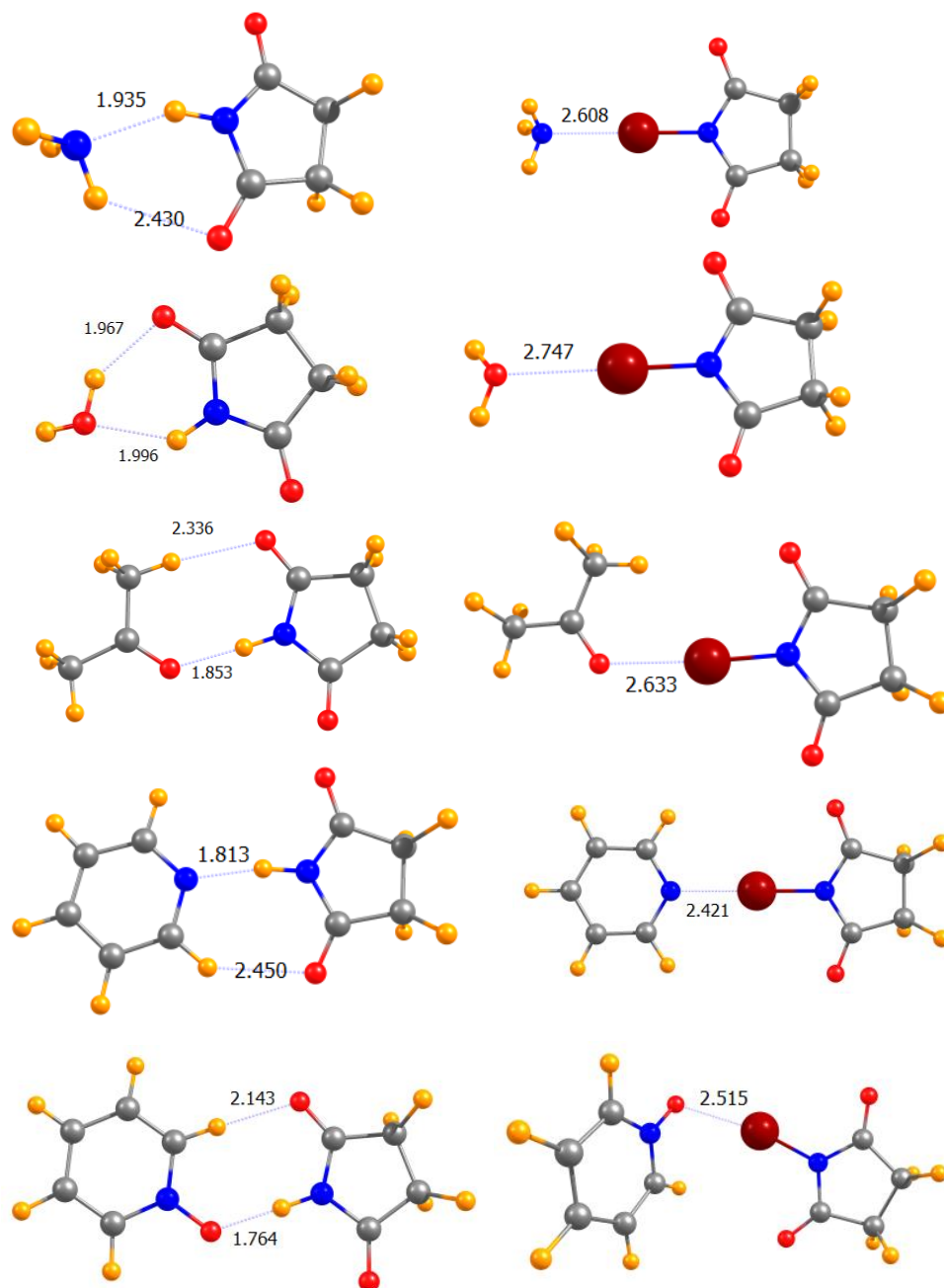
Figure 10-1. Geometries of complexes of succinimide and Br-succinimide with five lone-pair electron donors. Distances in Å.
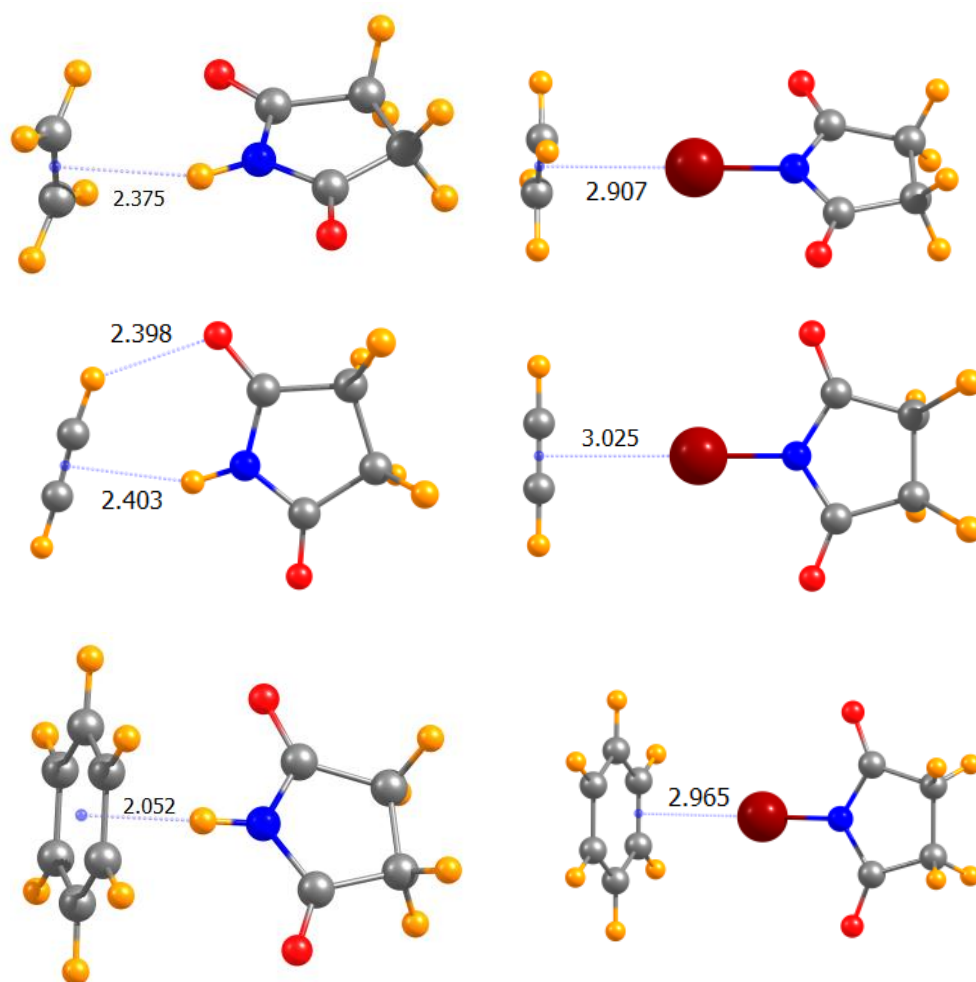
Figure 10-2. Geometries of complexes of succinimide and Br-succinimide with three π-electron donors. Distances in Å.
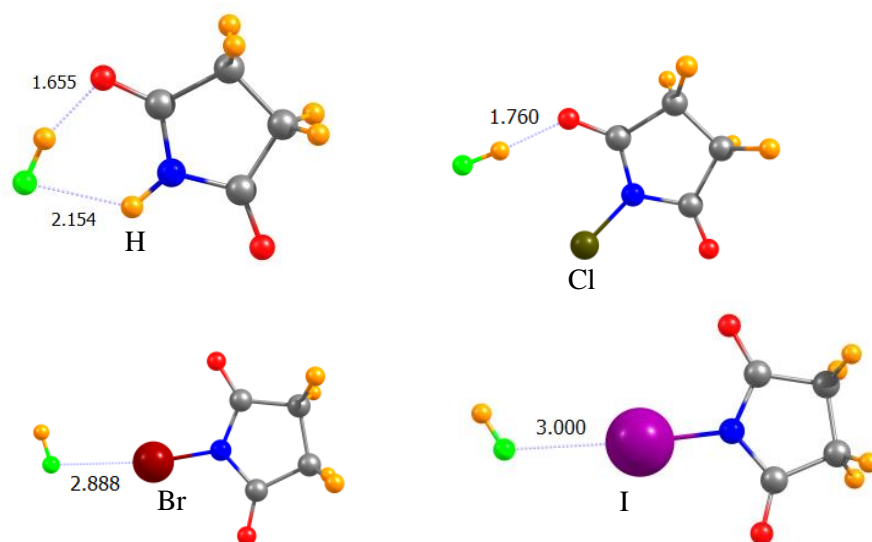
Figure 10-3. Geometries of complexes of HF with succinimide and halosuccinimides. Distances in Å.

| 45.00 kcal/mol | 20.83 kcal/mol | 30.95 kcal/mol | 38.96 kcal/mol |
| H | Cl | Br | I |

| 47.69 kcal/mol | 18.80 kcal/mol | 29.58 kcal/mol | 39.73 kcal/mol |

0.02 ▮▮▮ -0.001 au
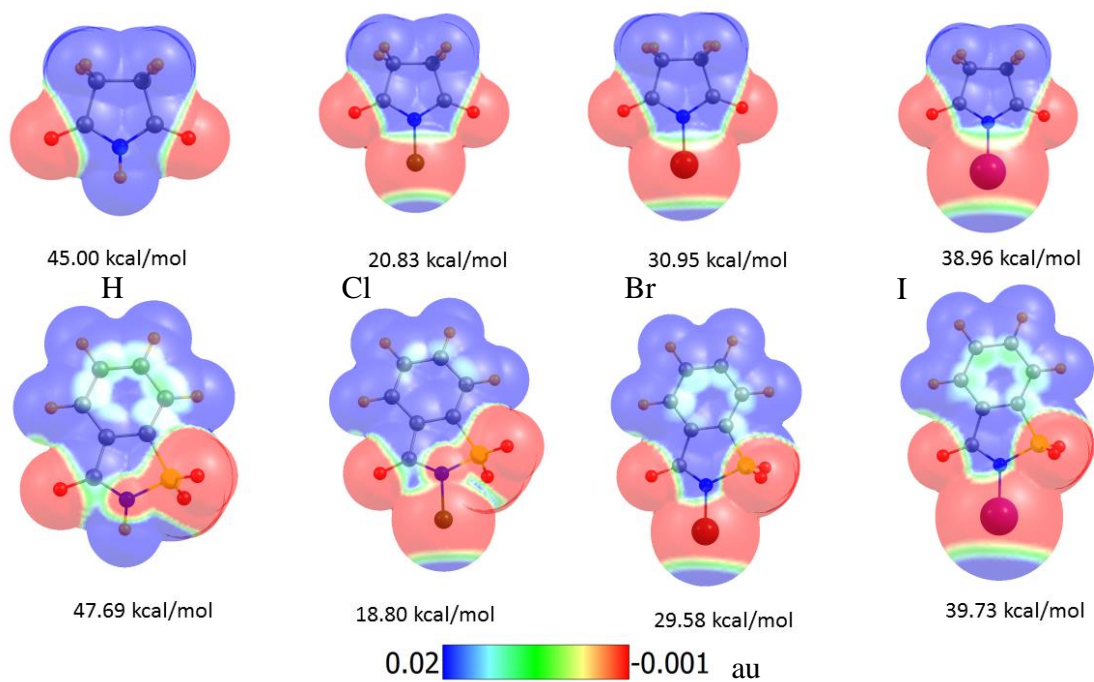
Figure 10-4. Molecular electrostatic potentials (MEPs) of succinimide (top) and saccharin (bottom), and their halosubstituted derivatives. Numerical values correspond to $V_{s,max}$.
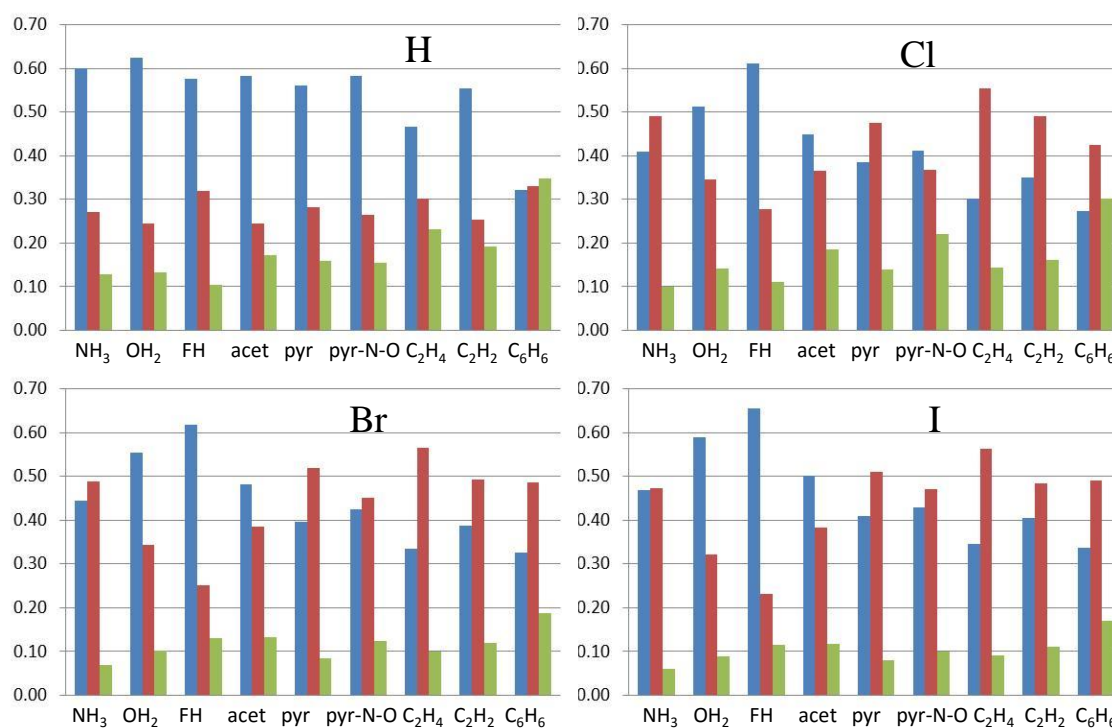
Figure 10-5. Fractional contributions of electrostatic (blue), induction (red), and dispersion (green) to total attraction energy in complexes with succinimide and its indicated halosubstituted derivatives.

CHAPTER 11

SUMMARY

This dissertation has presented a number of electronic and energetic aspects of various charge assisted noncovalent interactions. First of all, the effect of charge on charge assisted C-H$\cdots\pi$ and N-H$\cdots\pi$ interaction were investigated by directly comparing the charge assisted model systems with their neutral analogues. The π electron sources employed for the studies were ethene, acetylene, butadiene, benzene, imidazole, phenol and indole which cover both aliphatic and aromatic as well as systems with biological interest. The C-H$\cdots\pi$ H-bonds formed by trimethyl amine(TMA) with various π electron donors varies from less than 1 kcal/mol for simple ethylene or acetylene to as high as 4.5 kcal/mol for the imidazole system. But once TMA is replaced by tetramethyl ammonium cation (TMA+) H-bond energies increase to 4.7 kcal/mol for simple ethylene or acetylene to as high as 15.5 kcal/mol for indole. These results clearly show the two ways by which the strength of C-H$\cdots\pi$ H-bonds can be increased. First, by increasing the number of electrons in the electron donors. There is a trend of increasing HB strength as the simple C=C bond of ethylene or acetylene is conjugated, as in butadiene. The aromaticity of benzene enhances the binding, which is further enhanced by a –OH substituent as in phenol, with even greater effects arising in the heteroaromatic imidazole or indole. The second and the most effective way is introducing positive charge in the proton donor systems. Due to the introduction of the positive charge on the proton donor in our model systems, the binding energies increase by a factor between 4 and 7. Regarding the most important question, whether these charge assisted C-H$\cdots\pi$ interactions are truly H-bonds

or mostly other kinds of interaction, different quantum mechanical tools like SAPT analysis, NBO charge transfer studies, electron density shift calculation as well as NMR studies clearly show that these charge assisted bonds fall under the definition of H-bonds and hence are true H-bonds.

Some previous studies suggested hydrogen bonds formed by C-H donors can be strong enough to extract anions from the solution both selectively and effectively.[1-3] Our quantum mechanical study is able to not only quantify the strength of C-H···Anion interactions but also able to provide the basic and fundamental understanding of these interactions. Firstly, C-H···Anion interactions are very sensitive to the magnitude of charge present in the anion. With CF_3H as the exemplary proton donor the binding energies are 12-17 kcal/mol for the mono anions like CN^-, Cl^-, Br^-, NO_3^-, $HCOO^-$, CH_3COO^-, HSO_4^- and $H_2PO_4^-$, ~27 kcal/mole for dianions like SO_4^{2-} and HPO_4^{2-} and 45 kcal/mole for trianion PO_4^{3-}. One exception to above is F^- anion, which has a binding energy of 26 kcal/mol. The anionic H-bond energies are not very sensitive to the nature of the anions. But an increase in the number of acceptor atoms in the anions decreases the binding energy due to the dispersal of the charge on the anion. One of the interesting features of C-H···X H-bonds where X is the acceptor, is compression of the C-H bond length or blue-shifting of the C-H stretching frequency which is opposite to the classical notion that H-bond formation leads to the elongation and red shifting of the D-H bonds, where D is the proton donor. But opposite to the neutral C-H···X hydrogen bonds, in C-H···X^{n-} hydrogen bonds, the C-H bond is elongated and its stretching frequency red-shifted.[4-6] The energy decomposition

analysis by SAPT method reveals that the binding energies are composed of 52-65% electrostatic, 20-38% induction and remaining dispersion components.

Owing to the energetics of C-H$\cdots$X^{n-} H-bonds, the potency of the C-H hydrogen bond donors to solvate the above anions and their micro solvation energetics were analyzed taking CF$_3$H as the prototypical proton donor. Our studies show that C-H$\cdots$X^{n-} H-bonds form well-structured solvation cage around anions. The monoatomic anions like halides tends to form a geometry based on VSEPR theory. For example, with two CF$_3$H molecules, a liner geometry is obtained. Similarly, trigonal planar, tetrahedral, trigonal bipyramidal and octahedral geometries were obtained with coordination number 3, 4, 5 and 6 respectively. Such types of regular geometries are not possible for larger asymmetric anions with multiple H-bond acceptor atoms. Although, the total binding energy increases with the increase in number of coordinated CF$_3$H molecules, the binding energy per solvent molecule undergoes a steady decline. The plots of the free energies of the solvation as a function of number of CF$_3$H molecules yield a more or less parabolic curve which means free energy of solvation increases in the negative direction first, becomes most negative and starts to increase in the positive direction.

Similar to the covalent bonds, some special types of noncovalent interactions like hydrogen and halogen bonds have certain directional properties and they try to maintain linearity in their bond angles as much as possible.[7,8] The distortion of the bond angles from the equilibrium geometry always involves certain amount of destabilization energy. This dissertation compares charge assisted H-bonds with their neutral analogues for the sensitivity of bond angle distortion. Our results show that ionic H-bonds suffer a greater

loss of H-bond energy than their neutral analogues. However, if the bending force constant is normalized with the intrinsic H-bond energy, the distinction is less. SAPT analysis further shows that the source of destabilization arises from exchange repulsion. Similar to the bond angle distortion, the non-covalent interactions are also sensitive to bond stretching. The drop in interaction energy with the bond stretch were studied and fitted to the equation, ΔR^n and R^n where n indicates the exponent, R indicates noncovalent bond length and ΔR indicates bond length change from the equilibrium values. The values follow the pattern H-bond < pnicogen < chalcogen < halogen bond which means halogen bonds are most sensitive to the bond stretching. Similarly, ionic H-bonds have lower values of n than the neutral ones. SAPT analysis shows that among three components, the decay is slowest for the electrostatic term, followed by induction and then by dispersion.

The remaining portion of this dissertation has explored some of the practical applications of the charge assisted hydrogen and halogen bonds. Most articles or books still say that hydrogen bond is the strongest force of interaction among different noncovalent interactions. However, some recent experimental results suggested that the halogen bond is actually superior to the H-bond under similar conditions.[9-11] That is the reason the halogen bond has replaced the H-bond in some degree in some applied fields like anion receptor chemistry, crystal engineering, catalysis etc.[12-14] The detailed comparative studies between neutral as well as charged hydrogen and halogen bonds has been made for their performance to extract halide anions from aqueous solution using bis-triazole pyridinium(BTP) model system. Our results indicate that in both neutral and charged systems the strength for halide binding follows the order, I-bond > Br-bond $\cong$ H-bond >

Cl-bond. Except for the F⁻ binding, the binding energies for other halides with I-bond donor is almost double that of H-bond donors in both charged and neutral systems. Another important implication of this study is the positive charge in the binding unit largely affects the binding performance of the halides. By using dicationic systems, the binding energy for F⁻ can be increased by as much as 8 kcal/mol with respect to the neutral system. Molecular electrostatic potential maps fail to explain why I-bond is stronger than H-bond as the maximum in the electrostatic potential is much higher for H-bond donor than I-bond donor. So it might be induction or dispersion component which makes I-bond stronger than H-bond. Another important way to increase the binding performance of anion receptors is introducing suitable electron withdrawing functional groups into the system. The electronic effects of the different substituent groups, both electron releasing and electron withdrawing, on the binding of halides in bis-triazole benzene (BTB) systems has been studied in detail. Our study shows that the binding energy for halides can be increased as much as $30-50\%$ when NH_2 group is substituted by NO_2. Sensitivity to substituent is larger for I-bond donor receptors than H-bond donors on a magnitude basis. Similarly, dicationic receptors have higher substituent effect than neutral receptors if results are compared again on a magnitude basis.

The charge assisted H-bonds can be applied to the activation of the quinones for their use as oxidizing reagent. The H-bond donors help to increase the electron affinity of the quinones by stabilizing the semiquinone radical anions by charge assisted H-bonds. This type of activation is effective only for the electron rich quinones and only a small amount of activation is achieved in case of electron deficient quinones unless the H-bond

donor is cationic.[15] This marked discrepancy between electron rich and electron deficient quinones has been explored by taking a series of electron rich and electron deficient quinones and varying strengths of H-bond donor systems. The discrepancy is due to the tendencies of the neutral H-bond donors to undergo stacking interactions with the quinones before the reduction. The stacking propensity is higher for electron deficient quinones than electron rich which results in the discrepancy between electron rich and electron deficient quinones towards H-bond activation.

The last part of the dissertation has explored the energetics and the properties of N-X$\cdots$Y halogen bonds and made the direct comparisons with N-H$\cdots$Y H-bonds. Our results indicate that the strengths of bonds follow the order Cl-bond $<$ Br-bond $\cong$ H-bond $<$ I-bond. Coulombic forces represents the largest attractive component in the H-bond while induction energy surpasses electrostatics in several cases in halogen bonds.

Overall, this dissertation has explained some fundamental properties of charge assisted hydrogen and halogen bonds. In most of the cases, comparative studies have been made between them. This dissertation has also provided some insightful results in anion receptor chemistry. I believe the works presented in this dissertation will have large implications in chemistry and biochemistry. For example, the study of effect of charge on noncovalent interactions provides an important way to tune the strength of these interactions in a more rational way for various applications like catalysis, anion receptor chemistry, drug design, crystal engineering, self-assemblies etc. The results from the study of long range behavior of noncovalent interactions will be helpful for incorporation of these interactions into the force field for molecular dynamics simulation. The results from the

study of angular distortion of various noncovalent bond angles from their equilibrium geometry will have similar application in force field development. The parallel and comparative study of hydrogen and halogen bonds is able to change the longtime notion that H-bond is the strongest noncovalent interaction. This might lead to the more extensive use of halogen bond for various applications.

References

(1)   Mo, H.-J.; Shen, Y.; Ye, B.-H. *Inorg. Chem.* **2012**, *51*, 7174.

(2)   Gale, P. A.; Busschaert, N.; Haynes, C. J. E.; Karagiannidis, L. E.; Kirby, I. L. *Chem. Soc. Rev.* **2014**, *43*, 205.

(3)   Lee, S.; Chen, C.-H.; Flood, A. H. *Nat Chem* **2013**, *5*, 704.

(4)   Hobza, P.; Havlas, Z. *Chem. Rev.* **2000**, *100*, 4253.

(5)   Hermansson, K. *J. Phys. Chem. A* **2002**, *106*, 4695.

(6)   Li, X.; Liu, L.; Schlegel, H. B. *J. Am. Chem. Soc.* **2002**, *124*, 9639.

(7)   Politzer, P.; Murray, J. S.; Clark, T. *Phys. Chem. Chem. Phys.* **2010**, *12*, 7748.

(8)   Scheiner, S. *Acc. Chem. Res.* **2013**, *46*, 280.

(9)   Mullaney, B. R.; Partridge, B. E.; Beer, P. D. *Chem. Eur. J.* **2015**, *21*, 1660.

(10)   Langton, M. J.; Robinson, S. W.; Marques, I.; Félix, V.; Beer, P. D. *Nat Chem* **2014**, *6*, 1039.

(11)   Zapata, F.; Caballero, A.; White, N. G.; Claridge, T. D. W.; Costa, P. J.; Félix, V. t.; Beer, P. D. *J. Am. Chem. Soc.* **2012**, *134*, 11533.

(12)   Beale, T. M.; Chudzinski, M. G.; Sarwar, M. G.; Taylor, M. S. *Chem. Soc. Rev.* **2013**, *42*, 1667.

(13)   Kniep, F.; Jungbauer, S. H.; Zhang, Q.; Walter, S. M.; Schindler, S.; Schnapperelle, I.; Herdtweck, E.; Huber, S. M. *Angew. Chem. Int. Ed.* **2013**, *52*, 7028.

(14)   Meyer, F.; Dubois, P. *CrystEngComm* **2013**, *15*, 3058.

(15)   Turek, A. K.; Hardee, D. J.; Ullman, A. M.; Nocera, D. G.; Jacobsen, E. N. *Angew. Chem. Int. Ed.* **2016**, *55*, 539.

APPENDICES

APPENDIX A. Copy Right Permissions

Copyright Clearance Center

RightsLink®

Home | Account Info | Help

ACS Publications
Most Trusted. Most Cited. Most Read.

Title: Effect of Ionic Charge on the CH···n Hydrogen Bond

Author: Binod Nepal, Steve Scheiner

Publication: The Journal of Physical Chemistry A

Publisher: American Chemical Society

Date: Oct 1, 2014

Copyright © 2014, American Chemical Society

Quick Price Estimate

Permission for this particular request is granted for print and electronic formats, and translations, at no charge. Figures and tables may be modified. Appropriate credit should be given. Please print this page for your records and provide a copy to your publisher. Requests for up to 4 figures require only this record. Five or more figures will generate a printout of additional terms and conditions. Appropriate credit should read: "Reprinted with permission from {COMPLETE REFERENCE CITATION}. Copyright {YEAR} American Chemical Society." Insert appropriate information in place of the capitalized words.

I would like to... ❓   reuse in a Thesis/Dissertation ⌄

Requestor Type ❓   Author (original work) ⌄

Portion ❓   Full article ⌄

Format ❓   Print and Electronic ⌄

Will you be translating? ❓   No ⌄

Select your currency   USD - $ ⌄

Quick Price   Click Quick Price

This service provides permission for reuse only. If you do not have a copy of the article you are using, you may copy and paste the content and reuse according to the terms of your agreement. Please be advised that obtaining the content you license is a separate transaction not involving Rightslink.

QUICK PRICE   CONTINUE

Copyright Clearance Center

RightsLink®

ACS Publications
Most Trusted. Most Cited. Most Read.

Title: Effect of Ionic Charge on the CH···п Hydrogen Bond

Author: Binod Nepal, Steve Scheiner

Publication: The Journal of Physical Chemistry A

Publisher: American Chemical Society

Date: Oct 1, 2014

Copyright © 2014, American Chemical Society

PERMISSION/LICENSE IS GRANTED FOR YOUR ORDER AT NO CHARGE

BACK   CLOSE WINDOW

JOHN WILEY AND SONS LICENSE
TERMS AND CONDITIONS
Jun 29, 2016

License Number	3898430530198
License date	Jun 29, 2016
Licensed Content Publisher	John Wiley and Sons
Licensed Content Publication	Chemistry - A European Journal
Licensed Content Title	Anionic CH⋯X− Hydrogen Bonds: Origin of Their Strength, Geometry, and Other Properties
Licensed Content Author	Binod Nepal,Steve Scheiner
Licensed Content Date	Nov 13, 2014
Licensed Content Pages	8
Type of use	Dissertation/Thesis
Requestor type	Author of this Wiley article
Format	Print and electronic
Portion	Full article
Will you be translating?	No
Title of your thesis / dissertation	QUANTUM MECHANICAL STUDIES OF CHARGE ASSISTED HYDROGEN AND HALOGEN BONDS
Expected completion date	Aug 2016
Expected size (number of pages)	375
Requestor Location	Binod Nepal 25 Aggie Village C LOGAN, UT 84341 United States Attn: Binod Nepal
Publisher Tax ID	EU826007151
Billing Type	Invoice

Binod Nepal
25 Aggie Village C

Billing Address

LOGAN, UT 84341
United States
Attn: Binod Nepal

Total   0.00 USD

Terms and Conditions

TERMS AND CONDITIONS

- With respect to the Wiley Materials, all rights are reserved. Except as expressly granted by the terms of the license, no part of the Wiley Materials may be copied, modified, adapted (except for minor reformatting required by the new Publication), translated, reproduced, transferred or distributed, in any form or by any means, and no derivative works may be made based on the Wiley Materials without the prior permission of the respective copyright owner.**For STM Signatory Publishers clearing permission under the terms of the [STM Permissions Guidelines](#) only, the terms of the license are extended to include subsequent editions and for editions in other languages, provided such editions are for the work as a whole in situ and does not involve the separate exploitation of the permitted figures or extracts,** You may not alter, remove or suppress in any manner any copyright, trademark or other notices displayed by the Wiley Materials. You may not license, rent, sell, loan, lease, pledge, offer as security, transfer or assign the Wiley Materials on a stand-alone basis, or any of the rights granted to you hereunder to any other person.

- The Wiley Materials and all of the intellectual property rights therein shall at all times remain the exclusive property of John Wiley & Sons Inc, the Wiley Companies, or their respective licensors, and your interest therein is only that of having possession of and the right to reproduce the Wiley Materials pursuant to Section 2 herein during the continuance of this Agreement. You agree that you own no right, title or interest in or to the Wiley Materials or any of the intellectual property rights therein. You shall have no rights hereunder other than the license as provided for above in Section 2. No right, license or interest to any trademark, trade name, service mark or other branding ("Marks") of WILEY or its licensors is granted hereunder, and you agree that you shall not assert any such right, license or interest with respect thereto

- NEITHER WILEY NOR ITS LICENSORS MAKES ANY WARRANTY OR REPRESENTATION OF ANY KIND TO YOU OR ANY THIRD PARTY, EXPRESS, IMPLIED OR STATUTORY, WITH RESPECT TO THE MATERIALS OR THE ACCURACY OF ANY INFORMATION CONTAINED IN THE MATERIALS, INCLUDING, WITHOUT LIMITATION, ANY IMPLIED WARRANTY OF MERCHANTABILITY, ACCURACY, SATISFACTORY QUALITY, FITNESS FOR A PARTICULAR PURPOSE, USABILITY, INTEGRATION OR NON-INFRINGEMENT AND ALL SUCH WARRANTIES ARE HEREBY EXCLUDED BY WILEY AND ITS LICENSORS AND WAIVED BY YOU.

- WILEY shall have the right to terminate this Agreement immediately upon breach of this Agreement by you.

- You shall indemnify, defend and hold harmless WILEY, its Licensors and their respective directors, officers, agents and employees, from and against any actual or

threatened claims, demands, causes of action or proceedings arising from any breach of this Agreement by you.

- IN NO EVENT SHALL WILEY OR ITS LICENSORS BE LIABLE TO YOU OR ANY OTHER PARTY OR ANY OTHER PERSON OR ENTITY FOR ANY SPECIAL, CONSEQUENTIAL, INCIDENTAL, INDIRECT, EXEMPLARY OR PUNITIVE DAMAGES, HOWEVER CAUSED, ARISING OUT OF OR IN CONNECTION WITH THE DOWNLOADING, PROVISIONING, VIEWING OR USE OF THE MATERIALS REGARDLESS OF THE FORM OF ACTION, WHETHER FOR BREACH OF CONTRACT, BREACH OF WARRANTY, TORT, NEGLIGENCE, INFRINGEMENT OR OTHERWISE (INCLUDING, WITHOUT LIMITATION, DAMAGES BASED ON LOSS OF PROFITS, DATA, FILES, USE, BUSINESS OPPORTUNITY OR CLAIMS OF THIRD PARTIES), AND WHETHER OR NOT THE PARTY HAS BEEN ADVISED OF THE POSSIBILITY OF SUCH DAMAGES. THIS LIMITATION SHALL APPLY NOTWITHSTANDING ANY FAILURE OF ESSENTIAL PURPOSE OF ANY LIMITED REMEDY PROVIDED HEREIN.

- Should any provision of this Agreement be held by a court of competent jurisdiction to be illegal, invalid, or unenforceable, that provision shall be deemed amended to achieve as nearly as possible the same economic effect as the original provision, and the legality, validity and enforceability of the remaining provisions of this Agreement shall not be affected or impaired thereby.

- The failure of either party to enforce any term or condition of this Agreement shall not constitute a waiver of either party's right to enforce each and every term and condition of this Agreement. No breach under this agreement shall be deemed waived or excused by either party unless such waiver or consent is in writing signed by the party granting such waiver or consent. The waiver by or consent of a party to a breach of any provision of this Agreement shall not operate or be construed as a waiver of or consent to any other or subsequent breach by such other party.

- This Agreement may not be assigned (including by operation of law or otherwise) by you without WILEY's prior written consent.

- Any fee required for this permission shall be non-refundable after thirty (30) days from receipt by the CCC.

- These terms and conditions together with CCC's Billing and Payment terms and conditions (which are incorporated herein) form the entire agreement between you and WILEY concerning this licensing transaction and (in the absence of fraud) supersedes all prior agreements and representations of the parties, oral or written. This Agreement may not be amended except in writing signed by both parties. This

Agreement shall be binding upon and inure to the benefit of the parties' successors, legal representatives, and authorized assigns.

- In the event of any conflict between your obligations established by these terms and conditions and those established by CCC's Billing and Payment terms and conditions, these terms and conditions shall prevail.

- WILEY expressly reserves all rights not specifically granted in the combination of (i) the license details provided by you and accepted in the course of this licensing transaction, (ii) these terms and conditions and (iii) CCC's Billing and Payment terms and conditions.

- This Agreement will be void if the Type of Use, Format, Circulation, or Requestor Type was misrepresented during the licensing process.

- This Agreement shall be governed by and construed in accordance with the laws of the State of New York, USA, without regards to such state's conflict of law rules. Any legal action, suit or proceeding arising out of or relating to these Terms and Conditions or the breach thereof shall be instituted in a court of competent jurisdiction in New York County in the State of New York in the United States of America and each party hereby consents and submits to the personal jurisdiction of such court, waives any objection to venue in such court and consents to service of process by registered or certified mail, return receipt requested, at the last known address of such party.

WILEY OPEN ACCESS TERMS AND CONDITIONS

Wiley Publishes Open Access Articles in fully Open Access Journals and in Subscription journals offering Online Open. Although most of the fully Open Access journals publish open access articles under the terms of the Creative Commons Attribution (CC BY) License only, the subscription journals and a few of the Open Access Journals offer a choice of Creative Commons Licenses. The license type is clearly identified on the article.

The Creative Commons Attribution License

The Creative Commons Attribution License (CC-BY) allows users to copy, distribute and transmit an article, adapt the article and make commercial use of the article. The CC-BY license permits commercial and non-

Creative Commons Attribution Non-Commercial License

The Creative Commons Attribution Non-Commercial (CC-BY-NC)License permits use, distribution and reproduction in any medium, provided the original work is properly cited and is not used for commercial purposes.(see below)

Creative Commons Attribution-Non-Commercial-NoDerivs License

The Creative Commons Attribution Non-Commercial-NoDerivs License (CC-BY-NC-ND) permits use, distribution and reproduction in any medium, provided the original work is properly cited, is not used for commercial purposes and no modifications or adaptations are made. (see below)

Use by commercial "for-profit" organizations

Use of Wiley Open Access articles for commercial, promotional, or marketing purposes requires further explicit permission from Wiley and will be subject to a fee.

Further details can be found on Wiley Online Library
http://olabout.wiley.com/WileyCDA/Section/id-410895.html

Other Terms and Conditions:

v1.10 Last updated September 2015

Questions? customercare@copyright.com or +1-855-239-3415 (toll free in the US) or +1-978-646-2777.

ELSEVIER LICENSE
TERMS AND CONDITIONS

Jun 29, 2016

This Agreement between Binod Nepal ("You") and Elsevier ("Elsevier") consists of your license details and the terms and conditions provided by Elsevier and Copyright Clearance Center.

License Number	3898420648930
License date	Jun 29, 2016
Licensed Content Publisher	Elsevier
Licensed Content Publication	Chemical Physics
Licensed Content Title	Microsolvation of anions by molecules forming CH··X− hydrogen bonds
Licensed Content Author	Binod Nepal,Steve Scheiner
Licensed Content Date	16 December 2015
Licensed Content Volume Number	463
Licensed Content Issue Number	n/a
Licensed Content Pages	8
Start Page	137
End Page	144
Type of Use	reuse in a thesis/dissertation
Intended publisher of new work	other
Portion	full article
Format	both print and electronic
Are you the author of this Elsevier article?	Yes
Will you be translating?	No
Order reference number	
Title of your thesis/dissertation	QUANTUM MECHANICAL STUDIES OF CHARGE ASSISTED HYDROGEN AND HALOGEN BONDS
Expected completion date	Aug 2016
Estimated size (number of pages)	375

Elsevier VAT number	GB 494 6272 12
Requestor Location	Binod Nepal
	25 Aggie Village C
	LOGAN, UT 84341
	United States
	Attn: Binod Nepal
Total	0.00 USD

Terms and Conditions

INTRODUCTION

1. The publisher for this copyrighted material is Elsevier. By clicking "accept" in connection with completing this licensing transaction, you agree that the following terms and conditions apply to this transaction (along with the Billing and Payment terms and conditions established by Copyright Clearance Center, Inc. ("CCC"), at the time that you opened your Rightslink account and that are available at any time at http://myaccount.copyright.com).

GENERAL TERMS

2. Elsevier hereby grants you permission to reproduce the aforementioned material subject to the terms and conditions indicated.

3. Acknowledgement: If any part of the material to be used (for example, figures) has appeared in our publication with credit or acknowledgement to another source, permission must also be sought from that source. If such permission is not obtained then that material may not be included in your publication/copies. Suitable acknowledgement to the source must be made, either as a footnote or in a reference list at the end of your publication, as follows:

"Reprinted from Publication title, Vol /edition number, Author(s), Title of article / title of chapter, Pages No., Copyright (Year), with permission from Elsevier [OR APPLICABLE SOCIETY COPYRIGHT OWNER]." Also Lancet special credit - "Reprinted from The Lancet, Vol. number, Author(s), Title of article, Pages No., Copyright (Year), with permission from Elsevier."

4. Reproduction of this material is confined to the purpose and/or media for which permission is hereby given.

5. Altering/Modifying Material: Not Permitted. However figures and illustrations may be altered/adapted minimally to serve your work. Any other abbreviations, additions, deletions and/or any other alterations shall be made only with prior written authorization of Elsevier Ltd. (Please contact Elsevier at permissions@elsevier.com)

6. If the permission fee for the requested use of our material is waived in this instance, please be advised that your future requests for Elsevier materials may attract a fee.

7. Reservation of Rights: Publisher reserves all rights not specifically granted in the combination of (i) the license details provided by you and accepted in the course of this licensing transaction, (ii) these terms and conditions and (iii) CCC's Billing and Payment terms and conditions.

8. License Contingent Upon Payment: While you may exercise the rights licensed immediately upon issuance of the license at the end of the licensing process for the transaction, provided that you have disclosed complete and accurate details of your proposed use, no license is finally effective unless and until full payment is received from you (either by publisher or by CCC) as provided in CCC's Billing and Payment terms and conditions. If full payment is not received on a timely basis, then any license preliminarily granted shall be deemed automatically revoked and shall be void as if never granted. Further, in the event that you breach any of these terms and conditions or any of CCC's Billing and Payment terms and conditions, the license is automatically revoked and shall be void as if never granted. Use of materials as described in a revoked license, as well as any use of the materials beyond the scope of an unrevoked license, may constitute copyright infringement and publisher reserves the right to take any and all action to protect its copyright in the materials.

9. Warranties: Publisher makes no representations or warranties with respect to the licensed material.

10. Indemnity: You hereby indemnify and agree to hold harmless publisher and CCC, and their respective officers, directors, employees and agents, from and against any and all claims arising out of your use of the licensed material other than as specifically authorized pursuant to this license.

11. No Transfer of License: This license is personal to you and may not be sublicensed, assigned, or transferred by you to any other person without publisher's written permission.

12. No Amendment Except in Writing: This license may not be amended except in a writing signed by both parties (or, in the case of publisher, by CCC on publisher's behalf).

13. Objection to Contrary Terms: Publisher hereby objects to any terms contained in any purchase order, acknowledgment, check endorsement or other writing prepared by you, which terms are inconsistent with these terms and conditions or CCC's Billing and Payment terms and conditions. These terms and conditions, together with CCC's Billing and Payment terms and conditions (which are incorporated herein), comprise the entire agreement between you and publisher (and CCC) concerning this licensing transaction. In the event of any conflict between your obligations established by these terms and conditions and those established by CCC's Billing and Payment terms and conditions, these terms and conditions shall control.

14. Revocation: Elsevier or Copyright Clearance Center may deny the permissions described in this License at their sole discretion, for any reason or no reason, with a full refund payable to you. Notice of such denial will be made using the contact information provided by you. Failure to receive such notice will not alter or invalidate the denial. In no event will Elsevier or Copyright Clearance Center be responsible or liable for any costs, expenses or damage incurred by you as a result of a denial of your permission request, other than a refund of the amount(s) paid by you to Elsevier and/or Copyright Clearance Center for denied permissions.

LIMITED LICENSE

The following terms and conditions apply only to specific license types:

15. **Translation**: This permission is granted for non-exclusive world **English** rights only unless your license was granted for translation rights. If you licensed translation rights you

may only translate this content into the languages you requested. A professional translator must perform all translations and reproduce the content word for word preserving the integrity of the article.

16. **Posting licensed content on any Website**: The following terms and conditions apply as follows: Licensing material from an Elsevier journal: All content posted to the web site must maintain the copyright information line on the bottom of each image; A hyper-text must be included to the Homepage of the journal from which you are licensing at http://www.sciencedirect.com/science/journal/xxxxx or the Elsevier homepage for books at http://www.elsevier.com; Central Storage: This license does not include permission for a scanned version of the material to be stored in a central repository such as that provided by Heron/XanEdu.

Licensing material from an Elsevier book: A hyper-text link must be included to the Elsevier homepage at http://www.elsevier.com . All content posted to the web site must maintain the copyright information line on the bottom of each image.

Posting licensed content on Electronic reserve: In addition to the above the following clauses are applicable: The web site must be password-protected and made available only to bona fide students registered on a relevant course. This permission is granted for 1 year only. You may obtain a new license for future website posting.

17. **For journal authors:** the following clauses are applicable in addition to the above:
Preprints:
A preprint is an author's own write-up of research results and analysis, it has not been peer-reviewed, nor has it had any other value added to it by a publisher (such as formatting, copyright, technical enhancement etc.).

Authors can share their preprints anywhere at any time. Preprints should not be added to or enhanced in any way in order to appear more like, or to substitute for, the final versions of articles however authors can update their preprints on arXiv or RePEc with their Accepted Author Manuscript (see below).

If accepted for publication, we encourage authors to link from the preprint to their formal publication via its DOI. Millions of researchers have access to the formal publications on ScienceDirect, and so links will help users to find, access, cite and use the best available version. Please note that Cell Press, The Lancet and some society-owned have different preprint policies. Information on these policies is available on the journal homepage.

Accepted Author Manuscripts: An accepted author manuscript is the manuscript of an article that has been accepted for publication and which typically includes author-incorporated changes suggested during submission, peer review and editor-author communications.

Authors can share their accepted author manuscript:
- – immediately
  - o via their non-commercial person homepage or blog
  - o by updating a preprint in arXiv or RePEc with the accepted manuscript

- via their research institute or institutional repository for internal institutional uses or as part of an invitation-only research collaboration work-group
- directly by providing copies to their students or to research collaborators for their personal use
- for private scholarly sharing as part of an invitation-only work group on commercial sites with which Elsevier has an agreement

- − after the embargo period
  - via non-commercial hosting platforms such as their institutional repository
  - via commercial sites with which Elsevier has an agreement

In all cases accepted manuscripts should:
- − link to the formal publication via its DOI
- − bear a CC-BY-NC-ND license - this is easy to do
- − if aggregated with other manuscripts, for example in a repository or other site, be shared in alignment with our hosting policy not be added to or enhanced in any way to appear more like, or to substitute for, the published journal article.

Published journal article (JPA): A published journal article (PJA) is the definitive final record of published research that appears or will appear in the journal and embodies all value-adding publishing activities including peer review co-ordination, copy-editing, formatting, (if relevant) pagination and online enrichment.

Policies for sharing publishing journal articles differ for subscription and gold open access articles:

Subscription Articles: If you are an author, please share a link to your article rather than the full-text. Millions of researchers have access to the formal publications on ScienceDirect, and so links will help your users to find, access, cite, and use the best available version.

Theses and dissertations which contain embedded PJAs as part of the formal submission can be posted publicly by the awarding institution with DOI links back to the formal publications on ScienceDirect.

If you are affiliated with a library that subscribes to ScienceDirect you have additional private sharing rights for others' research accessed under that agreement. This includes use for classroom teaching and internal training at the institution (including use in course packs and courseware programs), and inclusion of the article for grant funding purposes.

Gold Open Access Articles: May be shared according to the author-selected end-user license and should contain a CrossMark logo, the end user license, and a DOI link to the formal publication on ScienceDirect.

Please refer to Elsevier's posting policy for further information.

18. **For book authors** the following clauses are applicable in addition to the above: Authors are permitted to place a brief summary of their work online only. You are not allowed to download and post the published electronic version of your chapter, nor may you scan the printed edition to create an electronic version. **Posting to a repository:**

Authors are permitted to post a summary of their chapter only in their institution's repository.

19. **Thesis/Dissertation**: If your license is for use in a thesis/dissertation your thesis may be submitted to your institution in either print or electronic form. Should your thesis be published commercially, please reapply for permission. These requirements include permission for the Library and Archives of Canada to supply single copies, on demand, of the complete thesis and include permission for Proquest/UMI to supply single copies, on demand, of the complete thesis. Should your thesis be published commercially, please reapply for permission. Theses and dissertations which contain embedded PJAs as part of the formal submission can be posted publicly by the awarding institution with DOI links back to the formal publications on ScienceDirect.

Elsevier Open Access Terms and Conditions

You can publish open access with Elsevier in hundreds of open access journals or in nearly 2000 established subscription journals that support open access publishing. Permitted third party re-use of these open access articles is defined by the author's choice of Creative Commons user license. See our open access license policy for more information.

Terms & Conditions applicable to all Open Access articles published with Elsevier:

Any reuse of the article must not represent the author as endorsing the adaptation of the article nor should the article be modified in such a way as to damage the author's honour or reputation. If any changes have been made, such changes must be clearly indicated.

The author(s) must be appropriately credited and we ask that you include the end user license and a DOI link to the formal publication on ScienceDirect.

If any part of the material to be used (for example, figures) has appeared in our publication with credit or acknowledgement to another source it is the responsibility of the user to ensure their reuse complies with the terms and conditions determined by the rights holder.

Additional Terms & Conditions applicable to each Creative Commons user license:

CC BY: The CC-BY license allows users to copy, to create extracts, abstracts and new works from the Article, to alter and revise the Article and to make commercial use of the Article (including reuse and/or resale of the Article by commercial entities), provided the user gives appropriate credit (with a link to the formal publication through the relevant DOI), provides a link to the license, indicates if changes were made and the licensor is not represented as endorsing the use made of the work. The full details of the license are available at http://creativecommons.org/licenses/by/4.0.

CC BY NC SA: The CC BY-NC-SA license allows users to copy, to create extracts, abstracts and new works from the Article, to alter and revise the Article, provided this is not done for commercial purposes, and that the user gives appropriate credit (with a link to the formal publication through the relevant DOI), provides a link to the license, indicates if changes were made and the licensor is not represented as endorsing the use made of the work. Further, any new works must be made available on the same conditions. The full details of the license are available at http://creativecommons.org/licenses/by-nc-sa/4.0.

CC BY NC ND: The CC BY-NC-ND license allows users to copy and distribute the Article, provided this is not done for commercial purposes and further does not permit distribution of the Article if it is changed or edited in any way, and provided the user gives

appropriate credit (with a link to the formal publication through the relevant DOI), provides a link to the license, and that the licensor is not represented as endorsing the use made of the work. The full details of the license are available at http://creativecommons.org/licenses/by-nc-nd/4.0. Any commercial reuse of Open Access articles published with a CC BY NC SA or CC BY NC ND license requires permission from Elsevier and will be subject to a fee.

Commercial reuse includes:

- − Associating advertising with the full text of the Article
- − Charging fees for document delivery or access
- − Article aggregation
- − Systematic distribution via e-mail lists or share buttons

Posting or linking by commercial companies for use by customers of those companies.

20. **Other Conditions**:

v1.8

Questions? customercare@copyright.com or +1-855-239-3415 (toll free in the US) or +1-978-646-2777.

Copyright Clearance Center

RightsLink®

Home   Account Info   Help

ACS Publications
Most Trusted. Most Cited. Most Read.

Title: Enhancing the Reduction Potential of Quinones via Complex Formation
Author: Binod Nepal, Steve Scheiner
Publication: The Journal of Organic Chemistry
Publisher: American Chemical Society
Date: May 1, 2016

Copyright © 2016, American Chemical Society

Quick Price Estimate

Permission for this particular request is granted for print and electronic formats, and translations, at no charge. Figures and tables may be modified. Appropriate credit should be given. Please print this page for your records and provide a copy to your publisher. Requests for up to 4 figures require only this record. Five or more figures will generate a printout of additional terms and conditions. Appropriate credit should read: "Reprinted with permission from {COMPLETE REFERENCE CITATION}. Copyright {YEAR} American Chemical Society." Insert appropriate information in place of the capitalized words.

I would like to... ⍰   reuse in a Thesis/Dissertation ⌄

Requestor Type ⍰   Author (original work) ⌄

Portion ⍰   Full article ⌄

Format ⍰   Print and Electronic ⌄

Will you be translating? ⍰   No ⌄

Select your currency   USD - $ ⌄

Quick Price   Click Quick Price

QUICK PRICE   CONTINUE

This service provides permission for reuse only. If you do not have a copy of the article you are using, you may copy and paste the content and reuse according to the terms of your agreement. Please be advised that obtaining the content you license is a separate transaction not involving Rightslink.

Copyright Clearance Center

RightsLink®

ACS Publications
Most Trusted. Most Cited. Most Read.

Title: Enhancing the Reduction Potential of Quinones via Complex Formation

**Author:** Binod Nepal, Steve Scheiner

Publication: The Journal of Organic Chemistry

Publisher: American Chemical Society

Date: May 1, 2016

Copyright © 2016, American Chemical Society

PERMISSION/LICENSE IS GRANTED FOR YOUR ORDER AT NO CHARGE

BACK   CLOSE WINDOW

ELSEVIER LICENSE
TERMS AND CONDITIONS

Jun 29, 2016

This Agreement between Binod Nepal ("You") and Elsevier ("Elsevier") consists of your license details and the terms and conditions provided by Elsevier and Copyright Clearance Center.

License Number	3898390809911
License date	Jun 29, 2016
Licensed Content Publisher	Elsevier
Licensed Content Publication	Chemical Physics Letters
Licensed Content Title	Angular dependence of hydrogen bond energy in neutral and charged systems containing CH and NH proton donors
Licensed Content Author	Binod Nepal,Steve Scheiner
Licensed Content Date	16 June 2015
Licensed Content Volume Number	630
Licensed Content Issue Number	n/a
Licensed Content Pages	6
Start Page	6
End Page	11
Type of Use	reuse in a thesis/dissertation
Portion	full article
Format	both print and electronic
Are you the author of this Elsevier article?	Yes
Will you be translating?	No
Order reference number	
Title of your thesis/dissertation	QUANTUM MECHANICAL STUDIES OF CHARGE ASSISTED HYDROGEN AND HALOGEN BONDS

Expected completion date	Aug 2016
Estimated size (number of pages)	375
Elsevier VAT number	GB 494 6272 12
Requestor Location	Binod Nepal 25 Aggie Village C LOGAN, UT 84341 United States Attn: Binod Nepal
Total	0.00 USD

Terms and Conditions

INTRODUCTION

1. The publisher for this copyrighted material is Elsevier. By clicking "accept" in connection with completing this licensing transaction, you agree that the following terms and conditions apply to this transaction (along with the Billing and Payment terms and conditions established by Copyright Clearance Center, Inc. ("CCC"), at the time that you opened your Rightslink account and that are available at any time at http://myaccount.copyright.com).

GENERAL TERMS

2. Elsevier hereby grants you permission to reproduce the aforementioned material subject to the terms and conditions indicated.

3. Acknowledgement: If any part of the material to be used (for example, figures) has appeared in our publication with credit or acknowledgement to another source, permission must also be sought from that source. If such permission is not obtained then that material may not be included in your publication/copies. Suitable acknowledgement to the source must be made, either as a footnote or in a reference list at the end of your publication, as follows:

"Reprinted from Publication title, Vol /edition number, Author(s), Title of article / title of chapter, Pages No., Copyright (Year), with permission from Elsevier [OR APPLICABLE SOCIETY COPYRIGHT OWNER]." Also Lancet special credit - "Reprinted from The Lancet, Vol. number, Author(s), Title of article, Pages No., Copyright (Year), with permission from Elsevier."

4. Reproduction of this material is confined to the purpose and/or media for which permission is hereby given.

5. Altering/Modifying Material: Not Permitted. However figures and illustrations may be altered/adapted minimally to serve your work. Any other abbreviations, additions, deletions and/or any other alterations shall be made only with prior written authorization of Elsevier Ltd. (Please contact Elsevier at permissions@elsevier.com)

6. If the permission fee for the requested use of our material is waived in this instance, please be advised that your future requests for Elsevier materials may attract a fee.

7. Reservation of Rights: Publisher reserves all rights not specifically granted in the combination of (i) the license details provided by you and accepted in the course of this licensing transaction, (ii) these terms and conditions and (iii) CCC's Billing and Payment terms and conditions.

8. License Contingent Upon Payment: While you may exercise the rights licensed immediately upon issuance of the license at the end of the licensing process for the transaction, provided that you have disclosed complete and accurate details of your proposed use, no license is finally effective unless and until full payment is received from you (either by publisher or by CCC) as provided in CCC's Billing and Payment terms and conditions. If full payment is not received on a timely basis, then any license preliminarily granted shall be deemed automatically revoked and shall be void as if never granted. Further, in the event that you breach any of these terms and conditions or any of CCC's Billing and Payment terms and conditions, the license is automatically revoked and shall be void as if never granted. Use of materials as described in a revoked license, as well as any use of the materials beyond the scope of an unrevoked license, may constitute copyright infringement and publisher reserves the right to take any and all action to protect its copyright in the materials.

9. Warranties: Publisher makes no representations or warranties with respect to the licensed material.

10. Indemnity: You hereby indemnify and agree to hold harmless publisher and CCC, and their respective officers, directors, employees and agents, from and against any and all claims arising out of your use of the licensed material other than as specifically authorized pursuant to this license.

11. No Transfer of License: This license is personal to you and may not be sublicensed, assigned, or transferred by you to any other person without publisher's written permission.

12. No Amendment Except in Writing: This license may not be amended except in a writing signed by both parties (or, in the case of publisher, by CCC on publisher's behalf).

13. Objection to Contrary Terms: Publisher hereby objects to any terms contained in any purchase order, acknowledgment, check endorsement or other writing prepared by you, which terms are inconsistent with these terms and conditions or CCC's Billing and Payment terms and conditions. These terms and conditions, together with CCC's Billing and Payment terms and conditions (which are incorporated herein), comprise the entire agreement between you and publisher (and CCC) concerning this licensing transaction. In the event of any conflict between your obligations established by these terms and conditions and those established by CCC's Billing and Payment terms and conditions, these terms and conditions shall control.

14. Revocation: Elsevier or Copyright Clearance Center may deny the permissions described in this License at their sole discretion, for any reason or no reason, with a full refund payable to you. Notice of such denial will be made using the contact information provided by you. Failure to receive such notice will not alter or invalidate the denial. In no event will Elsevier or Copyright Clearance Center be responsible or liable for any costs, expenses or damage incurred by you as a result of a denial of your permission request, other than a refund of the amount(s) paid by you to Elsevier and/or Copyright Clearance Center for denied permissions.

LIMITED LICENSE

The following terms and conditions apply only to specific license types:

15. **Translation**: This permission is granted for non-exclusive world **English** rights only unless your license was granted for translation rights. If you licensed translation rights you may only translate this content into the languages you requested. A professional translator must perform all translations and reproduce the content word for word preserving the integrity of the article.

16. **Posting licensed content on any Website**: The following terms and conditions apply as follows: Licensing material from an Elsevier journal: All content posted to the web site must maintain the copyright information line on the bottom of each image; A hyper-text must be included to the Homepage of the journal from which you are licensing at http://www.sciencedirect.com/science/journal/xxxxx or the Elsevier homepage for books at http://www.elsevier.com; Central Storage: This license does not include permission for a scanned version of the material to be stored in a central repository such as that provided by Heron/XanEdu.

Licensing material from an Elsevier book: A hyper-text link must be included to the Elsevier homepage at http://www.elsevier.com . All content posted to the web site must maintain the copyright information line on the bottom of each image.

Posting licensed content on Electronic reserve: In addition to the above the following

clauses are applicable: The web site must be password-protected and made available only to bona fide students registered on a relevant course. This permission is granted for 1 year only. You may obtain a new license for future website posting.

17. **For journal authors:** the following clauses are applicable in addition to the above:

Preprints:

A preprint is an author's own write-up of research results and analysis, it has not been peer-reviewed, nor has it had any other value added to it by a publisher (such as formatting, copyright, technical enhancement etc.).

Authors can share their preprints anywhere at any time. Preprints should not be added to or enhanced in any way in order to appear more like, or to substitute for, the final versions of articles however authors can update their preprints on arXiv or RePEc with their Accepted Author Manuscript (see below).

If accepted for publication, we encourage authors to link from the preprint to their formal publication via its DOI. Millions of researchers have access to the formal publications on ScienceDirect, and so links will help users to find, access, cite and use the best available version. Please note that Cell Press, The Lancet and some society-owned have different preprint policies. Information on these policies is available on the journal homepage.

Accepted Author Manuscripts: An accepted author manuscript is the manuscript of an article that has been accepted for publication and which typically includes author-incorporated changes suggested during submission, peer review and editor-author communications.

Authors can share their accepted author manuscript:

- – immediately
  - via their non-commercial person homepage or blog
  - by updating a preprint in arXiv or RePEc with the accepted manuscript
  - via their research institute or institutional repository for internal institutional uses or as part of an invitation-only research collaboration work-group
  - directly by providing copies to their students or to research collaborators for their personal use
  - for private scholarly sharing as part of an invitation-only work group on commercial sites with which Elsevier has an agreement
- – after the embargo period
  - via non-commercial hosting platforms such as their institutional repository

> o via commercial sites with which Elsevier has an agreement

In all cases accepted manuscripts should:

- – link to the formal publication via its DOI
- – bear a CC-BY-NC-ND license - this is easy to do
- – if aggregated with other manuscripts, for example in a repository or other site, be shared in alignment with our hosting policy not be added to or enhanced in any way to appear more like, or to substitute for, the published journal article.

Published journal article (JPA): A published journal article (PJA) is the definitive final record of published research that appears or will appear in the journal and embodies all value-adding publishing activities including peer review co-ordination, copy-editing, formatting, (if relevant) pagination and online enrichment.

Policies for sharing publishing journal articles differ for subscription and gold open access articles:

Subscription Articles: If you are an author, please share a link to your article rather than the full-text. Millions of researchers have access to the formal publications on ScienceDirect, and so links will help your users to find, access, cite, and use the best available version.

Theses and dissertations which contain embedded PJAs as part of the formal submission can be posted publicly by the awarding institution with DOI links back to the formal publications on ScienceDirect.

If you are affiliated with a library that subscribes to ScienceDirect you have additional private sharing rights for others' research accessed under that agreement. This includes use for classroom teaching and internal training at the institution (including use in course packs and courseware programs), and inclusion of the article for grant funding purposes.

Gold Open Access Articles: May be shared according to the author-selected end-user license and should contain a CrossMark logo, the end user license, and a DOI link to the formal publication on ScienceDirect.

Please refer to Elsevier's posting policy for further information.

18. **For book authors** the following clauses are applicable in addition to the above: Authors are permitted to place a brief summary of their work online only. You are not allowed to download and post the published electronic version of your chapter, nor may you scan the printed edition to create an electronic version. **Posting to a repository:** Authors are permitted to post a summary of their chapter only in their institution's repository.

19. **Thesis/Dissertation**: If your license is for use in a thesis/dissertation your thesis may be submitted to your institution in either print or electronic form. Should your thesis be published commercially, please reapply for permission. These requirements include permission for the Library and Archives of Canada to supply single copies, on demand, of the complete thesis and include permission for Proquest/UMI to supply single copies, on demand, of the complete thesis. Should your thesis be published commercially, please reapply for permission. Theses and dissertations which contain embedded PJAs as part of the formal submission can be posted publicly by the awarding institution with DOI links back to the formal publications on ScienceDirect.

Elsevier Open Access Terms and Conditions

You can publish open access with Elsevier in hundreds of open access journals or in nearly 2000 established subscription journals that support open access publishing. Permitted third party re-use of these open access articles is defined by the author's choice of Creative Commons user license. See our open access license policy for more information.

Terms & Conditions applicable to all Open Access articles published with Elsevier:

Any reuse of the article must not represent the author as endorsing the adaptation of the article nor should the article be modified in such a way as to damage the author's honour or reputation. If any changes have been made, such changes must be clearly indicated.

The author(s) must be appropriately credited and we ask that you include the end user license and a DOI link to the formal publication on ScienceDirect.

If any part of the material to be used (for example, figures) has appeared in our publication with credit or acknowledgement to another source it is the responsibility of the user to ensure their reuse complies with the terms and conditions determined by the rights holder.

Additional Terms & Conditions applicable to each Creative Commons user license:

CC BY: The CC-BY license allows users to copy, to create extracts, abstracts and new works from the Article, to alter and revise the Article and to make commercial use of the Article (including reuse and/or resale of the Article by commercial entities), provided the user gives appropriate credit (with a link to the formal publication through the relevant DOI), provides a link to the license, indicates if changes were made and the licensor is not represented as endorsing the use made of the work. The full details of the license are available at http://creativecommons.org/licenses/by/4.0.

CC BY NC SA: The CC BY-NC-SA license allows users to copy, to create extracts, abstracts and new works from the Article, to alter and revise the Article, provided this is not

done for commercial purposes, and that the user gives appropriate credit (with a link to the formal publication through the relevant DOI), provides a link to the license, indicates if changes were made and the licensor is not represented as endorsing the use made of the work. Further, any new works must be made available on the same conditions. The full details of the license are available at http://creativecommons.org/licenses/by-nc-sa/4.0.

CC BY NC ND: The CC BY-NC-ND license allows users to copy and distribute the Article, provided this is not done for commercial purposes and further does not permit distribution of the Article if it is changed or edited in any way, and provided the user gives appropriate credit (with a link to the formal publication through the relevant DOI), provides a link to the license, and that the licensor is not represented as endorsing the use made of the work. The full details of the license are available at http://creativecommons.org/licenses/by-nc-nd/4.0. Any commercial reuse of Open Access articles published with a CC BY NC SA or CC BY NC ND license requires permission from Elsevier and will be subject to a fee.

Commercial reuse includes:

- – Associating advertising with the full text of the Article
- – Charging fees for document delivery or access
- – Article aggregation
- – Systematic distribution via e-mail lists or share buttons

Posting or linking by commercial companies for use by customers of those companies.

20. **Other Conditions**:

v1.8

Questions? customercare@copyright.com or +1-855-239-3415 (toll free in the US) or +1-978-646-2777.

ELSEVIER LICENSE
TERMS AND CONDITIONS
Jun 29, 2016

This Agreement between Binod Nepal ("You") and Elsevier ("Elsevier") consists of your license details and the terms and conditions provided by Elsevier and Copyright Clearance Center.

License Number	3898421264675
License date	Jun 29, 2016
Licensed Content Publisher	Elsevier
Licensed Content Publication	Chemical Physics
Licensed Content Title	Long-range behavior of noncovalent bonds. Neutral and charged H-bonds, pnicogen, chalcogen, and halogen bonds
Licensed Content Author	Binod Nepal,Steve Scheiner
Licensed Content Date	29 July 2015
Licensed Content Volume Number	456
Licensed Content Issue Number	n/a
Licensed Content Pages	7
Start Page	34
End Page	40
Type of Use	reuse in a thesis/dissertation
Intended publisher of new work	other
Portion	full article
Format	both print and electronic
Are you the author of this Elsevier article?	Yes
Will you be translating?	No
Order reference number	
Title of your thesis/dissertation	QUANTUM MECHANICAL STUDIES OF CHARGE ASSISTED HYDROGEN AND HALOGEN BONDS
Expected completion date	Aug 2016

Estimated size (number of pages)	375
Elsevier VAT number	GB 494 6272 12

Binod Nepal
25 Aggie Village C

Requestor Location

LOGAN, UT 84341
United States
Attn: Binod Nepal

Total	0.00 USD

Terms and Conditions

INTRODUCTION

1. The publisher for this copyrighted material is Elsevier. By clicking "accept" in connection with completing this licensing transaction, you agree that the following terms and conditions apply to this transaction (along with the Billing and Payment terms and conditions established by Copyright Clearance Center, Inc. ("CCC"), at the time that you opened your Rightslink account and that are available at any time at http://myaccount.copyright.com).

GENERAL TERMS

2. Elsevier hereby grants you permission to reproduce the aforementioned material subject to the terms and conditions indicated.

3. Acknowledgement: If any part of the material to be used (for example, figures) has appeared in our publication with credit or acknowledgement to another source, permission must also be sought from that source. If such permission is not obtained then that material may not be included in your publication/copies. Suitable acknowledgement to the source must be made, either as a footnote or in a reference list at the end of your publication, as follows:

"Reprinted from Publication title, Vol /edition number, Author(s), Title of article / title of chapter, Pages No., Copyright (Year), with permission from Elsevier [OR APPLICABLE SOCIETY COPYRIGHT OWNER]." Also Lancet special credit - "Reprinted from The Lancet, Vol. number, Author(s), Title of article, Pages No., Copyright (Year), with permission from Elsevier."

4. Reproduction of this material is confined to the purpose and/or media for which permission is hereby given.

5. Altering/Modifying Material: Not Permitted. However figures and illustrations may be altered/adapted minimally to serve your work. Any other abbreviations, additions, deletions

and/or any other alterations shall be made only with prior written authorization of Elsevier Ltd. (Please contact Elsevier at permissions@elsevier.com)

6. If the permission fee for the requested use of our material is waived in this instance, please be advised that your future requests for Elsevier materials may attract a fee.

7. Reservation of Rights: Publisher reserves all rights not specifically granted in the combination of (i) the license details provided by you and accepted in the course of this licensing transaction, (ii) these terms and conditions and (iii) CCC's Billing and Payment terms and conditions.

8. License Contingent Upon Payment: While you may exercise the rights licensed immediately upon issuance of the license at the end of the licensing process for the transaction, provided that you have disclosed complete and accurate details of your proposed use, no license is finally effective unless and until full payment is received from you (either by publisher or by CCC) as provided in CCC's Billing and Payment terms and conditions. If full payment is not received on a timely basis, then any license preliminarily granted shall be deemed automatically revoked and shall be void as if never granted. Further, in the event that you breach any of these terms and conditions or any of CCC's Billing and Payment terms and conditions, the license is automatically revoked and shall be void as if never granted. Use of materials as described in a revoked license, as well as any use of the materials beyond the scope of an unrevoked license, may constitute copyright infringement and publisher reserves the right to take any and all action to protect its copyright in the materials.

9. Warranties: Publisher makes no representations or warranties with respect to the licensed material.

10. Indemnity: You hereby indemnify and agree to hold harmless publisher and CCC, and their respective officers, directors, employees and agents, from and against any and all claims arising out of your use of the licensed material other than as specifically authorized pursuant to this license.

11. No Transfer of License: This license is personal to you and may not be sublicensed, assigned, or transferred by you to any other person without publisher's written permission.

12. No Amendment Except in Writing: This license may not be amended except in a writing signed by both parties (or, in the case of publisher, by CCC on publisher's behalf).

13. Objection to Contrary Terms: Publisher hereby objects to any terms contained in any purchase order, acknowledgment, check endorsement or other writing prepared by you, which terms are inconsistent with these terms and conditions or CCC's Billing and Payment terms and conditions. These terms and conditions, together with CCC's Billing and Payment terms and conditions (which are incorporated herein), comprise the entire

agreement between you and publisher (and CCC) concerning this licensing transaction. In the event of any conflict between your obligations established by these terms and conditions and those established by CCC's Billing and Payment terms and conditions, these terms and conditions shall control.

14. Revocation: Elsevier or Copyright Clearance Center may deny the permissions described in this License at their sole discretion, for any reason or no reason, with a full refund payable to you. Notice of such denial will be made using the contact information provided by you. Failure to receive such notice will not alter or invalidate the denial. In no event will Elsevier or Copyright Clearance Center be responsible or liable for any costs, expenses or damage incurred by you as a result of a denial of your permission request, other than a refund of the amount(s) paid by you to Elsevier and/or Copyright Clearance Center for denied permissions.

LIMITED LICENSE

The following terms and conditions apply only to specific license types:

15. **Translation**: This permission is granted for non-exclusive world **English** rights only unless your license was granted for translation rights. If you licensed translation rights you may only translate this content into the languages you requested. A professional translator must perform all translations and reproduce the content word for word preserving the integrity of the article.

16. **Posting licensed content on any Website**: The following terms and conditions apply as follows: Licensing material from an Elsevier journal: All content posted to the web site must maintain the copyright information line on the bottom of each image; A hyper-text must be included to the Homepage of the journal from which you are licensing at http://www.sciencedirect.com/science/journal/xxxxx or the Elsevier homepage for books at http://www.elsevier.com; Central Storage: This license does not include permission for a scanned version of the material to be stored in a central repository such as that provided by Heron/XanEdu.

Licensing material from an Elsevier book: A hyper-text link must be included to the Elsevier homepage at http://www.elsevier.com . All content posted to the web site must maintain the copyright information line on the bottom of each image.

Posting licensed content on Electronic reserve: In addition to the above the following clauses are applicable: The web site must be password-protected and made available only to bona fide students registered on a relevant course. This permission is granted for 1 year only. You may obtain a new license for future website posting.

17. **For journal authors:** the following clauses are applicable in addition to the above:

Preprints:

A preprint is an author's own write-up of research results and analysis, it has not been peer-reviewed, nor has it had any other value added to it by a publisher (such as formatting, copyright, technical enhancement etc.).

Authors can share their preprints anywhere at any time. Preprints should not be added to or enhanced in any way in order to appear more like, or to substitute for, the final versions of articles however authors can update their preprints on arXiv or RePEc with their Accepted Author Manuscript (see below).

If accepted for publication, we encourage authors to link from the preprint to their formal publication via its DOI. Millions of researchers have access to the formal publications on ScienceDirect, and so links will help users to find, access, cite and use the best available version. Please note that Cell Press, The Lancet and some society-owned have different preprint policies. Information on these policies is available on the journal homepage.

Accepted Author Manuscripts: An accepted author manuscript is the manuscript of an article that has been accepted for publication and which typically includes author-incorporated changes suggested during submission, peer review and editor-author communications.

Authors can share their accepted author manuscript:

- – immediately
    - o via their non-commercial person homepage or blog
    - o by updating a preprint in arXiv or RePEc with the accepted manuscript
    - o via their research institute or institutional repository for internal institutional uses or as part of an invitation-only research collaboration work-group
    - o directly by providing copies to their students or to research collaborators for their personal use
    - o for private scholarly sharing as part of an invitation-only work group on commercial sites with which Elsevier has an agreement
- – after the embargo period
    - o via non-commercial hosting platforms such as their institutional repository
    - o via commercial sites with which Elsevier has an agreement

In all cases accepted manuscripts should:

- – link to the formal publication via its DOI
- – bear a CC-BY-NC-ND license - this is easy to do
- – if aggregated with other manuscripts, for example in a repository or other site, be shared in alignment with our hosting policy not be added to or enhanced in any way to appear more like, or to substitute for, the published journal article.

Published journal article (JPA): A published journal article (PJA) is the definitive final record of published research that appears or will appear in the journal and embodies all value-adding publishing activities including peer review co-ordination, copy-editing, formatting, (if relevant) pagination and online enrichment.

Policies for sharing publishing journal articles differ for subscription and gold open access articles:

Subscription Articles: If you are an author, please share a link to your article rather than the full-text. Millions of researchers have access to the formal publications on ScienceDirect, and so links will help your users to find, access, cite, and use the best available version.

Theses and dissertations which contain embedded PJAs as part of the formal submission can be posted publicly by the awarding institution with DOI links back to the formal publications on ScienceDirect.

If you are affiliated with a library that subscribes to ScienceDirect you have additional private sharing rights for others' research accessed under that agreement. This includes use for classroom teaching and internal training at the institution (including use in course packs and courseware programs), and inclusion of the article for grant funding purposes.

Gold Open Access Articles: May be shared according to the author-selected end-user license and should contain a CrossMark logo, the end user license, and a DOI link to the formal publication on ScienceDirect.

Please refer to Elsevier's posting policy for further information.

18. **For book authors** the following clauses are applicable in addition to the above: Authors are permitted to place a brief summary of their work online only. You are not allowed to download and post the published electronic version of your chapter, nor may you scan the printed edition to create an electronic version. **Posting to a repository:** Authors are permitted to post a summary of their chapter only in their institution's repository.

19. **Thesis/Dissertation**: If your license is for use in a thesis/dissertation your thesis may be submitted to your institution in either print or electronic form. Should your thesis be published commercially, please reapply for permission. These requirements include

permission for the Library and Archives of Canada to supply single copies, on demand, of the complete thesis and include permission for Proquest/UMI to supply single copies, on demand, of the complete thesis. Should your thesis be published commercially, please reapply for permission. Theses and dissertations which contain embedded PJAs as part of the formal submission can be posted publicly by the awarding institution with DOI links back to the formal publications on ScienceDirect.

Elsevier Open Access Terms and Conditions

You can publish open access with Elsevier in hundreds of open access journals or in nearly 2000 established subscription journals that support open access publishing. Permitted third party re-use of these open access articles is defined by the author's choice of Creative Commons user license. See our open access license policy for more information.

Terms & Conditions applicable to all Open Access articles published with Elsevier:

Any reuse of the article must not represent the author as endorsing the adaptation of the article nor should the article be modified in such a way as to damage the author's honour or reputation. If any changes have been made, such changes must be clearly indicated.

The author(s) must be appropriately credited and we ask that you include the end user license and a DOI link to the formal publication on ScienceDirect.

If any part of the material to be used (for example, figures) has appeared in our publication with credit or acknowledgement to another source it is the responsibility of the user to ensure their reuse complies with the terms and conditions determined by the rights holder.

Additional Terms & Conditions applicable to each Creative Commons user license:

CC BY: The CC-BY license allows users to copy, to create extracts, abstracts and new works from the Article, to alter and revise the Article and to make commercial use of the Article (including reuse and/or resale of the Article by commercial entities), provided the user gives appropriate credit (with a link to the formal publication through the relevant DOI), provides a link to the license, indicates if changes were made and the licensor is not represented as endorsing the use made of the work. The full details of the license are available at http://creativecommons.org/licenses/by/4.0.

CC BY NC SA: The CC BY-NC-SA license allows users to copy, to create extracts, abstracts and new works from the Article, to alter and revise the Article, provided this is not done for commercial purposes, and that the user gives appropriate credit (with a link to the formal publication through the relevant DOI), provides a link to the license, indicates if changes were made and the licensor is not represented as endorsing the use made of the

work. Further, any new works must be made available on the same conditions. The full details of the license are available at http://creativecommons.org/licenses/by-nc-sa/4.0.

CC BY NC ND: The CC BY-NC-ND license allows users to copy and distribute the Article, provided this is not done for commercial purposes and further does not permit distribution of the Article if it is changed or edited in any way, and provided the user gives appropriate credit (with a link to the formal publication through the relevant DOI), provides a link to the license, and that the licensor is not represented as endorsing the use made of the work. The full details of the license are available at http://creativecommons.org/licenses/by-nc-nd/4.0. Any commercial reuse of Open Access articles published with a CC BY NC SA or CC BY NC ND license requires permission from Elsevier and will be subject to a fee.

Commercial reuse includes:

- − Associating advertising with the full text of the Article
- − Charging fees for document delivery or access
- − Article aggregation
- − Systematic distribution via e-mail lists or share buttons

Posting or linking by commercial companies for use by customers of those companies.

20. **Other Conditions**:

v1.8

Questions? customercare@copyright.com or +1-855-239-3415 (toll free in the US) or +1-978-646-2777.

JOHN WILEY AND SONS LICENSE
TERMS AND CONDITIONS
Jun 29, 2016

This Agreement between Binod Nepal ("You") and John Wiley and Sons ("John Wiley and Sons") consists of your license details and the terms and conditions provided by John Wiley and Sons and Copyright Clearance Center.

License Number	3898430780320
License date	Jun 29, 2016
Licensed Content Publisher	John Wiley and Sons
Licensed Content Publication	Chemistry - A European Journal
Licensed Content Title	Competitive Halide Binding by Halogen Versus Hydrogen Bonding: Bis-triazole Pyridinium
Licensed Content Author	Binod Nepal,Steve Scheiner
Licensed Content Date	Jul 31, 2015
Licensed Content Pages	6
Type of use	Dissertation/Thesis
Requestor type	Author of this Wiley article
Format	Print and electronic
Portion	Full article
Will you be translating?	No
Title of your thesis / dissertation	QUANTUM MECHANICAL STUDIES OF CHARGE ASSISTED HYDROGEN AND HALOGEN BONDS
Expected completion date	Aug 2016
Expected size (number of pages)	375
Requestor Location	Binod Nepal 25 Aggie Village C LOGAN, UT 84341 United States Attn: Binod Nepal
Publisher Tax ID	EU826007151
Billing Type	Invoice

Binod Nepal
25 Aggie Village C

Billing Address

LOGAN, UT 84341
United States
Attn: Binod Nepal

Total   0.00 USD

Terms and Conditions

TERMS AND CONDITIONS

This copyrighted material is owned by or exclusively licensed to John Wiley & Sons, Inc. or one of its group companies (each a"Wiley Company") or handled on behalf of a society with which a Wiley Company has exclusive publishing rights in relation to a particular work (collectively "WILEY"). By clicking "accept" in connection with completing this licensing transaction, you agree that the following terms and conditions apply to this transaction (along with the billing and payment terms and conditions established by the Copyright Clearance Center Inc., ("CCC's Billing and Payment terms and conditions"), at the time that you opened your RightsLink account (these are available at any time at http://myaccount.copyright.com).

Terms and Conditions

- The materials you have requested permission to reproduce or reuse (the "Wiley Materials") are protected by copyright.

- You are hereby granted a personal, non-exclusive, non-sub licensable (on a stand-alone basis), non-transferable, worldwide, limited license to reproduce the Wiley Materials for the purpose specified in the licensing process. This license, **and any CONTENT (PDF or image file) purchased as part of your order,** is for a one-time use only and limited to any maximum distribution number specified in the license. The first instance of republication or reuse granted by this license must be completed within two years of the date of the grant of this license (although copies prepared before the end date may be distributed thereafter). The Wiley Materials shall not be used in any other manner or for any other purpose, beyond what is granted in the license. Permission is granted subject to an appropriate acknowledgement given to the author, title of the material/book/journal and the publisher. You shall also duplicate the copyright notice that appears in the Wiley publication in your use of the Wiley Material. Permission is also granted on the understanding that nowhere in the text is a previously published source acknowledged for all or part of this Wiley Material. Any third party content is expressly excluded from this permission.

- With respect to the Wiley Materials, all rights are reserved. Except as expressly granted by the terms of the license, no part of the Wiley Materials may be copied, modified, adapted (except for minor reformatting required by the new Publication), translated, reproduced, transferred or distributed, in any form or by any means, and no derivative works may be made based on the Wiley Materials without the prior permission of the respective copyright owner.**For STM Signatory Publishers clearing permission under the terms of the [STM Permissions Guidelines](#) only, the terms of the license are extended to include subsequent editions and for editions in other languages, provided such editions are for the work as a whole in situ and does not involve the separate exploitation of the permitted figures or extracts,** You may not alter, remove or suppress in any manner any copyright, trademark or other notices displayed by the Wiley Materials. You may not license, rent, sell, loan, lease, pledge, offer as security, transfer or assign the Wiley Materials on a stand-alone basis, or any of the rights granted to you hereunder to any other person.

- The Wiley Materials and all of the intellectual property rights therein shall at all times remain the exclusive property of John Wiley & Sons Inc, the Wiley Companies, or their respective licensors, and your interest therein is only that of having possession of and the right to reproduce the Wiley Materials pursuant to Section 2 herein during the continuance of this Agreement. You agree that you own no right, title or interest in or to the Wiley Materials or any of the intellectual property rights therein. You shall have no rights hereunder other than the license as provided for above in Section 2. No right, license or interest to any trademark, trade name, service mark or other branding ("Marks") of WILEY or its licensors is granted hereunder, and you agree that you shall not assert any such right, license or interest with respect thereto

- NEITHER WILEY NOR ITS LICENSORS MAKES ANY WARRANTY OR REPRESENTATION OF ANY KIND TO YOU OR ANY THIRD PARTY, EXPRESS, IMPLIED OR STATUTORY, WITH RESPECT TO THE MATERIALS OR THE ACCURACY OF ANY INFORMATION CONTAINED IN THE MATERIALS, INCLUDING, WITHOUT LIMITATION, ANY IMPLIED WARRANTY OF MERCHANTABILITY, ACCURACY, SATISFACTORY QUALITY, FITNESS FOR A PARTICULAR PURPOSE, USABILITY, INTEGRATION OR NON-INFRINGEMENT AND ALL SUCH WARRANTIES ARE HEREBY EXCLUDED BY WILEY AND ITS LICENSORS AND WAIVED BY YOU.

- WILEY shall have the right to terminate this Agreement immediately upon breach of this Agreement by you.

- You shall indemnify, defend and hold harmless WILEY, its Licensors and their respective directors, officers, agents and employees, from and against any actual or

threatened claims, demands, causes of action or proceedings arising from any breach of this Agreement by you.

- IN NO EVENT SHALL WILEY OR ITS LICENSORS BE LIABLE TO YOU OR ANY OTHER PARTY OR ANY OTHER PERSON OR ENTITY FOR ANY SPECIAL, CONSEQUENTIAL, INCIDENTAL, INDIRECT, EXEMPLARY OR PUNITIVE DAMAGES, HOWEVER CAUSED, ARISING OUT OF OR IN CONNECTION WITH THE DOWNLOADING, PROVISIONING, VIEWING OR USE OF THE MATERIALS REGARDLESS OF THE FORM OF ACTION, WHETHER FOR BREACH OF CONTRACT, BREACH OF WARRANTY, TORT, NEGLIGENCE, INFRINGEMENT OR OTHERWISE (INCLUDING, WITHOUT LIMITATION, DAMAGES BASED ON LOSS OF PROFITS, DATA, FILES, USE, BUSINESS OPPORTUNITY OR CLAIMS OF THIRD PARTIES), AND WHETHER OR NOT THE PARTY HAS BEEN ADVISED OF THE POSSIBILITY OF SUCH DAMAGES. THIS LIMITATION SHALL APPLY NOTWITHSTANDING ANY FAILURE OF ESSENTIAL PURPOSE OF ANY LIMITED REMEDY PROVIDED HEREIN.

- Should any provision of this Agreement be held by a court of competent jurisdiction to be illegal, invalid, or unenforceable, that provision shall be deemed amended to achieve as nearly as possible the same economic effect as the original provision, and the legality, validity and enforceability of the remaining provisions of this Agreement shall not be affected or impaired thereby.

- The failure of either party to enforce any term or condition of this Agreement shall not constitute a waiver of either party's right to enforce each and every term and condition of this Agreement. No breach under this agreement shall be deemed waived or excused by either party unless such waiver or consent is in writing signed by the party granting such waiver or consent. The waiver by or consent of a party to a breach of any provision of this Agreement shall not operate or be construed as a waiver of or consent to any other or subsequent breach by such other party.

- This Agreement may not be assigned (including by operation of law or otherwise) by you without WILEY's prior written consent.

- Any fee required for this permission shall be non-refundable after thirty (30) days from receipt by the CCC.

- These terms and conditions together with CCC's Billing and Payment terms and conditions (which are incorporated herein) form the entire agreement between you and WILEY concerning this licensing transaction and (in the absence of fraud) supersedes all prior agreements and representations of the parties, oral or written. This Agreement may not be amended except in writing signed by both parties. This

Agreement shall be binding upon and inure to the benefit of the parties' successors, legal representatives, and authorized assigns.

- In the event of any conflict between your obligations established by these terms and conditions and those established by CCC's Billing and Payment terms and conditions, these terms and conditions shall prevail.

- WILEY expressly reserves all rights not specifically granted in the combination of (i) the license details provided by you and accepted in the course of this licensing transaction, (ii) these terms and conditions and (iii) CCC's Billing and Payment terms and conditions.

- This Agreement will be void if the Type of Use, Format, Circulation, or Requestor Type was misrepresented during the licensing process.

- This Agreement shall be governed by and construed in accordance with the laws of the State of New York, USA, without regards to such state's conflict of law rules. Any legal action, suit or proceeding arising out of or relating to these Terms and Conditions or the breach thereof shall be instituted in a court of competent jurisdiction in New York County in the State of New York in the United States of America and each party hereby consents and submits to the personal jurisdiction of such court, waives any objection to venue in such court and consents to service of process by registered or certified mail, return receipt requested, at the last known address of such party.

WILEY OPEN ACCESS TERMS AND CONDITIONS

Wiley Publishes Open Access Articles in fully Open Access Journals and in Subscription journals offering Online Open. Although most of the fully Open Access journals publish open access articles under the terms of the Creative Commons Attribution (CC BY) License only, the subscription journals and a few of the Open Access Journals offer a choice of Creative Commons Licenses. The license type is clearly identified on the article.

The Creative Commons Attribution License

The Creative Commons Attribution License (CC-BY) allows users to copy, distribute and transmit an article, adapt the article and make commercial use of the article. The CC-BY license permits commercial and non-

Creative Commons Attribution Non-Commercial License

The Creative Commons Attribution Non-Commercial (CC-BY-NC)License permits use, distribution and reproduction in any medium, provided the original work is properly cited and is not used for commercial purposes.(see below)

Creative Commons Attribution-Non-Commercial-NoDerivs License

Use by commercial "for-profit" organizations

Further details can be found on Wiley Online Library
http://olabout.wiley.com/WileyCDA/Section/id-410895.html

Other Terms and Conditions:

v1.10 Last updated September 2015

Questions? customercare@copyright.com or +1-855-239-3415 (toll free in the US) or +1-978-646-2777.

Copyright Clearance Center

RightsLink®

Home | Account Info | Help

ACS Publications
Most Trusted. Most Cited. Most Read.

Title: Substituent Effects on the Binding of Halides by Neutral and Dicationic Bis(triazolium) Receptors

Author: Binod Nepal, Steve Scheiner

Publication: The Journal of Physical Chemistry A

Publisher: American Chemical Society

Date: Dec 1, 2015

Copyright © 2015, American Chemical Society

Quick Price Estimate

I would like to...	reuse in a Thesis/Dissertation
Requestor Type	Author (original work)
Portion	Full article
Format	Print and Electronic
Will you be translating?	No
Select your currency	USD - $
Quick Price	Click Quick Price

This service provides permission for reuse only. If you do not have a copy of the article you are using, you may copy and paste the content and reuse according to the terms of your agreement. Please be advised that obtaining the content you license is a separate transaction not involving Rightslink.

QUICK PRICE | CONTINUE

Copyright Clearance Center

RightsLink®

Home | Account Info | Help

ACS Publications
Most Trusted. Most Cited. Most Read.

Title: Enhancing the Reduction Potential of Quinones via Complex Formation
Author: Binod Nepal, Steve Scheiner
Publication: The Journal of Organic Chemistry
Publisher: American Chemical Society
Date: May 1, 2016
Copyright © 2016, American Chemical Society

Quick Price Estimate

Permission for this particular request is granted for print and electronic formats, and translations, at no charge. Figures and tables may be modified. Appropriate credit should be given. Please print this page for your records and provide a copy to your publisher. Requests for up to 4 figures require only this record. Five or more figures will generate a printout of additional terms and conditions. Appropriate credit should read: "Reprinted with permission from {COMPLETE REFERENCE CITATION}. Copyright {YEAR} American Chemical Society." Insert appropriate information in place of the capitalized words.

I would like to... ❓   [reuse in a Thesis/Dissertation ⌄]

Requestor Type ❓   [Author (original work) ⌄]

Portion ❓   [Full article ⌄]

Format ❓   [Print and Electronic ⌄]

Will you be translating? ❓   [No ⌄]

Select your currency   [USD - $ ⌄]

Quick Price   Click Quick Price

QUICK PRICE   CONTINUE

This service provides permission for reuse only. If you do not have a copy of the article you are using, you may copy and paste the content and reuse according to the terms of your agreement. Please be advised that obtaining the content you license is a separate transaction not involving Rightslink.

Copyright Clearance Center

RightsLink®

Home | Account Info | Help

ACS Publications
Most Trusted. Most Cited. Most Read.

Title: Enhancing the Reduction Potential of Quinones via Complex Formation

Author: Binod Nepal, Steve Scheiner

Publication: The Journal of Organic Chemistry

Publisher: American Chemical Society

Date: May 1, 2016

Copyright © 2016, American Chemical Society

PERMISSION/LICENSE IS GRANTED FOR YOUR ORDER AT NO CHARGE

BACK | CLOSE WINDOW

NX···Y halogen bonds. Comparison with NH···Y H-bonds and CX···Y halogen bonds

B. Nepal and S. Scheiner, *Phys. Chem. Chem. Phys.*, 2016, Advance Article, **DOI:** 10.1039/C6CP03771B

If you are not the author of this article and you wish to reproduce material from it in a third party non-RSC publication you must formally request permission using RightsLink. Go to our Instructions for using RightsLink page for details.

Authors contributing to RSC publications (journal articles, books or book chapters) do not need to formally request permission to reproduce material contained in this article provided that the correct acknowledgement is given with the reproduced material.

Reproduced material should be attributed as follows:

- For reproduction of material from NJC:
  Reproduced from Ref. XX with permission from the Centre National de la Recherche Scientifique (CNRS) and The Royal Society of Chemistry.
- For reproduction of material from PCCP:
  Reproduced from Ref. XX with permission from the PCCP Owner Societies.
- For reproduction of material from PPS:
  Reproduced from Ref. XX with permission from the European Society for Photobiology, the European Photochemistry Association, and The Royal Society of Chemistry.
- For reproduction of material from all other RSC journals and books:
  Reproduced from Ref. XX with permission from The Royal Society of Chemistry.

If the material has been adapted instead of reproduced from the original RSC publication "Reproduced from" can be substituted with "Adapted from".

In all cases the Ref. XX is the XXth reference in the list of references.

If you are the author of this article you do not need to formally request permission to reproduce figures, diagrams etc. contained in this article in third party publications or in a thesis or dissertation provided that the correct acknowledgement is given with the reproduced material.

Reproduced material should be attributed as follows:

- For reproduction of material from NJC:
  [Original citation] - Reproduced by permission of The Royal Society of

Chemistry (RSC) on behalf of the Centre National de la Recherche Scientifique (CNRS) and the RSC
- For reproduction of material from PCCP:
  [Original citation] - Reproduced by permission of the PCCP Owner Societies
- For reproduction of material from PPS:
  [Original citation] - Reproduced by permission of The Royal Society of Chemistry (RSC) on behalf of the European Society for Photobiology, the European Photochemistry Association, and RSC
- For reproduction of material from all other RSC journals:
  [Original citation] - Reproduced by permission of The Royal Society of Chemistry

If you are the author of this article you still need to obtain permission to reproduce the whole article in a third party publication with the exception of reproduction of the whole article in a thesis or dissertation.

Information about reproducing material from RSC articles with different licences is available on our [Permission Requests page](#).

CURRICULUM VITAE

Binod Nepal

(July, 2016)

Department of Chemistry and Biochemistry

Utah State University

003 Old Main Hill

Logan, UT, 84322

Email: binod.nepal@aggiemail.usu.edu

Phone: (435)213-7310

EDUCATION

Ph.D. Student in Chemistry   **Current**

Department of Chemistry and Biochemistry

Utah State University

Logan, UT, 84322

Advisor: Prof. Steve Scheiner

M.Sc. in Chemistry   **2008**

Central Department of Chemistry

Tribhuvan University

Kirtipur, Kathmandu, Nepal

Advisor: Prof. Kedar Nath Ghimire

B.Sc. in Chemistry   **2004**

Amrit Science College

Tribhuvan University

Kathamndu, Nepal

AWARDS & HONORS

Outstanding Graduate Student in Chemistry   **2016**

Department of Chemistry and Biochemistry

Utah State University

Logan, UT, 84322

Doctoral Dissertation Enhancement Fund   **2016**

Office of Research and Graduate Studies

Utah State University, Logan, UT

Joseph Reuel Harris Graduate Scholarship   **2014**

Utah State University, Logan, UT

Chhita Bahadur Tuladhar Gold Medal

(For securing first position in Chemistry major in B.Sc.)   **2004**

Amrit Science College, Kathamndu, Nepal

RESEARCH EXPERIENCES

Graduate Research Assistant   **2013 - Present**

Department of Chemistry and Biochemistry

Utah State University

Logan, UT, 84322

Research Mentor: Steve Scheiner

- o Gained experiences in quantum mechanical studies of different non

  covalent interactions

- o Learned different tools and techniques in computational chemistry

Graduate Research Assistant   **2011-2013**

Department of Chemistry and Biochemistry

Utah State University

Logan, UT, 84322

Research Mentor: Siddhartha Das

- o Gained experiences in synthesis and design of ligand, metal organic

  frameworks etc.

- o Worked in water oxidation catalysis

- o Learned to use NMR, UV-VIS, IR, Powder X-ray diffraction, Cyclic

  Voltammetry

M.Sc. Dissertation Research   **2007-2008**

"Optimization of xanthation onto apple waste and its application for Al^{3+} and Fe^{3+} removal"

Central Department of Chemistry, Tribhuvan University, Kirtipur, Kathmandu, Nepal

Research Mentor: Prof. Kedar Nath Ghimire

- o Gained experiences in adsorption chemistry
- o Learned different analytical techniques, synthesis etc.

TEACHING EXPERIENCES

Graduate Teaching Assistant, Utah State University, Logan, UT

- o Teaching Assistant, CHEM 1215 (Spring 2012, Fall 2013, Summer 2014, Summer 2015)
- o Teaching Assistant, CHEM 1225 (Fall 2012, Spring 2013, Spring 2016, Summer 2016)
- o Recitation Instructor, CHEM 1210 (Fall 2014, Fall 2015)
- o Utah State University, Teaching Assistant Workshop, Fall 2011

Lecturer in Chemistry, Trinity Int. College, Dillibazar, Kathmandu, Nepal, **2009-2011**

Lecturer in Chemistry, Martyr Memorial Institute of science and Technology, Jawalakhel, Lalitpur, Nepal, **2008-2009**

Teacher of general science, Shishu Milan Secondary School, Chunikhel, Kathmandu, Nepal, **2004-2005**

PRESENTATION & PUBLISHED ABSTRACTS

1. Binod Nepal and steve scheiner "*Substituent Effects on the Binding of Halides by Neutral and DicationicBis(triazolium) Receptors*" Poster presented at the ACS National Meeting, San Diego, CA, March2016.

PUBLICATIONS

1. Nepal, B., & Das, S. (2013). Sustained Water Oxidation by a Catalyst Cage-Isolated in a Metal–Organic Framework. *Angew. Chem. Int. Ed.* **2013**, *52*, 7224.

2. Nepal, B., & Scheiner, S. (2014). Effect of Ionic Charge on the CH⋯π Hydrogen Bond. *J. Phys. Chem. A* **2014**, *118*, 9575.

3. Nepal, B., & Scheiner, S. (2015). Angular dependence of hydrogen bond energy in neutral and charged systems containing CH and NH proton donors *Chem. Phys. Lett.* **2015**, *630*, 6.

4. Nepal, B., & Scheiner, S. (2015). Anionic CH⋯X− Hydrogen Bonds: Origin of Their Strength, Geometry, and Other Properties. *Chem. Eur. J.* **2015**, *21*, 1474.

5. Nepal, B., & Scheiner, S. (2015). Building a Better Halide Receptor. Optimum Choice of Spacer, Binding Unit, and Halo substitution. *Chem Phys Chem 2016, 17, 836.*

6. Nepal, B., & Scheiner, S. (2015). Competitive Halide Binding by Halogen Versus Hydrogen Bonding: Bis-triazole Pyridinium. *Chem. Eur. J.* **2015**, *21*, 13330.

7. Nepal, B., & Scheiner, S. (2015). Long-range behavior of noncovalent bonds. Neutral and charged H-bonds, pnicogen, chalcogen, and halogen bonds. *Chem. Phys.* **2015**, *456*, 34.

8. Nepal, B., & Scheiner, S. (2015). Microsolvation of anions by molecules forming CH··X− hydrogen bonds. *Chem. Phys.* **2015**, *463*, 137.

9. Nepal, B., & Scheiner, S. (2015). Substituent Effects on the Binding of Halides by Neutral and Dicationic Bis(triazolium) Receptors. *J. Phys. Chem. A* **2015**, *119*, 13064.

10. Fick, R. J., Kroner, G. M.,Nepal, B., Magnani, R., Horowitz, S., Houtz. R. L., Scheiner, S., Trievel, R.C.,(2015) Sulfur – Oxygen Chalcogen Bonding Mediates AdoMet Recognition in the Lysine Methyltransferase SET7/9. *ACS Chemical Biology* **2016**, *11*, 748.

11. Nepal, B., & Scheiner, S. (2016). Enhancing the Reduction Potential of Quinones via Complex Formation. *J. Org. Chem.* **2016**, *81*, 4316.

12. Nepal, B., & Scheiner, S. (2016). NX··Y Halogen Bonds. Comparison with NH··Y H-bonds and CX··Y Halogen Bonds (PCCP, accepted article)